

DESIGN SCHEME DECISION-MAKING AND ON-GOING COMMISSIONING FOR HVAC SYSTEMS

by

Fulin Wang

B.E. in Environmental Engineering, Wuhan Urban Construction Institute, 1993

M.E. in Thermal Engineering, Tsinghua University, 2001

Submitted to the Graduate School of Engineering

in partial fulfillment of the requirements

for the degree of Doctor of Engineering



Department of Global Environment Engineering

Kyoto University

June 2004

CONTENTS

CONTENTS	I
LIST OF TABLES	IX
LIST OF FIGURES	XI
NOMENCLATURE	XVII
ABSTRACT	XXV
INTRODUCTION	1
0.1 Background	1
0.2 Objectives	2
0.3 Structure	2
0.3.1 Part 1: Design phase	2
0.3.2 Part 2: Operational phase.....	3
CHAPTER 1	9
LIFE CYCLE COST ESTIMATION METHOD FOR HVAC SYSTEMS AT DESIGN PHASE	9
1.1 Concept.....	9
1.2 Methodology	11
CHAPTER 2	15
LIFE CYCLE COST ESTIMATION USING NEURAL NETWORK AT BEGINNING OF DESIGN	15

2.1 Introduction	15
2.2 Influence factors	16
2.3 Sensitivity analysis	17
2.3.1 Sensitivity analysis of initial investment cost	17
2.3.2 Sensitivity analysis of operational cost	19
2.4 Cost estimation	19
2.4.1 Selection of neural network model.....	21
2.4.2 Training of neural network model.....	23
2.4.3 Estimation using neural network model.....	31
2.5 Summary	33
CHAPTER 3	34
LIFE CYCLE COST ESTIMATION FOR THE OTHER THREE DESIGN STAGES	34
3.1 introduction	34
3.2 Conceptual design stage	34
3.2.1 Influence factors	34
3.2.2 Sensitivity analysis	35
3.2.2.1 Sensitivity analysis of initial investment cost	35
3.2.2.2 Sensitivity analysis of operational cost	36
3.2.3 Cost estimation.....	38
3.2.3.1 Estimation of initial investment cost.....	38

3.2.3.2 Estimation of operational cost	38
3.3 Preliminary design stage	39
3.3.1 Cost estimation of terminal systems.....	39
3.3.1.1 Initial investment cost.....	39
3.3.1.2 Operational cost.....	42
3.3.2 Cost estimation of heating/cooling source systems.....	42
3.3.2.1 Initial investment cost.....	42
3.3.2.2 Operational cost.....	44
3.4 Detailed design stage.....	45
3.4.1 Initial investment cost.....	45
3.4.2 operational cost.....	46
3.5 summary	46
CHAPTER 4	49
ON-GOING COMMISSIONING METHODOLOGY FOR OPERATIONAL PHASE	49
4.1 Introduction	49
4.2 Introduction to commissioning.....	49
4.2.1 Definition of commissioning.....	49
4.2.2 Historical development of commissioning.....	51
4.2.3 Current research on building commissioning.....	52
4.3 On-going commissioning methodology	53

4.3.1 Simulation comparison approach	56
4.3.1.1 Coil	56
4.3.1.2 Valve and damper.....	57
4.3.1.3 VAV box	61
4.3.1.4 Fan subsystem	61
4.3.2 No-fault operational data comparison.....	64
4.3.2.1 Malfunctioning supply air temperature sensor	65
4.3.2.2 Malfunctioning room air temperature sensor	67
4.4 Summary	69
CHAPTER 5	70
TOTAL ENERGY CONSUMPTION MODEL OF FAN SUBSYSTEM SUITABLE FOR ON-GOING COMMISSIONING	70
5.1 Introduction	70
5.2 Models	70
5.2.1 Fan efficiency model	74
5.2.2 Driveline efficiency	76
5.2.3 Motor efficiency	76
5.2.4 Inverter efficiency	79
5.3 Model parameters, inpoputs, and output	79
5.3.1 Parameters	79
5.3.2 Inputs	80

5.3.3 Output	80
5.4 Experimental validation	80
5.4.1 Validation using normal fan subsystem	81
5.4.1.1 Coefficients fitting for fan model	82
5.4.1.2 Coefficients fitting for motor model	85
5.4.1.3 Coefficients fitting for inverter model.....	86
5.5 Application for automated on-going commissioning.....	88
5.6 Application case study.....	89
5.6 Summary	92
CHAPTER 6	94
EXPERIMENT STUDY ON THE ON-GOING COMMISSIONING OF A REAL VAV SYSTEM.....	94
6.1 Introduction	94
6.2 Low efficiency fan subsystem.....	97
6.2.1 Experimental method.....	97
6.2.2 Results, discussion and conclusions	100
6.3 Malfunctioning supply air and room air temperature sensor.....	101
6.3.1 Experimental method.....	101
6.3.2 Results, discussion and conclusions	102
6.4 Stuck AHU outdoor air damper.....	103
6.4.1 Experimental method.....	103

6.4.2 Results, discussion and conclusions	103
6.5 Stuck AHU water valve.....	105
6.5.1 Experimental method.....	105
6.5.2 Results, discussion and conclusions	105
6.6 Summary	105
CHAPTER 7	107
MODEL-BASED COMMISSIONING FOR FILTERS IN ROOM AIR-CONDITIONERS	107
7.1 Introduction	107
7.2 Models	109
7.2.1 Estimation using fan energy consumption data.....	112
7.2.2 Estimation using thermal performance data	112
7.3 Model parameters, inputs, and output	119
7.3.1 Parameters	119
7.3.2 Inputs	119
7.3.3 Output.....	120
7.4 Model validation.....	120
7.4.1 Validation results of estimating using fan power consumption data.....	125
7.4.2 Validation results of estimating using thermal performance data	125
7.5 Model-based commissioning method.....	128
7.6 Summary	130

CHAPTER 8	131
CONCLUSIONS.....	131
8.1 Efficiency should be ensured from very beginning using economic estimation method at design phase.....	131
8.1.1 Neural network method suits for economic estimation at beginning of design .	131
8.1.2 Empirical equations suit for economic estimation at other design stages.....	132
8.2 No-Fault Operation Comparison Methodology for operational phase ensures system efficiency during whole life cycle	132
8.2.1 Simulation using suitable models automates on-going commissioning.....	132
8.2.2 Past no-fault Operational data records suits for continuously commissioning sensors	133
8.3 Main achievements.....	133
REFERENCES	135
LIST OF PAPERS.....	141
1. Papers published and reviewed	141
2. Papers under reviewing	142
3. Papers presented	142
APPENDIX A	147
EXPERIMENTAL STUDY ON COMMISSIONING MULTI-EVAPORATOR GHP SYSTEMS.....	147
A.1 Objectives	147
A.1.1 Develop GHP performance simulation tool	147
A.1.2 Develop commissioning method for GHP Systems	148

A.2 Profile of experimental building and GHP system.....	148
A.3 Measurement items.....	152
A.3.1 Meteorological data	152
A.3.2 Indoor environment	153
A.3.3 GHP system performance.....	155
A.3.4 Ventilation system performance.....	159
A.4 Experimental results	163
A.1.1 Filter resistance estimation model.....	163
A.1.2 Comparison of simulated and measured heating/cooling load.....	163
A.1.3 Indoor unit air flow rate.....	164
A.1.3 Ventilation air flow rate.....	164
A.1.4 GHP COP calculation.....	165
A.4 Future research	183
ACKNOWLEDGEMENT	185

LIST OF TABLES

Table 1.1	Calculation parameter of sensitivity analysis.....	14
Table 2.1	Known information for LCC estimation at beginning of design stage.....	16
Table 2.2	Training sample buildings information.....	24
Table 2.3	Buildings for ADLINE model validation.....	32
Table 3.1	Known information for LCC estimation at conceptual design stage.....	35
Table 3.2	Estimation of pipe amount.....	41
Table 4.1	Parameters of valve control model.....	63
Table 5.1	Data for fan model coefficients fitting.....	83
Table 5.2	Data for motor model coefficients fitting.....	85
Table 5.3	Data for inverter model coefficients fitting.....	86
Table 6.1	Profile of experimental building and VAV system.....	95
Table 6.2	Experimental results of malfunctioning temperature sensor.....	102
Table 7.1	Profile of the experimental air-conditioner.....	122
Table 7.2	Indoor unit fan performance data for coefficients fitting.....	123
Table 7.3	Parameters for filter resistance estimation.....	124
Table A.1	Profile of Experimental room and GHP system.....	151
Table A.2	Measurement items.....	162
Table A.3	Raw data used for COP calculation of cooling operation.....	171

Table A.4	COP calculation results of cooling operation.....	173
Table A.5	Raw data used for COP calculation of heating operation.....	179
Table A.6	COP calculation results of heating operation.....	181

LIST OF FIGURES

Figure 0.1	Dissertation contents and structure.....	5
Figure 1.1	Complete assessments of HVAC schemes.....	10
Figure 1.2	Concept of LCC estimation stage-by-stage.....	11
Figure 1.3	Sample building for sensitivity analysis.....	13
Figure 2.1	Change of initial investment cost caused by consecutive variables.....	18
Figure 2.2	Change of initial investment cost caused by influence factors.....	18
Figure 2.3	Change of operational cost caused by consecutive variables.....	20
Figure 2.4	Change of operational cost caused by different factors.....	20
Figure 2.5	Structure of ADLINE model.....	21
Figure 2.6	Training process of Neural Network.....	31
Figure 2.7	Comparison of estimated and real IIC and OC.....	33
Figure 3.1	Initial investment changes caused by load and air volume.....	36
Figure 3.2	Operational cost changes caused by load and air volume.....	37
Figure 3.3	IIC and OC estimation results at conceptual design stage.....	39
Figure 4.1	Concept of on-going commissioning methodology.....	55
Figure 4.2	Valve model in SIMBAD.....	58
Figure 4.3	Demand valve position vs. PI.....	60
Figure 4.4	Simulink model for valve control simulation.....	62
Figure 4.5	Comparison of simulated and real valve positions.....	63

Figure 4.6	VAV system responses to supply air temperature sensor offset.....	66
Figure 4.7	Influence of supply air temperature sensor offset.....	67
Figure 4.8	VAV system responses to room air temperature sensor offset.....	68
Figure 4.9	Influence of room air temperature sensor offset.....	68
Figure 5.1	Fan efficiency vs. dimensionless air flow rate.....	71
Figure 5.2	Total efficiency of fan subsystem vs. dimensionless air flow rate.....	72
Figure 5.3	Components and energy flow of a fan subsystem.....	72
Figure 5.4	Comparison of measured and estimated fan rotational speed.....	75
Figure 5.5	Motor efficiency vs. load factor and power frequency.....	77
Figure 5.6	VAV system motor efficiency vs. load factor and power frequency.....	78
Figure 5.7	Inverter heat generating vs. load factor.....	79
Figure 5.8	Inverter efficiency vs. load factor.....	81
Figure 5.8	Measurement points and AHU configuration.....	81
Figure 5.9	Experiment step and parameters.....	82
Figure 5.10	Coefficients fitting results of fan model.....	85
Figure 5.11	Coefficients fitting results of motor model.....	86
Figure 5.12	Coefficients fitting results of inverter model.....	87
Figure 5.13	Simulation accuracy of total energy consumption model.....	87
Figure 5.14	Flowchart of automated on-going commissioning for fan subsystem using total energy consumption model.....	90
Figure 5.15	Total power consumption of a fan subsystem with slipping belts compared with simulated value with tight belts.....	92

Figure 6.1	Experimental building and VAV system location.....	95
Figure 6.2	Experimental VAV system plan configuration.....	96
Figure 6.3	Experimental VAV system components and control systems.....	96
Figure 6.4	Experiment steps and parameters of loose fan belts.....	98
Figure 6.5	Power consumption measurement point and instrument.....	98
Figure 6.6	Fan pressure head measurement.....	99
Figure 6.7	Experimental fan specification curve.....	100
Figure 6.8	Experiment results of loose fan belts.....	100
Figure 6.9	Experimental steps of stuck AHU outdoor air damper.....	103
Figure 6.10	Experimental results of stuck AHU outdoor air damper.....	104
Figure 6.11	Experimental steps of stuck AHU water valve.....	105
Figure 6.12	Experimental results of stuck AHU water valve.....	106
Figure 7.1	GHP heat production and fan efficiency vs. filter resistance.....	108
Figure 7.2	Measurement points in a typical cassette-shape indoor unit.....	111
Figure 7.3	Pressure curves of indoor units.....	111
Figure 7.4	Refrigeration cycle state points.....	111
Figure 7.5	Statistical distribution of indoor air humidity in summer period.....	113
Figure 7.6	Flowchart of estimating air-conditioner indoor unit outlet air humidity.....	115
Figure 7.7	Estimated and measured air humidity at four outlets of the indoor unit..	118
Figure 7.8	An air-conditioner's performance vs. filter resistance.....	119

Figure 7.9	Ducts and instruments for making filters having different resistance....	121
Figure 7.10	Ducts and instruments for making filters having different resistance....	121
Figure 7.11	Coefficients fitting results of indoor unit fan.....	123
Figure 7.12	Expansion valve orifice area vs. controller demand.....	124
Figure 7.13	Validation results of estimating using fan power consumption data.....	126
Figure 7.14	Validation results of estimating using thermal performance data.....	126
Figure 7.15	Filter resistance estimation results of three other indoor units.....	127
Figure 7.16	Filter resistance estimation results of three other indoor units.....	129
Figure A.1	Experimental building.....	149
Figure A.2	Experimental HVAC systems.....	150
Figure A.3	Outdoor air temperature, humidity and solar radiation sensor measurement.....	152
Figure A.4	Wind direction and speed measurement.....	153
Figure A.5.	Measurement of heat flux and solar radiation.....	154
Figure A.6	Measurement of room air temperature.....	154
Figure A.7	Measurement of the number of occupants.....	155
Figure A.8	Measurement of indoor unit inlet and outlet air temperature and humidity.....	156
Figure A.9	Measurement of indoor unit air flow rate.....	156
Figure A.10	Measurement of gas consumption.....	157
Figure A.11	Measurement of refrigerant flow rate.....	157
Figure A.12	Measurement of refrigerant flow rate.....	158

Figure A.13	Measurement of refrigerant flow rate.....	158
Figure A.14	Measurement of ventilation air flow rate.....	159
Figure A.15	Measurement of ventilation air temperature and humidity.....	160
Figure A.16	Data loggers and wiring.....	160
Figure A.18	Indoor unit air flow rate and filter weight.....	164
Figure A.19	Ventilation air flow rate.....	165
Figure A.20	GHP refrigerant system chart and measurement points.....	166
Figure A.21	COP calculation results on typical summer day.....	167
Figure A.22	COP calculation results on typical winter day.....	175

NOMENCLATURE

Roman symbols

A	Area (m^2)
A_c	Amount of chillers
a	Error of proportional band L_0
a_0, a_1, a_2, a_3, a_4	Fitted coefficients for the equation of C_h - C_f
b	Error of proportional band L_1
C_a	Influence coefficient of HVAC scheme to cost
C_{EV}	Flow rate coefficient of expansion valve
C_f	Dimensionless flow rate
C_h	Dimensionless pressure head
C_o	Influence coefficient of outside air supply scheme to cost
C_p	Specific heat (kJ/kg.k)
C_r	Dimensionless flow resistance
C_s	Influence coefficient of heating and cooling source scheme to cost
C_V	Valve resistance coefficient ($\text{kPa}/(\text{kg/s})^2$)
C_{V0}	Valve resistance coefficient when valve is full open ($\text{kPa}/(\text{kg/s})^2$)
CL	Total cooling load (kW)
CO_y	The cost in the y^{th} year, CO_0 is the initial investment cost
D	Diameter (m)

E	Energy consumption (kW)
EC	Electric power consumption (kW)
EP	Electric power price
e_0, e_1, e_2, e_3, e_4	Fitted coefficients for the equation of $\eta-C_f$
F	Frequency of power line (Hz)
f_0, f_1, f_2, f_3, f_4	Fitted coefficients for the equation of C_f-C_r
G	Bias when dead-band is considered ($^{\circ}\text{C}$)
GC	Gas Consumption (m^3/s)
g	Dead-band of valve control bias ($^{\circ}\text{C}$)
g_e	Error of dead-band of valve control bias ($^{\circ}\text{C}$)
g_o	Original dead-band of valve control bias ($^{\circ}\text{C}$)
H	Heat produced by unit fuel (kJ/kg)
HHV	Higher heat value (kJ/Nm^3)
hr	A building's opening hours
I	Integral control output (%)
IIC	Initial investment cost (RMB, unit of Chinese currency)
INV	Invert output (%)
i	Numbering of equipments
in	Interest
i_0, i_1, i_2, i_3, i_4	Fitted coefficients for the equation of inverter efficiency equation
I_V	Valve capacity index (m^3/h at 1 bar)

K	Coefficient of proportional action ($1/^\circ\text{C}$)
L	Proportional band ($^\circ\text{C}$)
L_0	Proportional band when inverter output is 0 ($^\circ\text{C}$)
L_1	Proportional band when inverter output is 100 ($^\circ\text{C}$)
LE	Length (m)
LF	Load factor
m	Mass flow rate (kg/s)
m_0, m_1, m_2, m_3, m_4	Fitted coefficients for the equation of motor efficiency
n	Life cycle (year)
N	Rotational speed (r/m)
O	Controller output for valve opening (%)
O_V	Valve relative opening
OC	Yearly operational cost (RMB/a)
P	Pressure (Pa)
PE	Price of energy
PF	Price of fuel
PH	Pressure head (Pa)
PI	Proportional-integral control output (%)
PO	Proportional control output (%)
Q	Cooling/heating production (kW)
R	Coefficient of flow resistance ($\text{Pa}/(\text{m}^3/\text{h})^2$)

r	Ratio
s	Iterative step
st	Saturated
T	Temperature ($^{\circ}\text{C}$)
t	Time (s)
t_o	Original integral time (s)
t_e	Error of integral time (s)
V	Volume flow rate (m^3/h)
v	Velocity (m/s)
W	Weight vector for ADLINE neural network model
W_a	Air humidity ratio (g/kg dry air)
W_f	The weight of valve linear characteristic
X	Input vector for ADLINE neural network model
Z	Bias of supply air temperature to set point ($^{\circ}\text{C}$)

Greek symbols

α	Learning speed for ADLINE neural network model
Δ	Difference
ε	Error between estimated value and expected value
η	Efficiency
λ	Leakage coefficient (closed flow/open flow at constant pressure)

ξ	Local loss coefficient
ρ	Density (kg/m ³)
τ	Time
φ	Relative humidity

Subscripts and superscripts

a	Air
atm	Atmosphere
c	Cooling
cp	Cooling plant
d	Demand valve
dl	Driveline
dp	Dew-point
EV	Expansion valve
f	Fan
ft	Filter
h	Heating
i	Inlet
id	Indoor
inv	Inverter
k	Numbering of training samples

<i>m</i>	Measured value
<i>mo</i>	Motor
<i>max</i>	Maximum value
<i>n</i>	Number
<i>nor</i>	Normal operational data
<i>o</i>	Outlet
<i>OC</i>	Coil etc. other components except filter and fan in the indoor unit of a room air-conditioner
<i>od</i>	Outdoor air
<i>off</i>	Offset operational
<i>r</i>	Rated value
<i>re</i>	Return air
<i>ref</i>	Refrigerant
<i>s</i>	Set point
<i>st</i>	Saturation
<i>su</i>	Summer
<i>t</i>	Total value
<i>ts</i>	Time step
<i>w</i>	Winter
<i>wv</i>	Water vapor
<i>1,2,3,4</i>	State points in a refrigeration cycle, defined in Figure 7.2

Abbreviations

ADLINE	Adaptive linear element
AHU	Air handling unit
BEMS	Building energy management system
CAV	Constant air volume
CMOAR	Constant minimum outside air rate
COP	Coefficient of performance
DeST	Designer's simulation toolkits
FCU	Fan coil unit
HHV	Higher heat value
HVAC	Heating, ventilation and air conditioning
IIC	Initial investment cost
LCC	Life cycle cost
LCCE	Life cycle cost economic
LMS	Least Mean Square
NFOC	No-fault operation comparison
OC	Operational cost
PI	Proportional and integral
RMB	Unit of Chinese currency
VAV	Variable air volume

VSD Variable speed drive

VOAR Variable outside air rate

ABSTRACT

DESIGN SCHEME DECISION-MAKING AND ON-GOING COMMISSIONING FOR HVAC SYSTEMS

Fulin Wang

Kyoto University, June 2004

The most important two aspects for energy efficiency and high performance of buildings' Heating Ventilation and Air-Conditioning (HVAC) systems are the selection of proper HVAC scheme at design phase and the maintenance of proper running of the HVAC system during operational phase.

For the purpose of selecting a proper HVAC scheme, Life Cycle Cost (LCC) is a good criterion to make the decision of HVAC scheme selection at design phase. This dissertation proposes the concept of estimating the Life Cycle Cost of a HVAC system stage-by-stage corresponding to the design progress of the HVAC system, which is gradually specified stage by stage. This dissertation divides the economic estimation of HVAC systems into four stages: beginning of design, conceptual design, preliminary design, and detailed design. The Life Cycle Cost Estimation (LCCE) suitable for different design stages are analyzed and proposed. At the beginning of design stage, because there is little information that can be used to estimate the economic character of HVAC systems, neural network models are built to estimate the economic parameters of HVAC systems. At conceptual design stage, different HVAC system scheme are simulated to compare how they satisfy the demand of air conditioning. The simulation results are used to estimate the economic value of the HVAC Schemes. At preliminary design stage, parts of the HVAC systems are simulated and compared and some detailed information about the HVAC equipment can be obtained and used to accurately calculate the costs. The unknown information of the HVAC systems is estimated to calculate their economic values. At detailed design stage, every part of the HVAC systems is simulated. Accurate calculation methods are analyzed according to the detailed design information.

For the operational phase, the on-going commissioning is considered to be the method that can maintain the high performance of a HVAC system. This dissertation proposes a on-going commissioning methodology of No-fault Operation Comparison (NFOC). The no-fault operation data of a HVAC system can be obtained from simulation or past no-fault operational data records. The data obtained from the simulation using the design conditions represent the no-fault performance. The simulation analysis realizes on-going commissioning through continuously comparing the HVAC systems real-time operational data with simulated data. This approach suits for the air or water processing components or subsystems, such as fan subsystems, valves, VAV boxes, and coils etc., whose processing results or outputs can be both simulated and measured. Past no-fault operation that are under the almost same heat conditions as current operation can be used to continuously compare with the real-time current operation during operational phase to check whether current operation has faults or not. This approach suits for commissioning components whose simulation models are not suitable for commissioning, such as temperature sensors, air flow rate sensors etc.

The main achievements of this research can be summarized as follows:

- 1) Develops a methodology for determining an optimal HVAC scheme from valid candidates using Economic Estimation Method at design stages.
- 2) Gives different economic estimation methods suitable for different design stages corresponding to the characteristics of different design stages: neural network method for the beginning of design and empirical estimations for conceptual design, preliminary design and detailed design phase.
- 3) Develops the No-Fault Operation Comparison methodology for on-going commissioning of HVAC systems during operational phase through comparing real-time operational data with no-fault operational data that are obtained from simulation and past no-fault operational data records.
- 4) Develops a total energy consumption model of fan subsystems that can estimate the measurement-easy total energy consumption of fan subsystems and is suitable for on-going commissioning.
- 5) Experimentally studies the on-going commissioning characteristics of a real VAV

system. The experimental study reveals the feasibility of automated on-going commissioning of HVAC systems through comparing real time operational data with no-fault operational data obtained from simulation or past no-fault operational data records.

6) Develops a filter resistance estimation model that can estimate filter resistance without pressure sensor only using thermal or energy performance data of air-conditioners and is suitable for on-going commissioning filters in room air-conditioners.

Keywords: HVAC, Design, Life cycle cost, Commissioning, Operation, Energy efficiency

INTRODUCTION

0.1 BACKGROUND

Energy efficiency measures and technologies began to be studied and taken as an important issue since the middle east war crisis of 1973-1974, when the oil embargo by a number of Arab producers made the main industrial countries become painfully aware of their vulnerability to the new economic power of the oil producer countries (Scott, 1994). Among the energy consumed by human beings, approximately one third of primary energy is consumed in non-industrial buildings (ECBCS, 2002). Hence the building sector represents a major contribution to fossil fuel use and carbon dioxide production. Considering the uncertainties in energy supply and the risk of global warming, many countries have now introduced target values for reduced energy use in building, which are aimed at reducing energy consumption by 15% to 30%. To achieve such a target, international co-operation, in which research activities and knowledge can be shared, is considered to be an effective way to fulfill the aim of reducing energy consumption. Recognizing the significance of energy use in buildings, the International Energy Agency (IEA) has established an Implementing Agreement on Energy Conservation in Buildings and Community Systems (ECBCS). The function of ECBCS is to undertake research and provide an international focus for building energy efficiency. The research projects sponsored by ECBCS are named Annex. These Annexes are directed at energy saving technologies and activities that support technology application in practice. Since 1976 till now, 44 Annexes have been launched.

However, some analyses on the data from the buildings participating in the energy conservation program revealed that many of the installed energy efficiency measures were not performing as expected (Bonneville Power Administration, 1992). So how to ensure energy efficiency measures perform well? Design phase and operational phase are considered by this research to be the critical phases that determine the energy efficiency and the performance of energy conservation measures. Therefore to ensure the performance of energy conservation measures, design phase and operational phase should be emphasized and studied in detail.

0.2 OBJECTIVES

This research focuses on studying the methodology for ensuring energy efficiency of the buildings' Heating Ventilation and Air-Conditioning (HVAC) systems, which is the major contribution to building energy consumption, at design phase and operational phase. Design is the beginning and basis of a HVAC project. The HVAC scheme selected in design phase will be realized into real HVAC system. The characteristics, such as energy efficiency, capability, accessibility, etc., of the designed HVAC scheme determine the performances of the realized HVAC system since the very beginning. Same as design phase, operational phase is also the decisive phase that continuously influences the performance of a HVAC system during its whole life cycle. Therefore this dissertation focuses on studying how to ensure high performance of a HVAC system during design phase and operational phase. For design phase, the methodology of how to determine an optimal HVAC scheme is discussed, which is stage-by-stage Life Cycle Cost Estimation (LCCE). For operational phase, the methodology of how to ensure the high performance of a HVAC system is analyzed, which is the No-Fault Operation Comparison (NFOC) methodology suitable for on-going commissioning of HVAC systems.

0.3 STRUCTURE

Accordingly this dissertation consists of two parts. The first part is the Economic Estimation Method for design phase. The second part is the No-Fault Operation Comparison methodology suitable for the on-going commissioning during operational phase.

0.3.1 PART 1: DESIGN PHASE

Chapter 1, Chapter 2 and Chapter 3 constitute the first part, which discusses the Economic Estimation Method for determining an optimal HVAC scheme at design phase. Life Cycle Cost (LCC) is used as a criterion to make the decision of selecting HVAC scheme at design phase.

Chapter 1 proposes the concept of estimating the life cycle cost of a HVAC system stage-by-stage corresponding to the design progress of the HVAC system, which is also gradually implemented stage by stage. The life cycle cost estimation of HVAC systems is divided into four stages: beginning of design, conceptual design, preliminary design, and detailed design.

Chapter 2 analyzes the method of life cycle cost estimation at the beginning of a design phase. At this stage, there is no much information that can be used to estimate the life cycle cost of HVAC systems. ADLINE (Adaptive Linear Element) neural network models are used to estimate the life cycle cost of HVAC systems.

Chapter 3 studies the methods of life cycle cost estimation for the other three stages, all of which are some kind of empirical methods. At conceptual design stage, different HVAC system scheme are simulated to compare whether they can fulfill the requirement of air conditioning. Heating/cooling load are used to estimate the life cycle cost. At preliminary design stage, subsystems of a HVAC system are simulated and compared. So some detailed information about the HVAC equipment, for example some equipments size and number, can be obtained and used to calculate the life cycle cost more accurately than that of the former two stages. The unknown information of the HVAC system is estimated empirically to calculate the life cycle cost. At detailed design stage, every part of the HVAC systems is simulated and determined. The life cycle cost of the HVAC systems can be calculated in detail according to the detailed design information.

0.3.2 PART 2: OPERATIONAL PHASE

Chapter 4, Chapter 5, Chapter 6 and Chapter 7 form the second part, which deals with how to ensure the energy efficiency and high performance of a HVAC system at operational phase during its whole life cycle. On-going commissioning is considered to be a viable method to ensure the high performance of a HVAC system.

Chapter 4 discusses the methodology for on-going commissioning during operational phase, which is named No-Fault Operation Comparison. The not-fault performance of a HVAC system can be obtained from either simulation or past no-faults operational data records. In order to simulate the no-fault operation of a HVAC system, suitable component, subsystem or whole system models are necessary. Current available simulation models are analyzed to check whether they are suitable for on-going commissioning or not. If the models are not suitable for on-going commissioning, it is necessary to develop new models suitable for on-going commissioning. This dissertation developed two new models suitable for on-going commissioning, which are total energy consumption model for fan subsystems and resistance estimation model for filters in room air-conditioner.

Chapter 5 describes a newly developed total energy consumption model for fan subsystems, which can be used to simulate the not-fault performance of a fan subsystem and suitable for on-going commissioning. The simulated not-fault performance is used to compare with real-time performance of a fan subsystem to determine whether the system has faults or not.

Chapter 6 describes a series of experiments conducted in a real VAV system to study the on-going commissioning characteristics of a VAV system. Four types of faults were introduced into a real VAV system. The faulty operation were measured and compared with no-fault operation. The experiments demonstrated the feasibility of commissioning these components using No-Fault Operation Comparison method.

Chapter 7 introduced a filter resistance estimation model suitable for commissioning the filters in room air-conditioners. The model-based commissioning method for filters in air-conditioners is discussed.

Chapter 8 summarizes this dissertation, draws the conclusions, and lists the main achievements of this research.

The contents and structure of this dissertation is shown in the following figure.

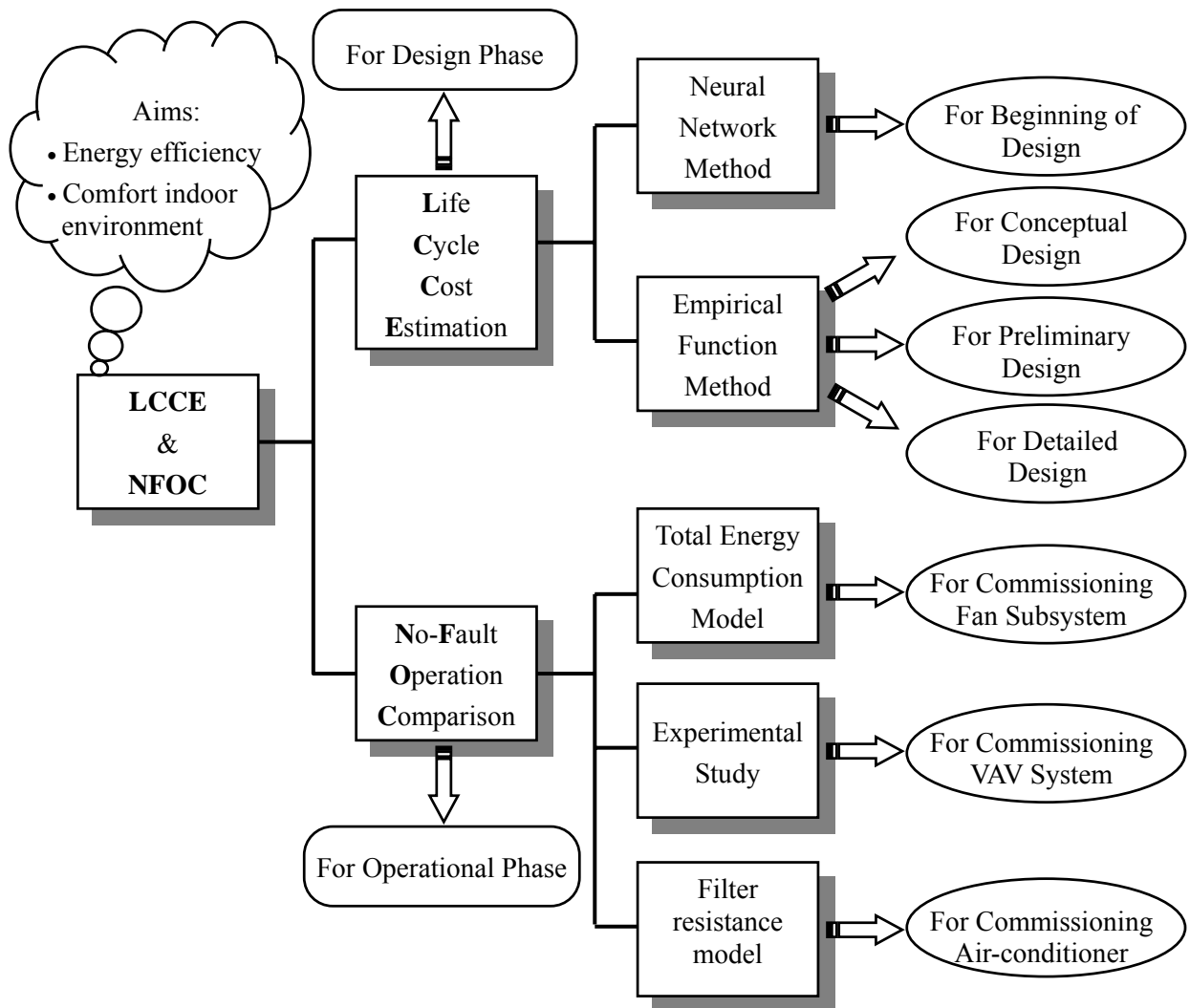


Figure 0.1 Dissertation contents and structure

PART I

This part of research was mainly done during the master course in Tsinghua University, Beijing, China.

LCC

ESTIMATION

AT

DESIGN

PHASE

CHAPTER 1

LIFE CYCLE COST ESTIMATION METHOD FOR HVAC SYSTEMS AT DESIGN PHASE

1.1 CONCEPT

Heating, Ventilating and Air Conditioning (HVAC) projects can be very complex. Typically there are many different HVAC designs that can satisfy the same set of HVAC requirements. How do we choose one design over another? What selection criteria should we use when considering the merits of two comparable designs? Should we select the system that implies less energy consumption, less initial investment cost, or less operation cost? Each HVAC design will perform differently with respect to these three properties.

Economic properties are an important aspect in assessing an HVAC scheme thoroughly. Two kinds of assessment should be performed to evaluate an HVAC scheme thoroughly. First it is important to assess how well a given design satisfies the HVAC requirements. This is typically done by simulating the design's year round performance. Second, it is important to evaluate the economic characteristics of the design by calculating the initial investment cost, operation cost and Life Cycle Cost (LCC) of the scheme. Satisfaction of HVAC requirements and economic characteristics (including initial investment cost and operation cost) are the basic points of evaluation for an HVAC design. Each aspect is balanced and limited by the others. A design that precisely fits the HVAC requirements may be associated with higher initial investment and operation costs. Increasing the initial investment through adding energy saving equipment, such as variable speed drive of pumps and fans, may decreased the operation cost. Figure 1.1 shows the complete description and assessment to an HVAC scheme.

A lot of research has been devoted to evaluating how well a given HVAC system

design fits a set of HVAC requirements. But very little research has been done on economic analysis of HVAC system designs, particularly economic analysis that is integrated into the design process. Griffith (1978) used LCC method to study the influence of window area to lighting, and Charette (1980) analyzed how to use LCC method for calculating building economic parameters, but they did not mention how to use LCC for analyzing HVAC systems. Griffin (1985) analyzed the cost of heating by electric power, Shitzer and Arkin (1979), Tsal and Adler (1986), Tsal and Behls (1987), Wang et al. (1984) studied cost optimization of duct and pipe system. Huang (1984), Lu et al. (1984), Li (1995), Long (1995), Tao (1996) and Kang et al. (1999) studied how to calculate the cost of some HVAC equipments and isolation material. Yang (2000) developed software for calculating the initial investment cost of HVAC systems.

However most of the published research addresses only specific aspects of HVAC systems and not entire systems and operational cost are estimated using equipment rated parameters with part load coefficient. Economic research has overlooked discussion of the models for economic estimation at different stages in the design process and the detailed analysis of whole year performance. At various stages, different information and evaluation methods are needed to make useful economic estimations. Incorporating economic evaluation at all stages in the design process allows engineers to discriminate between multiple designs which may satisfy the same given engineering requirements.

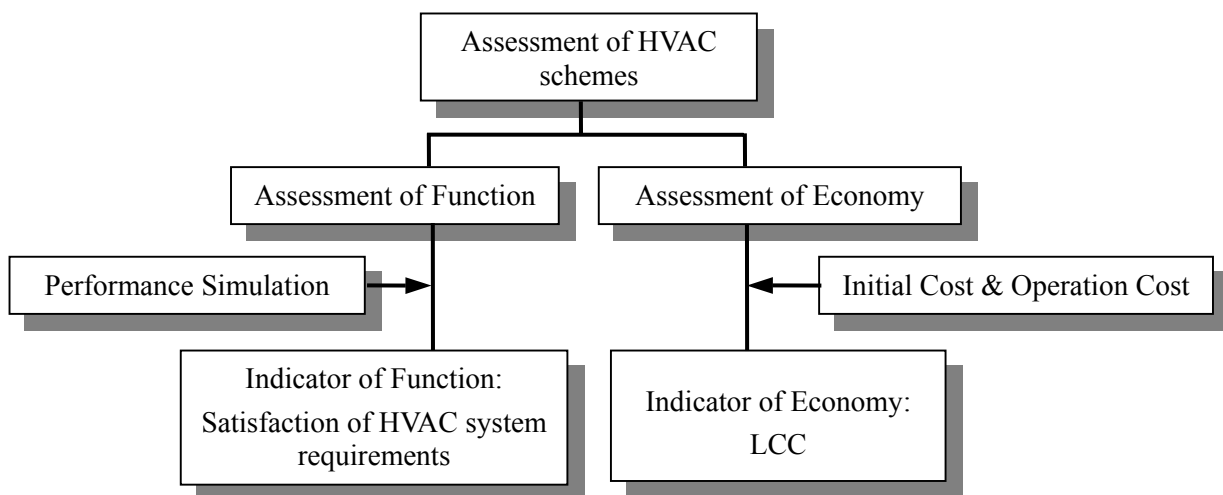


Figure 1.1 Complete Assessments of HVAC Schemes

This chapter analyzes the characteristics of design stages from concept to realization

and demonstrates different economic estimation methods suiting to each stage. For the purpose of this discussion, we recognize four discrete stages in the design process: Beginning of Design, Conceptual Design, Preliminary Design, and Detailed Design. Figure 1.2 shows the concept of economic estimation stage by stage accompanying the design steps.

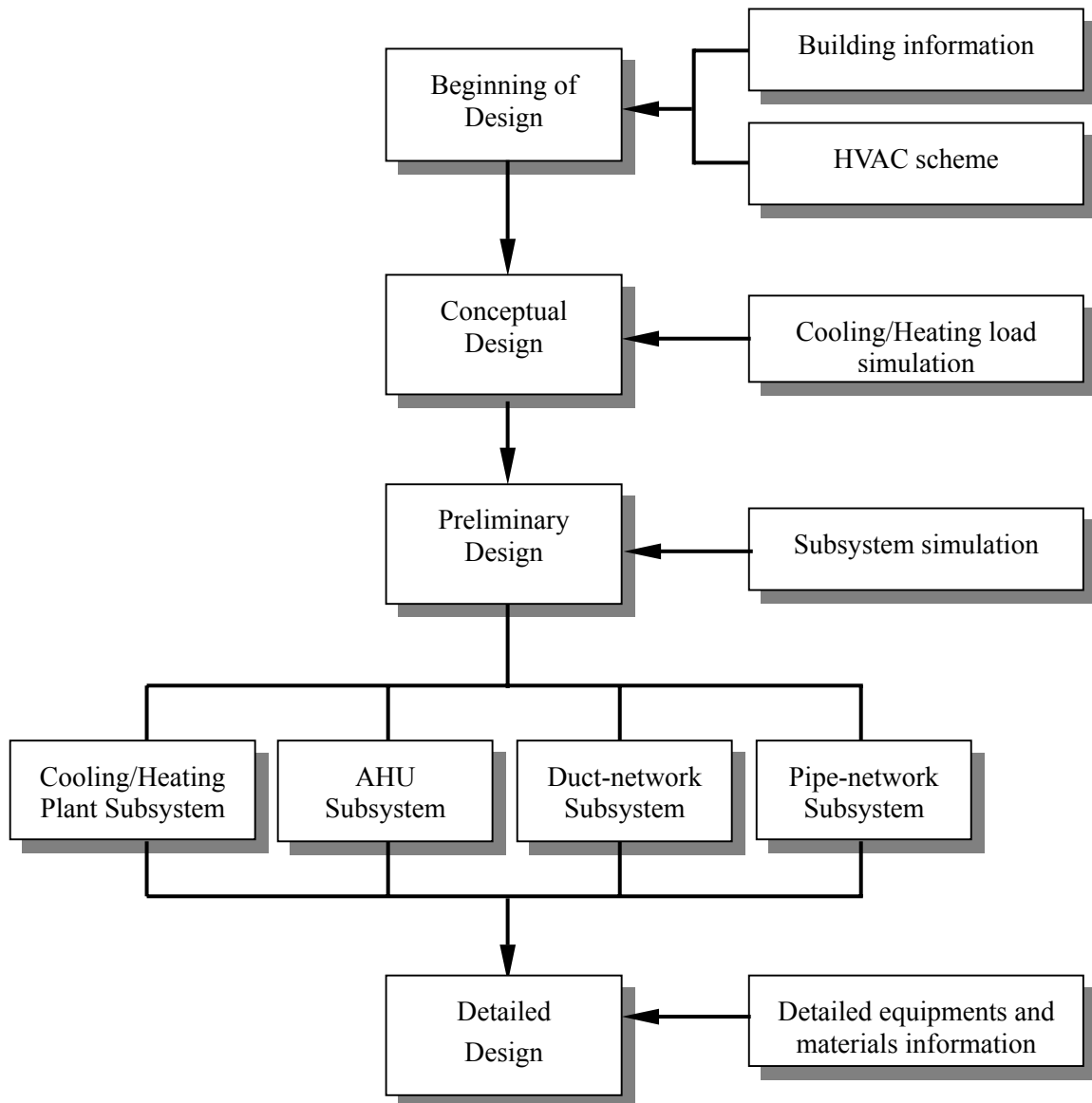


Figure 1.2 Concept of economic estimation stage-by-stage

1.2 METHODOLOGY

An HVAC system can be so complex that too many factors might influence its economic characteristics, for example, the building area, building use, building shape, envelope parameters, HVAC scheme, HVAC equipments price level, etc. Every different

factor influences the economic characteristics of the HVAC system differently, i.e., significantly, medially or little. In order to simplify the economic estimation to make the estimation possible to carry out, the sensitivity of economic estimations to changes in know information at each stage in the design process should be analyzed to check their influence power. The significant influence factors should be paid great attention to and the little influence factor should be ignored. Then evaluate economic estimation methods appropriate for each stage given the set of significant parameters available. The steps of estimating the economic characteristics of a HVAC system are as the following.

1) Determine all the possible factors that might influence the economic characteristics of a HVAC system as shown in Equation 1.1.

$$Cost = f(factor1, factor2, \dots) \quad (1.1)$$

2) Analyze the sensitivity of economic property to changes in know information to determine sensitive factors and ignore insensitive factors, as show in Equation 1.2.

$$Cost = f(sensitive\ factor1, sensitive\ factor2, \dots) \quad (1.2)$$

3) Determine the economic estimation methods appropriate for each stage using the set of sensitive factors. The initial investment and operation cost of HVAC systems can be obtained using these economic estimation methods. After the initial investment and operation cost is obtained, the Life Cycle Cost may be calculated to give a comprehensive evaluation as follows:

$$LCC = \sum_{y=0}^n \frac{CO_y}{(1 + in)^y} \quad (1.3)$$

Where y is the year during the life cycle of HVAC systems. So CO_0 is the initial investment cost and CO_y is the operational cost in the y^{th} year when y is larger than zero.

A building shown in Figure 1.3 is analyzed to study the economic sensitivity to changes in building area, building function, building envelope, area ratio of window to wall, shape coefficient (ratio of length to width), opening hours, outside air supply scheme, cooling and heating source scheme, and HVAC scheme. The initial investment and operation costs of the sample building's HVAC systems were analyzed in twenty-five

different scenarios by changing these parameters, as shown in Table 1.1.

Building uses are divided into three types according to indoor heat generation: hotels (including residential buildings), office buildings (including libraries and hospitals), and shopping centers (including restaurants, dancing halls, exhibition halls and gymnasiums).

Two kinds of window were analyzed: single-glazing aluminum alloy windows, and double-glazing aluminum alloy windows.

Two kinds of outside air supply scheme were analyzed: a constant outside air rate of 0.1, and a variable outside air rate of from 0.1 to 1.

Three kinds of regular scheme of HVAC secondary system were analyzed: FCU, CAV, and VAV.

Five kinds of regular cooling and heating source scheme were analyzed:

- 1) Compressor driven by electric power and gas fired hot water or steam boiler
- 2) Compressor driven by electric power and water boiler using electric power
- 3) LiBr absorber driven by vapor and gas fired boiler
- 4) Gas fired LiBr absorber and heater
- 5) Air source heating pump

The factors mentioned above are used as inputs to analyze the sensitivity of LCC responding to these factors at each design stage. Based on the sensitivity analysis, the necessary inputs required by each design stage can be determined.

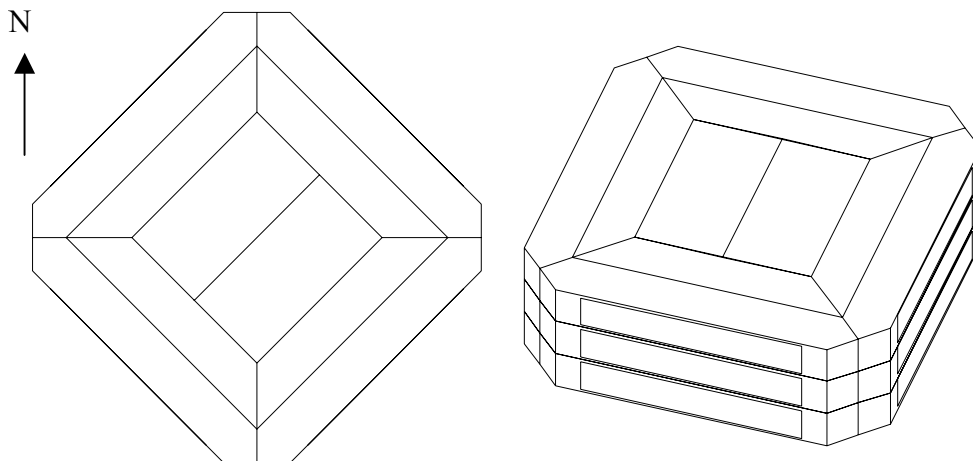


Figure 1.3 Sample Building for Sensitivity Analysis (plan and perspective)

Table 1.1 Calculation parameter of sensitivity analysis

No.	Building Area (m ²)	Area ratio of window to wall	Ratio of length to width	Building use	Window type	Opening hours	Outside air supply scheme	HVAC scheme	Cooling heating source
1	948.2	0.7	1	2	1	9	2	FCU	1
* 2	2844.6	0.7	1	2	1	9	2	FCU	1
3	5689.2	0.7	1	2	1	9	2	FCU	1
4	8533.8	0.7	1	2	1	9	2	FCU	1
5	2844.6	0.1	1	2	1	9	2	FCU	1
6	2844.6	0.5	1	2	1	9	2	FCU	1
7	2844.6	0.9	1	2	1	9	2	FCU	1
8	2844.6	0.7	2	2	1	9	2	FCU	1
9	2844.6	0.7	3	2	1	9	2	FCU	1
10	2844.6	0.7	4	2	1	9	2	FCU	1
11	2844.6	0.7	5	2	1	9	2	FCU	1
12	2844.6	0.7	1	1	1	9	2	FCU	1
13	2844.6	0.7	1	3	1	9	2	FCU	1
14	2844.6	0.7	1	2	2	9	2	FCU	1
15	2844.6	0.7	1	2	1	9	2	CAV	1
16	2844.6	0.7	1	2	1	9	2	VAV	1
17	2844.6	0.7	1	2	1	12	2	FCU	1
18	2844.6	0.7	1	2	1	16	2	FCU	1
19	2844.6	0.7	1	2	1	20	2	FCU	1
20	2844.6	0.7	1	2	1	24	2	FCU	1
21	2844.6	0.7	1	2	1	9	1	FCU	1
22	2844.6	0.7	1	2	1	9	2	FCU	2
23	2844.6	0.7	1	2	1	9	2	FCU	3
24	2844.6	0.7	1	2	1	9	2	FCU	4
25	2844.6	0.7	1	2	1	9	2	FCU	5

* Note: building #2 represents the standard configuration against which the relative value of other configurations is judged.

CHAPTER 2

LIFE CYCLE COST ESTIMATION USING NEURAL NETWORK AT BEGINNING OF DESIGN

2.1 INTRODUCTION

The Beginning of Design stage is the very start of a HVAC system design progress. At this stage, the known information is about the building, such as building area, building use, building envelope parameter and so on. Besides these parameters, the desired HVAC scheme and refrigeration scheme can also influence the economic characteristic. But to calculate the economic parameters in detail, such as initial investment and operation cost, the information available at this stage is far from adequacy. In order to calculate the economic parameters in detail, at least the size and amount of the HVAC equipments and materials need to be known. However, at the beginning of the design stage, this information cannot be obtained. So there is a conflict between the situation of knowing few information of HVAC system and the demand of detailed information to evaluate economic characteristics at the beginning of design stage.

For the purpose of solving this conflict, some economic estimation method is needed other than detailed calculation. The estimation method should be able to process multi-variable problem because at the beginning of the design stage there are many variables that might influence the economic characteristic, such as building area, building use, building envelope parameters, the HVAC scheme and refrigeration scheme. Neural network method can solve this kind of problem for its self-adaptive ability and convenient multi-variable input-output function.

Neural network is ‘a network of interacting simple units together with a rule to adjust the strength of the connections between these units in response to externally supplied data’

(Lisboa 1992). There are two steps to use a neural network:

1) Training phase, which is to determine the weight of the connection between two neurons by inputting the parameters of training samples and comparing the output given by the neural network and the samples' output and adjusting the weight according to a certain study algorithm.

2) Recall phase, which is to use the trained neural network to estimate the value of an unknown object corresponding to its input parameters.

As discussed in Chapter 1, it needs three steps, determine influence factors, sensitivity analysis, and develop economic estimation method, to complete the economic estimation of HVAC systems. The following parts will describe the analysis for these three steps.

2.2 INFLUENCE FACTORS

At the beginning of design, the known information is about building area, building use, envelope parameters and desired HVAC schemes. So at this stage, the following influence factors are selected, building area, building use, envelope characteristics (area rate of window to wall, window structure, etc.), building shape factor (rate of length to width), desired HVAC schemes. Table 2.1 shows the influences to the HVAC system Life Cycle Cost given by the known information.

Table 2.1 Known information for LCC estimation at beginning of design stage

Known Information	Influences to HVAC Systems
Building area	Determine the scale of HVAC systems
Building use	Determine interior heating/cooling load and equipments size
Envelope characteristics	Determine external heating/cooling load and equipments size
Building shape factor	Determine the layout of duct/pipe network
Heating/cooling source scheme	Determine the cost of primary system
HVAC secondary system scheme	Determine the cost of secondary system

The following equations show the influence factors selected for analyzing the sensitivity of Initial Investment Cost (IIC) and Operational Cost (OC).

$IIC = f(\text{Building area, Window type, Building use, Area rate of window to wall, Rate of length to width, HVAC secondary system scheme, Heat/Cooling source scheme})$

$OC = g(\text{Building area, Window type, Building use, Area rate of window to wall, Rate of length to width, Outdoor air supply scheme, Building opening hours, HVAC secondary system scheme, Heat/Cooling source scheme})$

2.3 SENSITIVITY ANALYSIS

Because there are too many variables that might influence the life cycle cost, sensitivity analysis needs to be conducted to determine the important variables and eliminate the variables that influence the life cycle cost very slightly. The example building shown in Figure 1.3 is used to study the sensitivity of the HVAC system's life cycle cost to the changes of the influence factors. Twenty-five scenarios of different influence factors shown in Table 1.1, are analyzed to check the sensitivity of life cycle cost to these changes.

2.3.1 SENSITIVITY ANALYSIS OF INITIAL INVESTMENT COST

The calculation results of the 25 scenarios show that initial investment cost changes in direct ratio according to the changes of the consecutive variables, i.e. building area, rate of window area to wall and rate of length to wall. Building area has prevailing influence on the HVAC system's initial investment cost. Ratios of window area to wall and length to width have the same relative impact on HVAC initial investment, but are much less significant than building area. Figure 2.1 shows the change of initial investment cost according to the change of three consecutive variables.

A change of building use can impact HVAC initial investment by as much as 40%. Different window types can vary HVAC initial investment cost by 8%. Since the influence of window types is relatively small compared to other factors, the influence of window type can be ignored. The choice of HVAC secondary system scheme can impact the initial investment by as much as 50%. A change in cooling and heating sources can change the initial investment by 30%.

Figure 2.2 represents the changes in HVAC initial investment relative to our standard

building configuration given a change in any one of the parameters mentioned above, other than building area.

From the analysis above we can determine that the sensitive factors of initial investment are building area, building use, rate of window to wall, rate of length to width, HVAC secondary system scheme, cooling and heating source scheme. The changes of window type cause little influences to the initial investment and can be ignored.

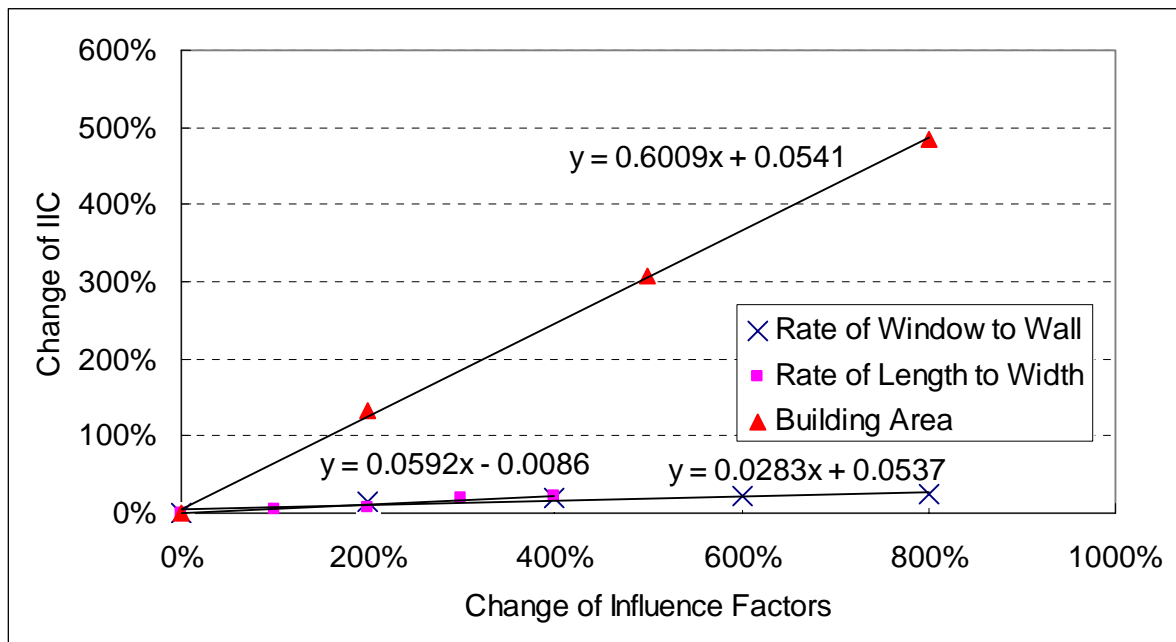


Figure 2.1 Change of initial investment cost caused by consecutive Variables

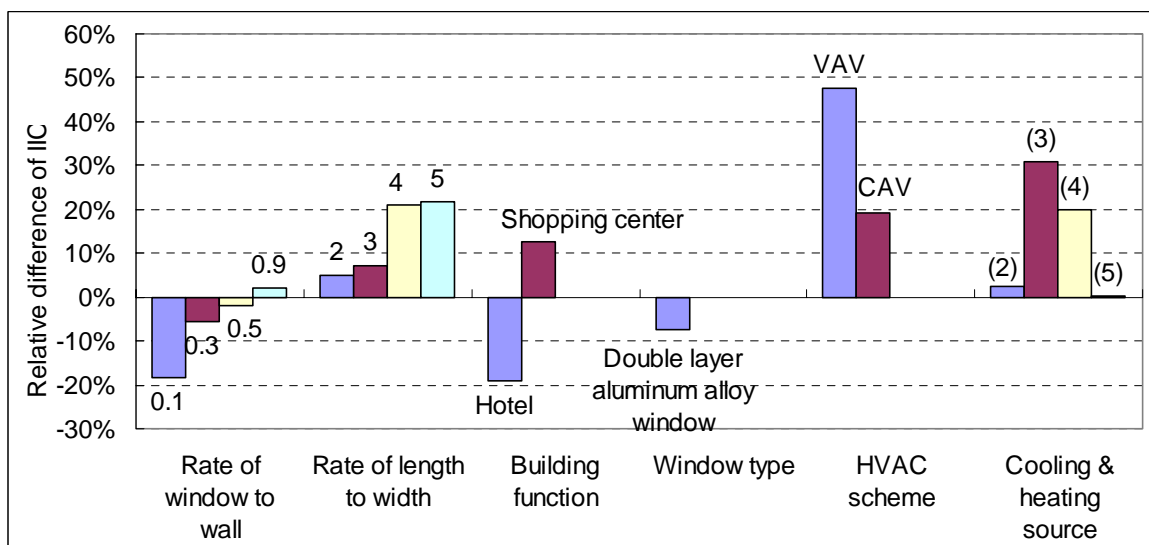


Figure 2.2 Change of initial investment cost caused by influence factors (The base line of this figure references the condition No. 2 in Table 1.1.)

2.3.2 SENSITIVITY ANALYSIS OF OPERATIONAL COST

Same as initial investment cost, The calculation results of the 25 scenarios show that the operational cost changes in direct ratio with the change of consecutive variables, i.e. building area, rate of window to wall, rate of length to width, and opening hours. Among the four factors, the building area and opening hours have same level influence and overwhelmingly influence the operational cost of the HVAC system. The rate of window area to wall and length to width can change the operation cost in same scale and much less than building area and opening hours. Figure 2.3 shows the operational cost change according to the changes of the four consecutive variables.

Building use can change the operation cost 2 to 3 times. Window type can change the operation cost 6%. The operation cost of constant outside air rate system is 30% higher than that of variable outside air rate. The HVAC secondary system scheme can change the operation cost change 50%~100%. Cooling and heating source scheme can change the operation cost 20%.

Figure 2.4 shows the HVAC systems operation cost change caused by changing the factors mentioned above except building area and opening hours that are prevailing, relative to the building in standard configuration.

This analysis illustrates that operation costs are significantly affected by building area, opening hours, building use, area rate of window to wall, rate of length to width, outside air supply scheme, HVAC secondary system scheme, and cooling and heating source schemes. A change of window type has little influences to operation costs and can be ignored.

2.4 COST ESTIMATION

At the beginning of design stage, it is necessary to consider eight factors as input variables to estimate HVAC system initial investment and operation costs, i.e. building area, building use, ratio of window area to wall, ratio of length to width, outside air supply scheme, opening hours, HVAC secondary system scheme, and cooling and heating source schemes. The large number of variables makes this a good application for neural networks. Neural networks are well suited to this kind of problem because they can easily process multi-variable input and output, and self-study functions can be used to adapt to the changes in parameters such as price. The following parts discuss how to use neural network for

estimating the cost of HVAC systems.

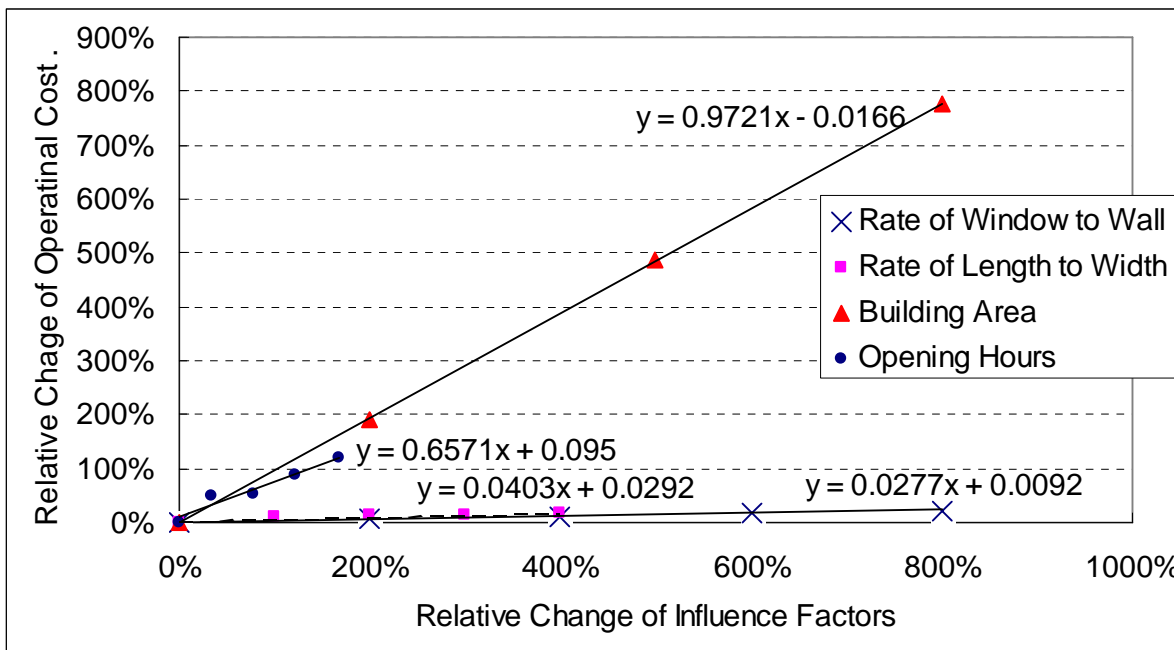


Figure 2.3 Change of operational cost caused by consecutive variables

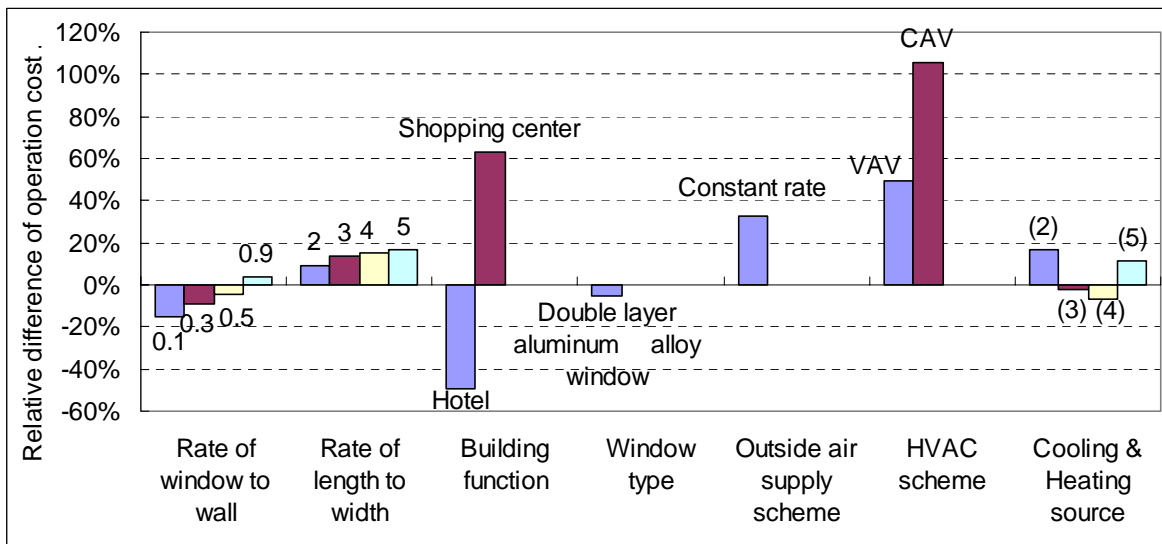


Figure 2.4 Change of operational cost caused by different factors
(The base line of this figure references the condition No. 2 in Table 1.1.)

2.4.1 SELECTION OF NEURAL NETWORK MODEL

There are near 60 different types of neural network models according to the structure and the algorithm used to define them (Cai, 1998). Among these neural network models, Adaptive Linear Element (ADLINE) is suitable for estimating economic values. One reason is that there are successful application examples. E. Shoneburg had successfully used ADLINE to predict the changing of several stocks (Hu, 1993). Another reason is that the initial investment and operation cost of HVAC systems have obviously linear relations with the building area and opening hours, which have the overwhelm influence to the economic values of HVAC systems according to the sensitivity analysis. The difference between ADLINE and linear regression method is that ADLINE uses iterative method to calculate the weight of every variable, which is convenient for calculating using computer. Furthermore, it is convenient to adjust weights when new samples are added to the sample set.

Figure 2.5 shows the structure of the ADLINE model.

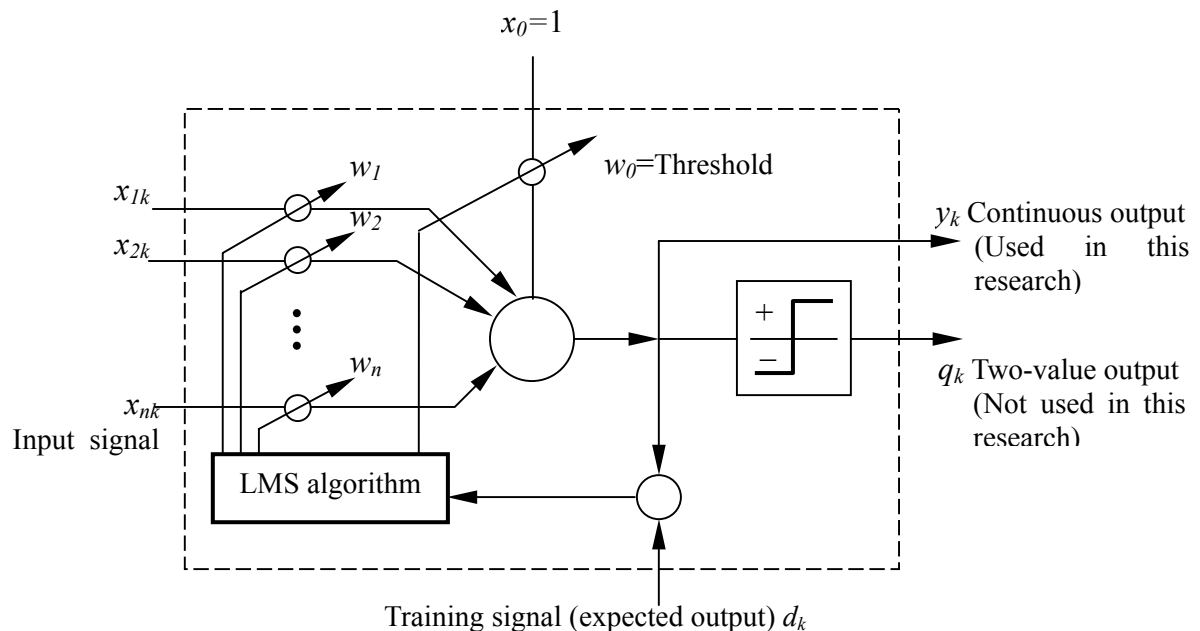


Figure 2.5 Structure of ADLINE model

The input vector is $(x_0, x_{1k}, x_{2k}, \dots, x_{nk})^T$ and weight vector is $(w_0, w_1, w_2, \dots, w_n)^T$. The continuous output is

$$Y_k = X_k^T W = W^T X_k \quad (2.1)$$

During training phase, the Least Mean Square (LMS) algorithm is used to adjust the weight to adapt the neural network to the characteristics of training samples. The error between neural network estimated value and expected value at step s is defined as follow.

$$E_k(s) = \frac{1}{2} [d_k - y_k(s)]^2 = \frac{1}{2} \varepsilon_k(s)^2 \quad (2.2)$$

The weight vector at time $t+1$ is

$$W(s+1) = W(s) - \psi \frac{\partial E_k(s)}{\partial W(s)} \quad (2.3)$$

$$\begin{aligned} \frac{\partial E_k(s)}{\partial W(s)} &= \frac{\partial}{\partial W(s)} \left\{ \frac{1}{2} [d_k - y_k(s)]^2 \right\} = \frac{\partial}{\partial W(s)} \left\{ \frac{1}{2} [d_k - W(s) \cdot X_k]^2 \right\} \\ &= -[d_k - y_k(s)] X_k = -\varepsilon_k(s) X_k \end{aligned} \quad (2.4)$$

Let $\psi = \frac{\alpha}{\|X_k\|_2^2}$, then

$$W(s+1) = W(s) + \frac{\alpha}{\|X_k\|_2^2} \varepsilon_k(s) X_k = W(s) + \frac{\alpha}{\sum_{i=0}^n |x_{ik}|^2} \varepsilon_k(s) X_k \quad (2.5)$$

Learning speed is controlled by α . When $0 < \alpha < 2$, the iterative computation is convergent (Cai, 1998).

When the total error of all training samples is less than the predetermined error threshold, the training processing is finished.

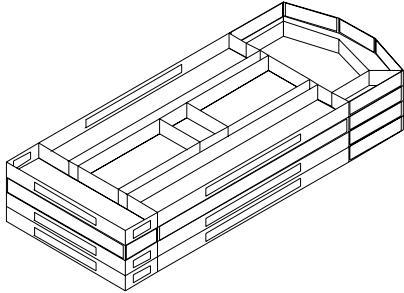
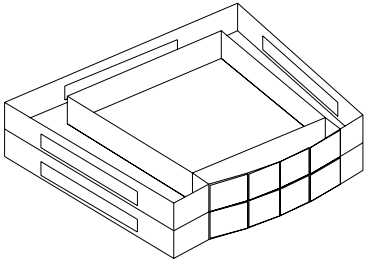
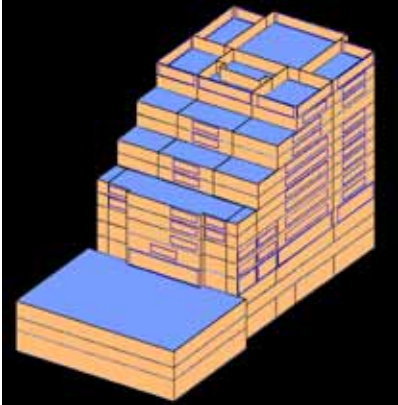
Because ADLINE is a linear model, the influence of nonlinear variables, such as building use, HVAC scheme, cooling and heating source scheme, can only be reflected through using amending coefficients, which can be determined according to the sensitivity

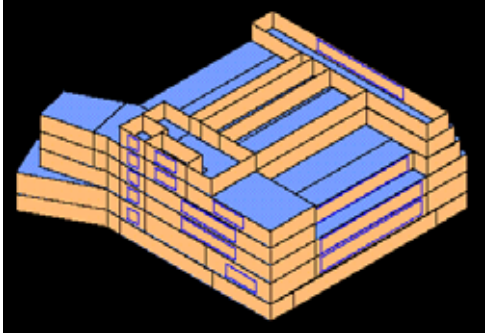
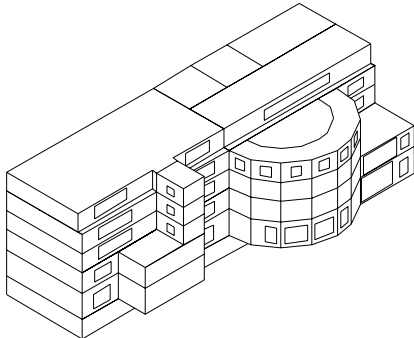
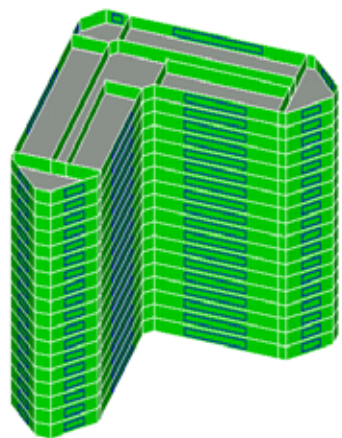
analysis. The consecutive variables are the input of the neural network model. Because the operation costs vary proportionally to the opening hours, operation cost can be calculated through multiplying the estimated operation cost per hour by opening hours.

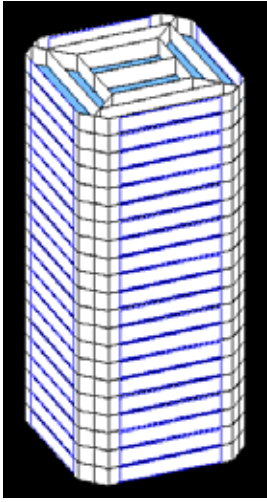
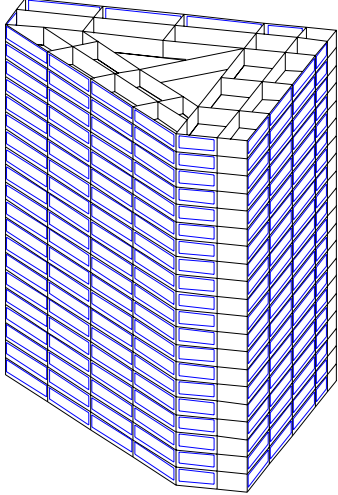
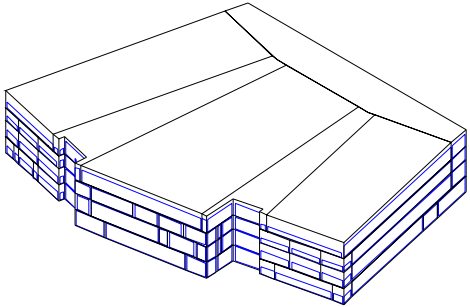
2.4.2 TRAINING OF NEURAL NETWORK MODEL

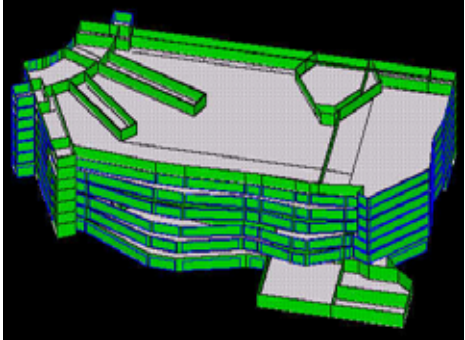
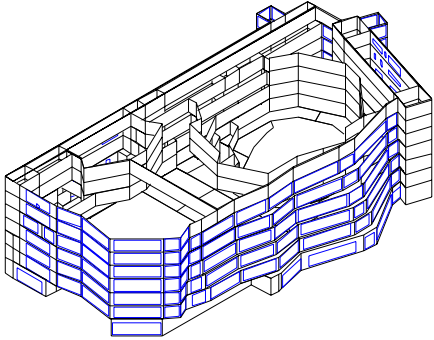
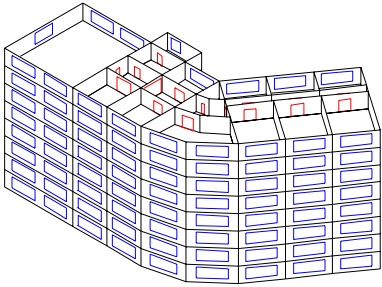
The first step in preparing a neural network to make economic estimations about HVAC systems is to train it using known data set from existing buildings. Once trained, the characteristics of the samples are stored in the neural network. When we input the parameters of a building to be predicted, the neural network will output estimated initial investment and operation costs according to the characteristics learned from the sample buildings. For this purpose, data from 21 different buildings were used as samples to train the neural network. First the initial investment and operation cost of these sample buildings were calculated in detail. DeST (Chen, 1999), simulation software developed by Tsinghua University, was used to simulate the whole year performance of an HVAC scheme. Through simulation we can obtain the size and quantity of HVAC equipments and materials used by a design scheme, which can in turn be used to calculate initial investment and operation cost. Table 2.2 lists the information of the 21 training sample buildings.

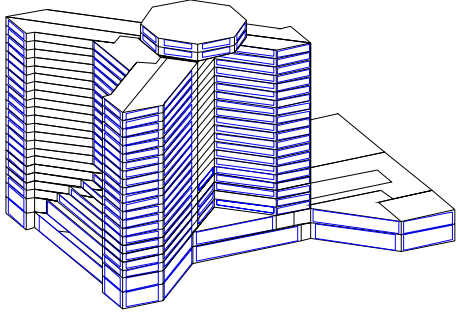
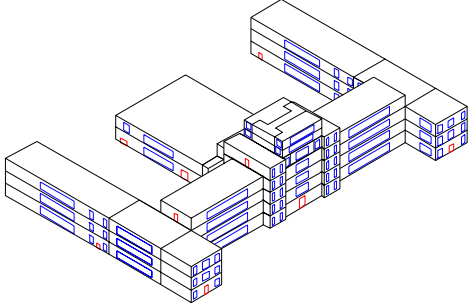
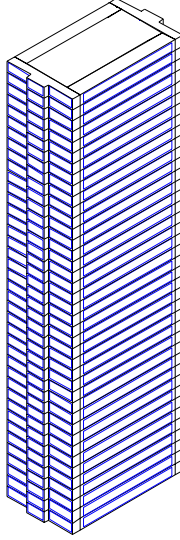
Table 2.2 Training sample buildings information

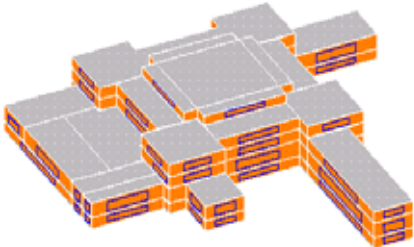
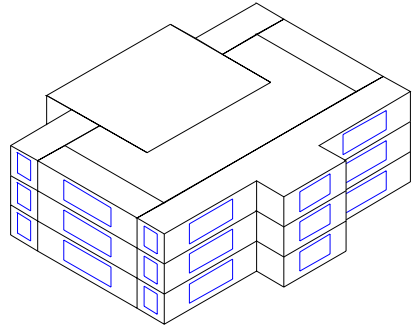
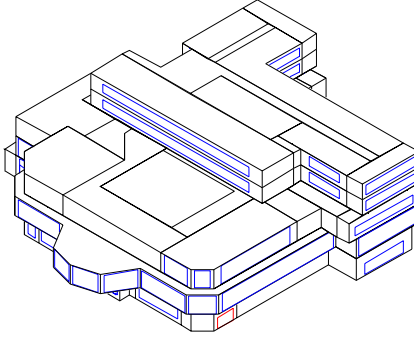
Name	Building Information		Building Model
Changqing Tower	Area (m ²)	10453.2	
	Use	Office	
	Rate of window to wall	0.55	
	Shape factor	2.31	
	Opening hours	10	
	Ratio of outside air	Constant	
	HVAC scheme	FCU	
	Heating/cooling source scheme	(1)	
	Initial investment cost (RMB)	4380477	
	Operational cost (RMB/yr)	480918	
Wuzhou Hotel	Area (m ²)	4140	
	Use	Office	
	Rate of window to wall	0.36	
	Shape factor	1.19	
	Opening hours	17	
	Ratio of outside air	Variable	
	HVAC scheme	CAV	
	Heating/cooling source scheme	(1)	
	Initial investment cost (RMB)	2428537	
	Operational cost (RMB/yr)	405525	
Cuiwei Tower	Area (m ²)	32088	
	Use	Office	
	Rate of window to wall	0.38	
	Shape factor	2.23	
	Opening hours	9	
	Ratio of outside air	Variable	
	HVAC scheme	FCU	
	Heating/cooling source scheme	(1)	
	Initial investment cost (RMB)	13385233	
	Operational cost (RMB/yr)	1018582	

Jinan-Jiaozhuan Library	Area (m ²)	16505	
	Use	Office	
	Rate of window to wall	0.20	
	Shape factor	1.11	
	Opening hours	14	
	Ratio of outside air	Variable	
	HVAC scheme	FCU	
	Heating/cooling source scheme	(1)	
	Initial investment cost (RMB)	5219282	
	Operational cost (RMB/yr)	617208	
Yikang Club	Area (m ²)	6503	
	Use	Office	
	Rate of window to wall	0.1	
	Shape factor	3.88	
	Opening hours	17	
	Ratio of outside air	Variable	
	HVAC scheme	CAV	
	Heating/cooling source scheme	(5)	
	Initial investment cost (RMB)	3288657	
	Operational cost (RMB/yr)	443459	
Landmark Hotel	Area (m ²)	25559	
	Use	Hotel	
	Rate of window to wall	0.22	
	Shape factor	4.8	
	Opening hours	24	
	Ratio of outside air	Variable	
	HVAC scheme	FCU	
	Heating/cooling source scheme	(3)	
	Initial investment cost (RMB)	11577872	
	Operational cost (RMB/yr)	1106737	

Landmark Tower	Area (m ²)	19913	
	Use	Office	
	Rate of window to wall	0.56	
	Shape factor	1	
	Opening hours	9	
	Ratio of outside air	Variable	
	HVAC scheme	FCU	
	Heating/cooling source scheme	(4)	
	Initial investment cost (RMB)	9964008	
	Operational cost (RMB/yr)	568998	
Fazhan Tower	Area (m ²)	37323	
	Use	Office	
	Rate of window to wall	0.54	
	Shape factor	1	
	Opening hours	10	
	Ratio of outside air	Variable	
	HVAC scheme	VAV	
	Heating/cooling source scheme	(1)	
	Initial investment cost (RMB)	21769455	
	Operational cost (RMB/yr)	1971079	
Shenyang Exhibition Center	Area (m ²)	36220	
	Use	Auditorium	
	Rate of window to wall	0.76	
	Shape factor	1.32	
	Opening hours	10	
	Ratio of outside air	Variable	
	HVAC scheme	CAV	
	Heating/cooling source scheme	(1)	
	Initial investment cost (RMB)	21131961	
	Operational cost (RMB/yr)	2081074	

Shenzhen Library	Area (m ²)	47056	
	Use	Office	
	Rate of window to wall	0.35	
	Shape factor	2.16	
	Opening hours	12	
	Ratio of outside air	Variable	
	HVAC scheme	CAV	
	Heating/cooling source scheme	(1)	
	Initial investment cost (RMB)	23533977	
	Operational cost (RMB/yr)	3975550	
Shenzhen Concert Hall	Area (m ²)	35815	
	Use	Auditorium	
	Rate of window to wall	0.32	
	Shape factor	2.15	
	Opening hours	13	
	Ratio of outside air	Variable	
	HVAC scheme	CAV	
	Heating/cooling source scheme	(1)	
	Initial investment cost (RMB)	17917645	
	Operational cost (RMB/yr)	3278403	
Yinji Tower	Area (m ²)	9968	
	Use	Office	
	Rate of window to wall	0.30	
	Shape factor	3.05	
	Opening hours	9	
	Ratio of outside air	Variable	
	HVAC scheme	FCU	
	Heating/cooling source scheme	(1)	
	Initial investment cost (RMB)	4183458	
	Operational cost (RMB/yr)	318957	

Great Wall hotel	Area (m ²)	87934	
	Use	Hotel	
	Rate of window to wall	0.49	
	Shape factor	2.42	
	Opening hours	24	
	Ratio of outside air	Variable	
	HVAC scheme	FCU	
	Heating/cooling source scheme	(3)	
	Initial investment cost (RMB)	39689270	
	Operational cost (RMB/yr)	3793292	
Military Museum	Area (m ²)	51486	
	Use	Auditorium	
	Rate of window to wall	0.26	
	Shape factor	18.92	
	Opening hours	13	
	Ratio of outside air	Variable	
	HVAC scheme	CAV	
	Heating/cooling source scheme	(1)	
	Initial investment cost (RMB)	30200890	
	Operational cost (RMB/yr)	3861003	
Qihuo Tower	Area (m ²)	46380	
	Use	Office	
	Rate of window to wall	0.64	
	Shape factor	1.67	
	Opening hours	13	
	Ratio of outside air	Variable	
	HVAC scheme	VAV	
	Heating/cooling source scheme	(1)	
	Initial investment cost (RMB)	27056110	
	Operational cost (RMB/yr)	3184031	

Tsinghua University Library	Area (m ²)	17884	
	Use	Office	
	Rate of window to wall	0.24	
	Shape factor	1.43	
	Opening hours	13	
	Ratio of outside air	Variable	
	HVAC scheme	FCU	
	Heating/cooling source scheme	(1)	
	Initial investment cost (RMB)	7462310	
	Operational cost (RMB/yr)	819579	
Tianjin Customs Tower	Area (m ²)	2738	
	Use	Office	
	Rate of window to wall	0.28	
	Shape factor	1.6	
	Opening hours	9	
	Ratio of outside air	Variable	
	HVAC scheme	FCU	
	Heating/cooling source scheme	(2)	
	Initial investment cost (RMB)	1158706	
	Operational cost (RMB/yr)	105909	
Tianqiao Hotel	Area (m ²)	12103	
	Use	Office	
	Rate of window to wall	0.40	
	Shape factor	2.18	
	Opening hours	24	
	Ratio of outside air	Variable	
	HVAC scheme	FCU	
	Heating/cooling source scheme	(1)	
	Initial investment cost (RMB)	4224815	
	Operational cost (RMB/yr)	540413	

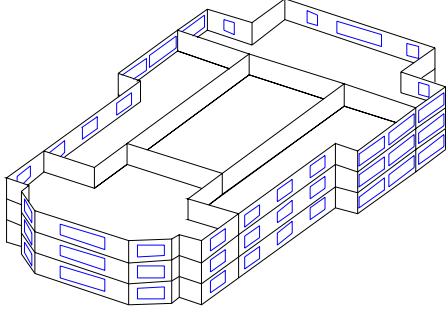
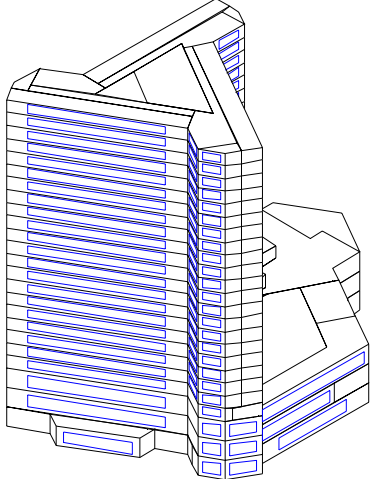
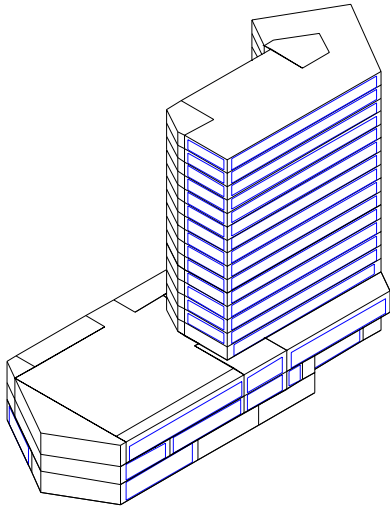
Tongchan Tower	Area (m ²)	8031	
	Use	Office	
	Rate of window to wall	0.26	
	Shape factor	2.12	
	Opening hours	9	
	Ratio of outside air	Variable	
	HVAC scheme	FCU	
	Heating/cooling source scheme	(1)	
	Initial investment cost (RMB)	3367330	
	Operational cost (RMB/yr)	256658	
Newcentury Hotel	Area (m ²)	41136	
	Use	Hotel	
	Rate of window to wall	0.39	
	Shape factor	1.13	
	Opening hours	24	
	Ratio of outside air	Variable	
	HVAC scheme	FCU	
	Heating/cooling source scheme	(1)	
	Initial investment cost (RMB)	14286924	
	Operational cost (RMB/yr)	1829521	
Newcentury Tower	Area (m ²)	26624	
	Use	Office	
	Rate of window to wall	0.58	
	Shape factor	2.07	
	Opening hours	14	
	Ratio of outside air	Variable	
	HVAC scheme	FCU	
	Heating/cooling source scheme	(1)	
	Initial investment cost (RMB)	8612849	
	Operational cost (RMB/yr)	1018425	

Figure 2.6 shows the changing of relative error accompanying the iterative times during the LMS iterative calculation. The iterative speed control factor $\alpha = 0.5$.

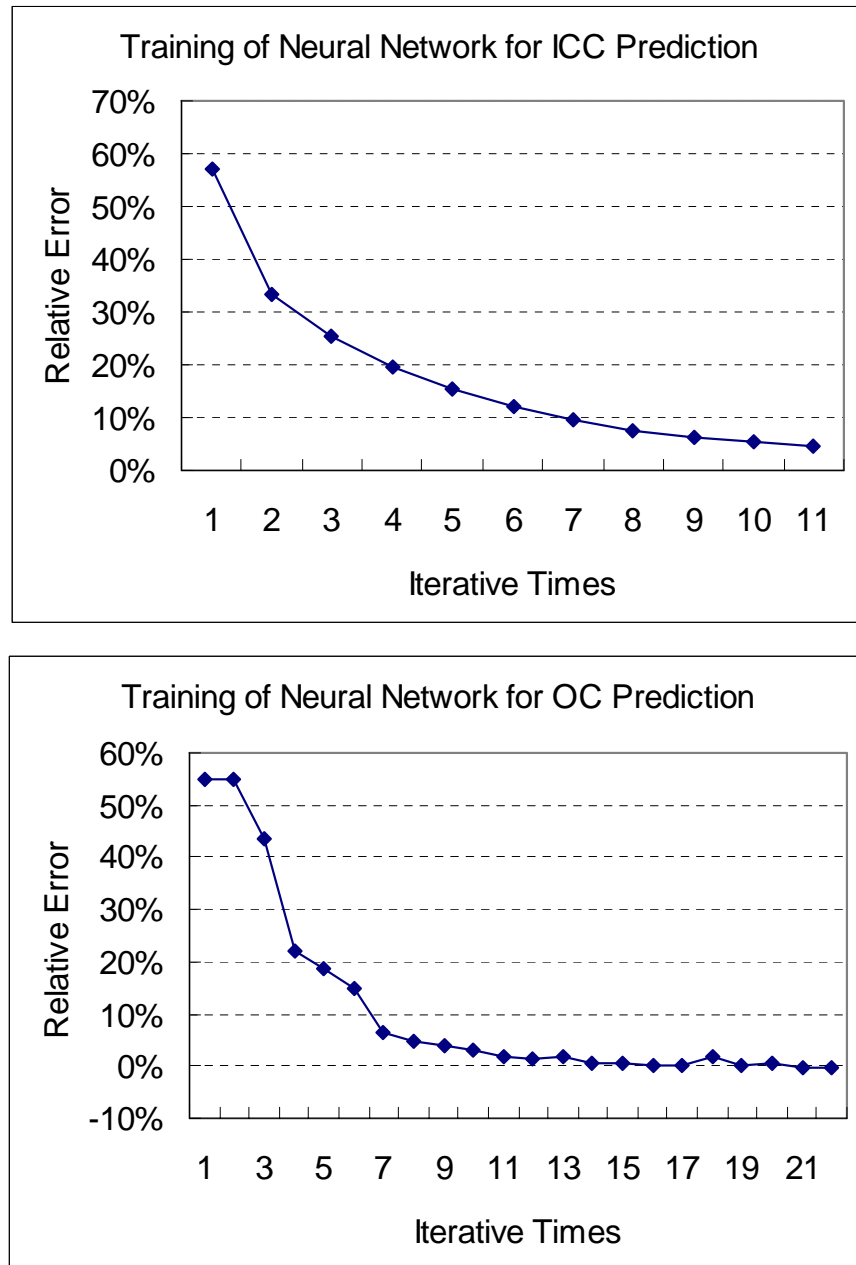


Figure 2.6 Training process of neural network

2.4.3 ESTIMATION USING NEURAL NETWORK MODEL

After the neural network training is finished, the characteristics of the samples are stored in the neural network. When we input the parameters of the building to be estimated,

the neural network will output the HVAC systems' initial investment and operation cost as the estimation result according to the characteristics stored in it. The estimation accuracy of the trained ADLINE model is checked through comparing the estimated cost and real cost of 5 buildings, which are beyond the training sample set. The information of the five buildings is list in Table 2.3. Figure 2.7 shows the difference between the initial investment and operation cost calculated in detail and estimated using the neural network. The maximum difference is 6%, which is accurate enough for the decision-making at the beginning of design stage.

The biggest predominance of estimation using neural network is the self-adaptive function, which makes it possible to adapt to the change of some factor such as price.

Because the training of neural network is to adjust the weight between the nodes according to the input samples, the trained neural network reflects the mean character of the samples. If the difference among the samples is too large, the training process cannot converge to relatively high accuracy. Then more detailed input variables are needed to obtain high accuracy of training.

Table 2.3 Buildings for ADLINE model validation

Building Number	1	2	3	4	5
Area (m ²)	2844.6	5689.2	8533.8	2844.6	2844.6
Use	Office	Office	Office	Hotel	Shopping center
Rate of window to wall	0.7	0.7	0.7	0.7	0.7
Shape factor	1	1	1	1	1
Opening hours	9	9	9	24	9
Ration of outside air	Variable	Variable	Variable	Variable	Variable
HVAC scheme	FCU	FCU	FCU	FCU	CAV
Heating/cooling source scheme	(4)	(4)	(4)	(4)	(1)
Initial investment cost (RMB)	1312910	2399144	3448996	959626	1554894
Operational cost (RMB/yr)	81581	181266	271886	151075	214149

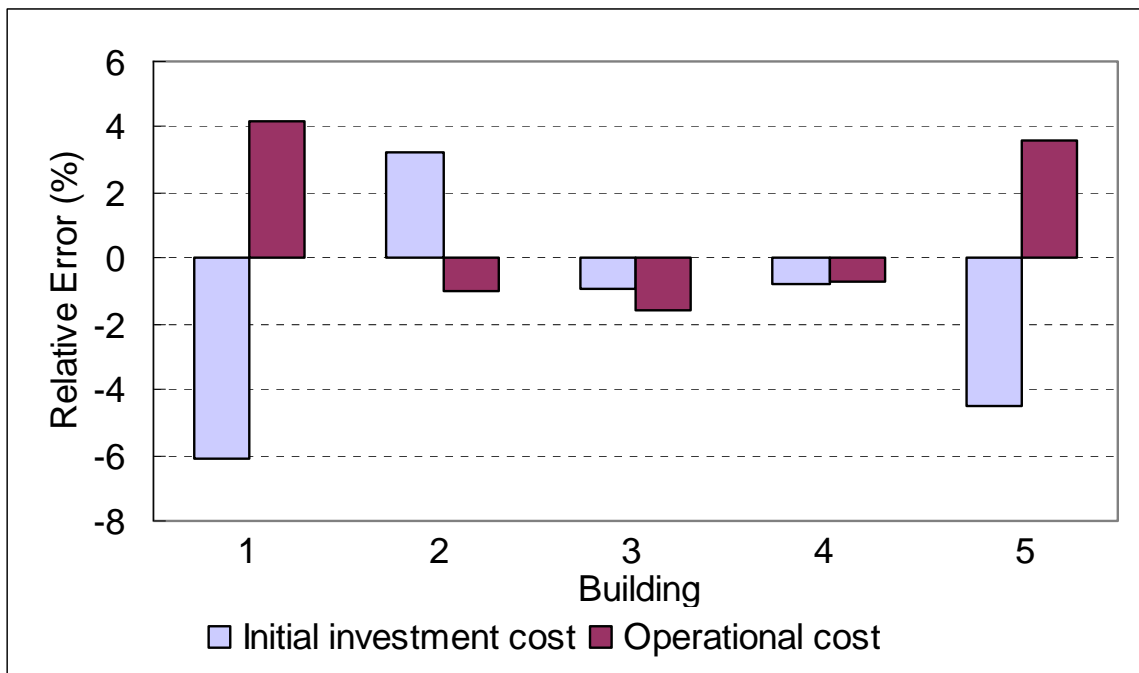


Figure 2.7 Comparison of estimated and real IIC and OC

2.5 SUMMARY

For the purpose of make good decision of HVAC design scheme, it is important to evaluate the economic performance of several valid HVAC schemes at the beginning of the design stage. Neural network method is suitable to estimate the economic parameters at the beginning of the design stage for the lack of detailed information of HVAC equipments and materials. Because there are many factors that might influence the economic characteristics of a HVAC system, sensitivity analysis is carried out to determine large influence factors and ignore minor influence factors. Then how to use neural network method to estimate the economic parameters at the beginning of design is discussed using the large influence factors as input. The ADLINE neural network method is used for the estimation and can successfully estimate the economic characteristics of HVAC systems at the beginning of the design stage. The maximum difference between ADLINE estimation results and the values calculated in detail is 6%, which is accurate enough for the decision-making at the beginning of design stage.

CHAPTER 3

LIFE CYCLE COST ESTIMATION FOR THE OTHER THREE DESIGN STAGES

3.1 INTRODUCTION

This dissertation divides the design progress into four stages. Previous chapter discusses the life cycle cost estimation for the first stage, beginning of design. This chapter analyzes the life cycle cost estimation for the other three stages, i.e. conceptual design, preliminary design and detailed design. Same as the beginning of design stage, influence factors analysis, sensitivity analysis and economic estimation method analysis are carried out for these three stages.

The method of the life cycle cost estimation for the three stages in common is that empirical equations are used to estimate the economic characteristics of a HVAC system. The empirical equations are obtained from the sensitivity analysis or statistically summarizing typical HVAC projects.

3.2 CONCEPTUAL DESIGN STAGE

3.2.1 INFLUENCE FACTORS

At the conceptual design stage, different indoor environment control schemes are simulated to obtain the hourly indoor air temperature, supply air temperature, supply air volume and the heating and cooling load of terminal equipment. At this stage, we can obtain more useful information to calculate the economic parameters of HVAC systems than that was available in the previous stage, as shown in Table 3.1. At this stage the influences of building area, building use and building envelope are reflected by heating/cooling load and supply air volume, which can more accurately describe the characteristics of a HVAC

system and permit to calculate the initial investment and operational cost more accurately than that at the beginning of design stage.

Table 3.1 Known information for LCC estimation at conceptual design stage

Known Information	Influences to HVAC Systems
Total Heating/cooling load	Determine size of heating/cooling source equipments
Supply air volume	Determine size of terminal equipments and duct/pipe
Zoning information	Determine AHU size and number
HVAC secondary system scheme (CAV, VAV, or FCU)	Determine cost of terminal systems

The following equations show the influence factors selected for analyzing the sensitivity of initial investment cost and operational cost.

$IIC = f$ (Total heating/cooling load, Total supply air volume, Scheme of HVAC secondary system, Scheme of heating and cooling source)

$OC = g$ (Total heating/cooling load, Total supply air volume, Scheme of outside air supply, Opening hours, Scheme of HVAC secondary system, Scheme of heating and cooling source)

3.2.2 SENSITIVITY ANALYSIS

3.2.2.1 Sensitivity analysis of initial investment cost

Through sensitivity analysis of initial investment we may conclude the following:

1) Total cooling load and total supply air volume exert similar influence on the initial investment costs of HVAC systems, as shown in Figure 3.1. The reason for this is that there is a fixed transfer relationship between total cooling load and total supply air volume. From cooling load, supply air volume can be calculated, and vice versa. So total cooling load and total supply air volume therefore are not both independent variables. Only one of them is independent. Thus, we need only select one of them as an input variable to estimate the economic parameters of HVAC systems.

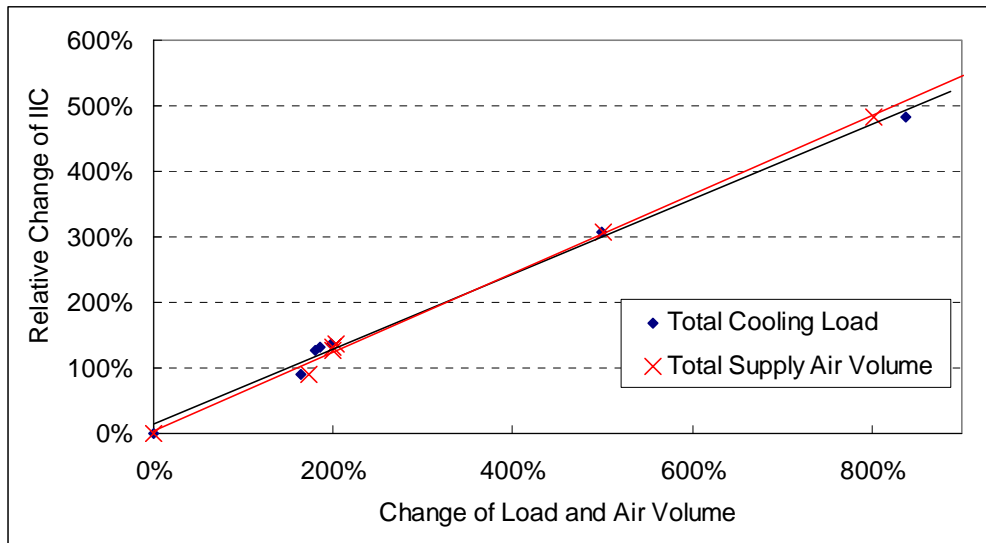


Figure 3.1 Initial investment cost changes caused by load and air volume

2) The initial investment cost rate of different HVAC schemes can be expressed as follows:

$$\text{FCU} : \text{VAV} : \text{CAV} = 1 : 1.4 : 1.2 \quad (3.1)$$

3) The following are initial investment cost rate associated with the different heating and cooling source schemes, which are defined earlier in Chapter 1.

$$(1) : (2) : (3) : (4) : (5) = 1 : 1 : 1.3 : 1.2 : 1 \quad (3.2)$$

Through sensitivity analysis of initial investment for the conceptual design stage we may identify the sensitive elements of initial investment at this stage as being: HVAC system scheme, heating and cooling source scheme, and either total cooling load or total supply air volume.

3.2.2.2 Sensitivity analysis of operational cost

From sensitivity analysis of operational cost at this stage, we may conclude the following:

1) Same as initial investment cost, total cooling load and total supply air volume exert similar influence on the operational costs of HVAC systems, as shown in Figure 3.2. The reason for this is that there is a fixed transfer relationship between total cooling load and total supply air volume. Only one of total cooling load and total supply air volume are

independent variable. Thus, we may select only one of them as an input variable to estimate the operational cost of HVAC systems.

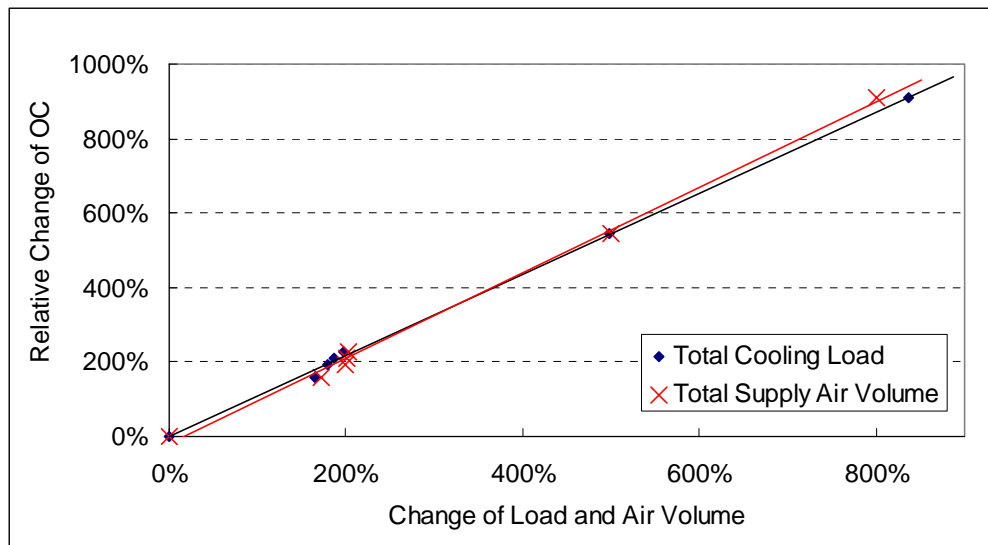


Figure 3.2 Operational cost changes caused by load and air volume

2) The operational cost rate of different HVAC schemes can be expressed as follows:

$$\text{FCU} : \text{VAV} : \text{CAV} = 1 : 1.5 : 2.0 \quad (3.3)$$

3) The following are operation cost rates for the different heating and cooling source schemes described earlier in chapter 1.

$$(1) : (2) : (3) : (4) : (5) = 1 : 1.2 : 1 : 0.9 : 1.1 \quad (3.4)$$

4) The annual operation cost of a constant minimum outside air rate is 30% higher than that of a variable outside air rate. So using low temperature outdoor air to cool indoor environments can significantly reduce operation costs. The following are operation cost rates for Constant Minimum Outside Air Rate (CMOAR) and Variable Outside Air Rate (VOAR):

$$\text{VOAR} : \text{CMOAR} = 1 : 1.3 \quad (3.5)$$

4) The operational cost of HVAC systems increases by a ratio of 1:1 with the increase of opening hours.

Through sensitivity analysis of operational costs for the conceptual design stage we

may identify the sensitive elements of initial investment at this stage as being: HVAC system scheme, heating and cooling source scheme, scheme of outside air supply, opening hours, and either total cooling load or total supply air volume.

3.2.3 COST ESTIMATION

3.2.3.1 Estimation of initial investment cost

According to the sensitivity analysis we can derive the following equation to estimate the initial investment of HVAC systems:

$$IIC = C_a C_s (4892CL + 472202) \quad (3.6)$$

The influence coefficient of HVAC secondary system scheme C_a is an impact factor caused by HVAC scheme, for FCU system, $C_a=1$, for VAV system, $C_a=1.4$, and for CAV system, $C_a=1.2$.

The influence of heating and cooling source scheme is amended by coefficient C_s . The value of the five schemes mentioned in chapter 1 is as following: for scheme (1), $C_s=1$, for scheme (2), $C_s=1$, for scheme (3), $C_s=1.3$, for scheme (4), $C_s=1.2$, and for scheme (5), $C_s=1$.

3.2.3.2 Estimation of operational cost

According to the sensitivity analysis we can derive the following equation to estimate the operation cost of HVAC systems.

$$OC = 44C_a C_s C_o CLhr \quad (3.7)$$

The influence coefficients of HVAC scheme for operational cost C_a are as follows: for FCU, $C_a=1$, for VAV, $C_a=1.5$, for CAV, $C_a=2.0$.

The influence coefficients of heating and cooling source scheme C_s are as following: for scheme (1), $C_s=1$, for scheme (2), $C_s=1.2$, for scheme (3), $C_s=1$, for scheme (4), $C_s=0.9$, and for scheme (5), $C_s=1.1$.

The influence coefficients of outside air supply scheme C_o are as follows: for VOAR, $C_s=1$, and for CMOAR, $C_s=1.3$.

Figure 3.3 shows the real initial investment and operation cost compared with the

values that are estimated using the method mentioned above. The difference between the real value and the estimated value is less than 8%.



Figure 3.3 IIC and OC estimation results at conceptual design stage

3.3 PRELIMINARY DESIGN STAGE

At the preliminary design stage, main subsystems of a HVAC system needs to be analyzed to check its performance. The simulation results can give more detailed information about the HVAC system than that of the former two stages. Therefore the economic estimation can be more accurate than the former two stages. In general an HVAC project can be divided into four main subsystems: terminal subsystems, heating and cooling source, duct networks and pipe networks. This dissertation analyzes economic estimation of terminal systems and heating and cooling sources. The economic estimation for duct networks and pipe networks is not studied in this dissertation because of the lack of time.

3.3.1 COST ESTIMATION OF TERMINAL SYSTEMS

3.3.1.1 Initial investment cost

a) All air systems

Air handling units (AHU) are the main part of an all air system. Terminal system simulations make it possible to calculate required air volume and cooling load, from which it is possible to determine the size and number of AHU required. Terminal system initial

investment costs may be calculated given the number and size of AHUs.

b) Air-water systems

Fan coil units (FCU) are the main part of an air water system. A similar process to that just described makes it possible to calculate initial investment costs for FCU terminal systems.

c) Ducts and isolation materials

Based on statistics gathered from typical duct layouts, we can express the relationship between the surface area of ducts and the supply air volume, as follows:

$$A=0.02V \tag{3.8}$$

With respect to the outside air ducts of air-water systems, we can estimate the surface area of ducts using the supply air volume as follows, based on statistics gathered from typical air duct layouts:

$$A=0.05V \tag{3.9}$$

Given the total surface area of ducts we can calculate the investment cost of ducts.

Given the total surface area of ducts and the thickness of thermal isolation material we can calculation the investment cost of thermal isolation material.

d) Air outlets and other accessories

Because at the preliminary design stage the detailed size and quantity of air outlets and other accessories are not yet known, it is necessary to estimate their size and quantity by extrapolation from existing HVAC systems. As a general rule of thumb, we can estimate that there will be two 300 mm * 300 mm air diffusers for inlet and outlet per 1000 m³/h supply air volume. With water systems we can assume roughly two 1000 mm * 200 mm louvers for air inlet and outlet per FCU.

Generally there is a muffler and a damper at the supply air outlet and the return air inlet of an AHU respectively. The size of the muffler and the damper can be estimated according to the supply air volume and the air flow velocity recommended by standard design

handbooks.

e) Pipes and thermal isolation materials

All-air systems have so few pipes that it is safe at this stage in the design process to ignore the cost of pipes in economic forecasts for all-air systems.

Air-water terminal systems on the other hand do use significant amounts of pipe. The amounts of pipe may be estimated at this stage by referring data summarized from similar existing HVAC systems, as presented in Table 3.2.

The first line of Table 3.2 is the building area charged by the air-water system whose pipe amount is to be estimated. The column under a building area is the amount of pipe required for the air-water system given different pipe diameters. The amount of the pipe thermal isolation material can be calculated given to the pipe diameter and length, and the thermal isolation material thickness.

The initial investment cost for pipes and thermal isolation material can be calculated given their type and the amount obtained above.

Table 3.2 Estimation of pipe amount (m)

Building Area (m ²) \ Diameter (mm)	50	100	150	300	600	650	900	2000	2750	4750	12500
20	0.3 * Building Area	Same as Left	Same as Left	Same as Left	Same as Left	Same as Left	Same as Left	Same as Left	Same as Left	Same as Left	Same as Left
25	-	25	25	25	25	25	25	25	25	25	25
32	-	-	12	12	12	12	12	12	12	12	12
40	-	-	-	45	45	45	45	45	45	45	45
50	-	-	-	-	45	45	45	45	45	45	45
70	-	-	-	-	-	60	60	60	60	60	60
80	-	-	-	-	-	-	60	60	60	60	60
100	-	-	-	-	-	-	-	110	110	110	110
125	-	-	-	-	-	-	-	-	140	140	140
150	-	-	-	-	-	-	-	-	-	400	400
200	-	-	-	-	-	-	-	-	-	-	770

3.3.1.2 Operational cost

a) Operation cost of AHU

During the preliminary design stage the hourly pressure drop of ducts is unknown, yet operation cost of an AHU fans still need to be estimated.

With respect to CAV systems, we can estimate the required power rating of a fan according to the supply air volume, fan pressure head (generally 700 ~ 1000 Pa) and the fan efficiency (generally 60% ~ 80%). The operation cost can be calculated using the operational hours, rated power of the fan and electric fee.

$$OC = \sum_{ts} EC_r EP_{ts} \quad (3.10)$$

With respect to VAV systems, because the power consumed hourly by a fan is in direct ratio to the supply air volume raised with a power tree, we can estimate power consumption of a fan according to the following equation:

$$OC = \sum_{ts} \left(\frac{V_{ts}}{V_r} \right)^3 EC_r EP_{ts} \quad (3.11)$$

b) Operation cost of FCU

Generally the fan of a FCU never stops during opening hours. So we can multiply the power rating, the opening hours and electric fee to calculate operation cost using equation 3.10.

3.3.2 COST ESTIMATION OF HEATING/COOLING SOURCE SYSTEMS

3.3.2.1 Initial investment cost

a) Initial investment of chillers and cooling towers

After cooling plant simulation we can obtain the size and number of chillers and cooling towers. Given the size and number of chillers and cooling towers, we can calculate the initial investment.

b) Initial investment of chilled water pumps

With respect to one-grade pump water systems, the water mass flow rate can be obtained according to the chill amount produced by chillers and temperature difference between supply and return chilled water. In general the pump pressure head is 30 ~ 40 meters, from which can determine the pump size. The number of pumps generally is equal to the number of chillers plus one spare pump.

With respect to two-grade pump water systems, the primary pumps' water mass flow rate can be obtained using the method mentioned above. The primary pump pressure head generally is 15 meters. The number of primary pumps equals the number of chillers plus one spare pump. The size and number of secondary pumps should be determined according to the division and operation schedule of the terminal systems. At this design stage however, this information is unknown, so we can use the same size and number as primary pumps to estimate their economic parameters.

c) Initial investment of cooling water pumps

The water volume flow rate of cooling water pumps may be calculated using the following equation.

$$V = \frac{Q_c (1 + COP)}{1.16 \Delta T \cdot COP} \quad (3.12)$$

Where 1.16 is used to convert the unit of Q_c from kW to kkal/h for the purpose of making the unit of volume flow rate be m³/h.

The cooling water pump pressure head generally is 30 meters and the number of the cooling water pumps is the number of the chillers plus one spare pump.

d) Initial investment in water pipe materials

The size and amount of water pipe materials need to be estimated because at this design stage the layout of pipe in the cooling plant has not been designed. The amount of the water pipe can be estimated using the following equation, which is obtained empirically from the statistics of common projects.

$$LE = 80A_{cp} + 100 \quad (3.13)$$

Where 80 and 100 are coefficients fitted through statistically analyzing the data of real

HVAC projects.

The diameter of the general water pipe can be derived from the total cooling load, as follows:

$$3600 \frac{\pi D^2}{4} v = \frac{Q_c}{1.16 \Delta T} \quad (3.14)$$

$$D = \sqrt{\frac{4Q_c}{1.16 \times 3600 \pi \Delta T v}} = \sqrt{\frac{1.098 Q_c}{3600 \Delta T v}} \quad (3.15)$$

With respect to the water flow rate v , according to the design handbook (Qian 1990) 1.5 ~ 2 m/s can be used to estimate the pipe diameter.

Temperature difference between supply and return chilled water generally is 5°C.

e) Initial investment cost for boilers

We can determine the number and size of boilers according to the total heating load.

f) Initial investment cost for heating water pumps

The water mass flow rate of pumps can be obtained according to the heating load and temperature difference of supply and return water. The number of pumps is equal to the number of boilers plus one spare pump. The pump pressure head generally is 15 to 20 meters.

g) Initial investment cost for water treatment equipment

We can derive the size of water treatment equipment from the total cooling and chilled water mass flow rate. Generally there is one water treatment unit in the cooling water system and chilled water system respectively.

3.3.2.2 Operational cost

a) Operation cost of chillers

Cooling plant simulation allows us to obtain the hourly energy consumption of chillers, from which we can calculate their operation cost.

b) Operation cost of boilers

The operation cost of boilers can be calculated through summing up the hourly fuel cost and electric power cost, as follows:

$$OC = \sum_{ts} \left(\frac{Q_{h,ts}}{H\eta} PF + EC_r EP_{ts} \right) \quad (3.16)$$

c) Operation cost of chilled water pumps

It is possible to approximate operation costs for constant rotation speed pumps given their power rating and running hours. With respect to variable rotation speed pumps, because the chilled water mass flow rate is in direct ratio to the cooling load, it is necessary to use the following equation to estimate hourly power consumption:

$$EC_{ts} = \left(\frac{Q_{c,ts}}{Q_{c,r}} \right)^3 EC_r \quad (3.17)$$

d) Operation cost of cooling water pumps and cooling towers

Cooling water pumps and cooling towers generally run at constant rotation speed, so we can derive an estimate of their operation cost from power rating and running hours.

3.4 DETAILED DESIGN STAGE

The detailed design stage is the period after performance simulations have been completed for the AHU, heating and cooling source, duct networks and pipe networks. At this stage the size and quantity of every equipment and material can be known and hourly performance of the AHUs, chillers, boilers, fans and pumps can be obtained. So a detailed calculation of the initial investment and operation cost can be carried out.

3.4.1 INITIAL INVESTMENT COST

Detailed calculation of initial investment of HVAC systems may be performed as follows:

$$IIC = \sum_n (\text{Price of HVAC equipment } n \times \text{Amount of equipment } n) + \text{Installing and commissioning fee} + \text{Tax} + \text{Other management fee} \quad (3.18)$$

3.4.2 OPERATIONAL COST

At detailed design stage the operational cost can be calculated in detail as follows:

$$OC = \sum_n \sum_{ts} E_{n,ts} PE_{n,ts} \quad (3.19)$$

3.5 SUMMARY

This chapter analyzes the methods of economic estimation of HVAC systems at conceptual design, preliminary design and detailed design stages. These economic estimation methods make use of what is known at each stage in the design process, and offer rules for estimating unknown parameters in order to facilitate calculation of initial investment and operational cost at every step along the way. At conceptual design phase, the heating and cooling load obtained from simulating the possible HVAC schemes are used to estimate the initial and operational cost. At preliminary design phase, because the performance of main HVAC subsystems is simulated, the HVAC design becomes more detailed and more information can be used to estimate initial and operational cost more accurately. At the last design phase, detailed design stage, detailed HVAC equipments capacity and quantity can be known and detailed initial and operational cost calculation method is discussed. This method of successive cost estimation is intended to give the engineer a more reliable means of designing cost effective HVAC systems.

PART II

This part of research was done during doctoral course in Kyoto University, Kyoto, Japan.

ON-GOING COMMISSIONING AT OPERATIONAL PHASE

CHAPTER 4

ON-GOING COMMISSIONING METHODOLOGY FOR OPERATIONAL PHASE

4.1 INTRODUCTION

In the former chapters, how to select an energy efficient HVAC scheme at design stage is discussed. The following chapters will analyze how to ensure a HVAC system performs as design intents and to keep energy efficiency and high performance during operational phase.

Commissioning is considered as a effective method of ensuring building HVAC system performance, reducing energy use, and improve indoor air quality and comfort level (Bonneville Power Administration, 1992). During operational phase, commissioning a HVAC system continuously to ensure high performance is named On-going commissioning or continuous commissioning. The following chapters of this dissertation focus on studying the methodology of on-going commissioning for HVAC systems at operational phase.

4.2 INTRODUCTION TO COMMISSIONING

4.2.1 DEFINITION OF COMMISSIONING

According to Merriam-Webster Collegiate Dictionary, commissioning is to put a facility to be “ready for active service, in use or in condition for use”. Therefore the meaning of building commissioning is to make a building ready for active service or in condition for use. For this purpose, several organizations give detailed definition of building commissioning.

The Bonneville Power Administration (1992) gives building commissioning a detailed definition as “ In the broadest sense, a process for achieving, verifying, and documenting

that the performance of a building and its various systems meet design intent and the owner and occupants' operational needs. The process ideally extends through all phase of a project, from concept to occupancy and operation. In a narrower sense, the act of statically and dynamically testing the operation of equipment and building systems to ensure they operate as designed and can satisfactorily meet the needs of the building throughout the entire range of operating conditions.”

American Society of Heating, Refrigeration, and Air conditioning Engineers (ASHRAE, 1996) defines commissioning as “the process of ensuring that systems are designed, installed, functionally tested, and capable of being operated and maintained to perform in conformity with the design intent.”

The Society of Heating, Air-Conditioning and Sanitary Engineers of Japan (SHASE) takes a broader view of commissioning by acknowledging the impact of building operation on the global environment and by specifically recommending that commissioning be performed throughout the life of the building from production (design and construction) to demolition. The objective of commissioning, as outlined by the SHASE guideline, can be summarized as follows: “The objective of commissioning is to diagnose and verify system performance in order to optimize the operation of building service systems by minimizing global environmental impacts and energy waste, while improving indoor environmental conditions and facility usage. Furthermore, when appropriate, commissioning should lead to proposals regarding measures for improving building performance. To accomplish the commissioning objective, it is recommended that buildings be commissioned throughout their life. This process is referred to as life-cycle commissioning.” (Annex 40, 2001)

Building commissioning extends through all phase of a project. So the building commissioning can be divided into two categories, new constructed buildings commissioning and existing building commissioning. Building commissioning begins with the program phase and continues across design phase, construction phase, acceptance phase and post-acceptance phase (ASHRAE 1996). Post-acceptance phase commissioning includes commissioning continuously during whole life cycle of a building, which is named on-going commissioning, the commissioning of building systems that are changed or retrofitted during operation phase, which is named retro-commissioning, and perform commissioning procedure again for a building system, which is named re-commissioning.

4.2.2 HISTORICAL DEVELOPMENT OF COMMISSIONING

Building commissioning is a nascent industry that has begun to be considered as a business opportunity in the last decade (Haasl, 2001). Prior to 1990s, commissioning was a component of building construction typically done to correct problems that originated earlier in the building process. However, after 1990s the meaning of commissioning was gradually extended. Commissioning is increasingly recognized as a cost-effective method of ensuring building performance, reducing energy use, and improve indoor air quality and comfort level. Many indicators show that commissioning industry is about to enter a period of expansion, for example, large architectural and engineering firms are entering the commissioning market, commissioning is causing the attention of more and more people, the number of commissioning researchers is increasing steadily (Haasl, 2001).

The origination of this situation can be cast back to the Middle East War crisis of 1973-1974. The oil embargo by a number of Arab producers made the main industrial countries became painfully aware of their vulnerability to the new economic power of the oil producing countries (Scott, 1994). The urgent need for oil security management and energy policy co-operation led to the creation of the International Energy Agency (IEA) in 1974. One of the main objectives of IEA is to promote rational energy policies in a global context. Approximately one third of primary energy supply is consumed in buildings. Despite a substantial improvement in the thermal performance of buildings, much energy is still inefficiently used. Therefore IEA established an implementing agreement on Energy Conservation in Buildings and Community Systems (ECBCS) in 1976 aiming at initiating research and providing an international focus for building energy efficiency. The primary rationale for ECBCS is to undertake a series of research projects so-called “Annexes” (ECBCS homepage). Since then, a lot of building energy efficiency measures and technologies have been studied and put forward, for example, Energy Conservation in Residential Buildings (Annex 3), Building Energy Management Systems (Annex 16, User Interfaces and System Integration; Annex 17, Evaluation and Emulation Techniques), Real Time HEVAC Simulation and Fault Detection and Diagnosis (Annex 25).

However, some analyses on the data from the buildings participating in the energy conservation program revealed that many of the installed energy efficiency measures were not performing as expected (Bonneville Power Administration, 1992). In order to address this issue, the Bonneville Power Administration held a meeting in October 1989, where the

idea of a commissioning pilot project was conceived. From then on, the awareness is growing that commissioning is a viable method to help ensure buildings and their Efficiency Conservation Measures (ECMs). In 1992, Bonneville Power Administration published a guideline for building commissioning. ASHRAE brought forward its guideline for commissioning in 1996. The first National Conference on Building Commissioning of USA was held in Sacramento in 1993, which is developed out of a 1992 Commissioning Round-table meeting sponsored by Bonneville Power Administration. This conference developed the definition of commissioning and established the goal of making commissioning “business as usual” (Benner, 1997). In April 2001, a new research project sponsored by ECBCS was launched and named Annex 40, Commissioning of Building HVAC Systems for Improving Energy Performance. The objective of Annex 40 is to develop, validate and document tools for commissioning buildings and building services that will help to facilitate the achievement of this goal (Annex 40 homepage). Research on building commissioning enters the period of flourish.

From the history and development of building commissioning, two reasons can be brought out for the rapid expansion of commissioning. The first is the necessity of developing commissioning technology to improve the energy efficiency under the pressure of energy crisis. The second is the attraction of business opportunity. The energy use intensity of office buildings in USA varies by over 400% and the potential energy saving of existing buildings average approximately 30% (Haasl, 2001). From energy cost alone, the simple payback of commissioning existing buildings is 1.8 years and of commissioning new construction is 9.9 years (Haasl, 2001). These two reasons make commissioning rapidly expand and attract great attention.

4.2.3 CURRENT RESEARCH ON BUILDING COMMISSIONING

Current research on building commissioning mainly consists of the following six aspects:

- 1) Building commissioning guideline: Building Commissioning Guidelines (Bonneville Power Administration, 1992), ASHRAE Guideline 1-1996 (ASHRAE, 1996), Commissioning Resource: Procedural Guidelines, Specifications, and Functional Test (Portland Energy Conservation Incorporated homepage), Building Commissioning Guide (U. S. Department of Energy, 1998), General Commissioning Procedure for DDC Systems

(Pacific Gas and Electric, 2001), etc.

2) Study on commissioning market: Haasl (2001), Tseng (1993), Yoshida (2001), etc.

3) Commissioning process and procedure: Choat (1993), DuBose (1993), Uncerwood (1993), etc.

4) Commissioning a design: English (2001), Stum (2001), etc.

5) Commissioning tools: Bearg (1999), Brambley (2002), Friedman (2001), Haves (1991, 1996), Smith (2002), Tseng (1994), etc.

6) Commissioning case study: Angle (1998), Cuevas (2003), Ellis (1996), Lawson (1993), Liu (2001), Naughton (1992), Richardson (1994), Wilkinson (2001), Nakahara (2003), etc.

7) Fault Detection and Diagnosis (FDD): As the method to detect and diagnose faults, FDD has been paid a large amount of research work to. ECBCS launched a research project named Annex 25, Real Time Simulation of HVAC Systems for Building Optimization, Fault Detection and Diagnostics.

This doctoral research participates in the Annex 40 Subtask D, Using of Model in Commissioning. The main objective of this subtask is to evaluate the feasibility of using computer simulation based on models, to verify the operational performance of the whole building, subsystems and components (Annex 40, 2001). Accordingly this dissertation aims at developing automated on-going commissioning method. Firstly this dissertation discusses the methodology for automated on-going commissioning. Then the past and current efforts to use simulation models are reviewed and checked whether they are suitable for commissioning or not. If a component or system model is checked not suitable for commissioning, new model suitable for commissioning should be developed. This doctoral research develops a total energy consumption model for fan subsystem and a filter resistance estimation model that are suitable for on-going commissioning.

4.3 ON-GOING COMMISSIONING METHODOLOGY

This research proposes a concept of on-going commissioning methodology that is comparison of the real-time operational data with no-fault operation, which is named

No-Fault Operation Comparison (NFOC). The no-fault operation can be obtained from either simulation or past no-fault operational data records. Accordingly NFOC consists of two aspects of approach. The first aspect is simulation analysis. This approach achieves on-going commissioning through continuously comparing the HVAC systems real-time operational data with the simulated data, which are calculated using the design conditions and models suitable for on-going commissioning. This simulated operation can be considered as no-fault operation. Real-time operational data can be obtained from Building Energy Management System (BEMS). If the differences between the real operational data and the simulated data do not exceed the predetermined threshold, a conclusion can be drawn that there is no fault in the HVAC system. Otherwise, if the difference is larger than the predetermined threshold, there might be some faults that are influencing the operation of the HVAC system. This approach suits for the air or water processing components or subsystems, such as fan subsystems, valves, VAV boxes, and coils etc., whose processing results or outputs can be both simulated and measured.

The second aspect of this methodology is no-fault operation records comparison. This approach is to continuously compare the real-time data during operational phase with the no-fault operation data records that are under the almost same heat conditions as current operation. This approach uses the same comparison method as simulation approach to detect faults. This approach suits for commissioning components whose simulation models are not applicable for commissioning, such as temperature sensors, air flow rate sensors etc. These components' simulation models are not suitable for commissioning because these models use real measured value as input to simulate the sensor output, for example HVACSIM+ temperature sensor model, type 7, simulates the sensor output signal (e.g. sensed temperature) given a temperature input. If the real measured value can be obtained, a sensor's output can be verified using real measured value instead of simulated value.

When comparing real-time operational data with no-fault data, it is important to determine a proper threshold for judging whether real operation is faulty or not. The threshold can be determined according to model validation accuracy or statistical analysis of the distribution of no-fault operational data. An empirical threshold of 20% is recommended by this research. Of course the threshold should be adjusted according to the characteristics of different components or systems.

When faults are detected in an HVAC system, the next step of on-going commissioning is to diagnose faults to find causes. The first is to determine fault diagnose methodology. Then use the operation symptoms and faults diagnostics methodology to find the causes for the faults.

Based on this methodology the on-going commissioning sequence consists of two steps, continuously monitoring and continuous Fault Detection and Diagnosis (FDD). During continuously monitoring, operational data are collected every one-minute and compared with the data simulated simultaneously or the data searched from past no-fault operational database. If real-time operational data do not match the simulated or records data, then diagnosis is activated to find causes for the difference. Figure 4.1 shows the main concept of this on-going commissioning methodology.

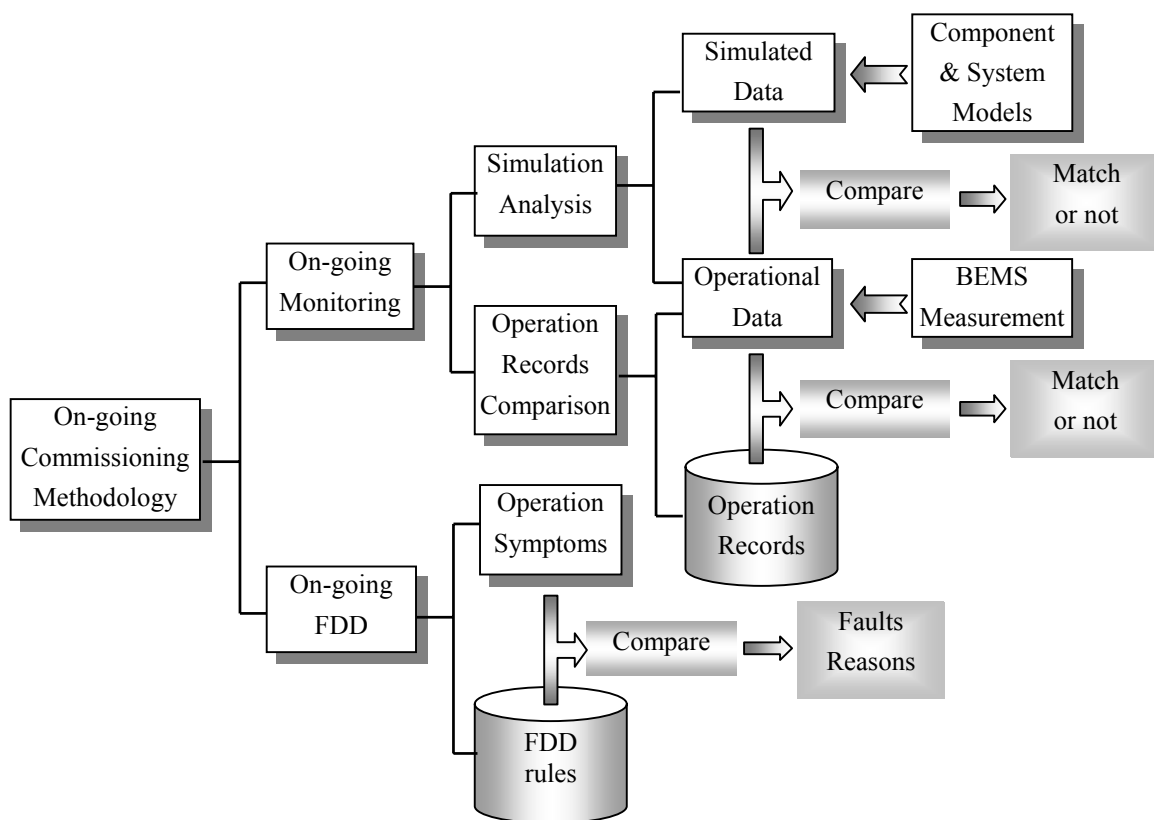


Figure 4.1 Concept of on-going commissioning methodology

This methodology can be used for developing an automated commissioning tool. The key components of an automated commissioning tool should include a set of models suitable for commissioning, a set of test sequences, and software to implement the test

sequences and to analyze data to give commissioning recommendation (Haves, 2002). The following parts of this chapter describe the models of several main HVAC components or subsystems suitable for commissioning and how to use these models and simulation to commission these components or subsystems. Then how to use operational records for continuously commissioning is analyzed. Based on this methodology, on-going commissioning tool can be developed, either stand-alone or be embedded in BEMS to continuously monitor the running of a building's HVAC systems and detect faults during operational phase.

4.3.1 SIMULATION COMPARISON APPROACH

Simulation analysis suits for commissioning the air or water processing components or subsystems, such as fan subsystems, valves, VAV boxes, and coils etc., whose processing results or outputs can be both simulated and measured. In order to use simulation for on-going commissioning, the first thing is to determine components and system models that are suitable for on-going commissioning. This research checked the models used in current popular simulation software, such as HVACSIM+ and SIMBAD, to find whether these models are suitable for on-going commissioning or not. If a model's inputs are easily available during operation phase and the models' outputs are useful for checking the performance of the HVAC system or components, this model can be considered suitable for on-going commissioning. The models suitable for on-going commissioning are used in this chapter to demonstrate the simulation comparison approach. Otherwise, new models suitable for on-going commissioning were developed. This dissertation studies how to continuously commission a VAV air conditioning system. The main components of a VAV system are fan subsystem, coil, water valve and VAV box. Modeling and commissioning a fan subsystem will be discussed in detail in next chapter. This section analyzed how to use simulation to commission coils, water valves and dampers, and VAV boxes.

4.3.1.1 Coil

The possible problem for coils during operation phase is that coils' tubes are fouling and fins are dirty. The symptoms caused by these faults are that the transferred heat amount is smaller than the normal coil and the outlet air and water temperature deviate from that of normal coils. In the case of a BEMS does not measure air and water flow rate, these data can be obtained from duct and pipe system simulation. If a BEMS measures the air flow rate,

supply, return and outdoor air temperature and humidity, water flow rate, and inlet and outlet water temperature, the on-going commissioning of a coil can be achieved through continuously comparing the simulated outlet air and water temperature with simulated value. Both HVACSIM+ and SIMBAD coil model are suitable for fulfilling this purpose.

Matsuoka (2002) studied the commissioning method for coils. So this dissertation does not discuss commissioning of coils in detail.

4.3.1.2 Valve and damper

On-going commissioning method of valve and damper are similar. The possible faults for valves and dampers are that they are stuck or positions driven by an actuator cannot match the desired positions. The symptoms of these faults are that the air or water flow rate cannot match the demand value. If a BEMS records the real opening of valves and dampers, on-going commissioning can be achieved through continuously comparing the real opening of valves and dampers with the ideal opening simulated using the valve and damper control algorithm. If a BEMS does not record the real positions of valves and dampers but record the water or air flow rate, we can compare the real air or water flow rate with the simulated value.

First of all, it is necessary to find a model suitable for on-going commissioning. For this purpose, the valve model used by HVACSIM+ (Clark, 1985) is shown in the following equations.

$$P_i = P_o + \text{sign}(m)C_v m^2 \quad (4.1)$$

$$C_v = \frac{W_f C_{v0}}{(O_v (1 - \lambda) + \lambda)^2} + (1 - W_f) C_{v0} \lambda^{(2O_v - 2)} \quad (4.2)$$

The 2-way valve model used by SIMBAD is shown in the following figure (CTSB, 2001).

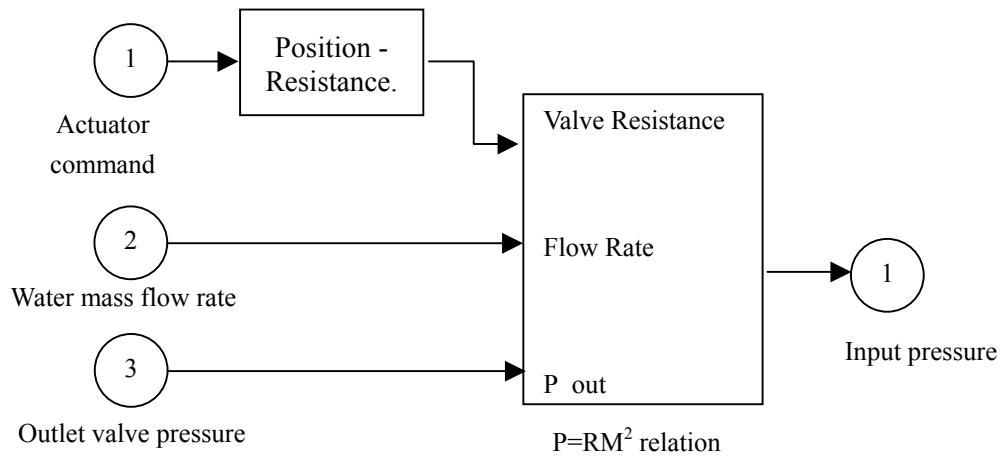


Figure 4.2 Valve model in SIMBAD

This model uses valve opening command, water mass flow rate and the water pressure at the outlet of valve to calculate the water pressure at the inlet of the valve. The model equations are shown as follows.

$$P_i = P_o + \text{sign}(m)C_v m^2 \quad (4.3)$$

$$C_v = \begin{cases} \frac{a}{I_v^2 (O_v (1 - \lambda) + \lambda)^2} & \text{(Linear characteristic valve)} \\ \frac{a}{I_v^2 ((1 - O_v)(1 - \lambda) + \lambda)^2} & \text{(Exponential characteristic valve)} \end{cases} \quad (4.4)$$

Where $a=1296$, which is the parameter used for simulating valve performance.

From the 2-way valve models described above, we can find that the both valve models in SIMBAD and HVACSIM+ are used for the calculation of the valve resistance at different opening. These models can be used for verify whether a valve is fouling or not by comparing the real measured pressure difference between the inlet and outlet of the valve with the pressure difference simulated using these models given the water flow rate and inlet or outlet pressure.

However, very few HVAC systems are being installed the water mass flow rate meter for an adjusting valve. So it is difficult to obtain the water mass flow rate used in the valve model. The main purpose of these two models is to simulate the performance of a valve,

which makes them not suitable for on-going commissioning. Furthermore, the fault that most often occurs is not the fouling of a valve because generally a water filter is designed and installed before the adjustable valve. The faults most often occur to a valve are that the valve is being stuck or the actuator is offsetting so that the real valve opening cannot match the demand opening.

Based on the two aspects of reason mentioned above, a new method is proposed to continuously commission a valve during operational phase, which is to continuously commission a valve's performance by comparing the real valve positions with the demand position if valve positions can be obtained from BEMS or simulated using the valve position control algorithm.

This dissertation studied a case of commissioning a stuck valve. The demand valve position was simulated using the valve Proportional Integral (PI) control algorithm, which is described in the following equations.

$$O = \begin{cases} 0 & (0 < PI) \\ \frac{15}{2} PI & (0 \leq PI \leq 2) \\ \frac{9PI - 270}{28} + 24 & (2 < PI \leq 30) \\ \frac{76}{70} PI - \frac{60}{7} & (30 < PI \leq 100) \\ 100 & (PI > 100) \end{cases} \quad (4.5)$$

$$PI = PO + I \quad (4.6)$$

$$PO = KZ \quad (4.7)$$

$$I = \frac{K}{t} \int_0^t G d\tau \quad (4.8)$$

$$K = \frac{100}{L} \quad (4.9)$$

$$Z = T - T_s \quad (4.10)$$

$$G = \begin{cases} L & (Z \geq L + g) \\ Z - g & (g < Z \leq L + g) \\ 0 & (0 \leq Z \leq g) \\ Z & (-(L - g) \leq Z < 0) \\ -L & (Z < -(L - g)) \end{cases} \quad (4.11)$$

$$L = (L_0 + a) - \frac{(L_0 + a) - (L_1 + b)}{100} INV \quad (4.12)$$

$$g = g_o + g_e \quad (4.13)$$

$$t = t_o + t_e \quad (4.14)$$

Equation 4.5 shows the output of the demand valve position given a PI valve. The coefficients value, such as 15, 2, 9, 270, et al, in Equation 4.5 shows different output rule at different range of PI values. Figure 4.3 shows the output demand valve positions versus PI valves.

Equations 4.6 to 4.14 are used to calculate the PI value according to the difference between AHU supply air temperature real-time value and set point.

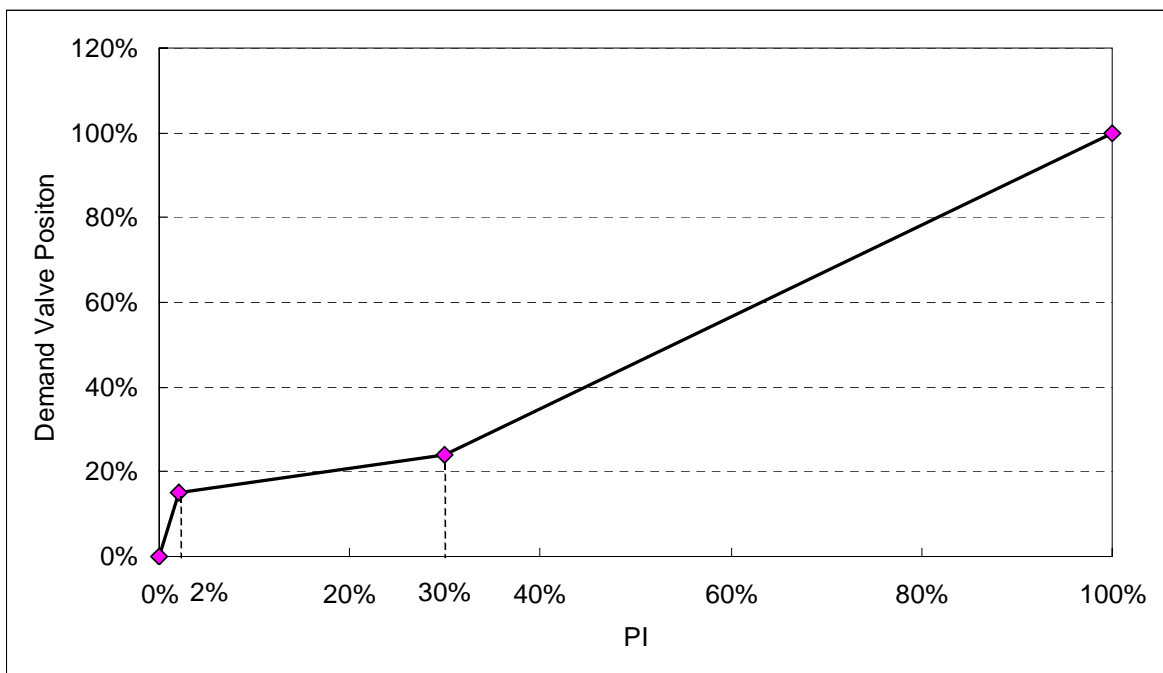


Figure 4.3 Demand valve position vs. PI

This valve control model was used to simulate the demand valve opening. The simulated valve positions were compared with real valve positions. In order to check whether this model can successfully detect faults of stuck valve or not, the valve real positions were set at 30% fixed, 70% fixed, 100% fixed and no fault of fixing.

Simulink was used to simulate the output of this valve control model, as shown in Figure 4.4. The parameters used by this valve model are shown in Table 4.1. The simulation and comparison results are shown in Figure 4.5. From this figure, we can find that when the valve had the fault of being fixed, the real valve positions were obviously different to the simulated positions, which were the desired positions to fulfill the air conditioning requirement. In the period of no faults existing, the real valve positions matched the simulated position well. Therefore if a valve's real positions can be obtained during operational phase, it is easy to achieve on-going commissioning for a valve.

4.3.1.3 VAV box

A VAV box generally consists of a plenum box and a damper controlled by a VAV controller. The most possible part that might have problem during operational phase is the VAV damper. The on-going commissioning method of VAV damper is similar to water valve, as discussed in previous section.

4.3.1.4 Fan subsystem

The first step for On-going commissioning a fan subsystem is to develop fan subsystem models suitable for on-going commissioning. Then use the model to simulate the no-fault performance of the fan subsystem and compare the no-fault performance with real-time performance. The on-going commissioning of a fan subsystem will be discussed in the next chapter in detail.

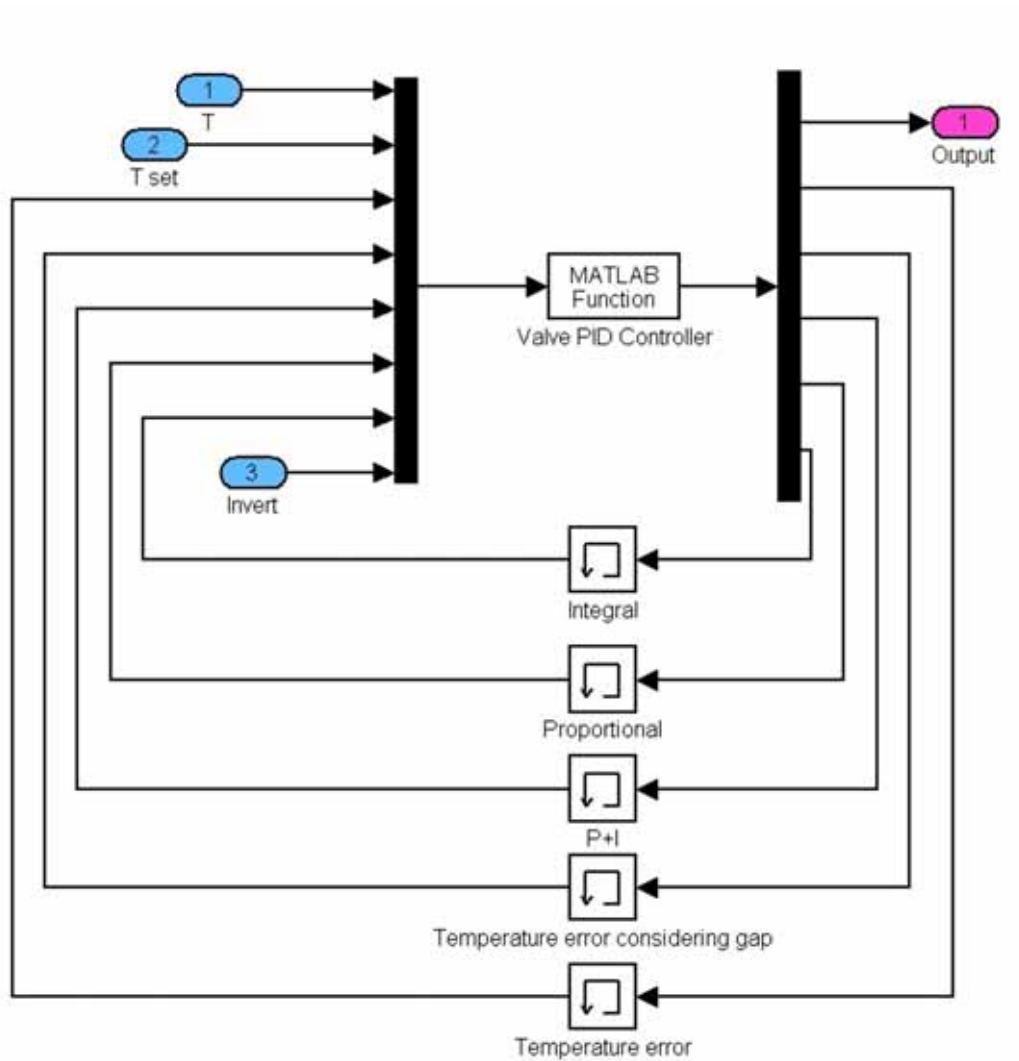
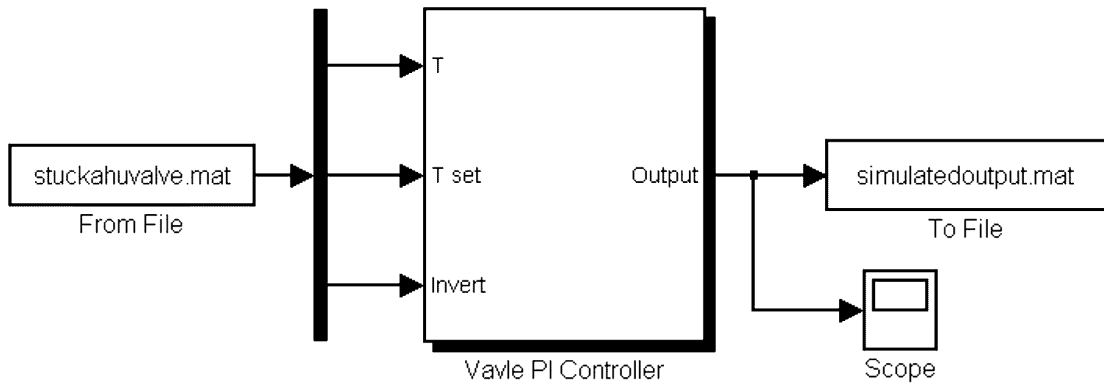


Figure 4.4 Simulink model for valve control simulation

Table 4.1 Parameters of valve control model

Parameter	Parameter Value
Integral time t_0 (s)	300
Gap of insensitivity g_0 (°C)	0.3
Proportional band at inverter=100% L_1 (°C)	8
Proportional band at inverter=0 L_0 (°C)	15
Control interval $d\tau$ (s)	10
Error of integral time t_e (s)	61.0887
Error of gap of insensitivity g_e (°C)	0.0123
Error of proportional band at inverter=100% b (°C)	-0.58
Error of proportional band at inverter=0 a (°C)	-1.8

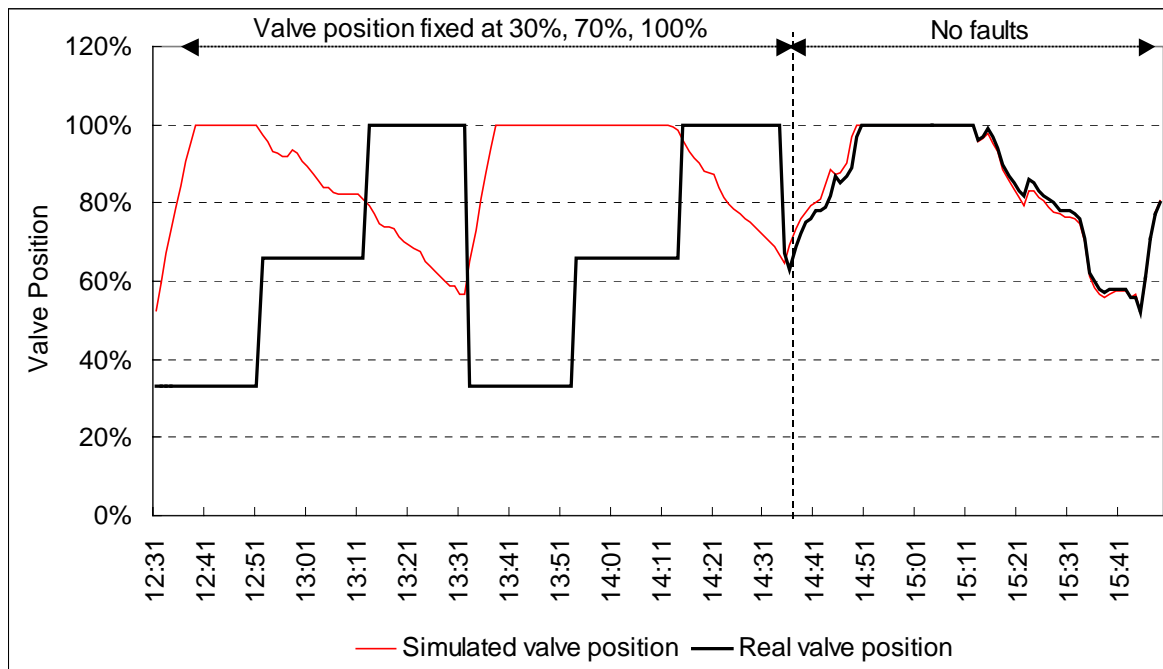


Figure 4.5 Comparison of simulated and real valve positions

4.3.2 NO-FAULT OPERATIONAL DATA COMPARISON APPROACH

No-fault operation data comparison is to continuously commission an HVAC system through continuously comparing the real-time operational data with the past no-fault operational data that were under the same heat conditions as the current operation. The key point of this approach is to search in the past no-fault operational database to find proper data to compare with the current operational data. The proper operation data valid for comparing are the data under the similar heat operation conditions, such as same weather condition, same indoor load condition, and other relative air processing parameters.

The components that are most suitable for being commissioned using this approach are sensors. Most sensor simulation models use measured value as input to simulate the output of a sensor. For example, the HVACSIM+ temperature sensor model uses measured temperature as an input to simulate the sensor output (Clark, 1985). The SIMBAD temperature sensor model uses measured convective temperature and mean radiant temperature as the inputs to simulate the sensor output (CTSB, 2001). If temperature is measured, the measured temperature can be used to verify the sensor's output instead of simulated value. However, these measured data are unavailable for on-going commissioning during operational phase because for common HVAC system only one sensor is installed for one measurement point. A possible approach for continuously commissioning a sensor is to compare the real time data with past no-fault operational data that is closely related to the sensor measurement. For instance, check the situation of supply air volume can verify whether the room air temperature sensor's measurement deviates much from true value or not, because the VAV controller decides the supply air volume according to the difference between measured room air temperature and set point. During construction phase and acceptance phase, every component has been commissioned. It is safe to assume the operation data of the commissioned HVAC system to be no fault. Therefore the past operation data can be used as criteria to verify the HVAC system running in the future. As an example, let us analyze the case of room air temperature sensor deviates from true value. A typical VAV system controller's output control demand using Proportional and Integral (PI) control algorithm, which is shown in the following equations.

$$V_d = V_{\max} (P + I) \quad (4.15)$$

$$P = K(T_m - T_s) \quad (4.16)$$

$$I = \frac{K}{t} \int_0^t (T_m - T_s) d\tau \quad (4.17)$$

If a sensor's offset is ΔT , the controller output will include deviation, as the following equation.

$$\hat{V}_d = V_{\max} \left[K(T_t + \Delta T - T_s) + \frac{K}{t} \int_0^t (T_t + \Delta T - T_s) d\tau \right] = V_d + V_{\max} \left(K\Delta T + \frac{K}{t} \int_0^t \Delta T d\tau \right) \quad (4.18)$$

The second term in Equation 4.18 is the difference between correct demand supply air volume and the faulty demand value given according to the faulty sensor measurements. This difference of supply air volume can be used to judge whether a sensor measurement deviates or not.

Two cases, malfunctioning supply air temperature sensor and room air temperature sensor, were studied to verify the validity of this operational comparison approach.

4.3.2.1 Malfunctioning supply air temperature sensor

In order to verify the validity of commissioning supply air temperature sensors using no-fault operational comparison approach, a case was studied that the supply air temperature sensor was made to offset 20% from the temperature set point 18°C. In the cooling operation case if the supply air temperature sensor measurement deviates from the true value, an automatically controlled VAV system's response should act as shown in Figure 4.6.

Figure 4.7 shows the changes of total supply air volume and room air temperature when supply air temperature sensor measurement offset was $\pm 20\%$ and no offset. When supply air temperature sensor offset was +20%, the average total supply air volume was 4% lower than that of no offset, and the supply air volume reached the minimum value, which caused the average room air temperature 0.7°C lower than set point. When the supply air temperature sensor offset was -20%, the average total supply air volume was 36.7% higher than that of no offset. The big difference between the normal operational data and sensor offset operational data shows the feasibility of on-going commissioning supply air temperature sensor using the method of no-fault operation comparison.

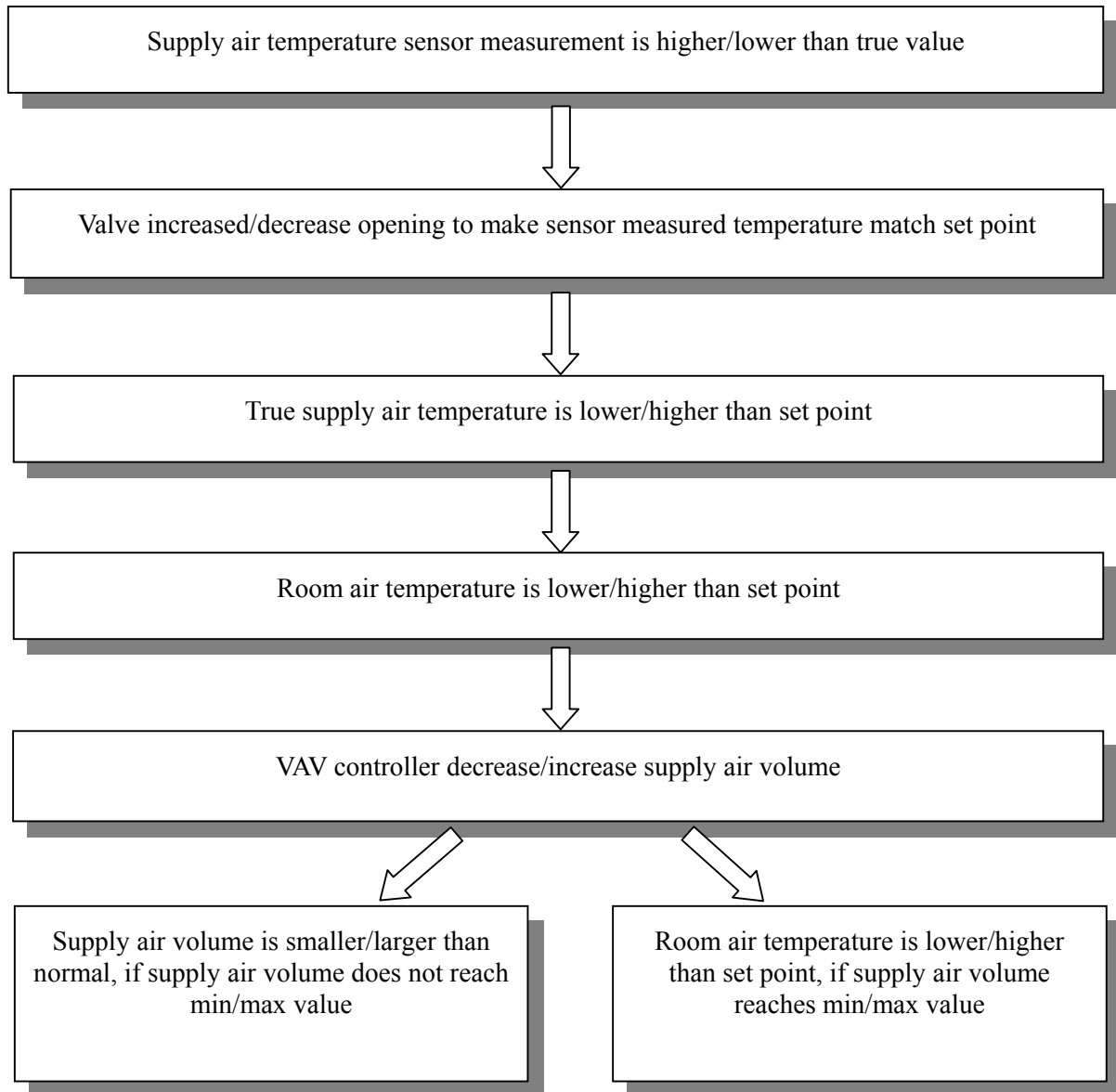


Figure 4.6 VAV system responses to supply air temperature sensor offset

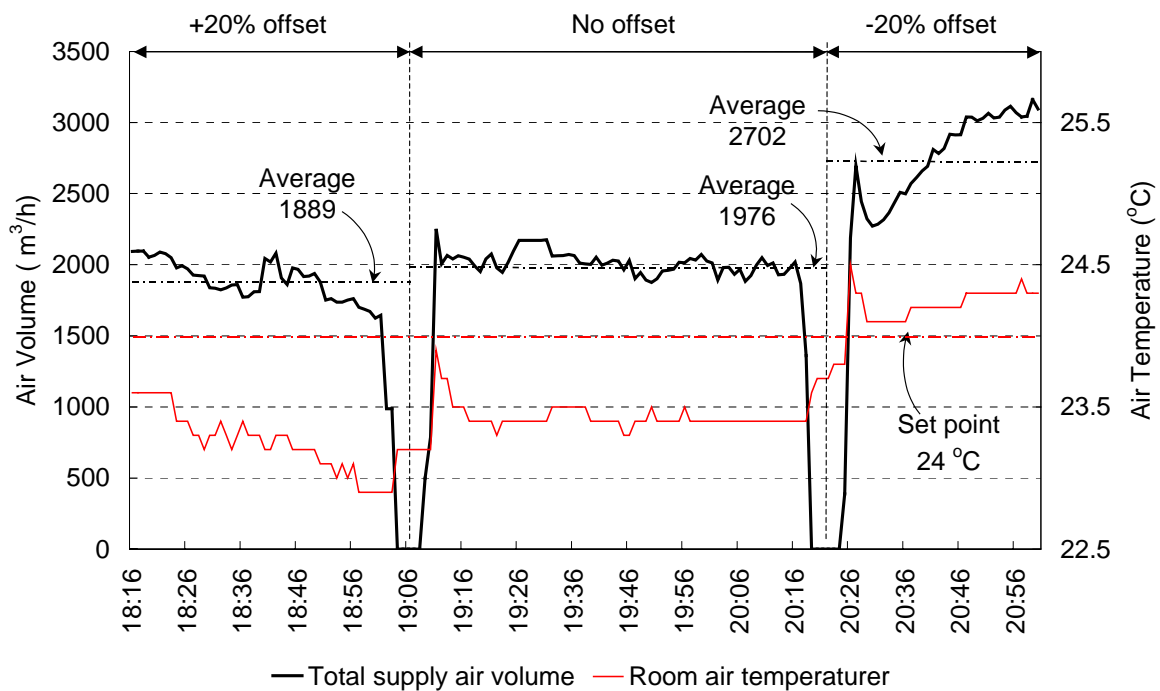


Figure 4.7 Influence of supply air temperature sensor offset

4.3.2.2 Malfunctioning room air temperature sensor

For the purpose of verifying the validity of commissioning room air temperature sensors using no-fault operation comparison approach, a case that the room air temperature sensor was made to offset 5% from the temperature set point 24°C was analyzed. For cooling operation if the room air temperature sensor measurement deviates from the true value, an automatically controlled VAV system should response as shown in Figure 4.8.

Figure 4.9 shows the situations of total supply air volume and room air temperature when room air temperature sensor offset was $\pm 5\%$ and no offset. When room air temperature sensor offset was +5%, the average supply air volume was 94.5% higher than that of no offset. When room air temperature sensor offset was -5%, the average supply air volume is 13.8% lower than that of no offset. Furthermore, when offset was -5%, the supply air volume reached the minimum value and room air temperature is 0.8 °C lower than set point. The differences between normal operational data and sensor offset operational data are so big that it is easy to detect the fault of sensor offset during operational phase through operational records comparison approach.

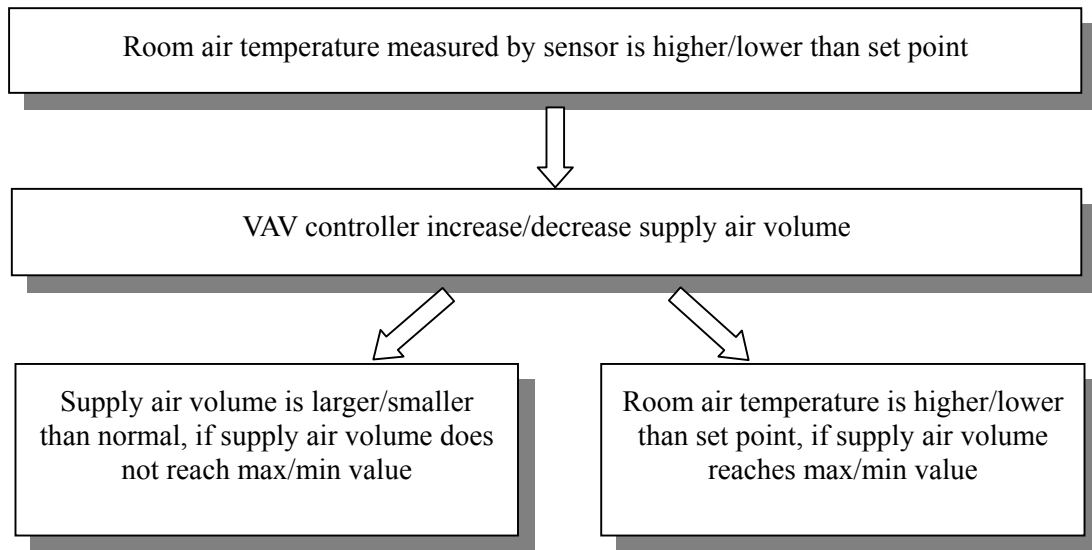


Figure 4.8 VAV system responses to room air temperature sensor offset

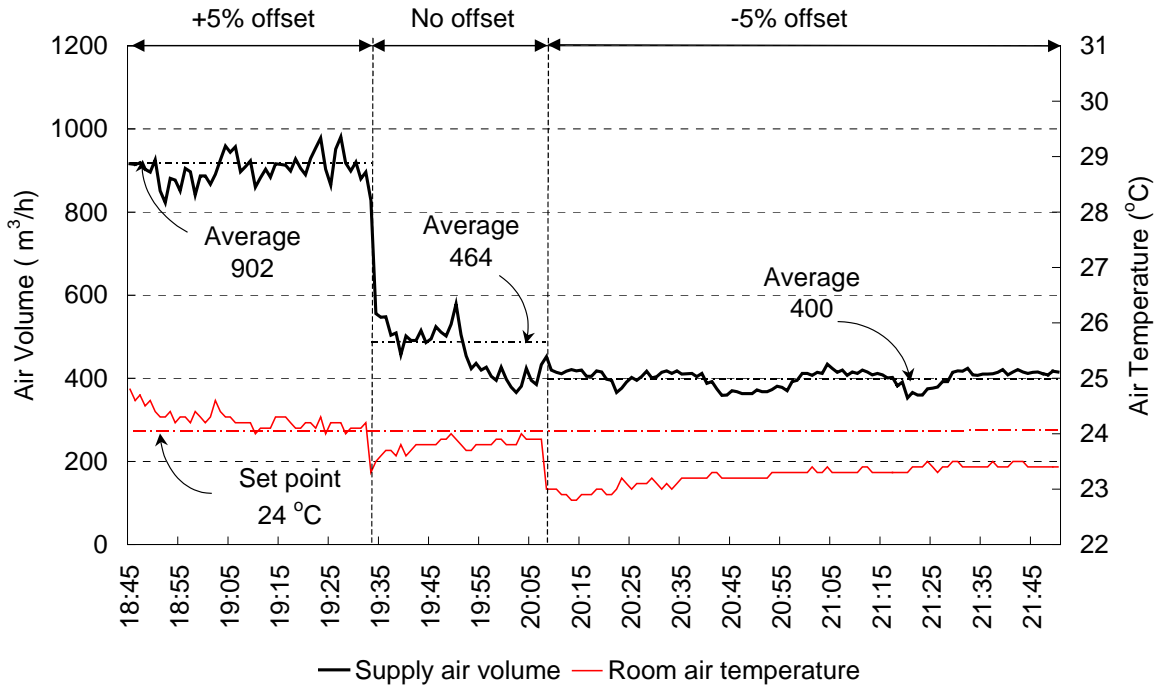


Figure 4.9 Influence of room air temperature sensor offset

4.4 SUMMARY

This chapter discussed an on-going commissioning methodology, which consists of two aspects of approach, simulation analysis comparison and past no-fault operation comparison. The simulation analysis comparison was demonstrated through commissioning a stuck valve and the past no-fault operation comparison was explained through the cases of commissioning malfunctioning supply air temperature sensor and room air temperature sensor. These case studies show that this on-going commissioning method is useful for monitoring the operation of main components of a secondary HVAC system and can successfully detect and diagnose some faults. Based on this methodology an on-going commissioning tool can be developed, which can either stand-alone or be embedded in BEMS.

CHAPTER 5

TOTAL ENERGY CONSUMPTION MODEL OF FAN SUBSYSTEM SUITABLE FOR ON-GOING COMMISSIONING

5.1 INTRODUCTION

For the purpose of automatically and continuously commissioning fan subsystems using simulation analysis during operational phase, currently available fan simulation models were checked to determine whether these models are suitable for on-going commissioning or not. Model validity checking showed that no fan model can give simulation results that match the experiment-measured data quite well. Therefore a new total energy consumption model of fan subsystem was developed, which is suitable and useful for on-going commissioning. This newly developed model's accuracy and validity for on-going commissioning were checked using experiments.

5.2 MODELS

The fan models used by currently available simulation tools can only simulate the performance of a fan itself. There are no models to simulate the performance of other components in fan subsystems, such as motors, inverters, etc. For example, SIMBAD can simulate a fan's energy consumption using an empirical equation by inputting maximum airflow rate, real-time airflow rate, and maximum energy consumption (CSTB 2001). HVACSIM+ is able to simulate a fan's energy consumption and a fan's pressure head using air flow rate and fan rotational speed by a series of equations fitted using manufacturer's data (Clark 1985).

However, it is difficult to commission the fan using these models because they

simulate the energy consumption of a fan itself and this energy consumption, which is named fan shaft power, is difficult to measure. Especially during the operational phase, there is no building energy management system that measures a fan's shaft power. But, it is very easy to measure the total power consumed by a fan subsystem, which includes the fan, driveline, motor and Variable Speed Drive (VSD), using a power meter set at the power input point such as the power switch. If the above-mentioned fan models are used to simulate the total power consumption of a fan subsystem, they will not give acceptable results. For instance, SIMBAD gives an average difference of 50%, and HVACSIM+ offers an average difference of 48% between the fan model simulated power consumption and measured fan subsystem power consumption. Therefore it is unreasonable to use these fan simulation models for a fan's on-going commissioning.

Furthermore, the characteristics of total efficiency of a fan subsystem are different from that of the fan itself. A fan's efficiency changes only according to a dimensionless air-flow rate C_f . The η - C_f curve shows a similar shape at different fan rotation speeds, as shown in Figure 5.1. Whereas the total efficiency of the fan subsystem changes according to not only C_f but also the fan rotational speed, as shown in Figure 5.2. Therefore new total efficiency models of the fan subsystem are needed to express the unique characteristics of the fan subsystem.

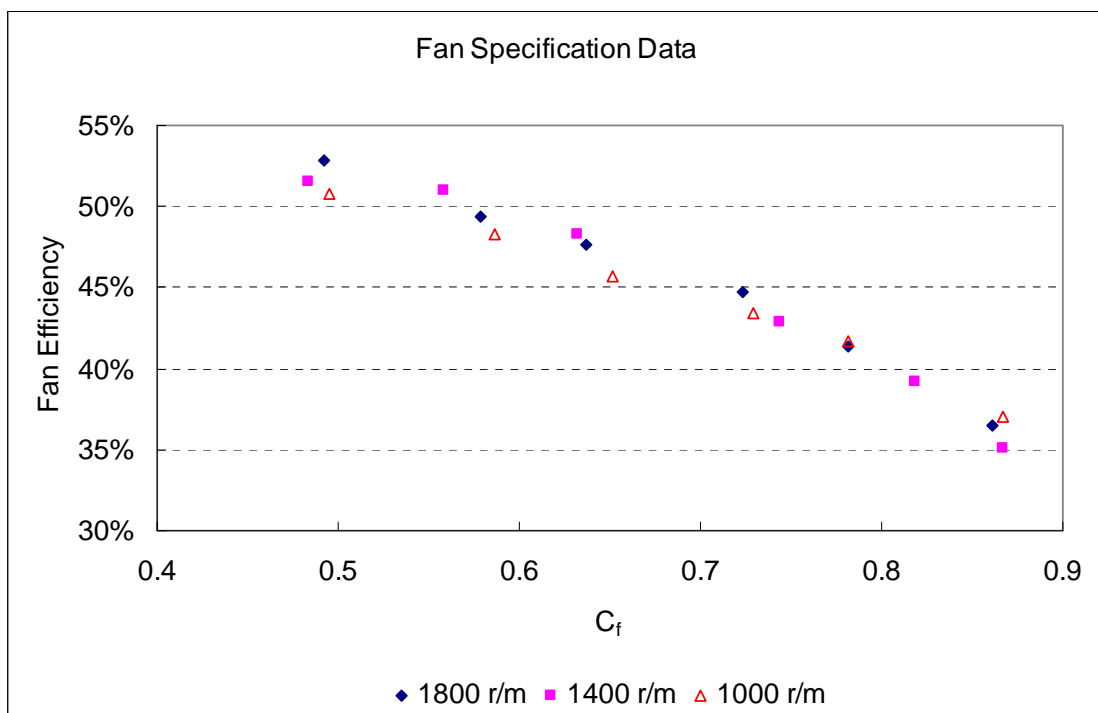


Figure 5.1 Fan efficiency vs. dimensionless air flow rate C_f

A total energy consumption model was proposed, which takes into account the performance of all the components in the fan subsystem, i.e. the fan, driveline, motor and VSD inverter. The components and energy flow of the typical fan subsystem are shown in Figure 5.3.

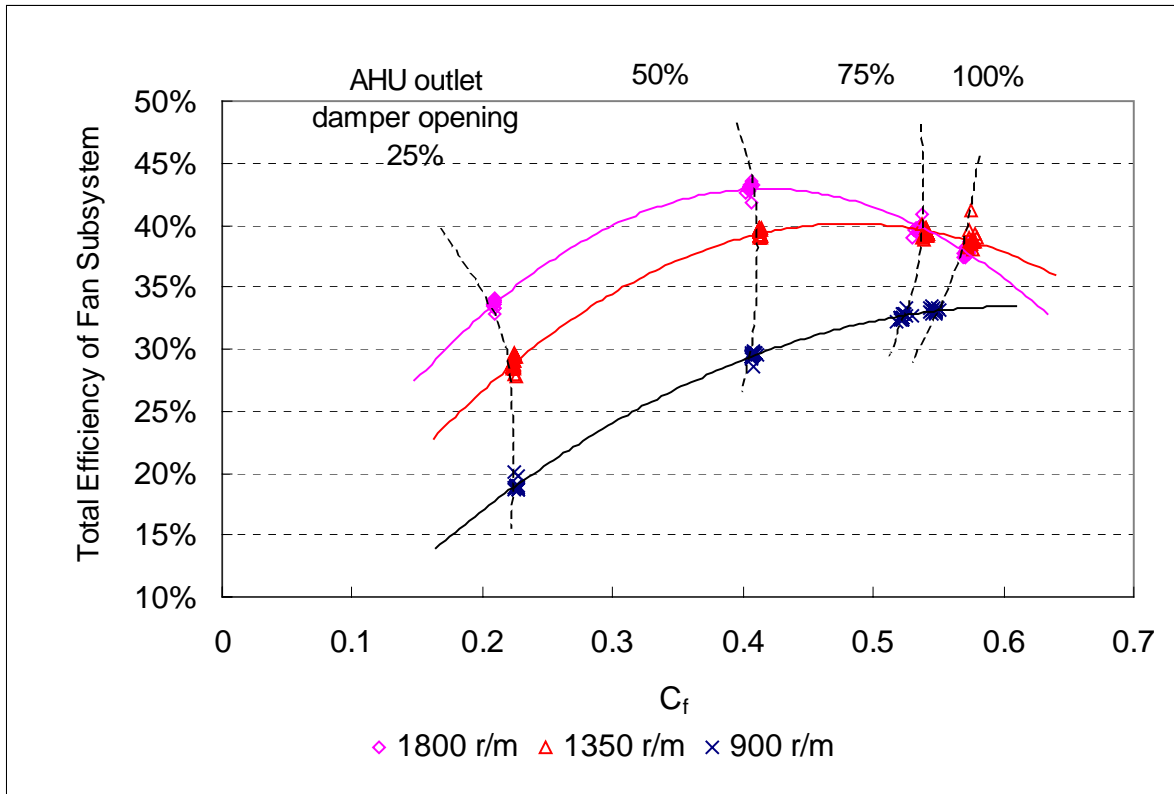


Figure 5.2 Total efficiency of fan subsystem vs. dimensionless air flow rate C_f

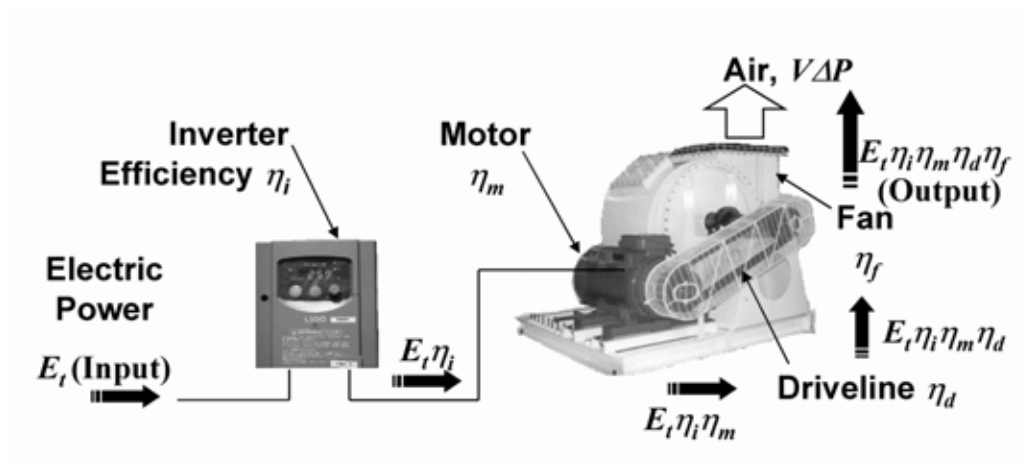


Figure 5.3 Components and energy flow of a fan subsystem

The total energy consumption model is defined by a total energy consumption equation and the associated every components efficiency equations, as follows.

$$E_t = \frac{V \cdot PH}{\eta_t} \quad (5.1)$$

$$\eta_t = \eta_f \eta_{dl} \eta_{mo} \eta_{inv} \quad (5.2)$$

$$\eta_f = e_0 + e_1 C_f + e_2 C_f^2 + e_3 C_f^3 + e_4 C_f^4 \quad (5.3)$$

$$\eta_{mo} = m_0 + m_1 LF + m_2 LF^2 + m_3 LF^3 + m_4 LF^4 \quad (5.4)$$

$$\eta_{inv} = i_0 + i_1 LF + i_2 LF^2 + i_3 LF^3 + i_4 LF^4 \quad (5.5)$$

$$LF = \frac{V \cdot PH}{\eta_f E_r} \quad (5.6)$$

$$C_f = f_0 + f_1 C_r + f_2 C_r^2 + f_3 C_r^3 + f_4 C_r^4 \quad (5.7)$$

$$C_r = \frac{\rho V^2}{PH \cdot D^4} \quad (5.8)$$

Equation 5.1 is used to calculate the total energy consumption of the fan subsystem using airflow rate, pressure head and total efficiency of the fan subsystem. Total efficiency of the fan subsystem is calculated using Equation 5.2 by multiplying the efficiency of all the components of the fan subsystem, i.e. the fan, driveline, motor and inverter. Equation 5.3 is used to calculate the fan efficiency using a 4th-order function of dimensionless airflow rate. This equation is taken from HVACSIM+ (Clark 1985). The motor and inverter efficiency is calculated using Equations 5.4 and 5.5 respectively, which are 4th-order functions of load factor. The load factor is calculated using Equation 5.6, which is the rate of fan shaft power to rated shaft power.

For the reason discussed in the following section, Equation 5.7 is used to calculate the dimensionless air-flow rate using dimensionless flow resistance, which is calculated using Equation 5.8, instead of the method used in HVACSIM+, which uses air-flow rate and fan rotation speed as shown in Equation 5.9. Fan rotation speed is estimated using Equation

5.10 from rated rotation speed and inverter output frequency.

If pressure head is not measured, it is necessary to estimate it. Firstly calculate fan rotation speed using Equation 5.10 and then calculate C_f using Equation 5.9. Pressure head can be calculated using Equation 5.11 and 5.12, which are the models used by HVACSIM+.

$$C_f = \frac{V}{ND^3} \quad (5.9)$$

$$N = \frac{INV}{INV_r} N_r \quad (5.10)$$

$$C_h = a_0 + a_1 C_f + a_2 C_f^2 + a_3 C_f^3 + a_4 C_f^4 \quad (5.11)$$

$$C_h = \frac{PH}{\rho N^2 D^2} \quad (5.12)$$

5.2.1 FAN EFFICIENCY MODEL

Equation 5.3 shows a fan efficiency model used in HVACSIM+. This fan efficiency model simulates a fan's efficiency using dimensionless air-flow rate C_f , which is calculated using air flow rate and fan rotational speed. However, for a gear driven or cog-belt driven fan subsystem, the fan rotation speed can be calculated using inverter output frequency and rated rotational speed as shown in Equation 5.10, because no slippage occurs in gear drivelines and cog-belt drivelines. Whereas for a v-belt or band belt driven fan subsystem, the belt slippage makes it inaccurate to calculate the transient fan rotation speed using the inverter output frequency and rated rotation speed. Furthermore, most BEMS are not installed with a sensor to measure the fan rotational speed. Therefore, for the purpose of on-going commissioning, other models must be used.

One alternate method is to simulate the fan efficiency using airflow rate and fan pressure head. For this purpose, a new dimensionless variable was proposed, dimensionless airflow resistance coefficient C_r , as shown in Equation 5.8. Dimensionless airflow resistance coefficient C_r is use to calculate C_f and then fan efficiency can be calculated using C_f and Equation 5.3.

Another method is to estimate fan rotational speed using inverter output frequency, as

shown in Equation 5.10. The accuracy that this estimation could achieve was checked by comparing the measured rotational speeds with estimated ones. The average difference between the measured and estimated rotational speed is 2.2% and the maximum difference is 9.0% as shown in Figure 5.4, when inverter output frequency gradually changed from 20% to 100% of rated frequency, 50 Hz. The accuracies of three fan efficiency simulation methods were compared to determine which one is most suitable for on-going commissioning. The input variables to the three simulation methods are as follows.

- 1) Air flow rate and head pressure
- 2) Air flow rate and measured fan rotational speed
- 3) Air flow rate and calculated fan rotational speed

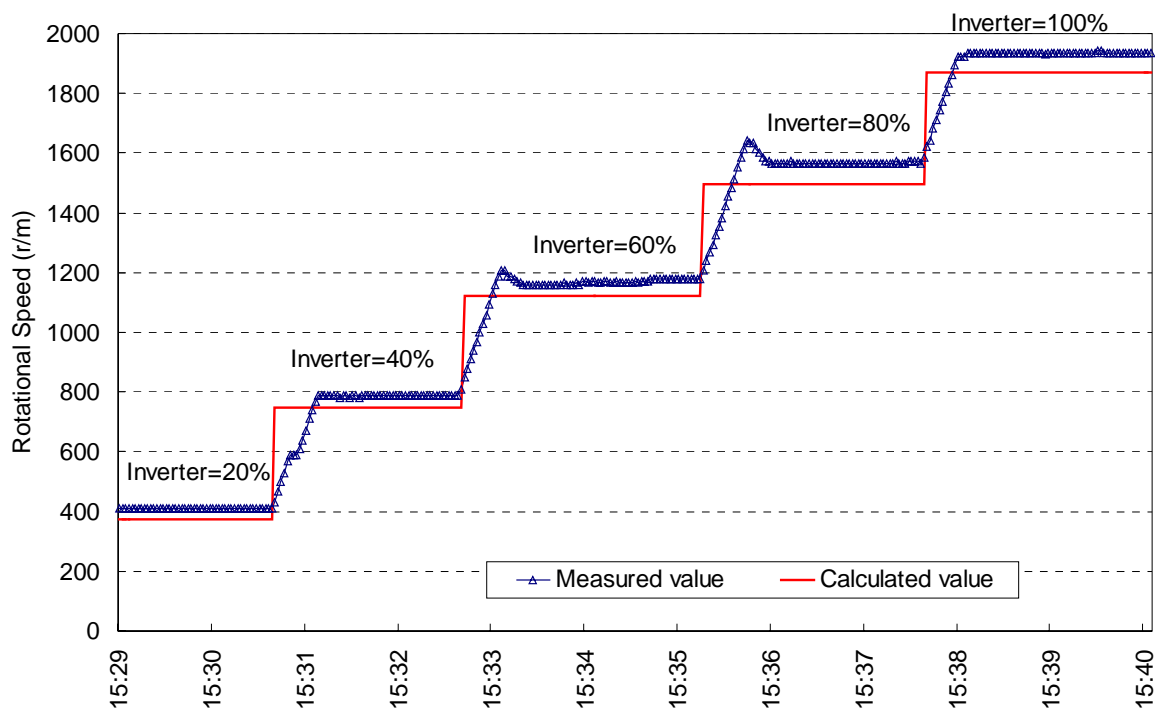


Figure 5.4 Comparison of measured and estimated fan rotational speed

The average differences between the measured total efficiency of the fan subsystem and the simulated total efficiency given by these three methods are 5.1%, 6.1% and 6.5% respectively. The simulation model using airflow rate and head pressure gave the most accurate simulation results. The simulation accuracy of 2) using measured fan rotational speed is 0.4% higher than using calculated fan rotation speed. So it is acceptable to simulate

the fan efficiency using calculated fan rotational speeds instead of measured ones when head pressure is unavailable.

5.2.2 DRIVELINE EFFICIENCY

The newly installed driveline efficiency can be used as a performance target value during the on-going commissioning phase, because the driveline efficiency changes due to aging. So as a driveline efficiency decreases because of aging, the real total efficiency of a fan subsystem will be lower than the total efficiency simulated using the newly installed driveline's efficiency. Therefore a newly installed driveline's efficiency can be used in the fan subsystem simulation to help detect the fault of belt aging and is useful for on-going commissioning. The recommended efficiency value for a newly installed V-belt is 95% and for newly installed cogged or synchronous belts the efficiency is 98% (OIT 2000).

5.2.3 MOTOR EFFICIENCY

Motor efficiency changes according to two variables, electric frequency and load factor, as shown in Figure 5.5. Load factor is the percentage of transient motor power output to rated power output. If fan belt efficiency is assumed to be constant at various loads and rated motor output is equal to rated fan power input, the load factor can be calculated through dividing the transient fan power input by rated fan power input, as shown in Equation 5.6.

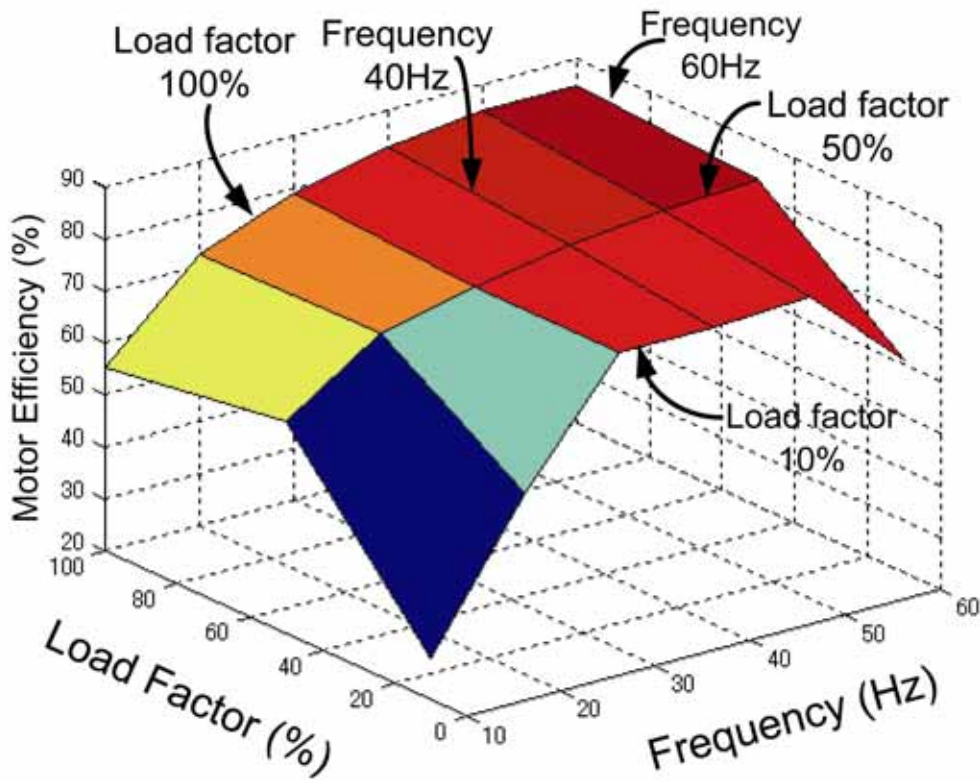


Figure 5.5 Motor efficiency vs. load factor and power frequency

For VSD-driven motors in a VAV system, the electric frequency input to the motor is not an independent variable. It is determined according to demand airflow rate and pressure, which determine the load on the motor. Therefore required motor input frequencies are related to load factors. The relationship between load factor LF and required frequency F can be derived, as shown in the Equations 5.13 to 5.15.

$$\frac{V}{V_r} = \frac{N}{N_r} = \frac{F}{F_r} \quad (5.13)$$

$$PH = RV^2 \quad (5.14)$$

$$LF = \frac{V \cdot PH}{V_r \cdot PH_r} = \left(\frac{V}{V_r} \right)^3 = \left(\frac{F}{F_r} \right)^3 \quad (5.15)$$

From Equation 5.15 it can be found that the required electric frequency has one definite value corresponding to one load factor value. Therefore load factor is the only independent

variable that can influence the motor efficiency. So for a VSD-driven motor in a VAV system, the relationship of motor efficiency and frequency and load factor is not a 3-dimensional surface, but 3-dimensional curves, as shown in Figure 5.6.

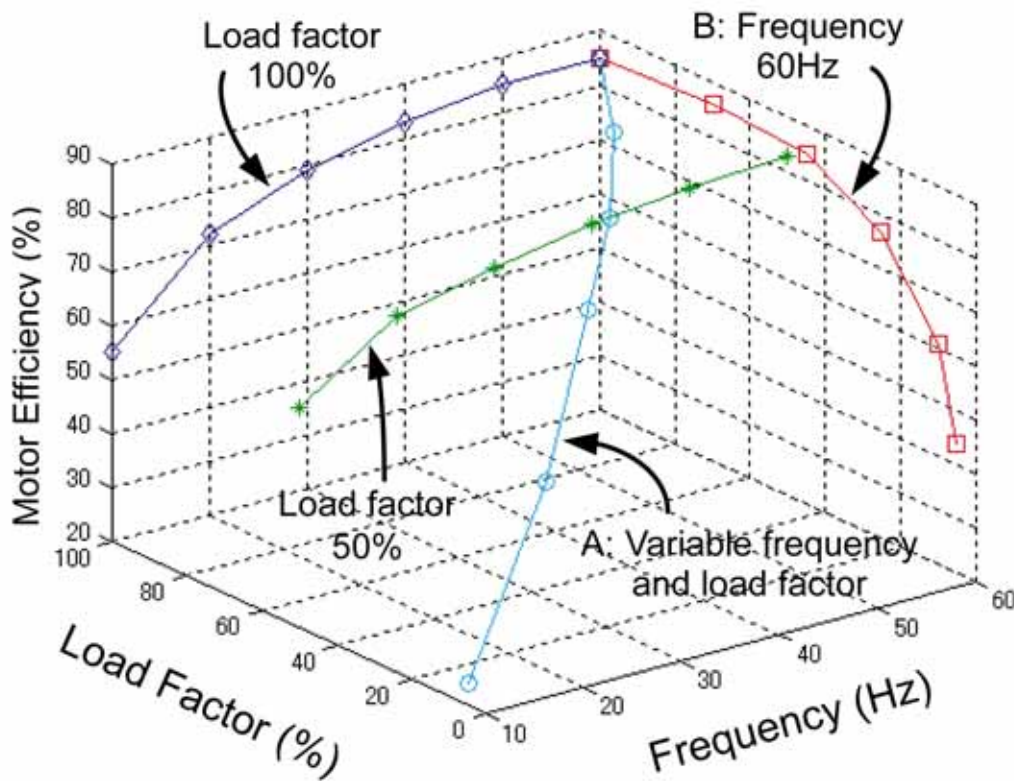


Figure 5.6 VAV system motor efficiency vs. load factor and power frequency

In order to simulate the motor efficiency accurately, Equation 5.4 needs to be fitted using the data with the relationship of $\eta_m-LF-\left(\frac{F}{F_r}\right)^3$, as shown by curve A in Figure 5.6.

However, most motor manufacturers only offer data on their motors' efficiency at the conditions of rated frequency and various load factors, as shown by curve B in Figure 5.6. Therefore these data have to be used to fit the motor efficiency model. Of course it is not accurate to simulate the motor efficiency in a VAV system using such a fitted model. So motor manufacturers should be urged to offer motor efficiency data with the relationship to load factor and frequency at the conditions of $\eta_m-LF-\left(\frac{F}{F_r}\right)^3$.

5.2.4 INVERTER EFFICIENCY

Inverters change the electric frequency to make motors' and fans' rotational speed variable. During frequency modulation, inverters consume some energy, which becomes heat and discharges to the local environment. Inverter manufacturers' literature shows the relationship between heat-generating losses and load factors, as shown in Figure 5.7 (Hitachi 2002).

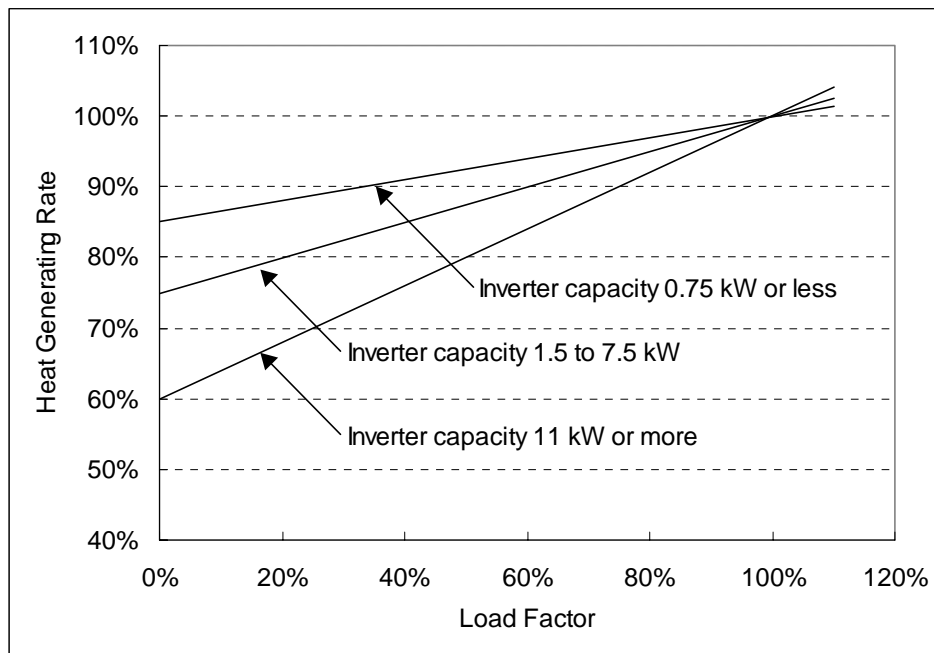


Figure 5.7 Inverter heat generating vs. load factor

Using the heat-generating rates, the inverter efficiency can be calculated as a function of changing load factor. Using these data of inverter efficiency vs. load factor, the inverter efficiency model can be fitted. The fitted inverter efficiency model can be used to simulate the inverter's efficiency during the operations phase to realize on-going commissioning of a fan subsystem.

5.3 MODEL PARAMETERS, INPUTS, AND OUTPUT

5.3.1 PARAMETERS

The necessary parameters are as follows.

a_0, a_1, a_2, a_3, a_4 – Fitted coefficients for the equation of C_h-C_f

D – Diameter of fan wheel (m)

e_0, e_1, e_2, e_3, e_4 – Fitted coefficients for the equation of $\eta-C_f$

f_0, f_1, f_2, f_3, f_4 – Fitted coefficients for the equation of C_f-C_r

E_r – Rated fan power consumption (W)

INV_r – Rated invert output frequency (Hz)

i_0, i_1, i_2, i_3, i_4 – Fitted coefficients of inverter efficiency equation using inverter specification data

m_0, m_1, m_2, m_3, m_4 – Fitted coefficients of motor efficiency equation using motor specification data

N_r – Rated fan rotational speed (r/s)

5.3.2 INPUTS

The inputs to the models are listed in the followings.

V – Air volume flow rate (m^3/s)

ΔP – Fan pressure head (Pa)

If fan pressure head is unavailable, the inputs should be as follows.

V – Air volume flow rate (m^3/s)

INV – Invert output frequency (Hz)

5.3.3 OUTPUT

The output of this model is the total energy consumed by all the components in a fan subsystem under no-fault operation.

E_t – Total energy consumption of fan subsystem (W)

5.4 EXPERIMENTAL VALIDATION

In order to validate this total energy consumption model of fan subsystem and its feasibility for on-going commissioning, experiments were conducted in August 2002 on a

real VAV system in an office building located in Tokyo. In the first experiment normal fan subsystem operation data were measured to check the total energy consumption model's accuracy. The second experiment checked whether this total energy consumption model could detect the fault of loose belts. The total electric power consumption, air volume and head pressure for the supply air fan in an AHU were measured. The measurement points and the configuration of the AHU are shown in Figure 5.8.

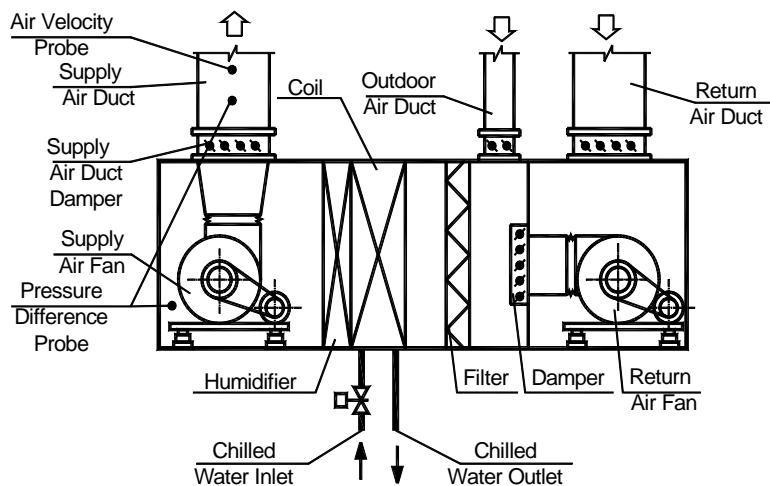


Figure 5.8 Measurement points and AHU configuration

5.4.1 VALIDATION USING NORMAL FAN SUBSYSTEM

For the purpose of validating the model, an experiment was carried out to measure the performance of a fan subsystem. Then the simulated data were compared with measured data to validate the model. In order to obtain the fan performance data at different load factor, the inverter output frequency was fixed at 100%, 75%, and 50%. Corresponding to each inverter output frequency, the AHU supply air outlet damper opening was set at 100%, 75%, 50%, and 25% respectively. The steps of setting these parameters are shown in Figure 5.9. Fan supply air volume, head pressure, and electric power consumption were measured every one minute and recorded using a data logger. Inverter output frequencies were obtained from the BEMS records.

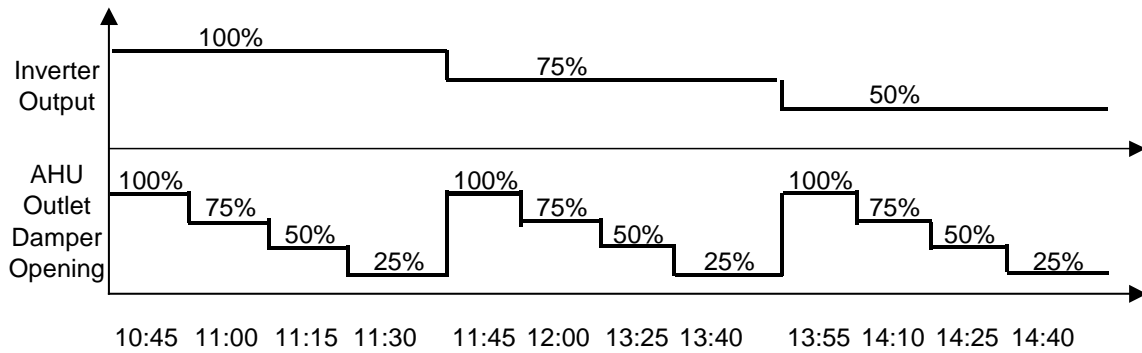


Figure 5.9 Experiment step and parameters

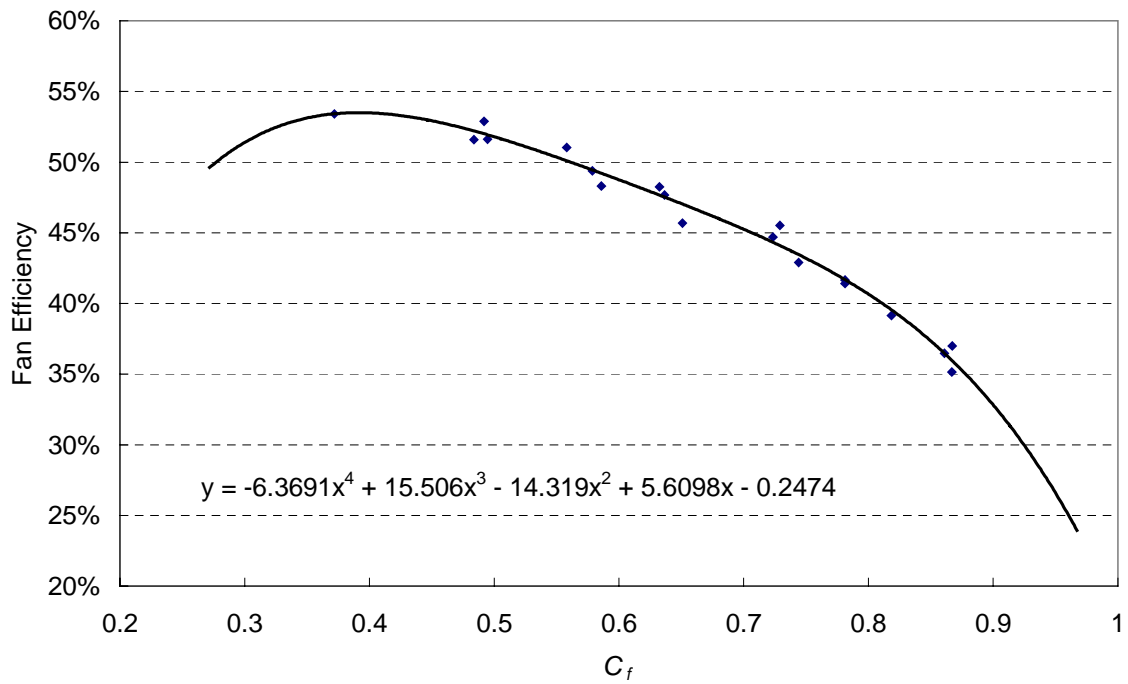
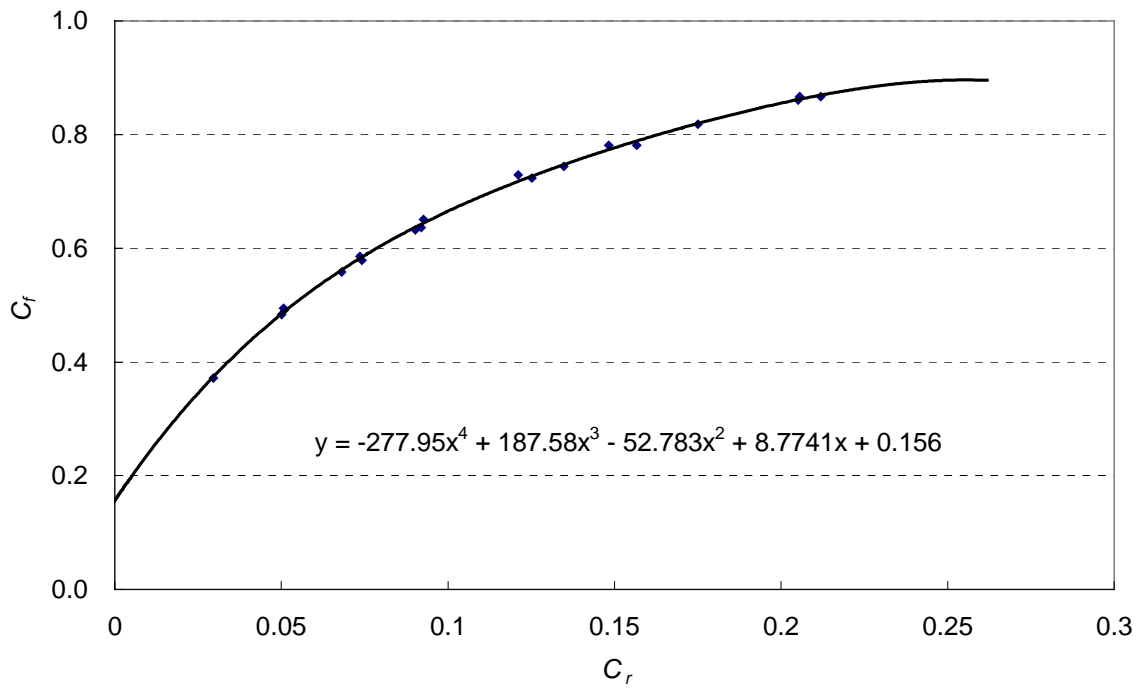
In order to estimate the performance of a fan subsystem using this model, firstly it is necessary to fit the coefficients used in the fan, motor and inverter models using manufacturer's specification data.

5.4.1.1 Coefficients fitting for fan model

The fan specification data used for coefficients fitting are list in Table 5.1. Coefficients fitting results of fan model are shown in Figure 5.10.

Table 5.1 Data for fan model coefficients fitting

Dimensionless flow resistance C_r	Dimensionless flow rate C_f	Dimensionless pressure head C_h	Fan efficiency η
0.0297	0.3720	4.6665	53.4188%
0.0501	0.4836	4.6665	51.5873%
0.0510	0.4919	4.7425	52.8889%
0.0507	0.4948	4.8293	51.6049%
0.0681	0.5580	4.5731	51.0417%
0.0741	0.5787	4.5167	49.3827%
0.0736	0.5859	4.6646	48.2955%
0.0902	0.6324	4.4332	48.2378%
0.0920	0.6366	4.4038	47.6667%
0.0927	0.6510	4.5732	45.6871%
0.1252	0.7234	4.1780	44.6860%
0.1211	0.7292	4.3902	45.5285%
0.1348	0.7440	4.1065	42.8850%
0.1567	0.7813	3.8957	41.4000%
0.1483	0.7812	4.1159	41.6667%
0.1751	0.8185	3.8265	39.1493%
0.2051	0.8608	3.6134	36.4751%
0.2119	0.8668	3.5465	35.1349%
0.2056	0.8672	3.6585	37.0000%



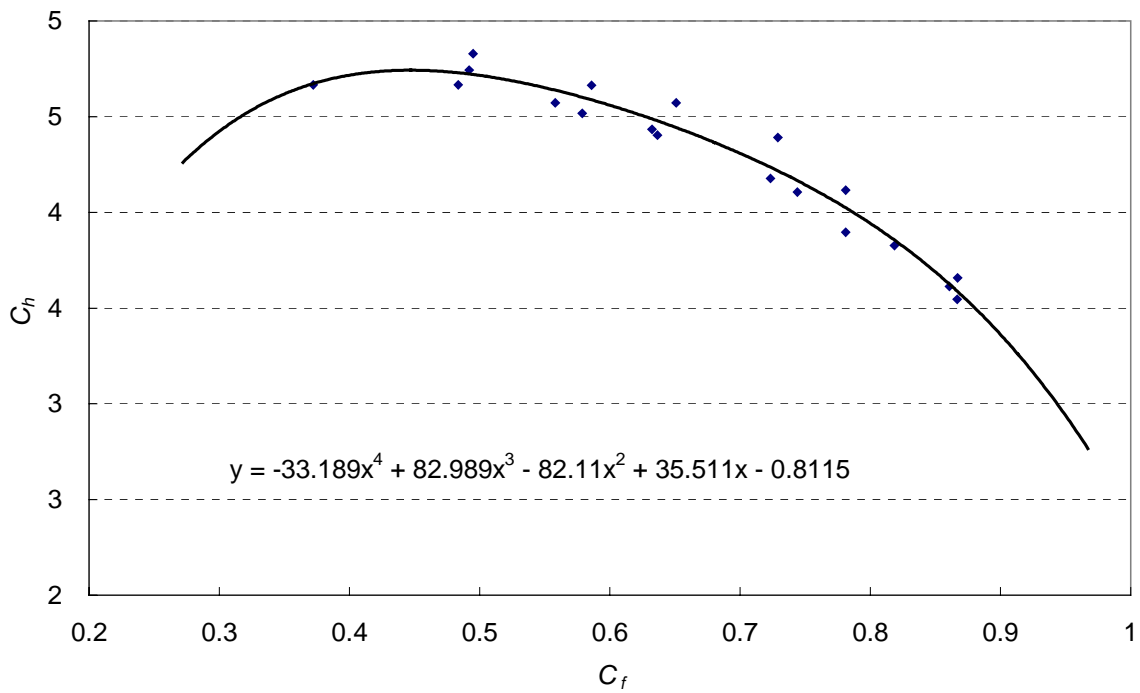


Figure 5.10 Coefficients fitting results of fan model

5.4.1.2 Coefficients fitting for motor model

The motor specification data used for coefficients fitting are list in Table 5.2. Coefficients fitting results of motor model are shown in Figure 5.11.

Table 5.2 Data for motor model coefficients fitting

Load factor LF	10%	25%	45%	70%	100%
Motor efficiency η	55.00%	77.00%	83.00%	86.00%	85.00%

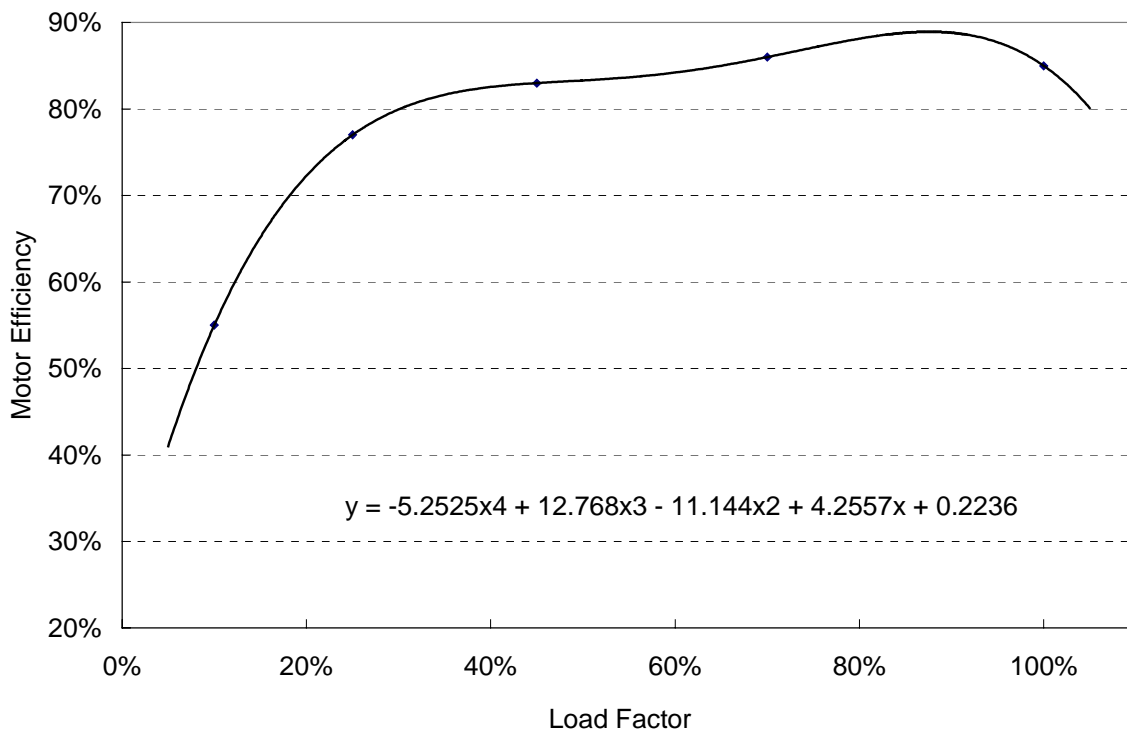


Figure 5.11 Coefficients fitting results of motor model

5.4.1.3 Coefficients fitting for inverter model

The inverter specification data used for coefficients fitting are list in Table 5.3. Coefficients fitting results of inverter model are shown in Figure 5.12.

Table 5.3 Data for inverter model coefficients fitting

Load factor <i>LF</i>	5%	10%	25%	45%	70%	100%	120%
Inverter efficiency <i>η</i>	81.16%	87.95%	91.79%	93.15%	93.84%	94.26%	94.54%

The simulated total efficiency of the fan subsystem using the total energy consumption model is shown in Figure 5.13 compared with the measured total efficiency of the fan subsystem. Before this total energy consumption model is developed, only fan model is available, so simulated fan efficiency using Equation 5.3 is also shown in Figure 5.13 for the purpose of checking the difference between measured fan subsystem total efficiency and simulated fan efficiency. Furthermore, before this total energy consumption model is developed, the only way to calculate fan subsystem total efficiency is to multiply fan real-time efficiency by rated driveline, motor and inverter efficiency. In order to check the

accuracy of simulated total efficiency of fan subsystem by multiplying fan real-time efficiency by rated driveline, motor and inverter efficiency, Figure 5.13 also shows the total efficiency of fan subsystem calculated using the original way.

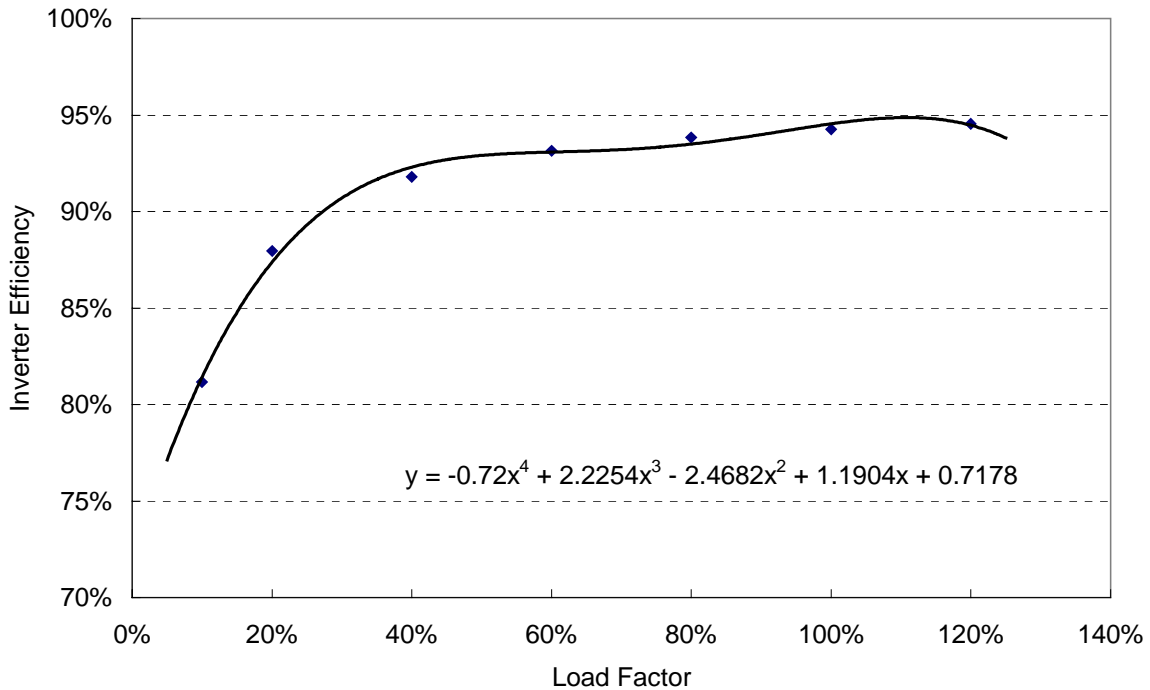


Figure 5.12 Coefficients fitting results of inverter model

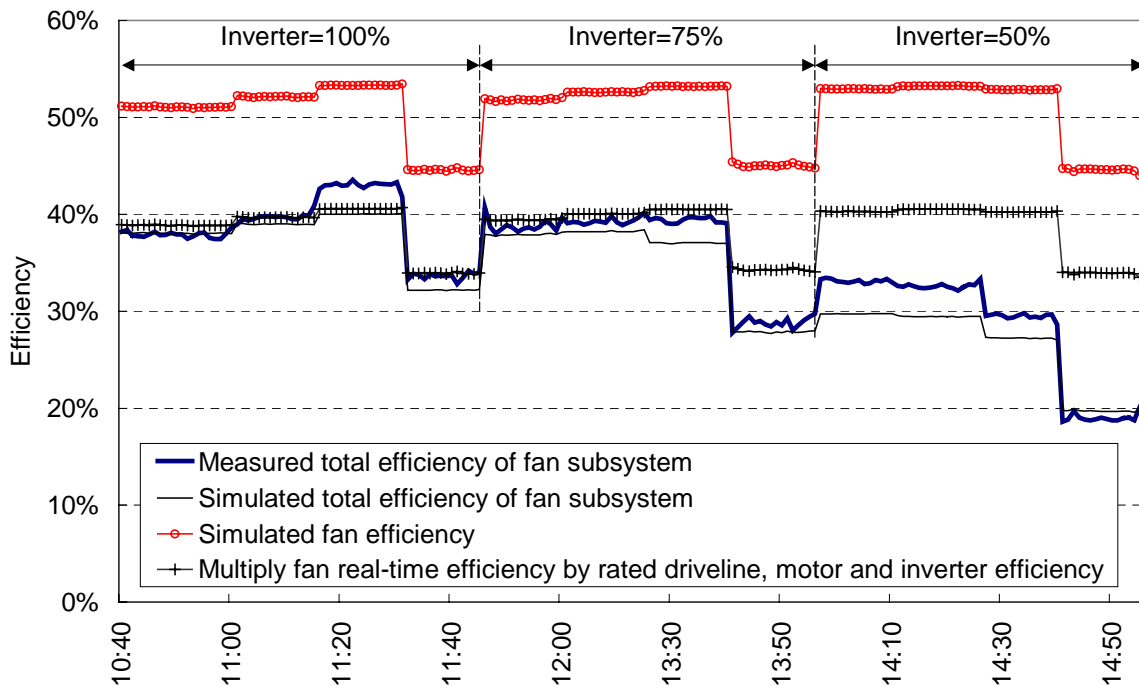


Figure 5.13 Simulation accuracy of total energy consumption model

The average difference between the simulated and measured total efficiency of fan subsystem is 5.1% and the maximum difference is 12.4%. There are two possible reasons that can explain the difference. One is that the belt efficiency is assumed to be constant, but in fact it varies at different fan rotation speeds. The other possible reason is that the motor efficiency model is fitted using the data at conditions of constant frequency and various load factors, whereas the motor actually ran under conditions of variable frequency and load factor. Nevertheless, the 5.1% average simulation difference is accurate enough for the applying this total energy consumption model to commission a fan subsystem.

5.5 APPLICATION FOR AUTOMATED ON-GOING COMMISSIONING

Automated on-going commissioning of fan subsystem is to continuously monitor the operation of a fan subsystem to determine whether the subsystem is running normally or not and detect and diagnose faults if the subsystem is running abnormally during the operational phase. This total energy consumption model of a fan subsystem can fulfill this purpose using the continuously measured fan supply air volume, fan head pressure or inverter output frequency, and total power consumption of the fan subsystem. Figure 5.14 shows how to use this total energy consumption model for automated on-going commissioning of a fan subsystem. The following procedure explains in detail the calculation step shown in Figure 5.14.

1) From BEMS collect data that are necessary for simulation, i.e. air volume, inverter output frequency or head pressure, and total energy consumption of a fan subsystem. Sample time interval is recommended to be one minute.

2) If pressure head is measured by BEMS, calculate the fan's dimensionless air-flow rate C_f using Equations 5.8 and 5.7.

3) If pressure head is not measured, calculate fan rotation speed using Equation 5.10 and then calculate C_f using Equation 5.9. Calculate head pressure using Equation 5.14 and 5.15.

4) Use Equation 5.3 and C_f to calculate the fan efficiency η_f .

5) Use Equation 5.6 and fan efficiency, airflow rate and pressure head to calculate load factor.

6) Use load factor and Equations 5.4 and 5.5 to calculate the motor and inverter efficiency.

7) Use Equations 5.2 and 5.1 to calculate the total efficiency and total energy consumption of the fan subsystem.

By comparing the simulated total power consumption of the fan subsystem with the measured real power consumption, it can be determined whether there are faults that are influencing the performance of the fan subsystem. If the measured data match the simulated data within the error range of the model, it can be concluded that the fan subsystem is running normally. Otherwise if differences between the measured power consumption and simulated power consumption exceed the predetermined threshold, the conclusion can be drawn that some faults are influencing the fan subsystem. We recommend that the threshold of the average difference between measured and simulated total power consumption during three hours is 15%. By comparing the symptom with a rule base, the most likely reason for the fault can be given as a diagnosis.

For a building with several identical fan subsystems, after this model is identified, it can be used to monitor all of them. It can save commissioning work, time and cost compared to measuring each of the subsystems one by one.

5.6 APPLICATION CASE STUDY

In order to verify whether this total energy consumption model can detect a fault occurring in a fan subsystem, an application case was studied in which the fan belts of a fan subsystem were loosened through replacing the proper size belts with larger size ones. Under this condition, the supply air volume, head pressure and total power consumption of the fan subsystem were measured once a minute.

In order to measure the fan performance over a full range, the inverter output frequencies were manually set at 100%, 75%, 50%, and 40% of rated frequency, 50 Hz, instead of being controlled automatically. Corresponding to every inverter output frequency, the VAV box demand supply air flow rates were manually set at 100%, 75%, 50%, and 30% of the rated airflow rate, which is 4000 m³/h.

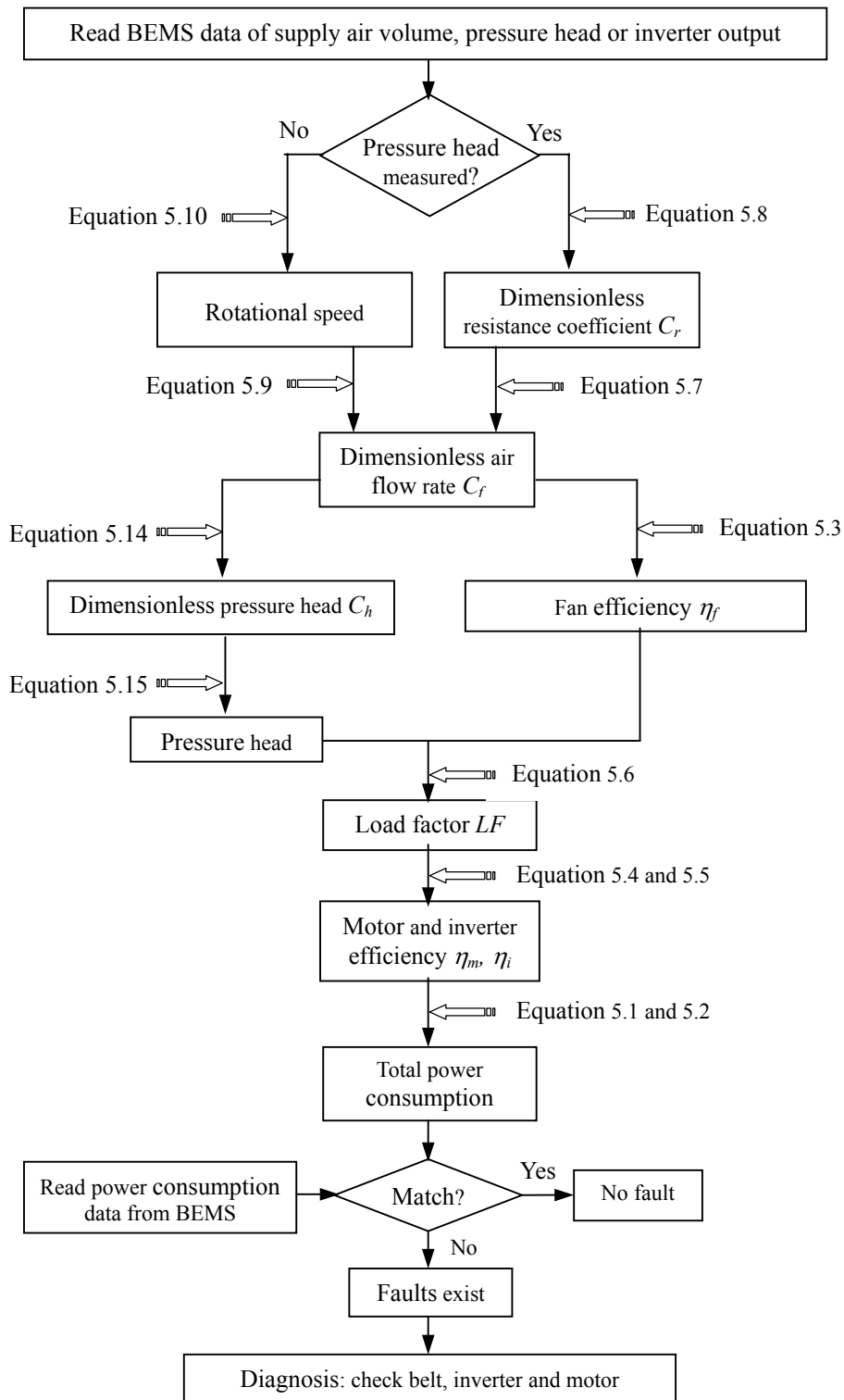


Figure 5.14 Flowchart of automated on-going commissioning for fan subsystem using total energy consumption model

The total energy consumption model was used to simulate the total power consumptions of the fan subsystem, which represent the performance of the fan subsystem without faults. The simulated and measured power consumptions were compared to determine whether there were some faults that were influencing the operation. In order to make the comparison reasonable and valid for detecting faults, the simulated power consumption was calculated using the same airflow rate and pressure as that of the fan subsystem with loose belts installed. If same the airflow rate and the same pressure are delivered, the power consumed by the fan subsystem with tight belts should be less than that consumed by the fan subsystem with slipping belts. Alternatively stated, a fan subsystem with loose belts would deliver less airflow and the motor would experience a reduced load, thus reducing the total power consumption of the fan subsystem. This fault condition could be detected using the fan subsystem model.

Figure 5.15 shows the difference between the simulated total power consumption of the fan subsystem without faults and measured total power consumption of the fan subsystem with the fault of loose belts. The average difference between the simulated and measured energy consumption of fan subsystem is 21.9% and the maximum difference is 61.7%. During high rotation speed, the influence of loose belts is significant and the difference between simulated and measure data is up to 61.7%. During low rotation speed, the influence of loose belts is insignificant and less than the simulation error. These symptoms can be used to develop rules used for fault detection and diagnosis. The average difference of 21.9% shows that the simulation using this total energy consumption model can easily detect this fault. This model is useful for on-going commissioning during the operations phase of a building.

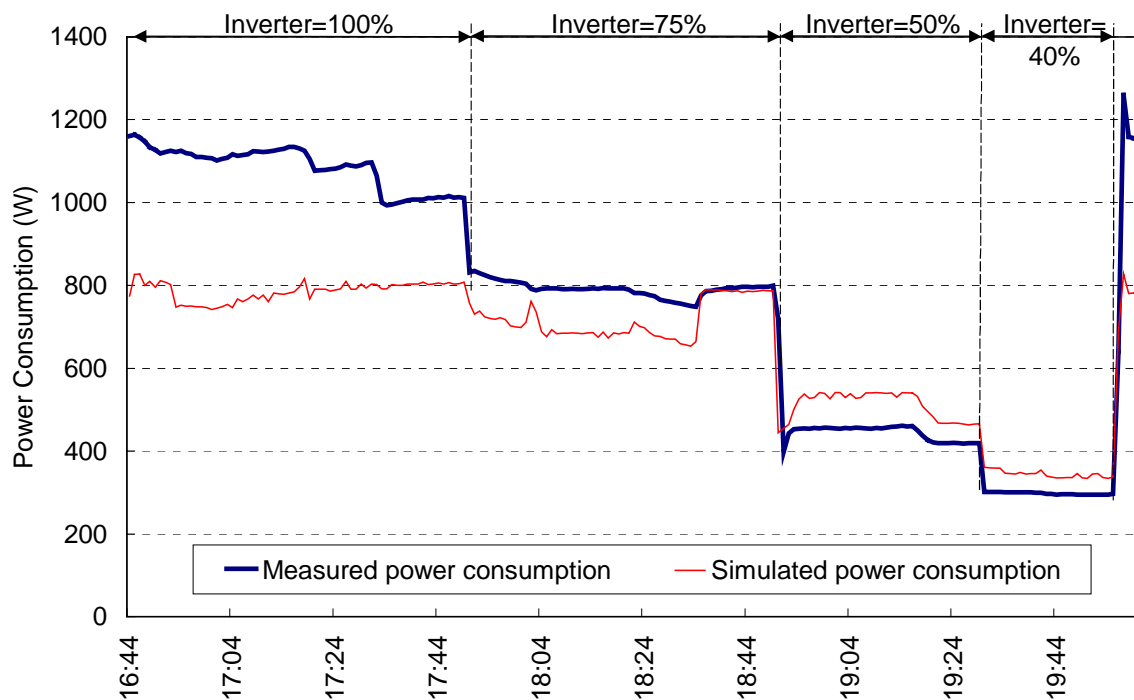


Figure 5.15 Total power consumption of a fan subsystem with slipping belts Compared with simulated value with tight belts

5.7 SUMMARY

From the discussion in this chapter, the following conclusions can be drawn.

1) This chapter proposed a total energy consumption model of a fan subsystem, in which motor, inverter, driveline and fan efficiency are taken into consideration. This total energy consumption model can simulate the total electric power consumption using fan supply air volume and fan head pressure. It avoids the difficulty of measuring a fan's shaft power to verify the performance of the fan during the operational phase. This model is useful for automated on-going commissioning of fan subsystem through continuously comparing the simulated total electric power consumption and measured data of a fan subsystem because its input variables can be obtained easily and continuously through a BEMS. This model is based on a theoretical analysis of the physical characteristics of fan subsystem components. It is suitable for all fan subsystems consisting of same components.

2) A dimensionless variable C_r , which is the dimensionless resistance coefficient of airflow, was proposed to simulate fan efficiency in order to solve the problem of determining the exact rotation speed of a fan subsystem with driveline that might slip, such as v-belt and band belt. VAV systems are increasingly installed with an airflow rate sensor

for VAV control, which can be utilized to provide data for this total energy consumption model.

3) The simulation accuracy of this total energy consumption model was verified using a real VAV system. The average difference between the simulated and the measured total electric power consumption of the VAV system is 5.1%, which is accurate enough to monitor the operation of fans, drivelines, motors and inverters during operational phase and to detect the faults of energy-inefficient of a fan subsystem.

4) Application of this total energy consumption model of fan subsystem for automated on-going commissioning was explained and demonstrated using an experimental study of a real fan subsystem with loose belts. The case study shows that using the model is able to detect the fault of loose belts. By using the model in a BEMS configured with an appropriate set of rules, the building operator could be given possible reasons for the fault as a diagnostic result.

CHAPTER 6

EXPERIMENT STUDY ON THE ON-GOING COMMISSIONING OF A REAL VAV SYSTEM

6.1 INTRODUCTION

This chapter studies the characteristics of on-going commissioning for a variable air volume (VAV) system through conducting a set of experiments on a real VAV system in the office building of the Yamatake Building System Company in Tokyo Japan. The experimental building and experimental VAV system position are shown in Figure 6.1. The experimental building and VAV system profile data is listed in Table 6.1. The plan of the experimental VAV system is shown in Figure 6.2.

This VAV system consists of one AHU and four VAV boxes. The AHU consists of return air fan section, mixing section, coil and humidifier section, and supply air fan section. Two automated control systems optimize the system operation. The first is supply air temperature control system, which controls the water valve position according to supply air temperature using proportional and integral algorithm. The second is the supply air volume control system, which controls the variable frequency inverter to change the fan rotational speed and air volume and controls the VAV box dampers' position according to the room air temperature and supply air pressure using PI algorithm. The components and control systems are shown in Figure 6.3.

Table 6.1 Profile of experimental building and VAV system

Parameter	Parameter Value
Building use	Office
Building area (m ²)	1404.5
Number of building floors	4
Floor area the VAV system takes charge of (m ²)	100.2
Rated air flow rate (m ³ /h)	4000
Minimum air flow rate (m ³ /h)	1400
Rated supply/return air fan pressure head (Pa)	879/586
Rated supply/return air fan power (kW)	2.2/1.5
Rated fan rotational speed (r/m)	1870
Fan wheel diameter (mm)	400
Number of VAV box	4



Figure 6.1 Experimental building and VAV system location

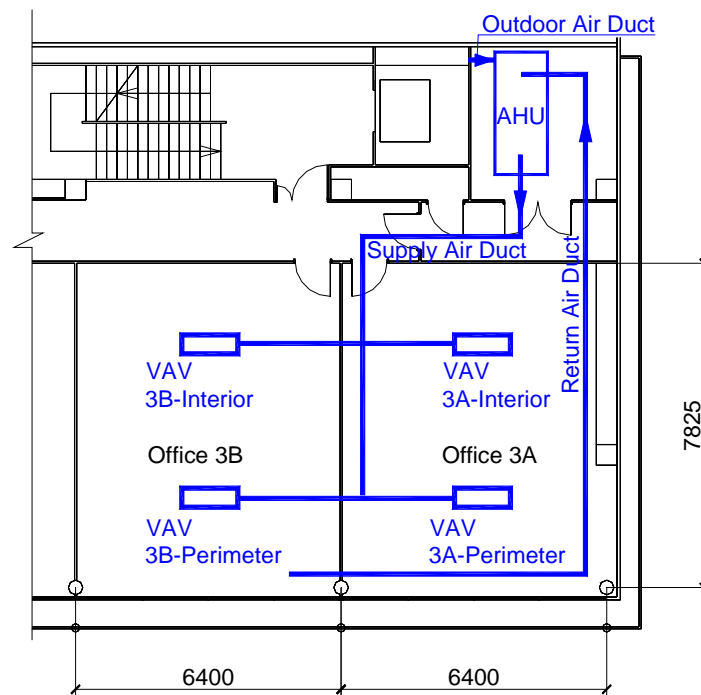


Figure 6.2 Experimental VAV system plan configuration

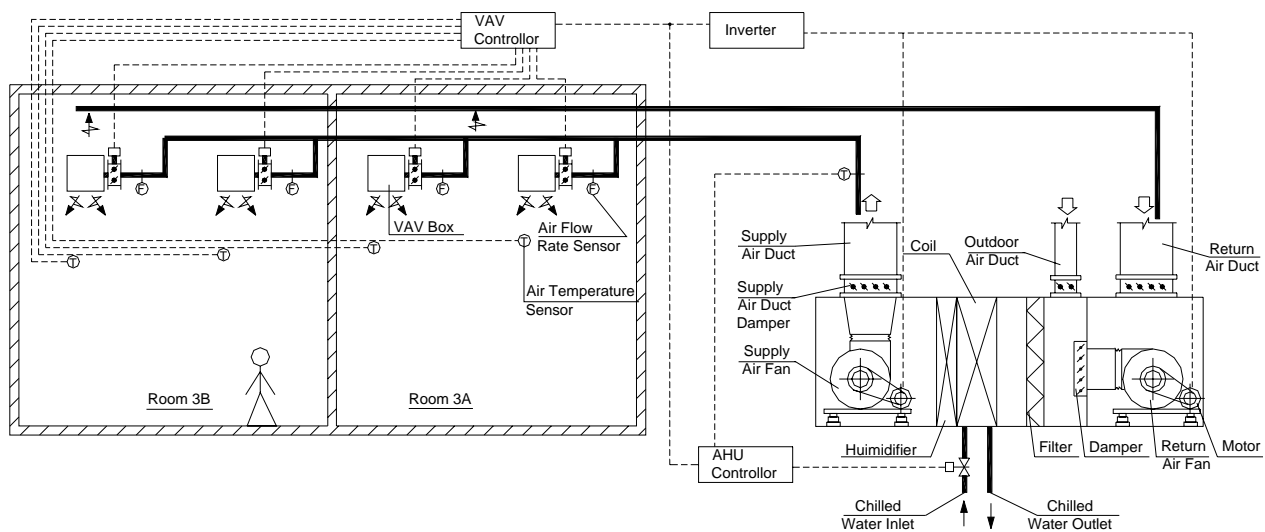


Figure 6.3 Experimental VAV system components and control systems

The building energy management system measures and records the supply, return and outdoor air volume, air temperature, and water temperature. These BEMS measured data were used to analyze the experiment results to check the commissioning characteristics of the VAV system. Because BEMS does not measure the supply air fan pressure head and supply air fan subsystem power consumption, they were measured using a manometer and a

power meter and automatically recorded every minute using a data logger.

The following four types of faults were selected to introduce into the VAV system, which are problems amenable to automated on-going commissioning (Yoshida, 1996, Brambley, 2002).

- 1) Low efficiency fan subsystem
- 2) Malfunctioning supply air and room air temperature sensor
- 3) Stuck outdoor air damper
- 4) Stuck AHU water valve

6.2 LOW EFFICIENCY FAN SUBSYSTEM

The purpose of this experiment is to check the performances of a fan subsystem that is running low-efficiently and use these data to verify or develop fan subsystem models suitable for on-going commissioning.

6.2.1 EXPERIMENTAL METHOD

The fan subsystem efficiency was lowered through loosening the fan belts. The normal size fan belts were replaced using bigger size belts. The invert output frequency and VAV demand supply air volume were set at several different values, as shown in Figure 6.4, to make the fan subsystem work in a full range. The invert output frequency was fixed at 100%, 75%, 50% and 40% of the rated frequency, 50 Hz. The set point of maximum demand air volume, 4000 m³/h, is used to make the VAV box dampers 100% open. The minimum demand air volume, 1440 m³/h, is to make the VAV box dampers be opened at the minimum level.

The total power consumption was measured every one minute. The measurement point is at the power switch so that this total power consumption includes the energy consumed by all the fan subsystem components, i.e., frequency inverter, motor, driveline, fan and the air kinetic energy. The measurement point and power consumption meter are shown in Figure 6.5.

The pressure differences between fan inlet and outlet were measures to obtain the fan

pressure heads using a manometer, as shown in Figure 6.6. The AHU supply air fan's specification curve is shown in Figure 6.7.

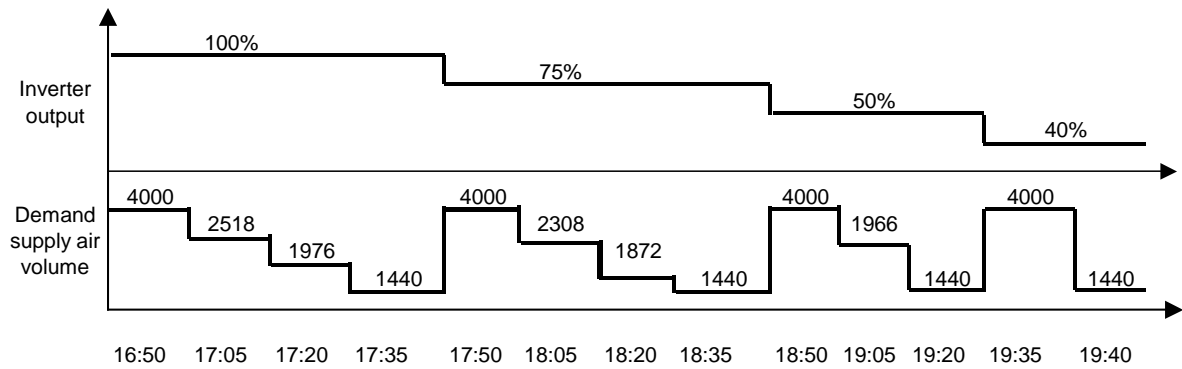


Figure 6.4 Experiment steps and parameters of loose fan belts



Figure 6.5 Power consumption measurement point and instrument



Figure 6.6 Fan pressure head measurement

Fan Performance Curve

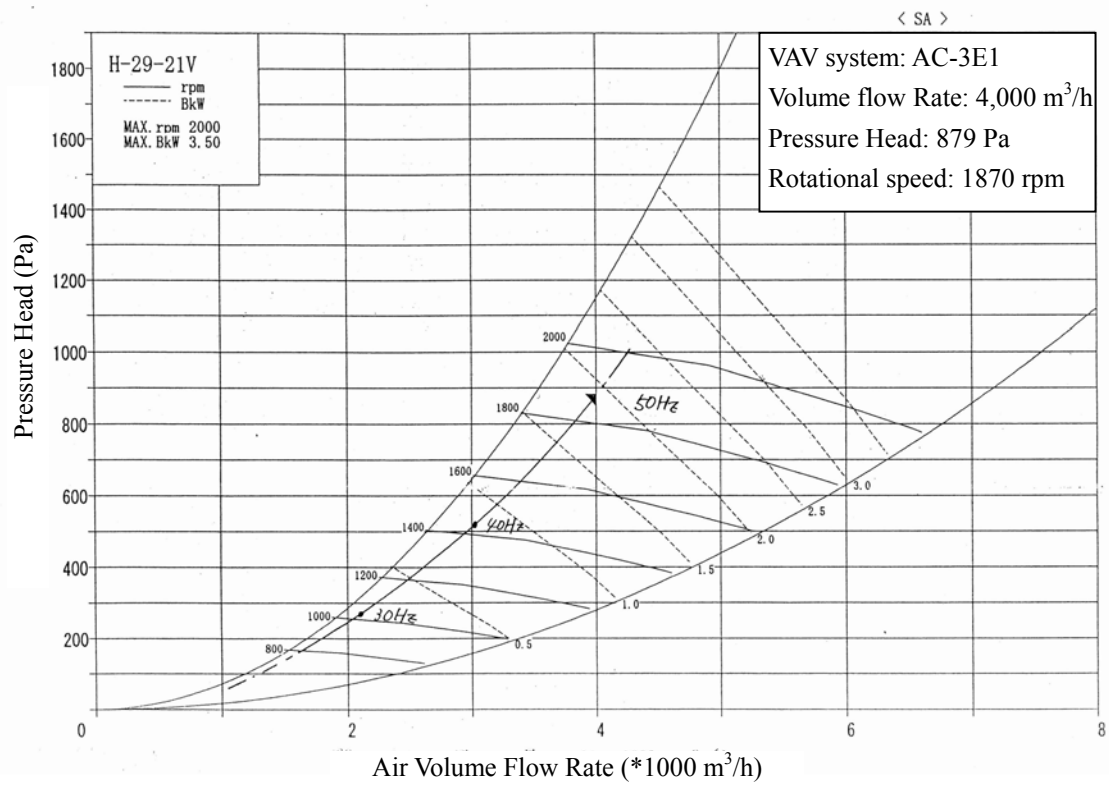


Figure 6.7 Experimental fan specification curves

As a reference, the performance of the fan subsystem with normal tight belts was measured using the same steps and parameters as the loose belts experiment.

6.2.2 RESULTS, DISCUSSION AND CONCLUSIONS

The experiment results were shown in Figure 6.8. The fan subsystem efficiency is calculated using Equation 6.1, which is the total efficiency including all the fan subsystem components' efficiency. The total efficiency of fan subsystem with loose belts was compared with the total efficiency of the fan subsystem with normal tight belts, which is calculated using the measured data of the fan subsystem with normal belts. The average efficiency difference between the fan subsystem with loose belts and normal belts is 26%, which can be easily detected and shows the possibility of automated commissioning of fan subsystem during operation phase through comparing measured real-time operation data with simulated normal operation data using design conditions.

$$\eta = \frac{V \cdot PH}{E_t} \tag{6.1}$$

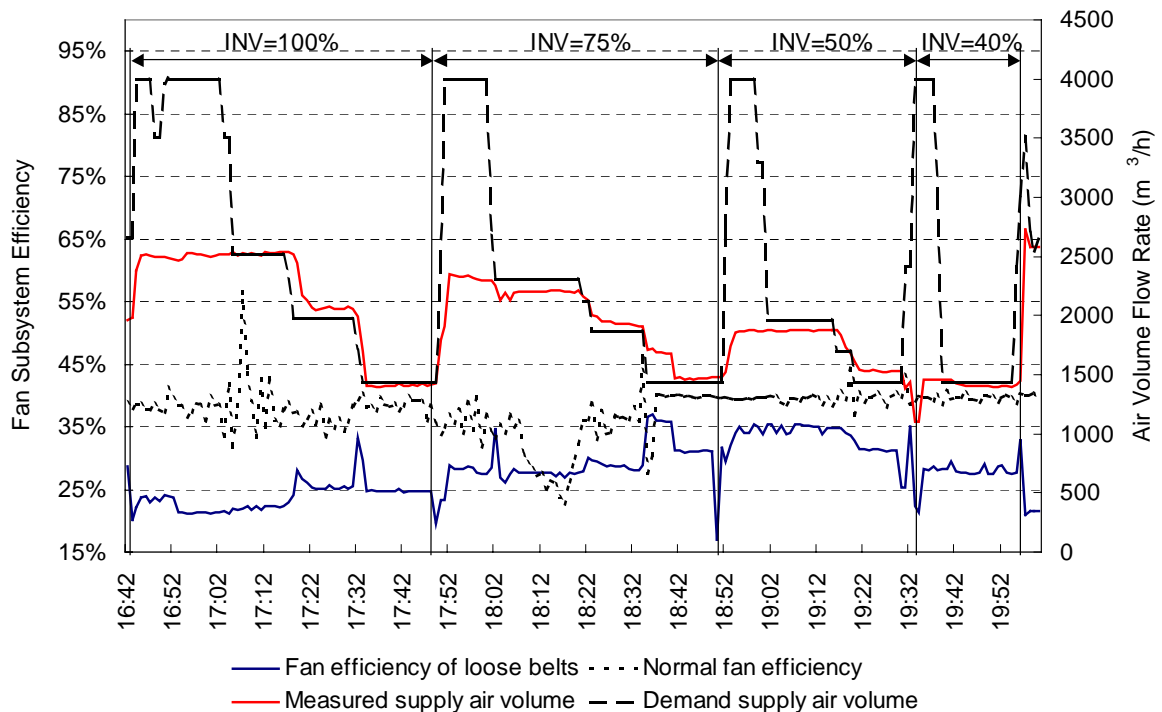


Figure 6.8 Experiment results of loose fan belts

Besides the total efficiency of fan subsystem, the actual supply air volume either cannot match the demand supply air volume especially when the demand air volume is close

to the maximum value. During the experiment period, the average measured supply air volume is 17.8% lower than the average of demand supply air volume, and the maximum supply air volume is 36.8% lower than demand value. This phenomenon shows that during operation phase this fault can be detected through comparing the real supply air volume with demand supply air volume.

From this experiment, it was found that hysteresis of BEMS data recording should be considered if BEMS data are used for on-line simulation. When the position of VAV box dampers changed, the BEMS recorded pressure, air flow rate, and power didn't change simultaneously. It took three minutes to reach steady state. The data in this hysteresis period should not be used for calculate, otherwise large error could be generated. For example, on 17:19 the fan rotation speed kept constant but the VAV box damper status changed. The pressure increased from 388 Pa to 458 Pa, power decreased from 1125 W to 1105 W, and air flow rate decreased from 2515 m³/h to 2446 m³/h. However, three minutes later at 17:22, pressure, power and air flow rate reached steady values of 477 Pa, 1079 W and 2062 m³/h. The calculated fan subsystem efficiency at 17:19 was 28.2%, compared with the efficiency of 23.7% in the steady period three minutes later. The relative error is 18.6%, which is considerably large. Therefore the BEMS data in the unsteady period after components' status change should be avoided using for simulation and calculation.

6.3 MALFUNCTIONING SUPPLY AIR AND ROOM AIR TEMPERATURE SENSOR

The purpose of these two experiments is to check respectively the performances of a VAV system when the supply air temperature sensor or room air temperature sensor is deviating from the correct measurement. The performances were analyzed to find a method that can be used for on-going commissioning.

6.3.1 EXPERIMENTAL METHOD

These two experiments used same method to make sensors deviate from normal measurement, which was that the sensor outputs were added an offset through building energy management system (BEMS). The offset of supply air temperature sensor was 3.6°C, which was the 20% of the temperature set point 18°C. The offset of room air temperature sensor was 1°C, which was the 5% of the temperature set point 24°C. The supply air volume flow rate was measured to analyze the influence of the sensor offset.

6.3.2 RESULTS, DISCUSSION AND CONCLUSIONS

During cooling period if the supply/room air temperature sensor measurement deviates from the true value, an automatically controlled VAV system's response should be as what is shown in Figure 4.6 and Figure 4.8 in chapter 4.

The experiment results are shown in Figure 4.7 and Figure 4.9 in chapter 4. When supply air temperature sensor offset was +20%, the average total supply air volume was 4% lower than that of no offset, and the supply air volume reached the minimum value, which caused the average air temperature of room 3B-perimeter 0.7°C lower than set point. When the supply air temperature sensor offset was -20%, the average total supply air volume was 36.7% higher than that of no offset. When room air temperature sensor offset was +5%, the average supply air volume was 94.5% higher than that of no offset. When room air temperature sensor offset was -5%, the average supply air volume is 13.8% lower than that of no offset. Furthermore, when offset was -5%, the supply air volume reached the minimum value and room air temperature is 0.8°C lower than set point. The experiments results are summarized in Table 6.2.

Table 6.2 Experimental results of malfunctioning temperature sensor

	Supply air temperature sensor		Room air temperature sensor	
	Offset +20%	Offset -20%	Offset +5%	Offset -5%
$\frac{V_{off} - V_{nor}}{V_{nor}}$	-4%	36.7%	94.5%	-13.8%
Supply air volume reached maximum?	No	No	No	No
Supply air volume reached minimum?	Yes	No	No	Yes
Room 3B-perimeter average air temperature deviated from set point?	0.7°C	No	No	-0.8°C

These experiment results show that during operational phase the fault of malfunctioning supply/room air sensor can be detected through comparing the real-time supply air volume with normal supply air volume that is controlled according to correct sensor measurement. Because during operational phase a large amount of operation data

might have been accumulated and recorded since the HVAC systems begin to serve and these recorded operational data are correct operation without faults because of the conducting of initial commissioning, these past operational data records can be used as criteria to verify the current operation. This past no-fault operational data records comparison is a possible on-going commissioning method for continuously commissioning sensor during operational phase.

6.4 STUCK AHU OUTDOOR AIR DAMPER

The purpose of this experiment is to check the VAV system performances when the AHU outdoor air damper is stuck and to find a method that can be used for on-going commissioning outdoor air damper.

6.4.1 EXPERIMENTAL METHOD

The outdoor air damper's opening was fixed at 100%, 70%, 40%, and 0%. Corresponding to every fixed position, the demand supply air volume was set at four statuses, which are 4000 m³/h, 3000 m³/h, 2000 m³/h, and automatically controlled. The experiment parameters are shown in Figure 6.9.

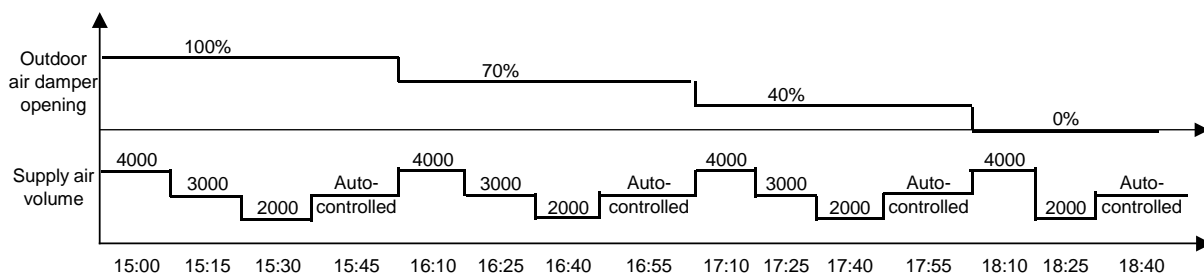


Figure 6.9 Experimental steps of stuck AHU outdoor air damper

6.4.2 RESULTS, DISCUSSION AND CONCLUSIONS

Figure 6.10 shows the experiment results. When outdoor air damper position changed from 100% to 40%, the ratio of outdoor air volume flow rate to supply air volume flow rate is almost constant. Only when the damper opening was very small, the outdoor air volume ratio became small. This is caused by that the nonlinear characteristic of the damper made the air flow resistance change little when damper opening changes from 100% to 40%, i.e. the air flow resistance coefficient of outdoor air duct branch R_{od} is almost constant.

The fault of fixed outdoor air damper can be detected through continuously monitoring

the ratio of outdoor air flow rate to supply air flow rate. If this ratio is almost constant, the outdoor air damper might be stuck. The reason is that the resistance of outdoor air duct branch will be constant if the outdoor air damper is stuck. The resistant of return air duct branch R_{re} is almost constant. Therefore the ratio of R_{re} to R_{od} is almost constant, assuming to be r . The total resistance coefficient of the parallel-connected outdoor air duct and return air duct are as shown in Equation 6.2. The pressure loss of the parallel-connected duct branch is equal, as shown in Equation 6.3. The ratio of outdoor air flow rate to supply air flow rate will be constant, as shown in Equation 6.4.

$$R_t = \frac{1}{\frac{1}{R_{od}} + \frac{1}{R_{re}}} = \frac{1}{\frac{1}{R_{od}} + \frac{1}{rR_{od}}} = \frac{R_{od}}{1 + \frac{1}{r}} \quad (6.2)$$

$$\Delta P = R_t V_t^2 = R_{od} V_{od}^2 \quad (6.3)$$

$$\frac{V_{od}}{V_t} = \sqrt{\frac{R_t}{R_{od}}} = \sqrt{\frac{1}{1 + \frac{1}{r}}} \quad (6.4)$$

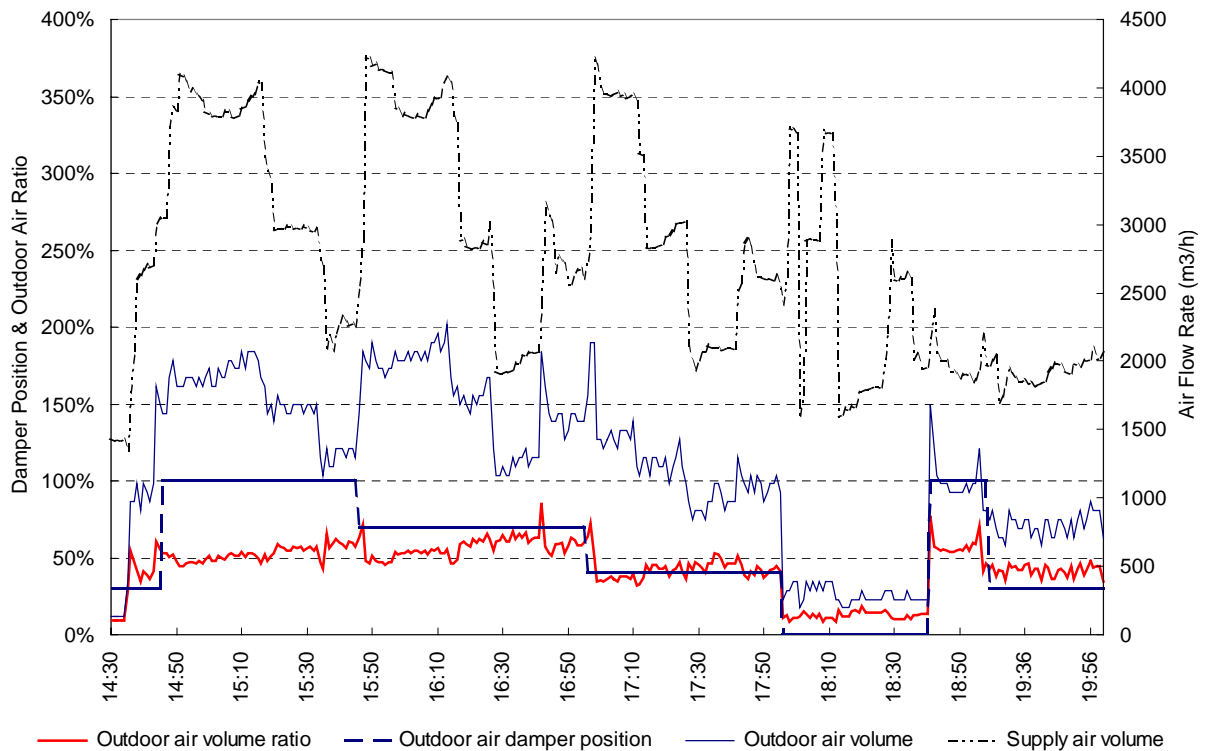


Figure 6.10 Experimental results of stuck AHU outdoor air damper

6.5 STUCK AHU WATER VALVE

The purpose of this experiment is to check the VAV system performances with a stuck AHU water valve and to develop a method that can be used for on-going commissioning AHU water valves.

6.5.1 EXPERIMENTAL METHOD

The AHU supply air flow rate was fixed at 4000, 3000, 2000 and 1440 m³/h. Corresponding to every flow rate, water valve was fixed at 100%, 66% and 33%. The experiment parameters and steps are shown in Figure 6.11.

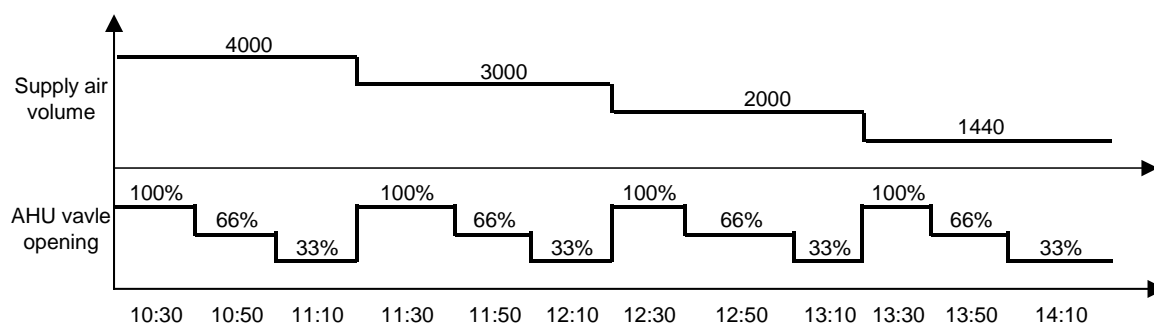


Figure 6.11 Experimental steps of stuck AHU water valve

6.5.2 RESULTS, DISCUSSION AND CONCLUSIONS

Figure 6.12 shows the experiment results. If the water valve was fixed, the supply air temperature cannot match the set point. The maximum supply air temperature is 5.2°C higher than the set point and minimum supply air temperature is 0.9°C lower than the set point. Therefore the on-going commissioning of water valve can be achieved through comparing the real supply air temperature with set point. Beside this, comparison of demand valve positions with real position can also detect the fault of stuck water valve, as discussed in chapter 4.

6.6 SUMMARY

This chapter described four experiments that focused on studying the on-going commissioning of a real VAV system. From these experiments three major conclusions can be drawn.

1) Automated on-going commissioning is feasible through using simulation analysis if simulation models suitable for on-going commissioning are available. The experiments' results show that the values of some parameter will deviate from normal range if some fault

is influencing the running of the VAV system. Therefore automated on-going commissioning can be achieved through continuously comparing the real-time performance data with simulated correct data. If the real-time values of some parameter are deviating from simulated value, some fault related to this parameter might exist and could be detected.

2) Operational records are useful for continuously commissioning sensors. If a sensor offsets, the automatic control result will make some parameters deviate from normal value. Through monitoring the supply air volume compared with recorded past no-fault operational data can detect whether supply air temperature sensors and room air temperature sensors offset or not.

3) Hysteresis should be considered in order to improve the on-line on-going commissioning accuracy. Experiment results show that when the status of a component changes, some variables, such as supply air volume and air temperature, do not change immediately and simultaneously but delay for about three minutes. The data in this period should be eliminated, otherwise calculated results using non-simultaneous data will produce large error.

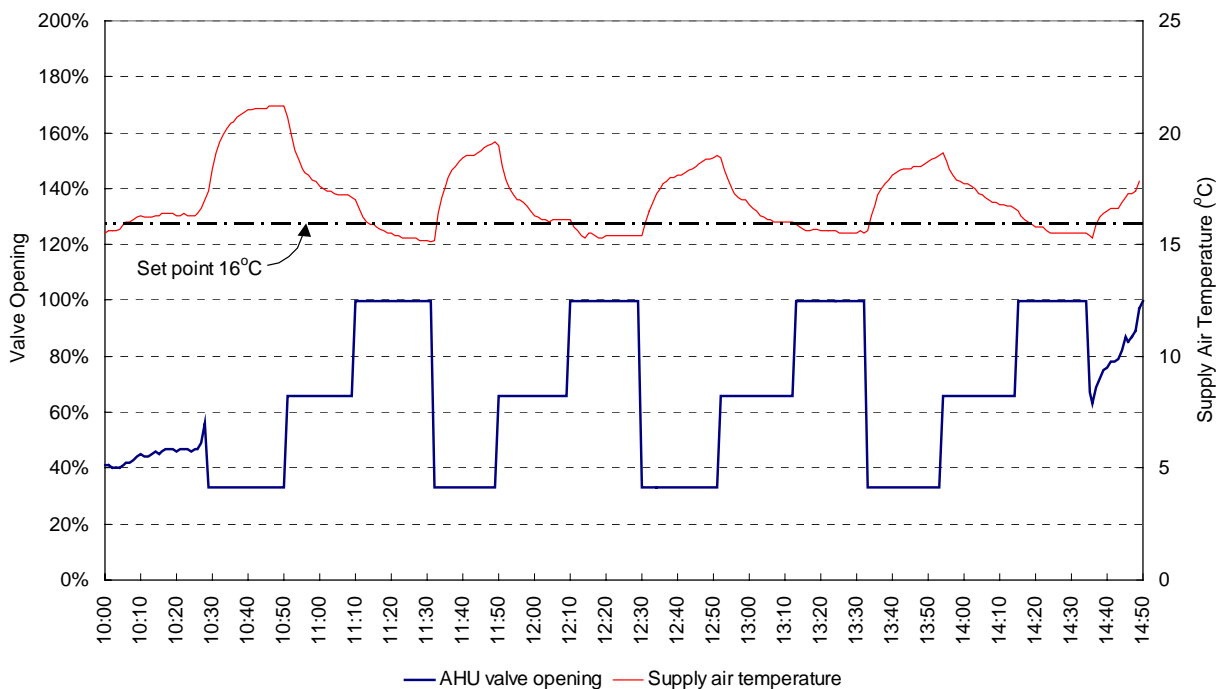


Figure 6.12 Experimental results of stuck AHU water valve

CHAPTER 7

MODEL-BASED COMMISSIONING FOR FILTERS IN ROOM AIR-CONDITIONERS

7.1 INTRODUCTION

Most researches about filters in a Heating, Ventilating and Air-Conditioning (HVAC) system study the capability of a filter to retain particles, dust, bacteria and molds (Moritz, 2001), survival and growth of microorganisms on a filter (Kemp, 2001), releasing Volatile Organic Compounds (VOC) from a filter (Hytinen, 2003, Ruden, 1999). Papers can seldom be found about the influence of filter fouling on energy consumption. However, a measurement done by this research shows that an Gas-fired-engine Heat Pump (GHP) indoor unit fan efficiency decreased 35.8% when the filter resistance increased to twice of initial resistance because of dust accumulation as shown in Figure 7.1. Furthermore, this research studied the heat produced by the GHP during winter. The heat production decreased 33.1% when the filter resistance doubled, as shown in Figure 7.1. So filter fouling can not only decrease fan efficiency, but also decrease the heating/cooling capacity of room air-conditioners. It is important to timely detect an over-fouled filter and clean or replace it. Generally room air-conditioners are not equipped with pressure sensor to measure air flow resistance through a filter, which represents the filter-fouling situation. So it is necessary to develop a method to estimate air flow resistance through a filter without the requirement of adding filter pressure sensor for the purpose of saving the cost of pressure sensors, which is relatively expensive.

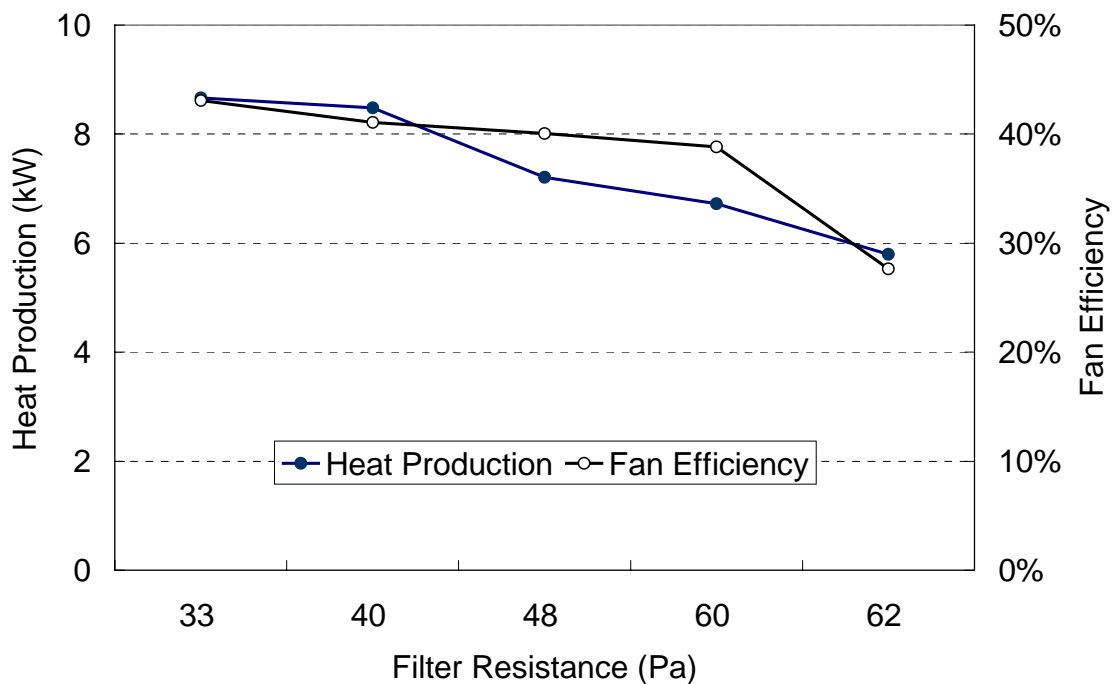


Figure 7.1 GHP heat production and fan efficiency vs. filter resistance

For the purpose of detecting filters’ fouling situations without pressure sensor, this research focuses on developing a model that is able to estimate the air flow resistance through a filter only using air-conditioner’s thermal or energy performance data. For the increasingly spreading multi-evaporator air-conditioners, which are equipped with refrigerant pressure and temperature sensor and room air temperature sensor for the purpose of controlling and balancing the heating/cooling capacity of each indoor unit, the air-conditioners’ thermal performance data are available requiring no additional sensor. So it is feasible to develop a model to estimate filter resistance using currently obtainable data.

Such a model is useful for commissioning a room air-conditioner. As defined by ASHRAE, building commissioning is the process of ensuring that building systems are designed, installed, functionally tested, and capable of being operated and maintained to perform in conformity with the design intent (ASHRAE, 1996). Commissioning is considered to be a viable method to help ensure energy-efficient operation of buildings and their efficiency conservation measures (BPA, 1992). Based on the filter model, a commissioning method for filters in room air-conditioners is proposed for the sake of ensuring the energy-efficient operation of room air conditioners.

7.2 MODELS

The model proposed to estimate filter resistance is shown in the following equations.

$$\Delta P_{ft} = \Delta P_f + \frac{\rho v_i^2}{2} - \Delta P_{OC} - \frac{\rho v_o^2}{2} \quad (7.1)$$

$$\Delta P_f = \rho_a N^2 D^2 C_h \quad (7.2)$$

$$C_h = a_0 + a_1 C_f + a_2 C_f^2 + a_3 C_f^3 + a_4 C_f^4 \quad (7.3)$$

$$C_f = \frac{V_a}{ND^3} \quad (7.4)$$

$$\Delta P_{OC} = \xi \frac{\rho_a v_{fo}^2}{2} \quad (7.5)$$

$$v_i = \frac{V_a}{A_i}, \quad v_o = \frac{V_a}{A_o}, \quad v_{fo} = \frac{V_a}{A_{fo}} \quad (7.6)$$

$$V_a = \frac{E \eta_f}{\Delta P_f} \quad (7.7)$$

$$\eta_f = e_0 + e_1 C_f + e_2 C_f^2 + e_3 C_f^3 + e_4 C_f^4 \quad (7.8)$$

If indoor unit fan power consumption E is unavailable, indoor unit air flow rate can be estimated using Equation 7.9, 7.10, and 7.11 instead of Equation 7.7 and 7.8.

$$V_{a,su} = \frac{m_{ref}(h_{ref1} - h_{ref3})}{\rho_a (h_{ao} - h_{ai})} \quad (7.9)$$

$$V_{a,w} = \frac{m_{ref}(h_{ref2} - h_{ref3})}{\rho_a C_{pa} (T_{ao} - T_{ai})} \quad (7.10)$$

$$m_{ref} = C_{EV} A_{EV} \sqrt{\rho_{ref} (P_3 - P_4)} \quad (7.11)$$

Equation 7.1 is used to calculate a filter's resistance to air flow ΔP_{ft} by subtracting resistance of coil etc. ΔP_{OC} from fan pressure head ΔP_f . A typical air-conditioner indoor unit

of cassette-shape, shown in Figure 7.2, is used as an example to explain the pressure distribution. The pressure curve of the indoor unit is shown in Figure 7.3. Fan pressure head ΔP_f is calculated using Equation 7.2, 7.3, and 7.4 using a 4th-order function of dimensionless airflow rate C_f . Equation 7.3 is taken from HVACSIM+ (Clark, 1985). Equation 7.5 is used to calculate pressure drop of coil etc ΔP_{OC} . Equation 7.6 is used to calculate the air flow velocity at fan inlet, outlet, and air-conditioner indoor unit outlet through dividing the air flow rate V_a by inlet and outlet area. Air flow rate V_a is calculated using Equation 7.7 and 7.8 if time series fan power consumption E can be available. If fan power consumption E is unavailable, the heat balance equations between air side and refrigerant side, as shown in Equation 7.9 for summer time and Equation 7.10 for winter time respectively can be used to calculate the air flow rate V_a . The refrigerant enthalpy h_{ref} in Equation 7.9 and Equation 7.10 can be calculated using refrigerant pressure P_{ref} and temperature T_{ref} . The refrigerant state points in a refrigeration cycle are defined in Figure 7.4. The refrigerant enthalpy at state point 4 is assumed to be equal to the enthalpy at state point 3. So cooling amount of refrigerant side during summer period is calculated using refrigerant enthalpy at state point 1 and state point 3. The refrigerant property calculation software REFPROP (NIST, 2002) is used to calculate refrigerant density and enthalpy by this research. The refrigerant flow rate m_{ref} can be estimated using the expansion valve characteristics shown in Equation 7.11.

As mentioned above, this model gives two ways to estimate filter resistance using two sorts of different inputs respectively, i.e. indoor unit fan power consumption data and air-conditioner thermal performance data. The first method is simpler than the second method. The reason for proposing the second method is because the second method based on heat balance is also useful for commissioning other components. The following sections discuss the two different estimation methods in detail.

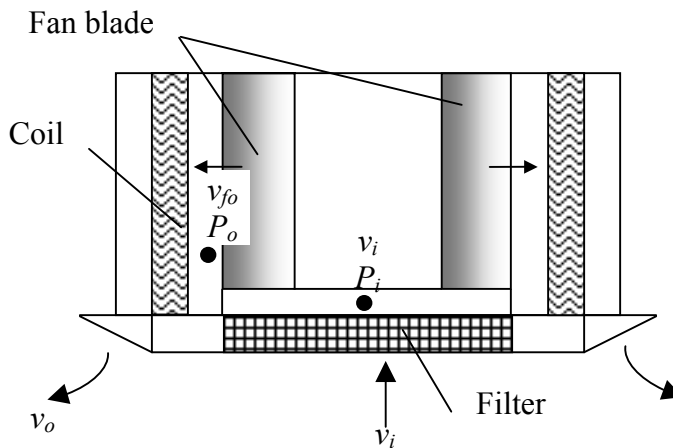


Figure 7.2 Measurement points in a typical cassette-shape indoor unit

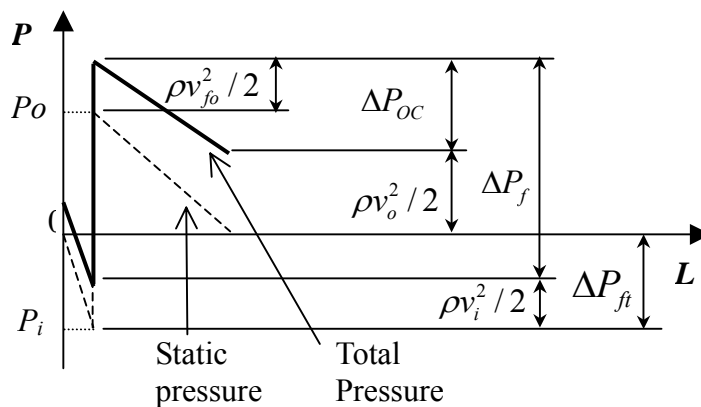


Figure 7.3 Pressure curves of indoor units

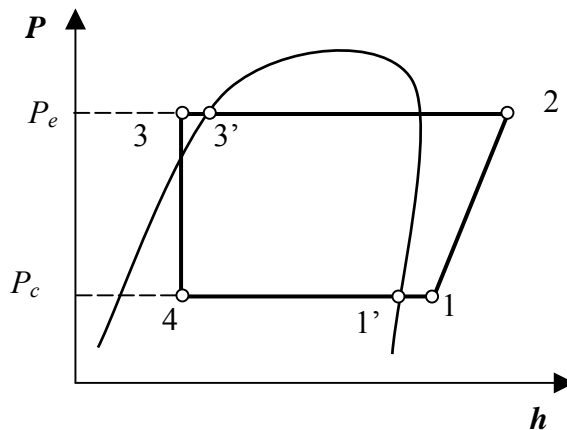


Figure 7.4 Refrigeration cycle state points

7.2.1 ESTIMATION USING FAN ENERGY CONSUMPTION DATA

As shown in Equation 7.7 and 7.8, using the power consumed by an air-conditioner's indoor unit fan is the second way to estimate air flow rate and then to estimate filter resistance. If substituting Equation 7.2, 7.4, and 7.8 into Equation 7.7, Equation 7.12 will be formed, which is an implicit function of dimensionless flow rate C_f . Iterative method can be used to solve this equation to obtain dimensionless flow rate C_f . Then filter resistance can be estimated.

$$C_f ND^3 = \frac{E(e_0 + e_1 C_f + e_2 C_f^2 + e_3 C_f^3 + e_4 C_f^4)}{\rho N^2 D^2 (a_0 + a_1 C_f + a_2 C_f^2 + a_3 C_f^3 + a_4 C_f^4)} \quad (7.12)$$

The method is suitable for the air-conditioners whose indoor unit fan power consumption is measured in real-time. Compared with the first method, which use air-conditioner thermal performance data to estimate filter resistance, this method uses less parameters and input data than the first method. The disadvantage of this method is that the fan power consumptions need to be measured.

7.2.2 ESTIMATION USING THERMAL PERFORMANCE DATA

As shown in Equation 7.9 and 7.10, an air-conditioner's thermal performance data, i.e. refrigerant condensation and evaporation pressure and temperature, supply and indoor air enthalpy or temperature, are used to calculate air flow rate and then to calculate filter resistance. For cooling operation, supply and indoor air enthalpy is used to calculate air flow rate, as shown in Equation 7.10, because air humidity changes and enthalpy is necessary to calculate the total heat exchange, which includes both sensible and latent heat. For heating operation, supply and indoor air temperature is used to calculate air flow rate, as shown in Equation 7.9 because air humidity does not change and total heat exchange equals to sensible heat exchange.

Among the required variables input to the model, only the supply air temperature is unavailable for common multi-evaporator air-conditioners. The other variables, i.e. refrigerant condensation and evaporation pressure and temperature, and indoor air temperature, are obtainable because these variables are needed for controlling the air-conditioners' operation. Because temperature sensor is cheaper than pressure sensor, it is reasonable to add a temperature sensor to an air-conditioner to measure the outlet air

temperature for estimating filter resistance instead of adding pressure sensor to measure filter resistance.

Although for heating operation adding a temperature sensor is enough to estimate filter resistance, for cooling operation only adding a temperature sensor is not enough because air enthalpy is necessary for the calculation. Not only air temperature but also air humidity is needed for calculating air enthalpy. It will not be acceptable to add both temperature and humidity sensor only for the purpose of estimating filter resistance. So air humidity has to be estimated. The following method is proposed to estimate indoor unit outlet air humidity using air temperature.

1) Indoor air relative humidity is assumed to be 54%. The reason for this assumption is that according to the statistical analysis of the room air humidity from 9:00 to 20:00 in the summer period of July 1 to August 30, 94.3% air relative humidity fall in the range of 50% to 66%, and the most frequent humidity is 54%. The statistical results are shown in Figure 7.5.

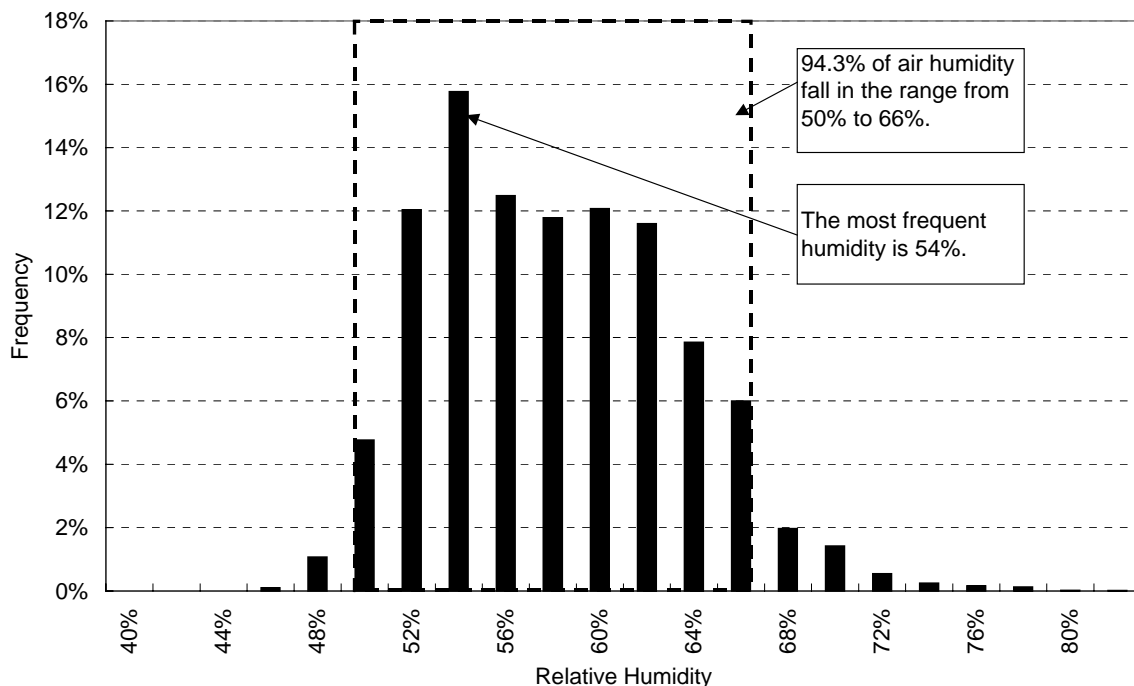


Figure 7.5 Statistical distribution of indoor air humidity in summer period

2) Outlet air humidity is determined by comparing the outlet air temperature with indoor air dew-point temperature, which can be calculated using indoor air humidity and

temperature, as shown in Equation 7.13 to 7.16 (ASHRAE, 1993). If supply air temperature is higher than indoor air dew-point temperature, the supply air humidity is assumed to be equal to indoor air humidity ratio. If supply air temperature is lower than indoor air dew-point temperature, the supply air relative humidity is assumed to be equal to 99%.

$$T_{dp} = C_{14} + C_{15} \ln(P_{wv}) + C_{16} [\ln(P_{wv})]^2 + C_{17} [\ln(P_{wv})]^3 + C_{18} P_{wv}^{0.1984} \quad (7.13)$$

$$P_{wv} = \phi P_{wv,st} \quad (7.14)$$

$$\ln(P_{wv,st}) = C_8 / T_{id} + C_9 + C_{10} T_{id} + C_{11} T_{id}^2 + C_{12} T_{id}^3 + C_{13} \ln(T_{id}) \quad (7.15)$$

$$W_a = 0.62198 \frac{P_{wv}}{P_{atm} - P_{wv}} \quad (7.16)$$

Where,

$$C_8 = -5.8002206 \text{ E} + 03$$

$$C_9 = -5.5162560 \text{ E} + 00$$

$$C_{10} = -4.8640239 \text{ E} - 02$$

$$C_{11} = 4.1764768 \text{ E} - 05$$

$$C_{12} = -1.4452093 \text{ E} - 08$$

$$C_{13} = 6.5459673$$

$$C_{14} = 6.54$$

$$C_{15} = 14.526$$

$$C_{16} = 0.7389$$

$$C_{17} = 0.09486$$

$$C_{18} = 0.4569$$

Here the dew-point temperature T_{dp} is in centigrade degree. Indoor air temperature T_{id} is in degree Kelvin.

The calculation flowchart of using this method to estimate air-conditioner outlet air humidity is shown in Figure 7.6.

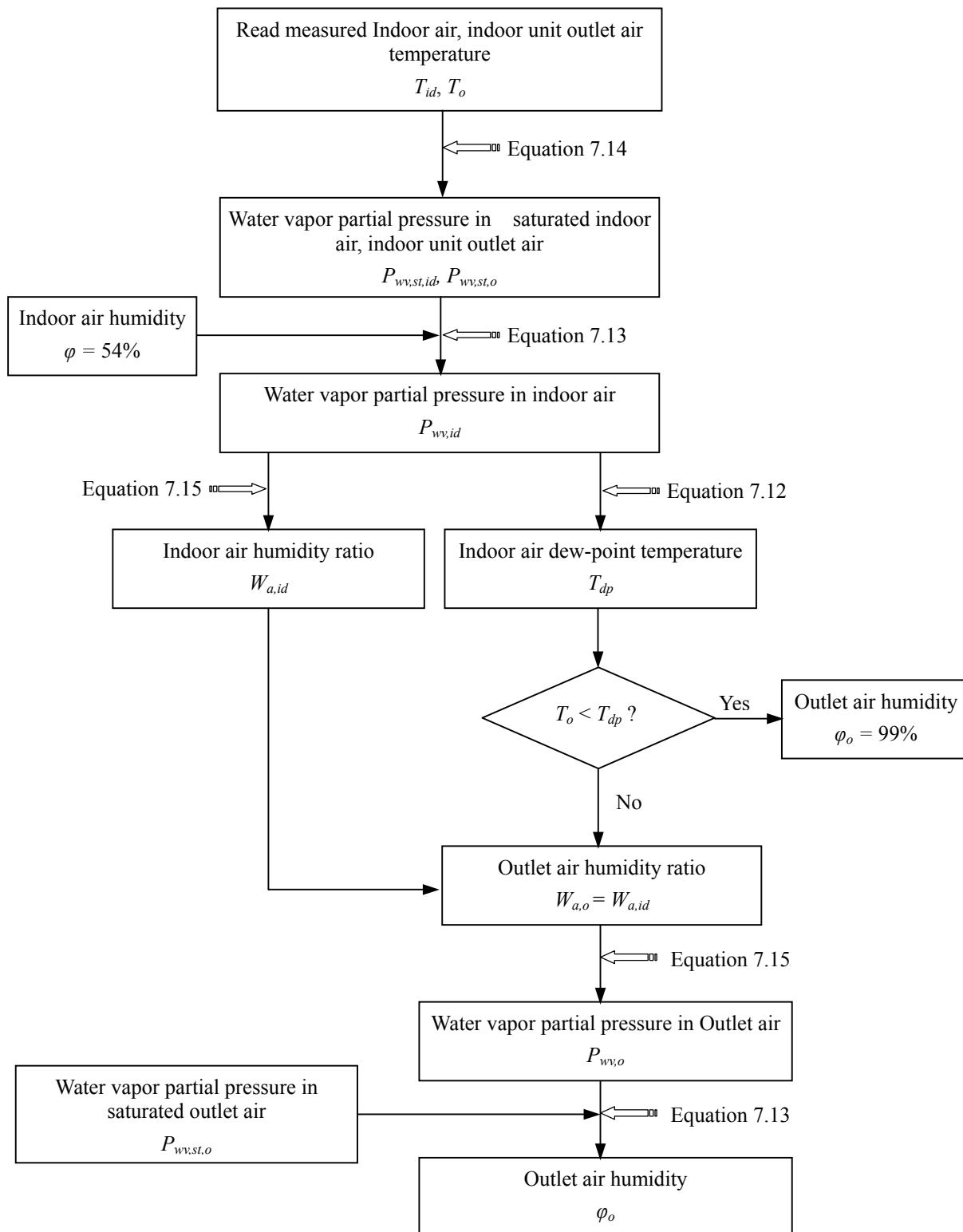
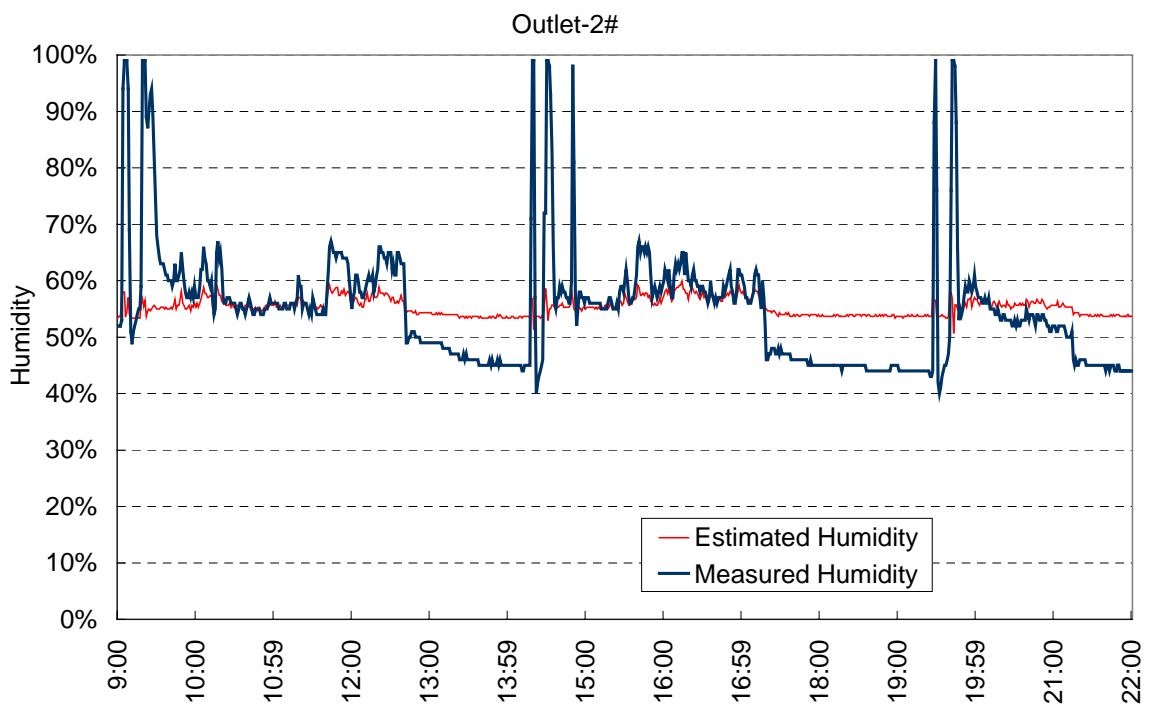
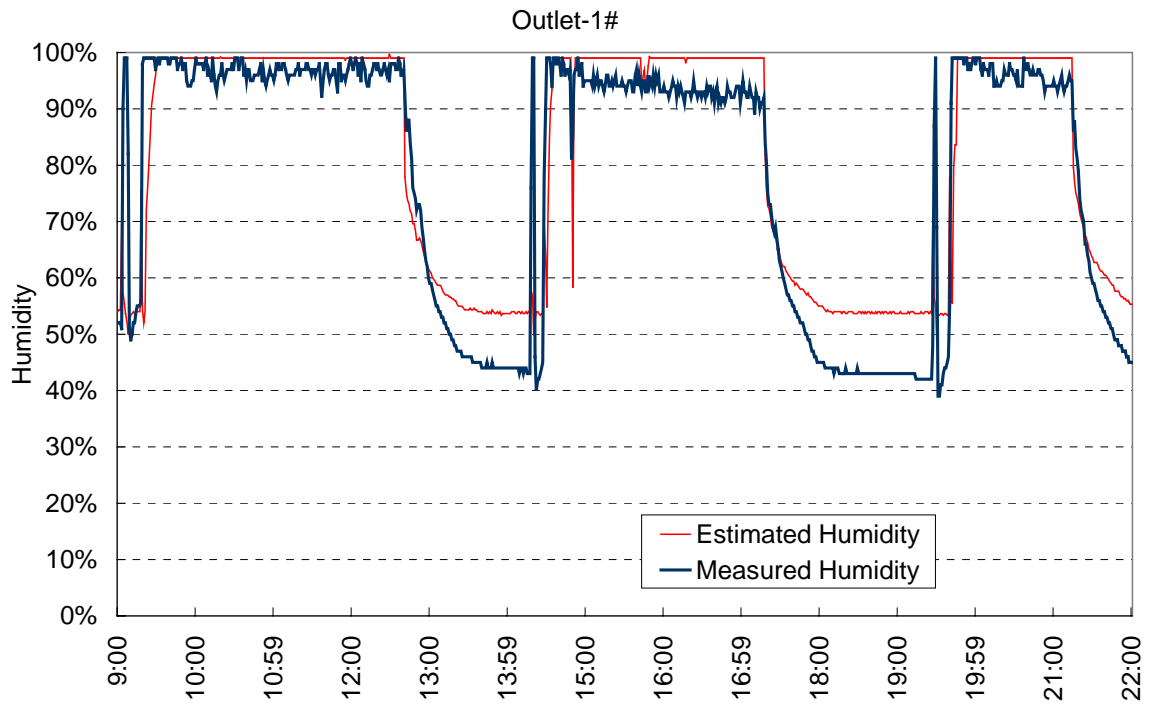


Figure 7.6 Flowchart of estimating air-conditioner indoor unit outlet air humidity

This method is tested by estimating the outlet air humidity of a GHP with four outlets on August 11, 2003. The estimated air humidity was compared with measured humidity, as shown in Figure 7.7. The whole average estimation error is 11.69%. The estimation error is large during the period when the GHP stopped. If only comparing the period when GHP was running, i.e. 9:31 to 12:40, 14:35 to 17:16, and 19:48 to 21:14, the average estimation error is only 5.54%. This estimation accuracy shows that this method is acceptable for estimating outlet air humidity. In the following summer, an experiment is planned to conduct to verify the accuracy of filter resistance estimation using this air humidity estimation. Different resistance filters will be installed in an air-conditioner's indoor unit. The thermal performance of the air-conditioner and filter resistances will be measured.

The reason why the inlet and outlet air temperature and enthalpy are used to estimate filter resistance instead of other performance data, for example refrigerant flow rate, is that the inlet and outlet air temperature and enthalpy have closer and clearer relations to the filter resistance, as shown in Figure 7.8. On December 23, when the filters having the largest resistance of 95 Pa are installed in the four indoor units, the average temperature difference between inlet and outlet air is the highest. When filter resistance decreased, the temperature difference decreased accordingly. But other performance data, such as GHP gas consumption and refrigerant flow rate did not show such a clear trend.



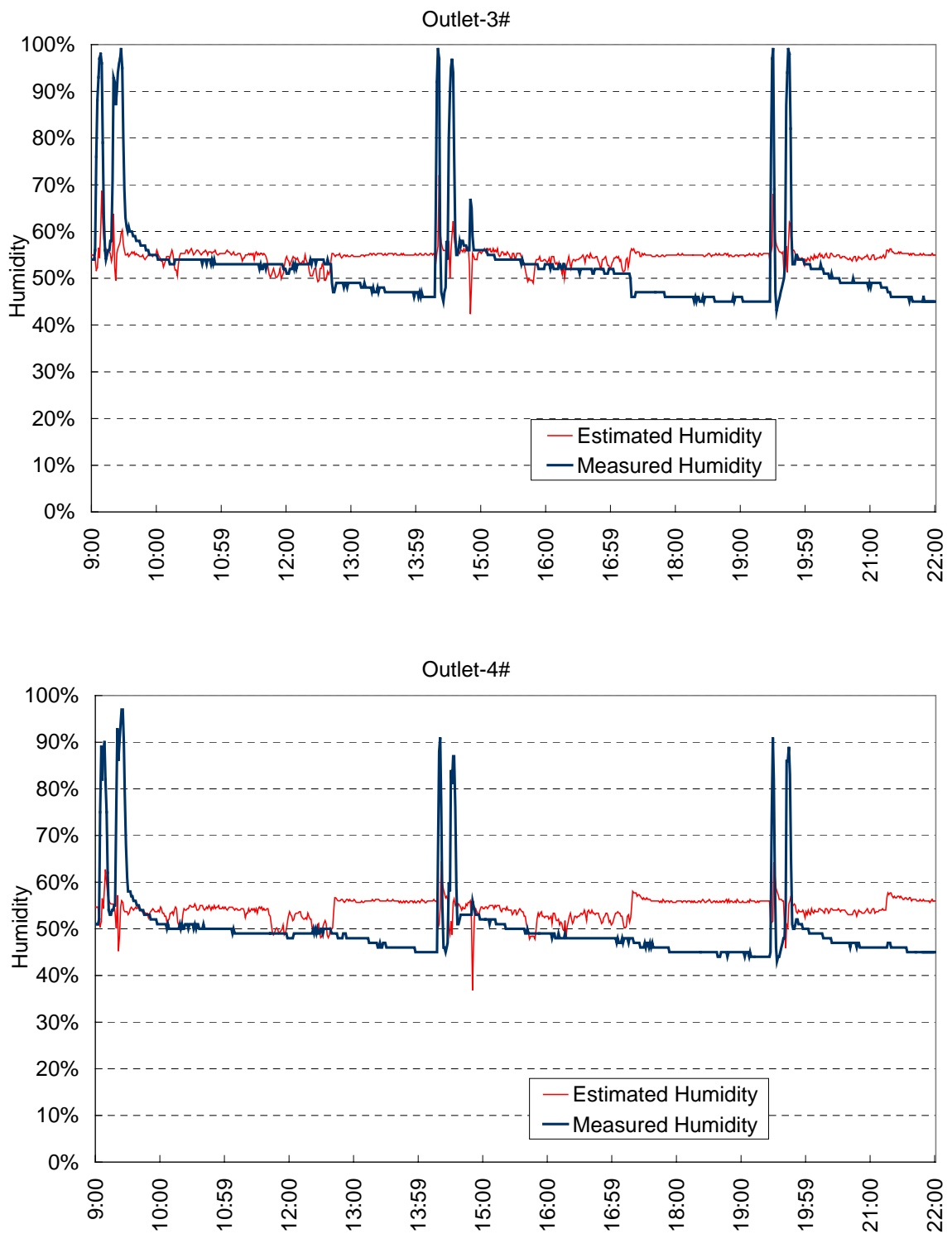


Figure 7.7 Estimated and measured air humidity at four outlets of the indoor unit

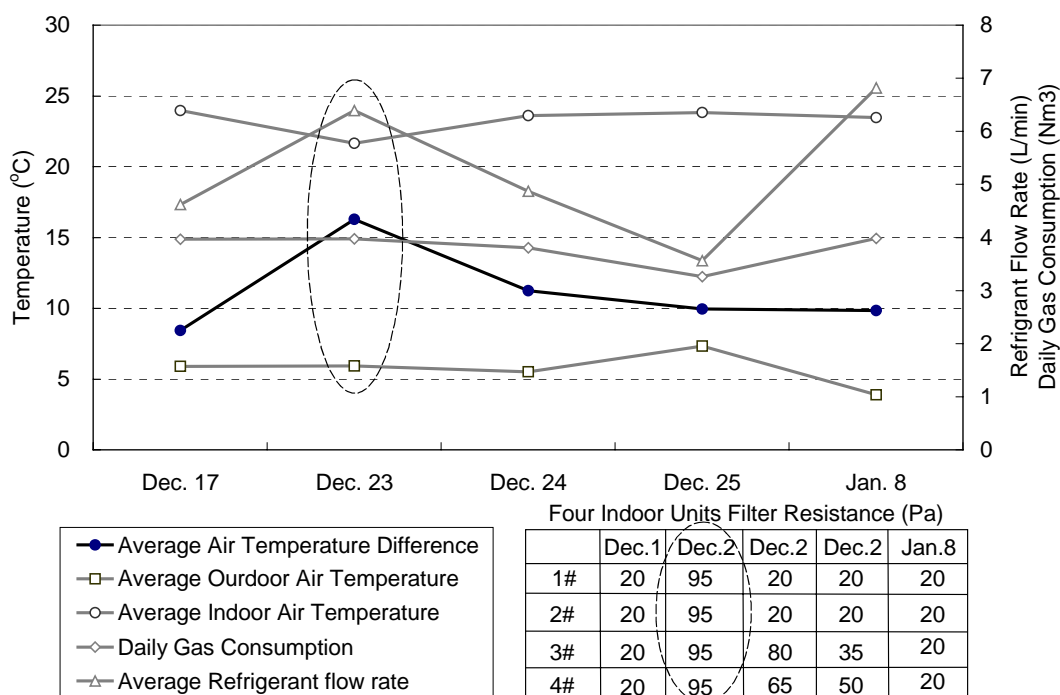


Figure 7.8 An air-conditioner's performance vs. filter resistance

7.3 MODEL PARAMETERS, INPUTS, AND OUTPUT

7.3.1 PARAMETERS

The necessary parameters are as follows.

a_0, a_1, a_2, a_3, a_4 – Fitted coefficients for the equation of C_h-C_f

A_i, A_o, A_{fo} – Area of inlet, outlet and fan outlet of indoor unit (m^2)

C_{EV} – Flow rate coefficient of expansion valve

D – Diameter of fan wheel (m)

e_0, e_1, e_2, e_3, e_4 – Fitted coefficients for the equation of $\eta-C_f$

ξ – Flow resistance coefficient of coil etc.

7.3.2 INPUTS

The inputs to the models are listed in the followings.

1) Inputs for the first estimation method:

N – Fan rotational speed (r/s)

E – Fan power consumption (W)

2) Inputs for the second estimation method:

N – Fan rotational speed (r/s)

A_{EV} – Expansion valve orifice area (m²), calculated from valve opening

$P_{r1}, P_{r2}, P_{r3}, P_{r4}$ – Refrigerant pressure at four state points (Pa)

T_{ai} – Air temperature at the inlet of an indoor unit (°C)

T_{ao} – Air temperature at the outlet of an indoor unit (°C)

T_{r1}, T_{r2}, T_{r3} – Refrigerant temperature at three state points (°C)

If fan power consumption is available, the inputs should be as follows.

7.3.3 OUTPUT

The model output is filter resistance.

ΔP_{ft} – Filter resistance to air flow (Pa)

7.4 MODEL VALIDATION

In order to check the accuracy of this filter resistance estimation model, experiments were conducted during heating period since December 2003 to April 2004 on a multi-evaporator GHP system in an office building in Maibara Japan. Because this period is in winter, the GHP was running under heating operation and indoor units were running as condensers. Equation 7.10 was used to calculate air flow rate.

Firstly, a duct system, as shown in Figure 7.9, was constructed to make filters of different fouling level. Five filters having different resistance, which are 35 Pa, 50 Pa, 65 Pa, 80 Pa, and 90 Pa, were made for purpose of making an air-conditioner work at different filter resistance conditions. The filters with different resistance are shown in Figure 7.10.

Next the five filters were installed into an air-conditioner's indoor unit respectively. Then the performance of the air-conditioner with different fouling level filters was measured.

Finally, the filter resistances were estimated using this model and compared with the measured filter resistances to check the estimation accuracy.

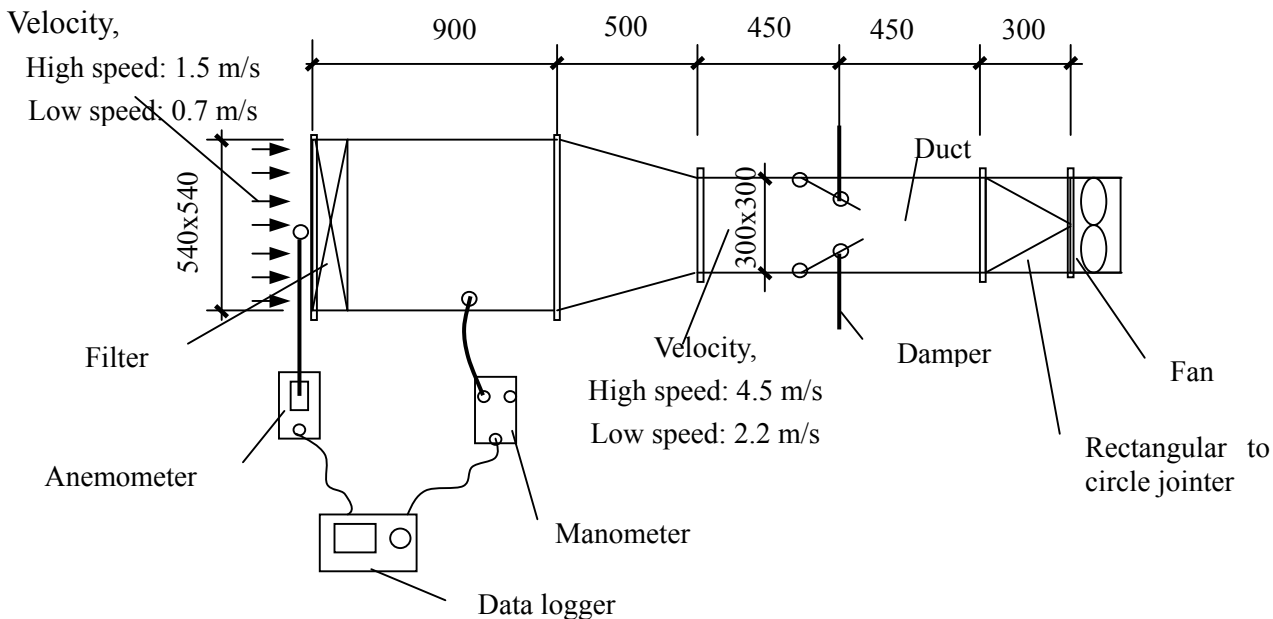


Figure 7.9 Ducts and instruments for making filters having different resistance



Figure 7.10 Filters having different resistance

The profile of the experimental air-conditioner is listed in Table 7.1. The fan specification data used to fit the coefficients in the equations of C_h-C_f and $\eta-C_f$ are listed in Table 7.2. The coefficients fitting results are shown in Figure 7.11. The parameters for the filter resistance estimation are listed in Table 7.3. The expansion valve orifice area is one of the inputs to the filter resistance estimation model. But in general only demanded valve opening from controller is available. It is necessary to know how to calculate valve orifice area from demanded valve opening. The relation between valve orifice area and demanded opening of the expansion valve in the experimental air-conditioner is shown in Figure 7.12. This figure is the specification of the expansion valve, which can be used to calculate the valve orifice area from valve opening.

In this calculation, the refrigerant pressure loss in the coil of indoor unit is ignored during calculating refrigerant enthalpy, i.e. P_{ref2} is assumed to be equal to P_{ref3} .

Table 7.1 Profile of the experimental air-conditioner

Heating / cooling capacity (kW)	42.5 / 35.5
Rated LPGconsumption (heating / cooling kW) (LPG HHV=90.27MJ/Nm ³)	28.0 / 28.5
Refrigerant	R407C
Outdoor unit rated power (heating / cooling kW)	1.09 / 1.09
Indoor unit rated power (heating / cooling, W)	93 / 92
Outdoor unit fan rated air flow rate (m ³ /h)	13800
Indoor unit fan rated air flow rate (high / low speed m ³ /h)	1200 / 900
Number of indoor unit	4

Table 7.2 Indoor unit fan performance data for coefficients fitting

Dimensionless flow rate C_f	Dimensionless pressure head C_h	Fan efficiency η
0.3384	2.5731	43.0955%
0.2959	2.6748	41.0555%
0.2755	2.7579	40.0656%
0.2232	3.0243	38.8360%
0.1545	2.9508	27.6441%

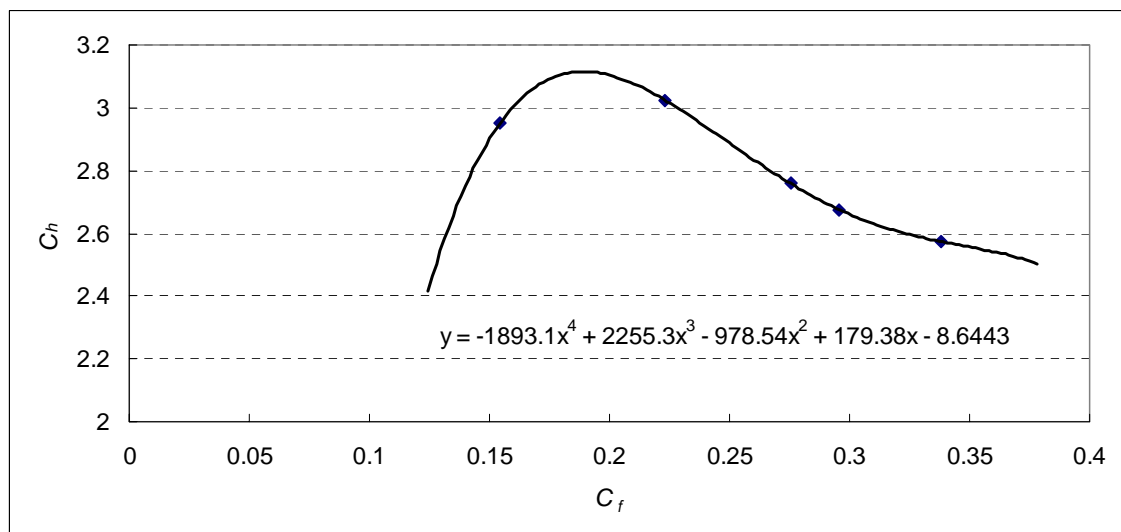
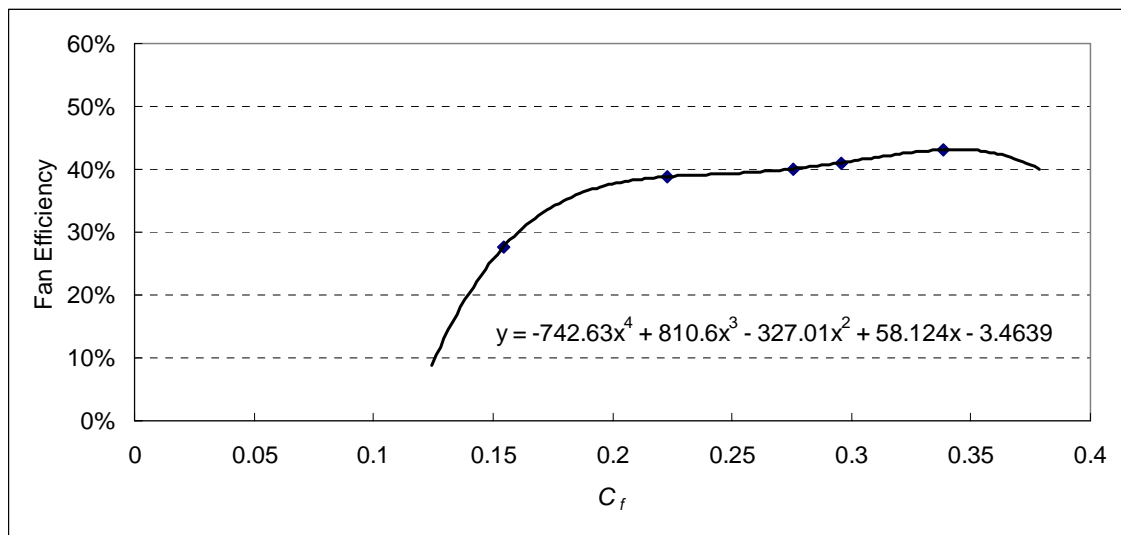


Figure 7.11 Coefficients fitting results of indoor unit fan

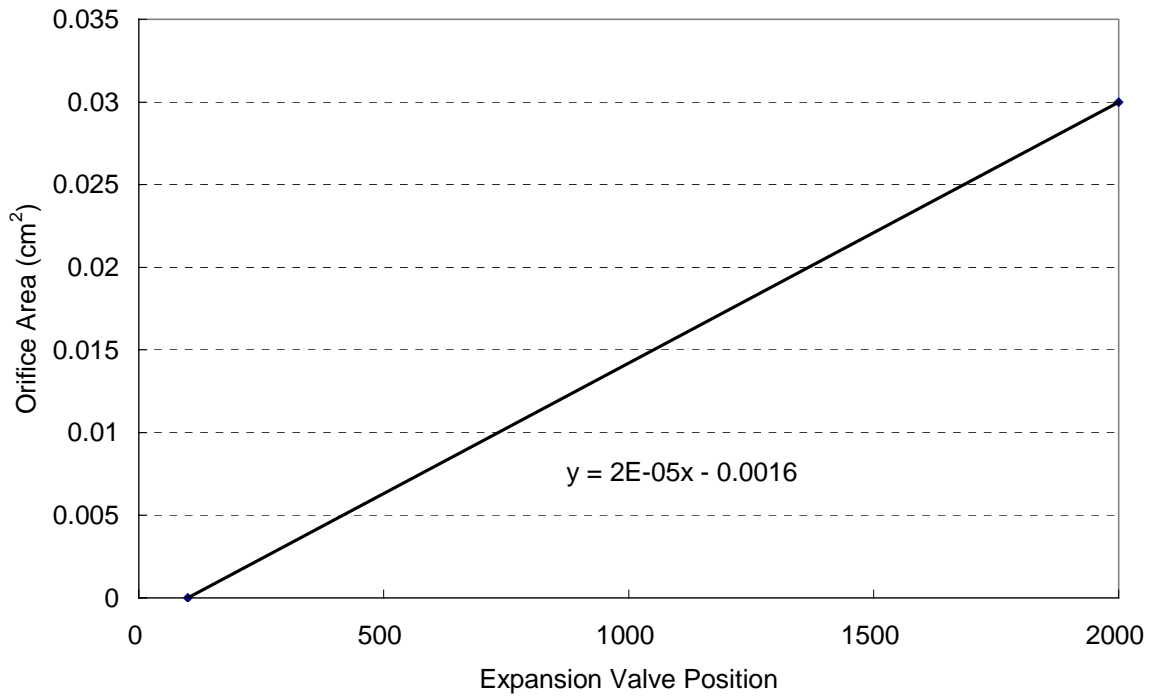


Figure 7.12 Expansion valve orifice area vs. controller demand

Table 7.3 Parameters for filter resistance estimation

a_0, a_1, a_2, a_3, a_4	-8.6443, 179.38, -978.54, 2255.3, -1893.1
A_i (m ²)	0.2916
A_o (m ²)	0.0706
A_{fo} (m ²)	0.1444
C_{EV}	0.6648
D (m)	0.46
e_0, e_1, e_2, e_3, e_4	-3.4639, 58.124, -327.01, 810.6, -742.63
ξ	2.1069

7.4.1 VALIDATION RESULTS OF ESTIMATING USING FAN POWER CONSUMPTION DATA

The validation results of estimating filter resistance using indoor unit fan power consumption are shown in Figure 7.13. The validation results show that the maximum estimation error is 12.72% and the average estimation error is 5.89%. So the estimation using fan power consumption is also accurate enough for estimating filter resistance during operating an air-conditioner.

Because of error accumulation, the estimated dimensionless flow rates are deviating from the dimensionless flow rates estimated using thermal performance data. A revising coefficient of 1.1609 is introduced to improve the estimation accuracy. The average estimation error did not become so small as 5.89% until this revising coefficient was introduced.

In order to validate the model universality, the coefficients fitted using one indoor unit data are used to estimate the filter resistance of three other indoor units whose model are same as the original indoor unit. The resistances of the filters currently used, pre-made 65 Pa filter and 95 Pa filter are measured and compared with the estimated resistance. The validation results are shown in Figure 7.15. Although the performance of the four units a littler differ from each other, the difference is not large. The filter resistances of three other indoor units estimated using the same parameters as the original indoor unit can match the measured filter resistances well. The maximum estimation error is 11.12% and the average estimation error is 4.88%. This estimation accuracy shows that the estimation using same parameter for all same type indoor units is acceptable.

7.4.2 VALIDATION RESULTS OF ESTIMATING USING THERMAL PERFORMANCE DATA

The validation results of estimating filter resistance using air-conditioner's thermal performance data are shown in Figure 7.14. The validation results show that the maximum estimation error is 13.12% and the average estimation error is 5.96%. So the model estimation is accurate enough for estimating filter resistance during the operational phase.

One issue that should be paid attention to is that the filter resistance estimation result is sensitive to refrigerant temperature when the refrigerant is not pure substance but mixture. For mixture refrigerant, the refrigerant density changes quite much if temperature changes

even a little when refrigerant is in two-phase region. For example, when the temperature of R407C changes from 36.4°C to 36.5°C at the pressure of 1.5484 MPa, its density changes from 544.16 to 471.77 kg/m³ because of the evaporation of some substance. The temperature difference of 0.1°C, which is in the range of temperature measurement error, can make the refrigerant density change 13.3%. This sensitivity makes the estimation accuracy not stable. When estimating filter resistance, attention should be paid for this.

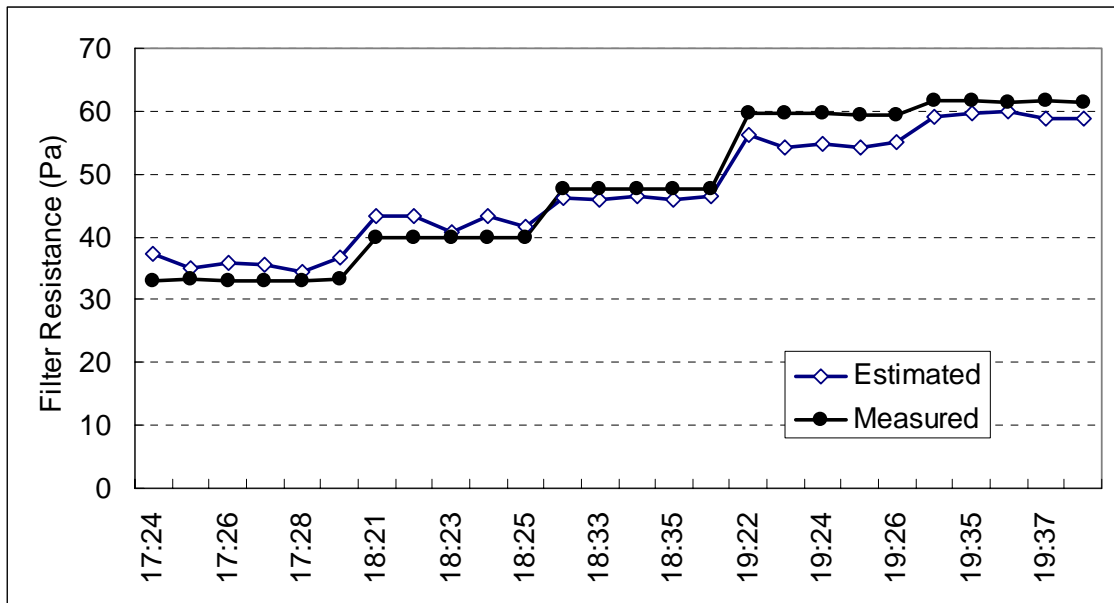


Figure 7.13 Validation results of estimating using fan power consumption data

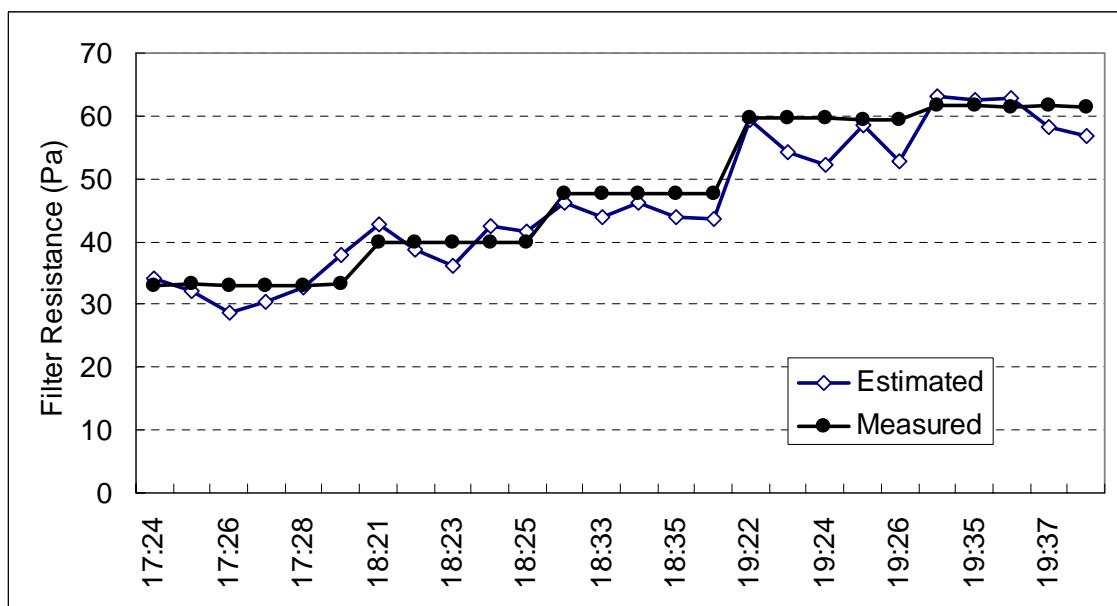


Figure 7.14 Validation results of estimating using thermal performance data

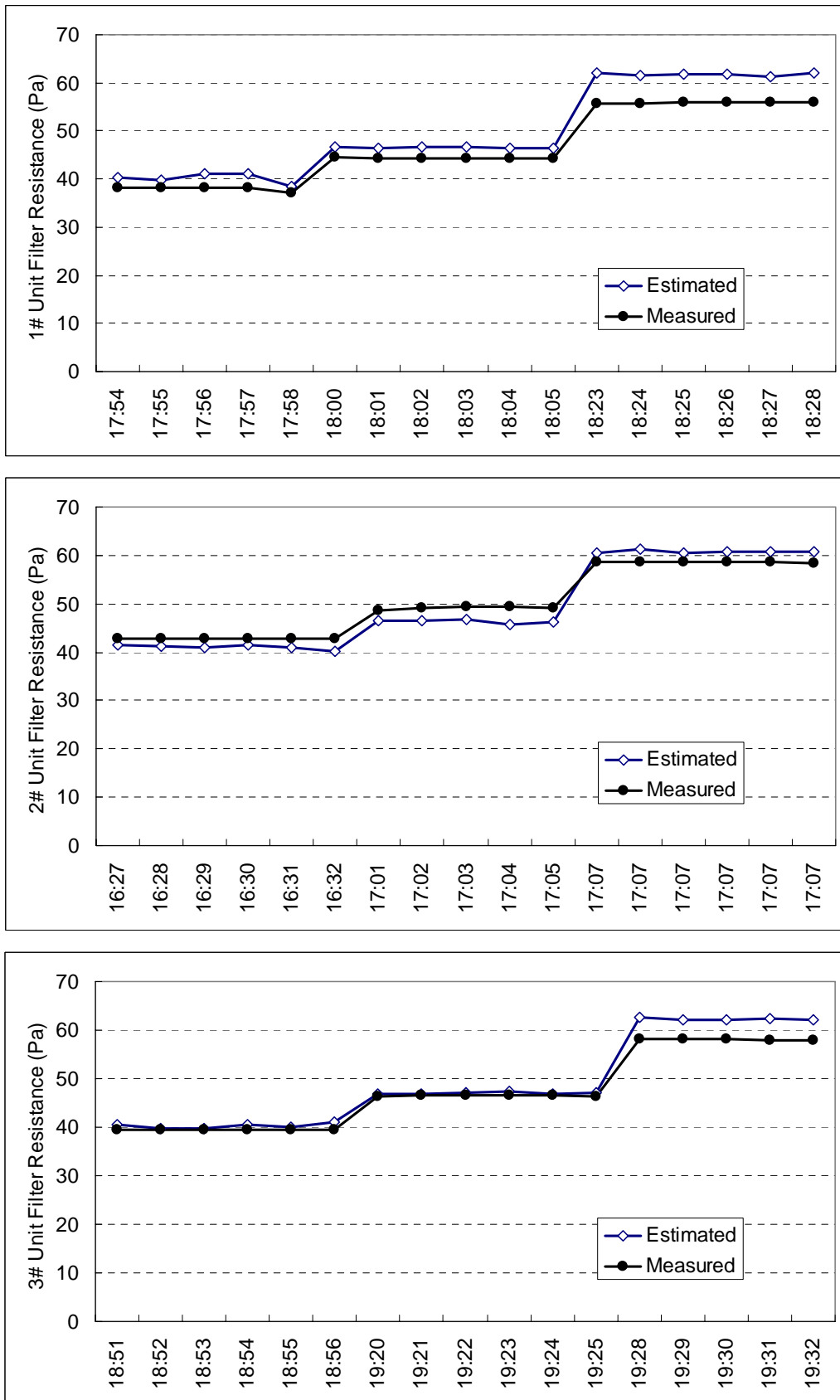


Figure 7.15 Filter resistance estimation results of three other indoor units

7.5 MODEL-BASED COMMISSIONING METHODOLOGY

Automated commissioning of a filter in an air-conditioner is to continuously monitor the fouling situation of the filter to determine whether the filter resistance reaches the predetermined threshold or not during operation. This filter resistance estimation model can fulfill this purpose using the continuously measured air-conditioner thermal performance data or indoor unit fan power consumption data. The following procedure shows how to achieve automated commissioning using this filter resistance estimation model.

1) Fit coefficients

The first step is to fit the coefficients of a_0, a_1, a_2, a_3, a_4 in Equation 7.3 and e_0, e_1, e_2, e_3, e_4 in Equation 7.8. These coefficients should be fitted using the manufacturer data of the fan in the air-conditioner to be commissioned.

2) Determine parameters

The second step of using this model for commissioning is to determine all the parameters related, as listed in section 7.3.1.

3) Commissioning

For the case of fan power consumptions being measured, input real-time fan rotational speed and power consumption to the models to calculate the filter resistance.

For the case of fan power consumptions not being measured, input real-time fan rotational speed, expansion valve opening, air temperature at the inlet and outlet of the indoor unit, and refrigerant pressure and temperature to estimate the filter resistance. Then compare the estimated resistance with the resistance threshold of filter-cleaning to check whether the filter should be cleaned or not.

The automated commissioning flow is described in Figure 7.16 in detail.

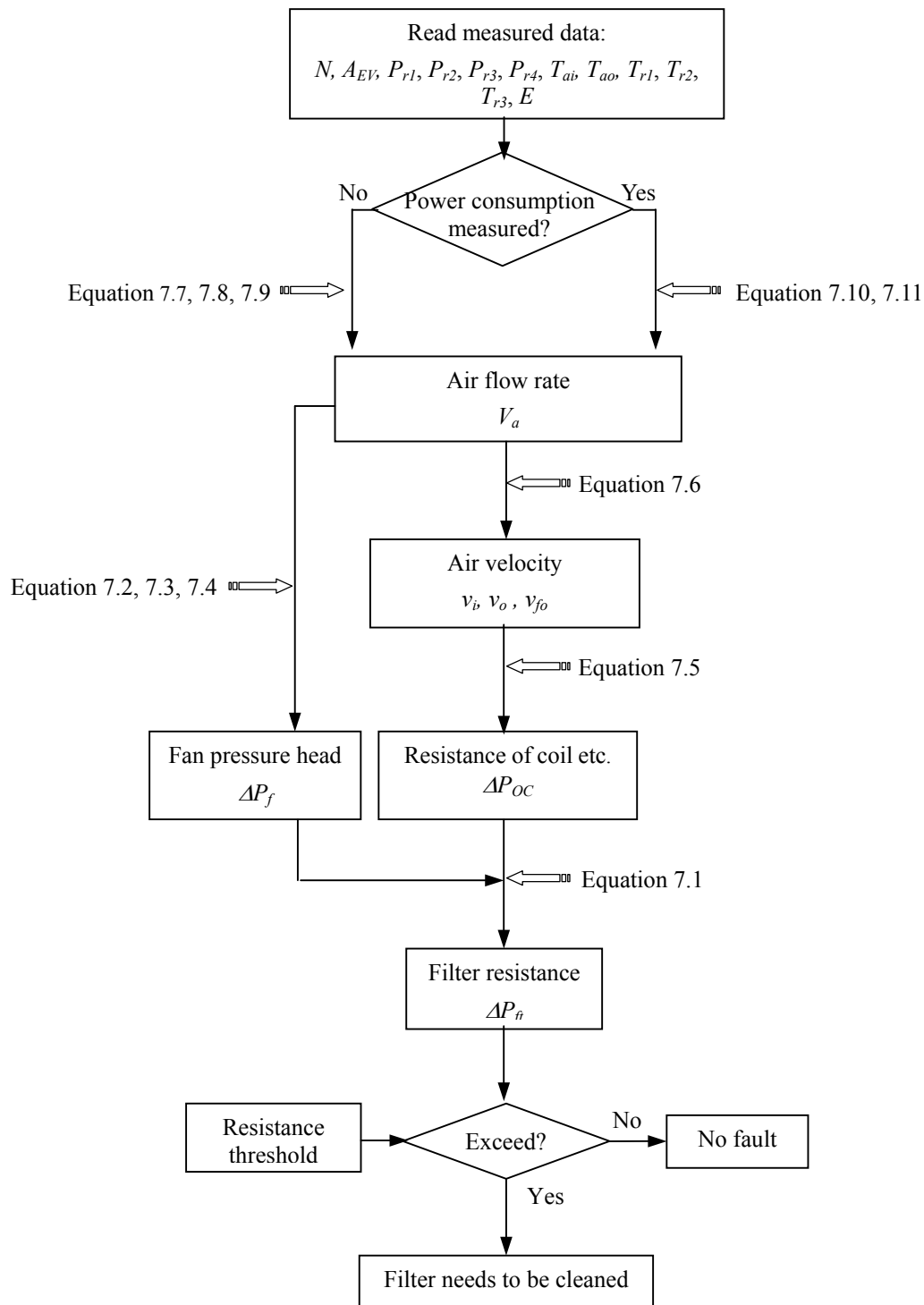


Figure 7.16 Flow chart of model-based automated commissioning for filters in air-conditioners

7.6 SUMMARY

This paper proposes a model that can estimate filter resistance. Two ways are proposed to estimate filter resistance. One is to use the thermal performance of a room air-conditioner as input and the other is to use the power consumed by the indoor unit fan as input. If refrigerant pressure and temperature is available, this model estimates filter resistance using the thermal performance data, i.e. refrigerant pressure and temperature, air temperature or enthalpy difference between indoor unit outlet and inlet air. If indoor unit fan power consumption is available, fan power consumptions are used as inputs to estimate filter resistance.

This model was validated using a multi-evaporator GHP system. The maximum and average difference between estimated and measured filter resistance are 13.12% and 5.96% when estimating using the air-conditioner thermal performance data, and 12.72% and 5.89% when estimating using indoor unit fan power consumption. For the purpose of checking the model universality, the coefficients fitted using one indoor unit data are used to estimate the filter resistance of three other indoor units whose model are same as the original indoor unit. The estimation for the three other indoor units shows that the maximum estimation error is 11.12% and the average estimation error is 4.88%. Hence this model is accurate enough for estimating filter resistance during operating a room air-conditioner. Based on this model, the method for commissioning filters in air-conditioners is proposed. This method is useful for automatically estimating filter resistance and reminding users to clean or replace a filter in time to save energy and to maintain desirable indoor environment.

CHAPTER 8

CONCLUSIONS

This dissertation discussed the methodology for achieving energy efficiency and ensuring high performance of buildings' HVAC systems. This dissertation argues that the most important things for ensuring energy efficiency and high performance of a HVAC system are the selection of proper HVAC scheme at design phase and the maintenance of proper running of the HVAC system during operational phase. The analysis and discussion in this dissertation support the following conclusions.

8.1 EFFICIENCY SHOULD BE ENSURED FROM VERY BEGINNING USING ECONOMIC ESTIMATION METHOD AT DESIGN PHASE

For the design phase, in order to selecting a proper HVAC scheme, this dissertation proposes to use life cycle cost (LCC) as a criterion to make the decision of selecting HVAC scheme at design phase and proposes the concept of estimating the life cycle cost of a HVAC system stage-by-stage corresponding to the design progress, which is also implemented stage by stage. The economic estimation of HVAC systems is divided into four stages, beginning of design, conceptual design, preliminary design, and detailed design, according to the characteristics of design progress.

8.1.1 NEURAL NETWORK METHOD SUITS FOR ECONOMIC ESTIMATION AT BEGINNING OF DESIGN

At the beginning of design stage, there is little known information that can be used to estimate the economic value of HVAC systems in detail. Neural network models are suitable for estimating the economic parameters of HVAC systems for its self-adaptive ability and convenient multi-variable input-output function. A neural network trained using known HVAC project information can successfully estimate the economic parameters of a HVAC system. The estimated economic values are useful judgment criteria for designers to

select a proper HVAC scheme from many possible design schemes.

8.1.2 EMPIRICAL EQUATIONS SUIT FOR ECONOMIC ESTIMATION AT OTHER DESIGN STAGES

At conceptual design stage, different HVAC system scheme are simulated to compare how they can fulfill the demand of air conditioning. From the simulation results, heating/cooling load can be obtained and used to summarize empirical equations to achieve proper economic estimation. At preliminary design stage, main subsystems of HVAC systems are simulated and compared. So some detailed information about air conditioning equipments can be obtained and used to calculate the initial investment and operation costs more accurately than the former two stages. The unknown information of the HVAC system is estimated using empirical equations derived from the statistics of existing HVAC projects. At detailed design stage, every part of the HVAC systems is simulated and determined. Accurate calculation methods for estimating life cycle cost are used to economically evaluate a HVAC system according to the detailed design information.

8.2 NO-FAULT OPERATION COMPARISON METHODOLOGY FOR OPERATIONAL PHASE ENSURES SYSTEM EFFICIENCY DURING WHOLE LIFE CYCLE

For the operational phase, the on-going commissioning is the viable method that can ensure the high performance and energy efficiency of a HVAC system. This dissertation proposes an on-going commissioning methodology of No-Fault Operation Comparison (NFOC). Through comparing no-fault operation with real-time operation, it can be judged that whether a HVAC system is running correctly or not. From the comparison results, faults can be detected and diagnosed. The no-fault performance of a HVAC system can be obtained from simulation or past no-fault operational data records.

8.2.1 SIMULATION USING SUITABLE MODELS AUTOMATES ON-GOING COMMISSIONING

The simulation analysis can achieve automated on-going commissioning through continuously comparing the HVAC systems real-time operational data with simulated data, which are calculated using the design conditions and represent the on-fault performance. This approach suits for the air or water processing components or subsystems, such as fan subsystems, valves, VAV boxes, and coils etc., whose processing results or outputs can be both simulated and measured. This dissertation checked whether the currently available

models of the main components in HVAC systems are suitable for automated on-going commissioning or not. For the components models that are not suitable for on-going commissioning, suitable models should be proposed. This dissertation proposed a total energy consumption model of fan subsystem and filter resistance estimation model, both of which are suitable for on-going commissioning.

8.2.2 PAST NO-FAULT OPERATIONAL DATA RECORDS SUITS FOR CONTINUOUSLY COMMISSIONING SENSORS

Past no-faults operational data records can be used to appraise the performance of current operation through continuously comparing them with the real-time operational data during operational phase. The past not-fault operation that were under the almost same heat conditions as current operation are criteria to judge whether current operation is correct or not. This approach suits for commissioning components whose simulation models are not suitable for commissioning, such as temperature sensors, air flow rate sensors etc.

8.3 MAIN ACHIEVEMENTS

The main achievements of this research can be summarized as follows.

1) Proposes a concept of HVAC design scheme decision-making from possible candidates using Life Cycle Cost Estimation method stage by stage at design phase. The life cycle cost, a comprehensive index of initial investment cost and operational cost, is a selection criterion to determine an energy efficient HVAC scheme.

2) Proposes different economic estimation methods suitable to the characteristics of different design stages. Neural network method suits for the beginning of design and empirical equations take effect for conceptual design, preliminary design and detailed design.

3) Proposes the No-Fault Operation Comparison methodology for on-going commissioning of HVAC systems during operational phase. Through comparing no-fault performance data with real-time data, it can be judged that whether a HVAC system is running correctly and efficiently or not. The no-fault operation data are obtained either from simulation using components or system models suitable for on-going commissioning or from past no-fault operational data records that were under the same heat conditions as the current operation.

4) Proposes a total energy consumption model of fan subsystem suitable for on-going commissioning. This model takes into account the efficiency of all the components of fan subsystem, i.e. fan, driveline, motor and variable speed drive. Because this model can be used to simulate the total energy consumption of a fan subsystem that is easy to obtain during operational phase, this model is useful for on-going commissioning of fan subsystem. The average simulation error of this model is 5.1%, which shows that this model is accurate enough for commissioning a fan subsystem.

5) Studied the on-going commissioning characteristics of VAV systems using experiments. Four types of typical fault, low efficiency fan, malfunctioning supply air and room air temperature sensor, stuck AHU outdoor air damper, and stuck AHU water valve, were introduced to a really running VAV system and the experiment results demonstrated the feasibility of commissioning these components using No-Fault Operation Comparison methodology.

6) Proposed a filter resistance estimation model, which is suitable for commissioning filters in room air-conditioners. Either the thermal performance of a room air-conditioner or the power consumed by the indoor unit fan can be used as input to estimate filter resistance. The maximum and average difference between estimated and measured filter resistance are 12.72% and 5.89% when estimating using indoor unit fan power consumption, and 13.12% and 5.96% when estimating using the air-conditioner thermal performance data. The parameters obtained from one indoor unit were used to estimate the filter resistance of another three indoor units whose model is same as the original one. The filter resistance estimation results show that the maximum estimation error is 11.12% and the average estimation error is 4.88%. The validation results show that this model is accurate enough for estimating filter resistance during operating a room air-conditioner and suitable for commissioning filters in air-conditioners.

To summarize, the new things created by this research are the following four items, two methods for ensuring energy efficiency of HVAC systems, LCCE for design phase and NFOC for operational phase, and two theoretical models suitable for on-going commissioning HVAC systems, total energy consumption model of fan subsystem and filter model for room air-conditioners.

REFERENCES

Annex 40, Annex 40 work program, 2001.

Annex 40, homepage, <http://www.commissioning-hvac.org/default.asp>

Angle, Steven L., H. Arkin, Commissioning lab buildings, *ASHRAE Journal*, Vol. 40 (11), 1998, Part 1, p.49.

ASHRAE, *ASHRAE Handbook, Fundamentals*, S.I. Edition, p. 6.7, American Society of Heating, Refrigerating, and Air-Conditioning Engineers, Inc., Atlanta, 1993.

ASHRAE, ASHRAE Guideline 1-1996, The HVAC Commissioning Process, 1996.

Bearg D. W., Use of Multipoint Monitoring as a Tool for Commissioning Building for IAQ, *ASHRAE Transactions*, Vol. 105, Part 1, 1999, pp. 1101-1110.

Benner N., Commissioning Retrospective: How Far Have We Come in Five Years?, *Proceedings of the 5th National Conference on Building Commissioning of USA*, 1997.

Bonneville Power Administration, *Building Commissioning Guidelines*, 1992.

Brambley M. R., R. Briggs, S. Katipamula, C. Dasher, L. Luskey, and L. Irvine, Investigating Potential Strategies for Automating Commissioning Activities, *Proceedings of the 10th National Conference on Building Commissioning of USA*, 2002.

Cai K., *Realization Technology of Neural Networks*, 1998, Press of Guofang University, Changshai, China.

Charette R.P, Life Cycle Cost Analysis For Buildings, *ASHRAE Transactions*, Vol. 86, 1980, Part 2, pp. 167-193.

Chen F., Yuchun Deng, Zhifeng Xue, Ruhong Wu, Tool pack for building environment simulation, *HV&AC*, 1999, 4th issue, pp. 58-63.

Choat E. E., Implementing the commissioning process, *ASHRAE Transactions*, Vol. 99, Part 1, 1993.

- Clark, R. D., *HVACSIM+ Building Systems and Equipment Simulation Program Reference Manual*, NBSIR 84-2996, 1985.
- CTSB (Centre Scientifique et Technique du Batiment), *Manual of SIMBAD Building and HVAC Toolbox*, Version 2.0.0, 2001.
- Cuevas C., P. Lacote, J. Lebrun, Re-commissioning of an Air Handling Unit, Documents of Annex 40 5th meeting, Kyoto, Japan, 2003.
- DuBose G. H., Odom J. D., Fairey P. W., Why HVAC commissioning procedures do not work in humid climates, *ASHRAE Journal*, Vol. 35 (12), 1993.
- ECBCS, homepage, <http://www.ecbcs.org/Annexes.htm>, International Energy Agency Energy Conservation in Buildings and Community Systems.
- ECBCS, *Annual Report 2001 – 2002*, International Energy Agency Energy Conservation in Buildings and Community Systems, p. 23.
- Ellis R.T., Commissioning a Museum and Archival Storage Facility, *ASHRAE Transactions*, Vol. 102, 1996.
- English M. C., Design Review During Commissioning, *Proceedings of the 9th National Conference on Building Commissioning of USA*, 2001.
- Friedman H., M. A. Piette, Comparison of Emerging Diagnostic tools for Large Commercial HVAC System, *Proceedings of the 9th National Conference on Building Commissioning of USA*, 2001.
- Griffith J.W, Benefits of Daylight-Cost and Energy Saving, *ASHRAE Transactions*, Vol. 83, 1978, Part 2, p421.
- Griffin T.M, Life-Cycle Costing Application for Building Energy Code Compliance, *ASHRAE Transactions*, Vol. 91, 1985, Part 1B, pp. 603-608.
- Haasl T., R. Friedmann, L. Irvine, E. Baxter and K. Stum, California Commissioning Market Characterization, *Proceedings of the 9th National Conference on Building Commissioning of USA*, 2001, p. 10.

- Haves P., Approach and work plan for IEA Annex 40 Subtask D1, 2002.
- Haves P., Dexter, A. L., Jorgensen, D. R., Ling K. V., Geng G., Use of a Building Emulator to evaluate techniques for improved commissioning and control of HVAC systems, *ASHRAE Transactions*, Vol. 97, Part 1, 1991, pp. 684-688.
- Haves P., Saksbury T. I., Jorgensen, D. R., Dexter, A. L., Development and testing of a prototype tool for HVAC control system commissioning, *ASHRAE Transactions*, Vol. 102, 1996.
- Hitachi, 2002, *Hitachi Inverter Technical Guidebook*, Tokyo, Hitachi, Ltd.
- Hu S., Qing Shen, Dewen Hu, Chun Shi, *Application Technique of Neural Network*, Press of Guofang University of Science and Technology, Nov. 1993, 1st edition.
- Huang S., Discussion of Performance and Generalized Economic Indicator of Isolation Material, *HV&AC*, 1984, 1st issue, pp. 3-6.
- Hyttinen M., P. Pasanen, J. Salo, M. Bjorkroth, M. Vartiainen, P. Kalliokoski, Reaction of ozone on ventilation filters, *Indoor and Built Environment*, Vol. 12 (3), 2003, pp. 151-158.
- Kang Y., Yi Jiang, Yanping Zhang, Operation Economic Analysis of the Outside Air Handling Unit with a Latent Heat Storage Subsystem, *HV&AC*, 1999, 4th issue, pp. 8-11.
- Kemp P. C., H. G. Neumeister-Kemp, G. Lysek, F. Murray, Survival and growth of micro-organisms on air filtration media during initial loading, *Atmospheric Environment*, Vol. 35 (28), 2001, pp. 4739-4749.
- Kitagawa H., Yoshida H., Wang F., Matsumoto K., Goto K., Comparison of Measured and Simulated Heating / Cooling Load of a Multi-evaporator GHP System, *Proceedings of the Annual Conference of the Society of Heating, Air-conditioning and Sanitary Engineers of Japan (SHASE)*, 2004.
- Lawson C. N., Commissioning Hospitals for Compliance, *ASHRAE Transactions*, Vol. 99, Part 2, 1993, pp. 1183-1190.

- Li S., Economic and Technical Comparison between Electric and Thermally Driven Chillers, *HV&AC*, 1995, 5th issue, pp. 22-25.
- Lisoa P. G. J. (1992). *Neural Networks - Current Applications*, Chapman & Hall, London, UK.
- Liu M., Y. Cui, Improving Building Energy Efficiency and Indoor Air Quality in Hospital and Research Facilities, *Proceedings of the 9th National Conference on Building Commissioning of USA*, 2001.
- Long W., Cunyang Fan, Feasibility Analysis of Using the ASHP Chiller in Shanghai Area, *HV&AC*, 1995, 5th issue, pp. 3-7.
- Lu Canren, Yitai Ma, Shunxing Gao, Weimin Zheng, Energy Saving Analysis of Heat Pump Using for Heating and Cooling Public Buildings in Beijing and Tianjin Areas, *HV&AC*, 1984, 1st issue, pp. 7-12.
- Matsuoka I., Study on Method of Automatic Commissioning in HVAC System based on Simulation Models, Master thesis, Kyoto University, 2002.
- Mitsubishi, 2002, *Test Report of Induction Motor*, Nagoya, Mitsubishi Electric Corporation.
- Moritz M., H. Peters, B. Nipko, H. Ruden, Capability of air filters to retain airborne bacteria and molds in heating, ventilating and air-conditioning (HVAC) systems, *International Journal of Hygiene and Environmental Health*, Vol. 203 (5-6), Jul. 2001, pp. 401-409.
- Naughton P. J., DCS commissioning for a microelectronic factory, *ASHRAE Transactions*, Vol. 98, Part 2, 1992.
- NIST, NIST Reference Fluid Thermodynamic and Transport Properties – REFPROP, Version 7.0, U.S. National Institute of Standards and Technology, Boulder, 2002.
- OIT. 2000. Replace V-belt With Cogged or Synchronous Belt Drives. Merrifield: Office of Industrial Technologies, U.S. Department of Energy.
- Pacific Gas and Electric, *General Commissioning Procedure for DDC Systems*, 2001.
- Portland Energy Conservation Incorporated, homepage, <http://www.peci.org/cx/guides.html>.

- Qian Y., *HVAC and Energy Saving in High Rise Buildings*, Press of Tongji University, Feb. 1990, 1st edition, p. 309.
- Richardson G., Commissioning of VAV Laboratories and the Problems Encountered, *ASHRAE Transactions*, Vol. 100, 1994, pp. 1393-1399.
- Ruden H., H. Schleibinger, Air filters from HVAC systems as possible source of volatile organic compounds (VOC) – laboratory and field assays, *Atmospheric Environment* Vol. 33 (28), 1999, pp. 4571-4577.
- Scott R., *The History of the International Agency, the First Twenty Years*, Volume I, Origins and Structure, 1994, p. 19.
- Shitzer A., H. Arkin, Computer Aided Optimal Life-Cycle Design of Rectangular Air Supply Duct Systems, *ASHRAE Transactions*, Vol. 85, 1979, Part1, pp. 197-212.
- Shitzer A., H. Arkin, Study of Economic and Engineering Parameters Related to the Cost of an Optimal Air Supply Duct System, *ASHRAE Transactions*, Vol. 85, 1979, Part2, pp. 363-373.
- Smith V. A., C. Scruton, Progress Update on Automated Commissioning and Diagnostics under the AEC PIER Research Program, *Proceedings of the 10th National Conference on Building Commissioning of USA*, 2002.
- Stum K., Understanding Owner Project Requirements Documentation, *Proceedings of the 9th National Conference on Building Commissioning of USA*, 2001.
- Stylianou M., Chillers and Heat Pumps, *Building Optimization and Fault Diagnosis Source Book*, IEA Annex 25, 1996, pp. 66.
- Tao X., Economic and Technical Analysis of a real cooling plant, *HV&AC*, 1996, 5th, issue, pp. 32-35.
- Tsal R.J., M.S.Adler, Evaluation of Duct Design Method, *ASHRAE Transactions*, Vol. 92, 1986, Part1, pp. 347-361.
- Tsal R.J., H.F.Behls, Evaluation of Numerical Methods for Ductwork and Pipeline Optimization, *ASHRAE Transactions*, Vol. 93, 1987, Part1, pp. 17-34.

- Tseng P. C., Stanton-Hoyle D. R., Withers W. M., Commissioning through Digital Control and an Advanced Monitoring System – a Project perspective, *ASHRAE Transactions*, Vol. 100, 1994, pp. 1382-1392.
- Tseng P. C., Harmon J., Edwards F. C., Commissioning and Construction Quality Control – a New Perspective on Facility Commissioning, *ASHRAE Transactions*, Vol. 99, Part 2, 1993, pp. 959-968.
- Underwood T. D., Commissioning process: How it affects the building owner and maintenance contractor, *ASHRAE Transactions*, Vol. 99, Part 1, 1993, pp. 863-866.
- U. S. Department of Energy and U. S. Department of General Service Administration, *Building Commissioning Guide*, 1998.
- Wang S.K., K.L.Leung, W.K.Wang, Sizing a Rectangular Supply Duct with Transversal Slots by Using Optimum Cost and Balanced Total Pressure Principle, *ASHRAE Transactions*, Vol. 90, 1984, Part 2A, pp. 414-430.
- Wilkinson R., Healthy Bugs and Healthy People: Commissioning the Montana State University Agriculture Bio-Science Facility, *Proceedings of the 9th National Conference on Building Commissioning of USA*, 2001.
- Yoshida H., VAV Air Handling Unit, *Building Optimization and Fault Diagnosis Source Book*, International Energy Agency Annex 25, August 1996.
- Yoshida H., Japanese Preliminary Questionnaire Study on Opportunities and Automation Possibilities in Commissioning Process With BEMS assistance, Working Documents of the Second Meeting of IEA Annex 40, 2001, Quebec, Canada.
- Yang Y., J. Liu, Design of Budget management software of HVAC project, *HV&AC*, 2000, 1st issue, pp. 55-56.
- Nakahara N., Study and Practice on HVAC System Commissioning, *Proceedings of the 4th International Symposium on Heating, Ventilation and Air Conditioning*, (ISHVAC2003), Beijing, China, 2003, Vol. I, pp. 44-61.

LIST OF PAPERS

1. PAPERS PUBLISHED AND REVIEWED

- 1) Fulin Wang, Harunori Yoshida, and Masato Miyata, Total Energy Consumption Model of Fan Subsystem Suitable for Continuous Commissioning, *ASHRAE Transactions*, American Society of Heating, Refrigerating, and Air-Conditioning Engineers, Inc., Atlanta, 2004, Vol. 110, Part 1, pp. 357-364.
- 2) Fulin Wang, Harunori Yoshida, Ipei Matsuoka, Makoto Tsubaki, and Kanako Itou, Experiment Study On On-going Commissioning a Real VAV System, *Proceedings of the 4th International Symposium on Heating, Ventilation and Air Conditioning*, (ISHVAC2003), ISBN 7-302-07326-0 / TU.206, Beijing, China, 2003, Vol. II, pp. 959-966.
- 3) Fulin Wang and Harunori Yoshida, A On-going Commissioning Tool Based on Operation Record and Simulation, *Proceedings of the 8th International Building Performance Simulation Association Conference, Building Simulation 2003 (BS2003)*, ISBN 90-386-1566-3, Eindhoven, Netherlands, 2003, Vol. III, pp. 1347-1353.
- 4) Kazuya Takahashi, Harunori Yoshida, Yuzo Tanaka, Noriko Aotake and Fulin Wang, Heat Flux Measurement of Urban Boundary Layers in Kyoto City and Its Prediction by CFD Simulation, *Proceedings of the 8th International Building Performance Simulation Association Conference, Building Simulation 2003 (BS2003)*, ISBN 90-386-1566-3, Eindhoven, Netherlands, Vol. III, pp. 1347-1353.
- 5) Fulin Wang, Economic Prediction of HVAC Systems at Different Design Stages, *ASHRAE Transactions*, ISSN 0001-2505, American Society of Heating, Refrigerating, and Air-Conditioning Engineers, Inc., Atlanta, 2003, Vol. 109, Part 1, pp.157-166.
- 6) Fulin Wang, Yi Jiang and Harunori Yoshida, Building HVAC Systems Economic Performance Evaluation Using Neural Network Method At Beginning of Design, *Proceedings of International Conference with the theme Advances in Building Technology (ABT2002)*, ISBN 0-08-044100-9, Hong Kong, 2002, Vol. II, pp.

1265-1272.

- 7) Harunori Yoshida, Yuuya Iguchi, Ippei Matsuoka, and Fulin Wang, Total Optimal Operation for HVAC system with Heat Source and Distribution System, *Proceedings of International Conference with the theme Advances in Building Technology (ABT2002)*, ISBN 0-08-044100-9, Hong Kong, 2002, Vol. II, pp. 1297-1304.
- 8) Fulin Wang, Qingmei Qi, Zhifeng Xue, Qingpeng Wei, Yi Jiang, and Xianting Li, Conducting a High-rise Building Design Work by Simulation of DeST, *Proceedings of International Conference of Air-conditioning in High-rise Buildings (ACHRB'2000)*, Shanghai, China, 2000, pp. 71-76.

2. PAPERS UNDER REVIEWING

- 1) Fulin Wang, Harunori Yoshida, Hiroaki Kitagawa, Keiji Matsumoto, Kyoko Goto, Model-based Commissioning Methodology for Filters of Room Air-conditioner, Submitted to The 4th International Conference for Enhanced Building Operation (ICEBO 2004), Paris, France, 2004.
- 2) Masato Miyata, Harunori Yoshida, Masahiko Asada, Fulin Wang, FDD Method of Multiple VAV Terminal Units for a Real Office Building, Submitted to The 4th International Conference for Enhanced Building Operation (ICEBO 2004), Paris, France, 2004.
- 3) Hiroaki Kitagawa, Harunori Yoshida, Fulin Wang, Keiji Matsumoto, Kyoko Goto, Comparison of Measured and Simulated Heating Load of a Multi-evaporator Gas-driven-engine Heat Pump System, Submitted to the annual conference of the Society of Heating, Air-conditioning and Sanitary Engineers of Japan (SHASE), 2004.

3. PAPERS PRESENTED

- 1) Fulin Wang, Harunori Yoshida, and Masato Miyata, Total Energy Consumption Model of Fan Subsystem Suitable for On-going Commissioning, Presented in ASHRAE Winter Meeting, Anaheim, US, Jan. 24-28, 2004.
- 2) Masato Miyata, Harunori Yoshida, Fulin Wang, Makoto Tubaki, Kanako Itou, Experimental Study on Model-based Commissioning Method of VAV Systems in a

- Real Building, Presented in The 3rd International Conference for Enhanced Building Operation (ICEBO 2003), Berkeley, US, Oct. 13-15, 2003.
- 3) Fulin Wang, Harunori Yoshida, Ipei Matsuoka, Makoto Tsubaki, and Kanako Itou, Experiment Study On On-going Commissioning a Real VAV System, Presented in the 4th International Symposium on Heating, Ventilation and Air Conditioning (ISHVAC2003), Beijing, China, Oct. 9-11, 2003.
 - 4) Fulin Wang and Harunori Yoshida, A On-going Commissioning Tool Based on Operation Record and Simulation, Presented in the 8th International Building Performance Simulation Association Conference, Building Simulation 2003 (BS2003), Eindhoven, Netherlands, Aug. 11-14, 2003.
 - 5) Kazuya Takahashi, Harunori Yoshida, Yuzo Tanaka, Noriko Aotake and Fulin Wang, Heat Flux Measurement of Urban Boundary Layers in Kyoto City and Its Prediction by CFD Simulation, Presented in the 8th International Building Performance Simulation Association Conference, Building Simulation 2003 (BS2003), Eindhoven, Netherlands, Aug. 11-14, 2003.
 - 6) Fulin Wang, Economic Prediction of HVAC Systems at Different Design Stages, Presented in ASHRAE Winter Meeting, Chicago, US, Jan. 24-28, 2003.
 - 7) Fulin Wang, Yi Jiang and Harunori Yoshida, Building HVAC Systems Economic Performance Evaluation Using Neural Network Method At Beginning of Design, Presented in the International Conference with the theme Advances in Building Technology (ABT2002), Hong Kong, China, Dec. 4-6, 2002.
 - 8) Harunori Yoshida, Yuuya Iguchi, Ipei Matsuoka, and Fulin Wang, Total Optimal Operation for HVAC system with Heat Source and Distribution System, Presented in the International Conference with the theme Advances in Building Technology (ABT2002), Hong Kong, China, Dec. 4-6, 2002.
 - 9) Fulin Wang, Qingmei Qi, Zhifeng Xue, Qingpeng Wei, Yi Jiang, and Xianting Li, Conducting a High-rise Building Design Work by Simulation of DeST, Proceedings of International Conference of Air-conditioning in High-rise Buildings (ACHRB'2000), Shanghai, China, Oct. 24-27, 2000.

APPENDIX

EXPERIMENTAL

STUDY

ON

COMMISSIONING

GHP

SYSTEMS

APPENDIX A

EXPERIMENTAL STUDY ON COMMISSIONING MULTI-EVAPORATOR GHP SYSTEMS

In June 2003, a research project cooperated with Yanmar Company Ltd. launched and will continue for two years. This research focuses on improving energy efficiency of multi-evaporator Gas-fired-engine driven Heat Pump (GHP) systems. Because commissioning is a viable method to ensure the energy efficiency of building systems, GHP system commissioning becomes one of the objectives of this research project and forms a part of this doctoral research. Since June 2003, measurement instruments are set up to measure a GHP system in real use. Data of climate, GHP performance, internal load, etc. are automatically recorded by three data loggers once a minute. This chapter introduces the details of this experimental study on commissioning the multi-evaporator GHP system.

A.1 OBJECTIVES

The main objective of this experimental study is to improve the energy efficiency of GHP systems. In detail the objectives are listed in the following.

A.1.1 DEVELOP GHP PERFORMANCE SIMULATION TOOL

Until now the rated performance of GHPs has been studied. The next necessary research is to study how to improve the annual performance of GHPs, especially to improve the energy efficiency during part load period. For this purpose, it is essential to simulate annual heating/cooling load, to measure the annual performance of a building and its GHP systems, and to analyze the relations between buildings and GHP systems. Based on the analysis on experiment data, building models and GHP models can be developed. Finally GHP performance simulation tool can be developed using these models.

The GHP performance simulation tool is expected to be able to fulfill the following achievements.

- 1) Optimize the operation control for GHP systems.
- 2) Improve GHP performance at part load conditions.
- 3) Simulate GHP energy consumption and load distribution.
- 4) Make standard energy efficient GHP operation pattern.

A.1.2 DEVELOP COMMISSIONING METHOD FOR GHP SYSTEMS

Commissioning is considered to be a viable way to ensure the energy efficiency of building systems. In order to ensure the energy efficiency of GHP systems, it is necessary to develop the commissioning method for GHP systems. This research focuses on the following items.

- 1) Develop component models suitable for commissioning GHP systems at component level.
- 2) Develop whole system commissioning method.

For the purpose of realizing the objectives mentioned above, measurement on really in use GHP system is continuing since June 2003. Both buildings thermal performance and GHP system performance are being measured continuously. The following parts will introduce the details of the experimental measurement and main achievements from the experiment up to now.

A.2 PROFILE OF EXPERIMENTAL BUILDING AND GHP SYSTEM

The experiment is conducted in building of the Development and Research Center, Yanmar Company, Ltd. at 1600-4 Umegahara, Sakata-gun, Maibara-cho, Shiga, Japan. The building's outlook is shown in Figure A.1.

The experimental room is on the third floor of this building. The room is used as a design office and occupied by 14 persons. The room faces to outdoor space at west side and north side. The east of the room is corridor and the south of the room is another office. Under this room is a precisely controlled constant temperature humidity room. Because the

third floor is top floor, the top of the room is roof.

The room is equipped with one GHP system and two ventilation systems. The GHP system consists of one outdoor unit on the roof and four indoor units. Each ventilation system consists of two outlet louvers, two inlet louvers, and one heat exchanger unit including a fan.

The HVAC systems in the experiment room are shown in Figure A.2. The profile data of experimental room and GHP system are listed in Table A.1.



Figure A.1 Experimental building

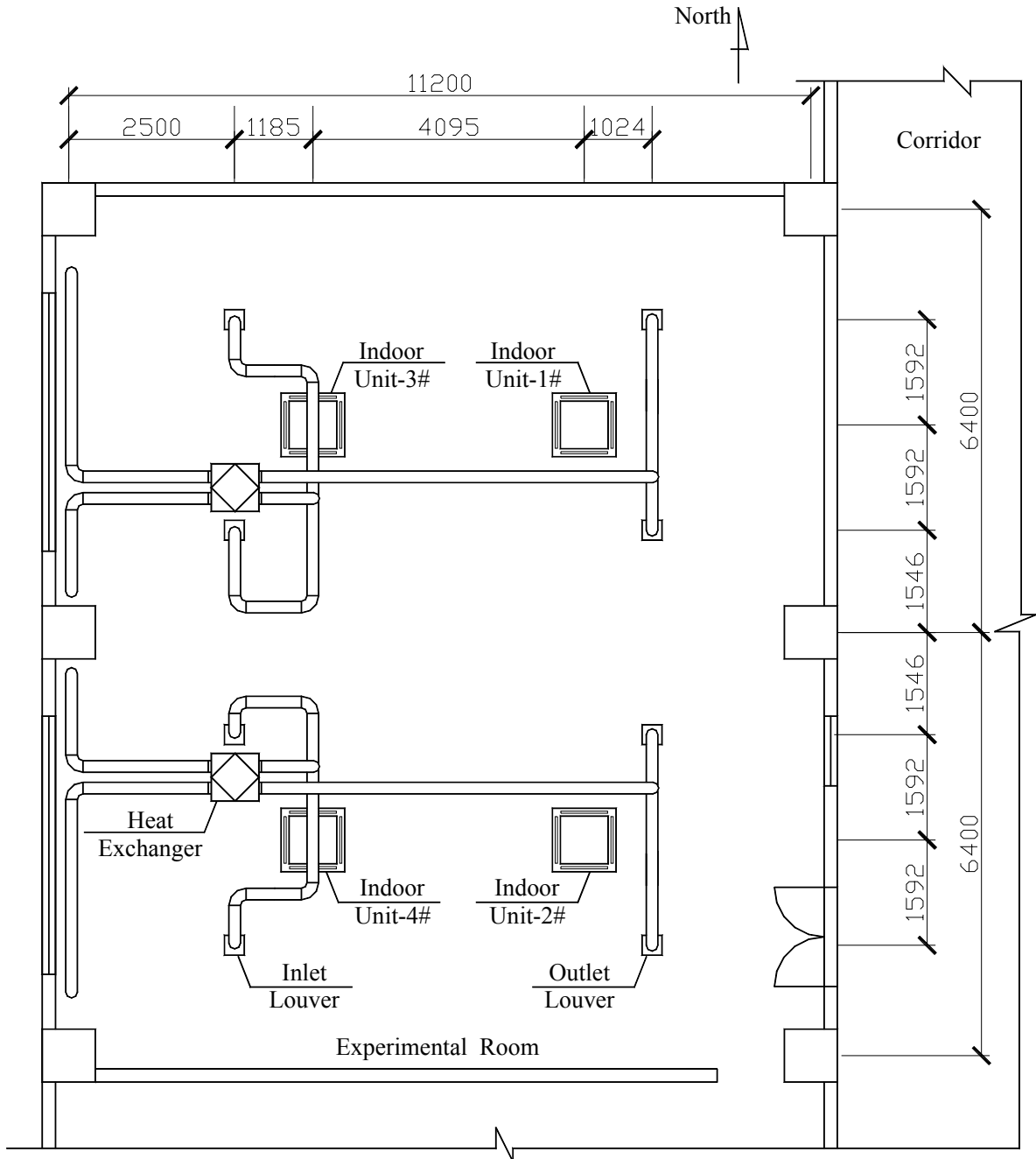


Figure A.2 Experimental HVAC systems

Table A.1 Profile of experimental room and GHP system

Room Information	Use	Office
	Floor area (m ²)	143.36
	Story height (m)	4.13
	Window area (m ²)	8.69
	Window type	Single-glazing aluminum alloy
	Glass thickness (mm)	8
	Window heat transfer coefficient (W/m ² °C)	5.47
	Lighting power (W)	1280
	Number of occupants	15
GHP System	Heating/cooling capacity (kW)	42.5 / 35.5
	Rated LPG consumption (heating / cooling kW) (LPG HHV=90.27MJ/Nm ³)	28.0/28.5
	Refrigerant	R22 (Before November 2003) R407C (After November 2003)
	Outdoor unit rated power (heating / cooling, kW)	1.09 / 1.09
	Indoor unit rated power (heating / cooling, W)	93/92
	Outdoor unit fan rated air flow rate (m ³ /h)	13800
	Indoor unit fan rated air flow rate (high/low speed, m ³ /h)	1200 / 900
Ventilation System	Number of indoor unit	4
	Rated air flow rate (high / low speed, m ³ /h)	350 / 220
	Rated power (high / low speed, W)	150 / 61
	Enthalpy exchange rate (cooling / heating)	62% / 65%

A.3 MEASUREMENT ITEMS

All the data related to the thermal and energy performance of the experimental room and HVAC systems are measured and recorded automatically using data loggers. In detail, four series of data, i.e. meteorological data, indoor environment, GHP system performance, and ventilation system performance, are measured and recorded.

A.3.1 METEOROLOGICAL DATA

The following meteorological data are measured, outdoor air temperature and humidity, solar radiation, wind direction and velocity. Outdoor air temperature and humidity are measured and recorded using combined temperature and humidity sensor and logger every two minutes, as shown in Figure A.3. Solar radiation is measured using solar radiation sensor putted on rooftop, as shown in Figure A.3. Wind direct and speed are measured using micro-vane and 3-Cup anemometer, as shown in Figure A.4.



Figure A.3 Outdoor air temperature, humidity and solar radiation measurement



Figure A.4 Wind direction and speed measurement

A.3.2 INDOOR ENVIRONMENT

Measured indoor environment data include heat flux through wall, window, flooring, and ceiling, solar radiation entering room through window, experimental room and surrounding room temperature, power consumed by lighting, computer, and other machines, number of occupants. Heat flux is measured using heat flux sensor, as shown in Figure A.5. Measurement of solar radiation entering room is shown in Figure A.5. Measurement of room air temperature distribution using thermal couple is shown in Figure A.6. Room air temperatures are measured at the southwest, center and northeast of the room and at the height of 700 mm, 1500 mm, and 2300 mm. The number of occupants is recorded through taking photos of the experimental room every five minutes using a digital camera, as shown in Figure A.7.



Figure A.5 Measurement of heat flux and solar radiation entering room



Figure A.6 Measurement of room air temperature



Figure A.7 Measurement of the number of occupants

A.3.3 GHP SYSTEM PERFORMANCE

In order to study the commissioning of GHP systems, the performance of the experimental GHP system is measured in detail, including indoor unit inlet and outlet air temperature and humidity, air flow rate, power consumption, outdoor unit inlet and outlet air temperature, power consumption, gas consumption, temperature of exhausted gas, refrigerant flow rate, refrigerant temperature and pressure at the four state points of refrigerating cycle. Indoor unit inlet and outlet air temperature is measured using thermal couple and humidity is measured using combined temperature and humidity sensor logger, as shown in Figure A.8. For the purpose of measuring the air flow rate of indoor unit, a duct is made to let the air velocity distribute uniformly, as shown in Figure A.9. Measurement of gas consumption and refrigerant flow rate are shown in Figure A.10 and Figure A.11. Measurement of refrigerant temperature and pressure are shown in Figure A.12 and Figure A.13.



Figure A.8 Measurement of indoor unit inlet and outlet air temperature and humidity



Figure A.9 Measurement of indoor unit air flow rate



Figure A.10 Measurement of gas consumption



Figure A.11 Measurement of refrigerant flow rate



Figure A.12 Measurement of refrigerant temperature



Figure A.13 Measurement of refrigerant pressure

A.3.4 VENTILATION SYSTEM PERFORMANCE

For ventilation system, air flow rate, inlet and outlet air temperature and humidity are measured. For the purpose of making air velocity distribute uniformly, a duct is used to measure the air velocity, as shown in Figure A.14. The air temperature is measured using thermal couple and humidity is measured using combine temperature and humidity sensor and logger, as shown in Figure A.15.

Three data loggers are used to record the measurement data, as shown in Figure A.16. Data are recorded once a minute.

In summary, all the measurement items are listed in Table A.2. Sensor locations are shown in Figure A.17.



Figure A.14 Measurement of ventilation air flow rate



Figure A.15 Measurement of ventilation air temperature and humidity



Figure A.16 Data loggers and wiring

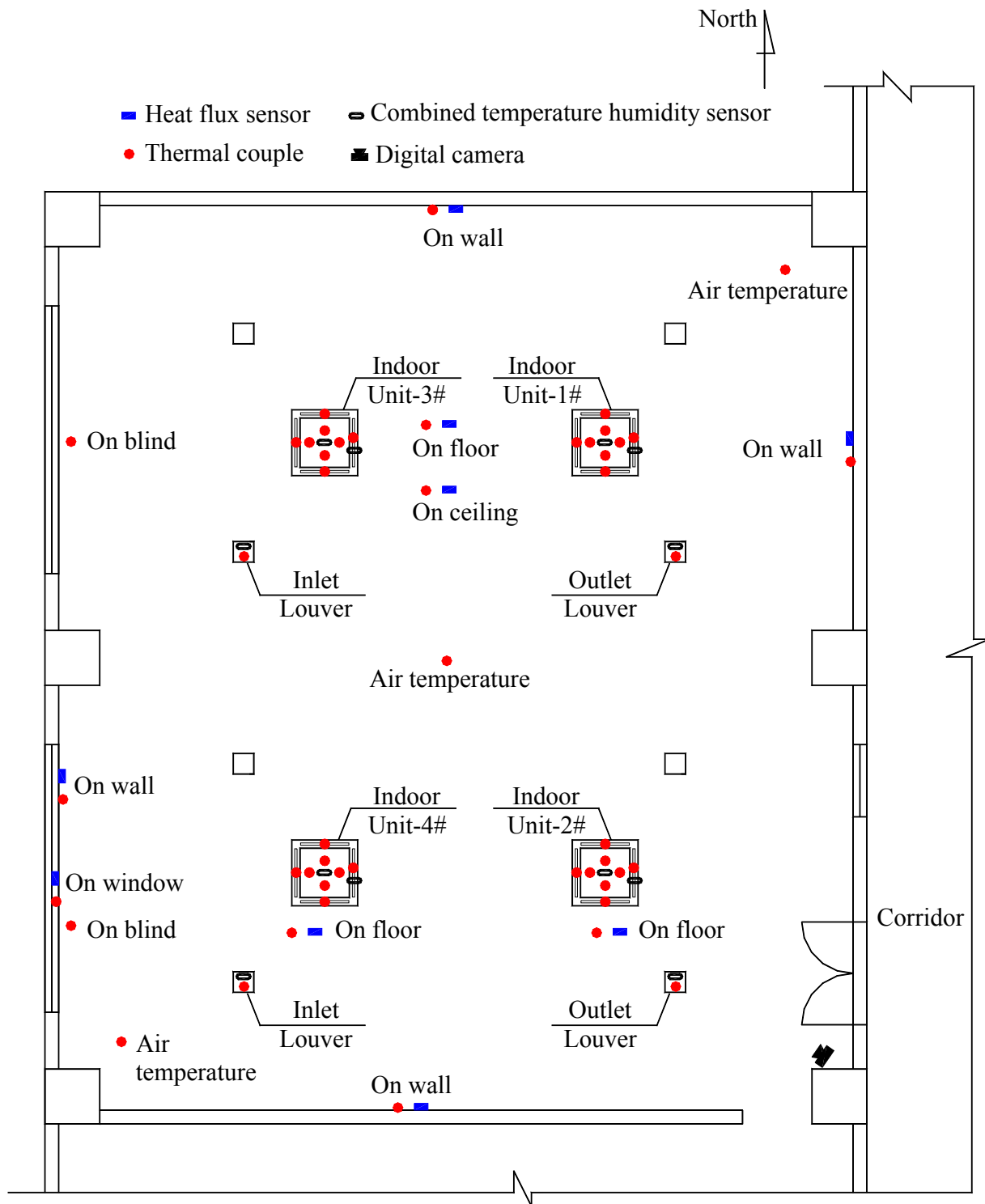


Figure A.17 Measurement sensor location

Table A.2 Measurement items

Series	Measurement Items	Instrument	Location
Meteorological Data	Outdoor air temperature and humidity	Combined temperature / humidity sensor / logger	Outdoor ventilated case
	Solar radiation	Solar radiation sensor	Rooftop
	Wind direction	Micro-vane wind direction sensor	Rooftop
	Wind speed	3-Cup anemometer	Rooftop
Indoor Environment	Heat flux	Heat flux sensor	Wall, window, ceiling, floor
	Surface temperature	Thermal couple	Wall, window, ceiling, floor
	Indoor air temperature	Thermal couple	West, center, east in experimental room, Adjacent room
	Number of occupants	Digital camera	Experimental room
	Electric power consumed by lighting and office machines	Electric power meter	Experimental room
GHP Outdoor Unit Performance	Gas consumption	Gas flow meter	Rooftop
	Electric power consumption	Electric power meter	Rooftop
	Refrigerant flow rate	Refrigerant flow rate meter	Rooftop
	Refrigerant pressure	Refrigerant pressure sensor	Rooftop
	Refrigerant temperature	Thermal couple	Rooftop
	Inlet / outlet air temperature	Thermal couple	Rooftop
	Exhausted gas temperature	Thermal couple	Rooftop
	Engine rotational speed	GHP monitoring system	Control center
	Compressor inlet / outlet refrigerant temperature	GHP monitoring system	Control center
	Compressor inlet / outlet refrigerant pressure	GHP monitoring system	Control center
	Expansion valve position	GHP monitoring system	Control center
	Operation mode	GHP monitoring system	Control center
On / Off state	GHP monitoring system	Control center	

GHP Indoor Unit Performance	Inlet / outlet air temperature	Thermal couple	Experimental room
	Inlet / outlet air humidity	Combined temperature / humidity sensor / logger	Experimental room
	Electric power consumption	Electric power meter	Experimental room
	Air flow rate	Anemometer	Measured one time
	Expansion valve position	GHP monitoring system	Control center
	Operation mode	GHP monitoring system	Control center
	On / Off state	GHP monitoring system	Control center
	Thermostat On / Off state	GHP monitoring system	Control center
	Refrigerant vapor / liquid temperature	GHP monitoring system	Control center
Ventilation System	Inlet / outlet air temperature	Thermal couple	Experimental room
	Inlet / outlet air humidity	Combined temperature / humidity sensor / logger	Experimental room
	Electric power consumption	Electric power meter	Experimental room
	Operation mode	Relay output	Experimental room
	On / Off state	Relay output	Experimental room
	Fan speed level	Relay output	Experimental room
	Air flow rate	Anemometer	Measured one time

A.4 EXPERIMENTAL RESULTS

A.1.1 FILTER RESISTANCE ESTIMATION MODEL

Using the data obtained from this experimental study on the GHP system, the filter resistance estimation model was developed. The details of the model are described in Chapter 7.

A.1.2 COMPARISON OF SIMULATED AND MEASURED HEATING/COOLING LOAD

The hourly heating/cooling load of the experimental room during a year was simulated using the simulation software HASP. The simulated heating/cooling load was compared with three types of measured load, which are heat transferred through building envelopes, load calculated from GHP indoor unit enthalpy difference between inlet and outlet air, and

enthalpy difference between inlet and outlet refrigerant. The comparison results show that the simulated load can well match the three type of measured load in summer period and simulated load can well match load calculated from building envelope heat transfer and from air side enthalpy difference in winter period. In winter period the simulated load cannot match the load calculated from refrigerant enthalpy difference because the refrigerant flow rate was not measured accurately because of refrigerant foaming (Kitagawa, et al., 2004).

A.1.3 INDOOR UNIT AIR FLOW RATE

The indoor unit air flow rate was measured before and after filter cleaning respectively. The filters were cleaned through blowing using high-pressure air. The measurement results are shown in Figure A.18

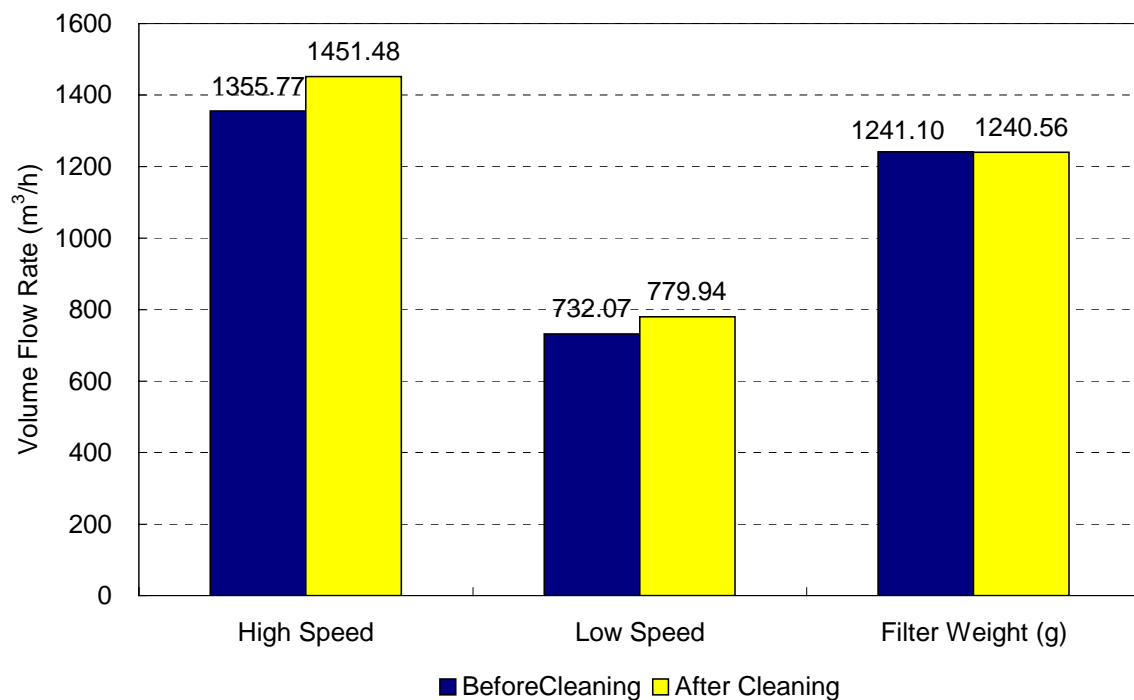


Figure A.18 Indoor unit air flow rate and filter weight

A.1.3 VENTILATION AIR FLOW RATE

The measurement results of ventilation are shown in Figure A.19

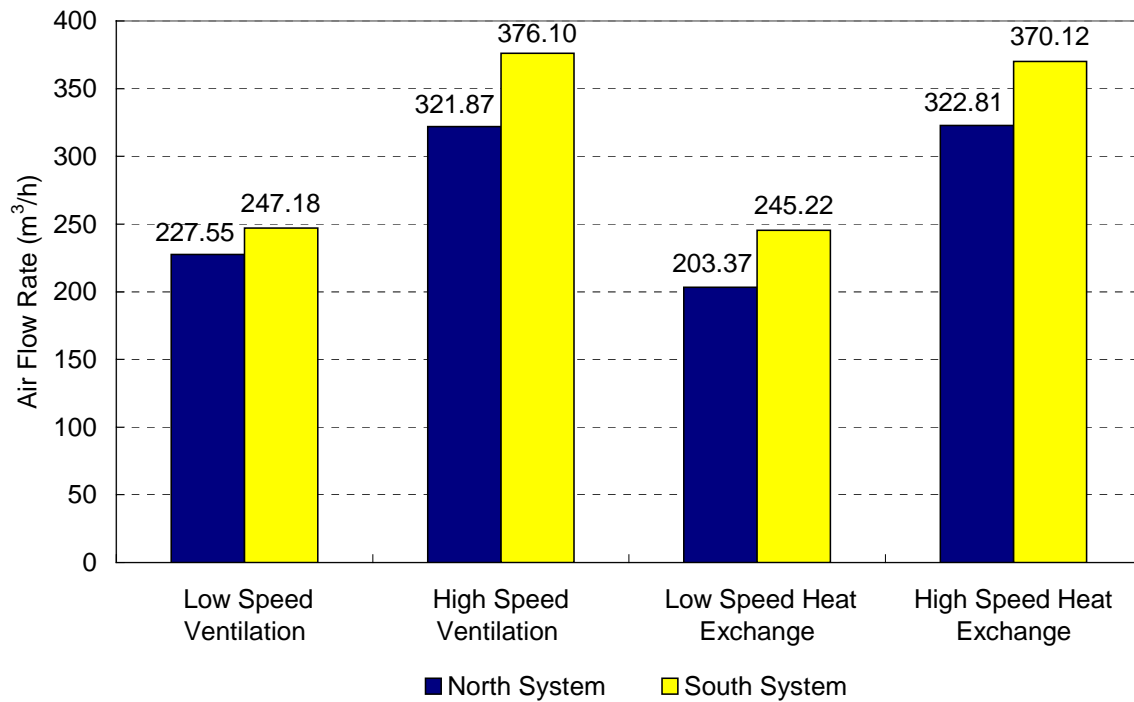


Figure A.19 Ventilation air flow rate

A.1.4 GHP COP CALCULATION

The Coefficient Of Performance (COP) based on primary energy of the GHP is calculated using the minutely measured GHP system performance data. During cooling operation in summer, the COP is calculated using Equation (A.1). During heating operation in winter, the COP is calculated using Equation (A.2).

$$COP_{su} = \frac{HHV \cdot GC + EC / 0.3}{m_{ref}(h_{ref1} - h_{ref3})} \quad (A.1)$$

$$COP_w = \frac{HHV \cdot GC + EC / 0.3}{m_{ref}(h_{ref2} - h_{ref3})} \quad (A.2)$$

Where 0.3 is the coefficient of converting electric power to primary energy.

The GHP refrigerant system chart and refrigerant flow rate, pressure, and temperature measurement points are shown in Figure A.20.

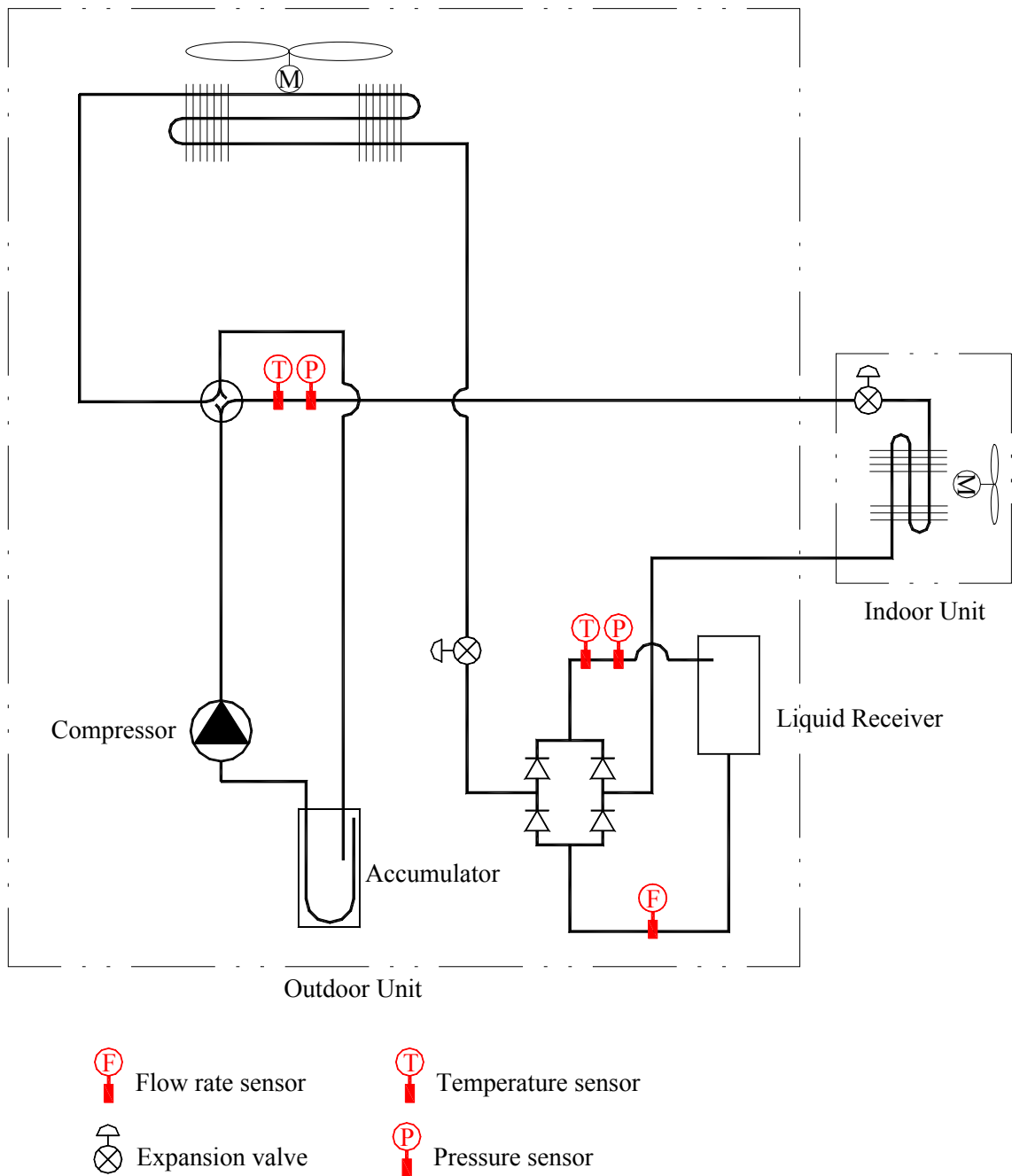


Figure A.20 GHP refrigerant system chart and measurement points

A MATLAB program is written to automatically scan the raw data and calculate the primary energy based COP once a minute. For summertime, the refrigerant enthalpy at state point 1 and 3 are used to calculate the cooling produced by the GHP. The MATLAB program code is shown in the following part. The COP calculation results on typical summer day are shown in Figure A.21. A sample of raw data used for COP calculation is shown in Table A.3. and calculation results are shown in Table A.4.

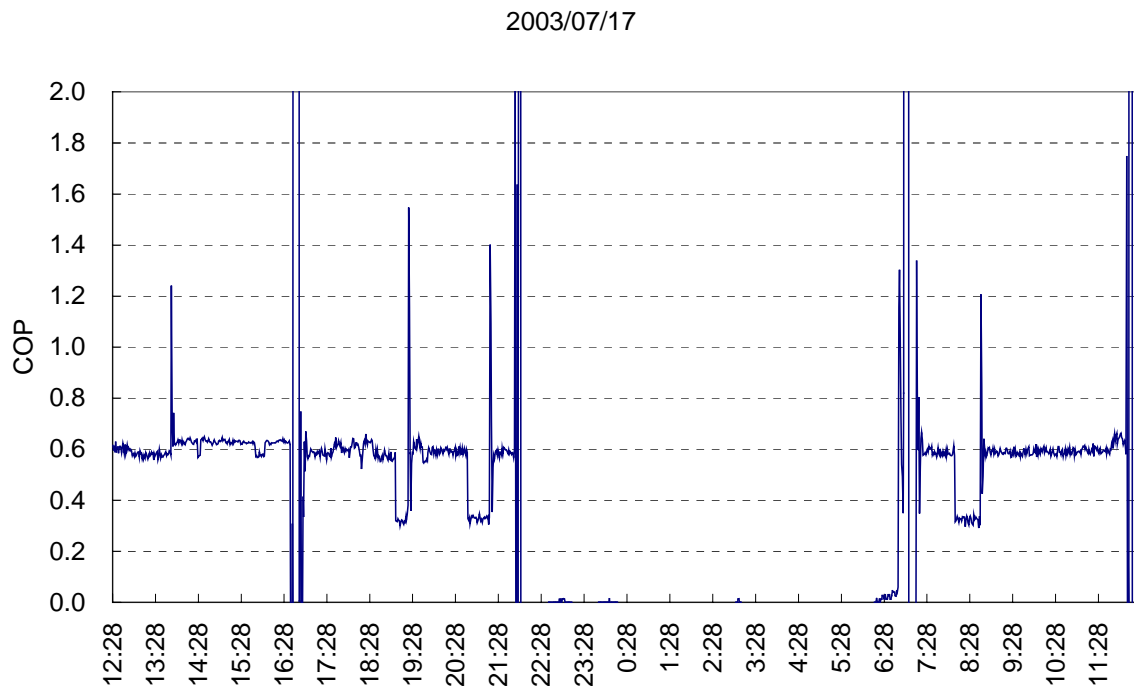


Figure A.21 COP calculation results on typical summer day

From Figure A.21 it can be found that the COP of the GHP system during refrigerant cycle is about 0.6. This COP is not high compared with the catalog COP of 1.08 and the potential of improving the performance of the GHP system can be seen.

```
%File name:GHPCOP_Summer_StandardTimeStyle.m
%Written by Fulin Wang
%February 23, 2004
%This program is used to calculate a GHP's primary energy COP during cooling period in
summer.
%Measured refrigerant flow rate, pressure and temperature at state points
%3 and 1 are used to calculate the cooling amount produce by the GHP.
%The Thermodac Data(RF) files are read to get raw data.
%Set the current path as the folds where Thermodac Data(RF) data to be analyzed are stored.
%The raw data style of left two columns recording date and time should be standard date/time
value style, for example, 37824 0.519803
%instead of date/time style, 2003/7/22 12:28:31.
%The data number in every row must be same. It is better to check the first and last row in the
raw data file.
```

```
clear all

HHV = 90.27; % LPG Higher Heating Value, MJ/Nm3
tic;

for month = 1:12 %Scan and read all the Thermodac(RF) files in current directory.
    if month < 10
        eval(['FileNameMonth = ['0',int2str(month),'];']);
    else
        FileNameMonth = int2str(month);
    end
    for date = 1:31
        if date < 10
            eval(['FileNameDate = ['0',int2str(date),'];']);
        else
            FileNameDate = int2str(date);
        end
        eval(['FileID = fopen('',FileNameMonth,FileNameDate,'1228.csv');']);
        if FileID == -1
            eval(['FileID = fopen('',FileNameMonth,FileNameDate,'1015.csv');']);
            if FileID == -1
                eval(['FileID = fopen('',FileNameMonth,FileNameDate,'0918.csv');']);
            end
        end
        end
        if FileID ~= -1

            for line = 1:5
                t = fgets(FileID); %Read five lines table title
            end
            clear RawData P1 T1 P3 T3 H1 H4 Density3 LPGHeat RefFlowRate
CoolingAmount COP

            RawData = fscanf(FileID, '%f%c', [64,inf]);
            %Read raw data. The data style of left two columns recording date and time
            %should be standard style instead of date/time style.
            %The data number in every row must be same. Check the first and last row
```

```

%in the raw data file.

RawData = RawData';
RawData = RawData(:,1:2:41); %Eliminate space column

RowNo = size(RawData);
for row = 1:RowNo(1,1)
    P1 = RawData(row,19)*9.8E4+101325; %Refrigerant pressure of State
point 1, converted from kg/cm2 to Pa
    P3 = RawData(row,10)*9.8E4+101325;
    T1 = RawData(row,20)+273.15; %Refrigerant Temperature of State point 1,
converted from Centigrade to Kelvin
    T3 = RawData(row,11)+273.15;
    H1(row,1) = property ('H','T',T1,'P',P1,'R22'); % Refrigerant enthalpy, J/kg
    H1(row,1) = property ('H','T',T1,'P',P1,'R22');
%Because of the bug of refrigerant property calculation program,
%the first call of the program gives strange answers.
%So every property has to be calculated two times to get correct results.
    H4(row,1) = property ('H','T',T3,'P',P3,'R22');
% Refrigerant enthalpy at state point 4,
% assumed to be equal to the enthalpy at state point 3
    H4(row,1) = property ('H','T',T3,'P',P3,'R22');
    Density3(row,1) = property ('D','T',T3,'P',P3,'R22'); % Refrigerant density
at state point 3, kg/m3
    Density3(row,1) = property ('D','T',T3,'P',P3,'R22');
end
LPGHeat = RawData(:,7)*HHV*1.0E6/3600; % LPG heat generation, W
RefFlowRate = RawData(:,9).*Density3*1.0E-3/60;
% Refrigerant flow rate, converted from L/min to kg/s
CoolingAmount = RefFlowRate.*(H1-H4);
% Cooling amount = Refrigerant flow rate * Delta enthalpy
COP = CoolingAmount./(LPGHeat+RawData(:,8)./0.3); %Converse electric
consumption to primary energy consumption (RawData(:,8)./0.3)

figure
plot(COP,'r','LineWidth',1)
grid on
ylabel('COP')

```

```

eval(['title('"',FileNameMonth,'/',FileNameDate,'"')]);
axis auto
fclose(FileID);
set(gca,'ylim',[0 3])
set(gca,'xlim',[0 1440])
set(gca,'xTick',[0:120:1440])
set(gca,'xTickLabel',[0:120:1440])
eval(['hgsave("COP',FileNameMonth,FileNameDate,'.fig")']);

Results = [RawData(:,1) RawData(:,2) RawData(:,7) RawData(:,8) RawData(:,9)
RawData(:,10) RawData(:,11) RawData(:,19) RawData(:,20) H4 H1 Density3 CoolingAmount
COP];

eval(['SaveFileName=["COP',FileNameMonth,FileNameDate,'.csv"];']);
eval(['SaveFileID = fopen('"',SaveFileName,'"","w");']);
if SaveFileID ~= -1
    TableTitle1 = ['Date,Time,GasConsumption,ElectricConsumption,RefrigerantFlowRate',...
    'Pressure3,Temperature3,Pressure1,Temperature1,Enthalpy3,Enthalpy1,Density3,CoolingAmo
unt,COP'];
    TableTitle2 = ['-,-,Nm3/h,W,L/min,kg/cm2,C,kg/cm2,C,J/kg,J/kg,kg/m3,W,-'];

    fprintf(SaveFileID,'%s,\n',TableTitle1);
    fprintf(SaveFileID,'%s,\n',TableTitle2);
    fprintf(SaveFileID,'%d,%d,%d,%d,%d,%d,%d,%d,%d,%d,%d,%d,%d,%d,\n',Results');
    fclose(SaveFileID);
end

end

end

end

toc;
hours = fix(toc/3600);
minutes = fix(mod(toc,3600)/60);
seconds = mod(mod(toc,3600),60);
['Calculation time: ',int2str(hours),'hours, ',int2str(minutes),'minutes, ',int2str(seconds),'seconds']

```


Table A.3 Raw data for COP calculation of cooling operation

29	CH	0	1	2	3	4	5	6	7	8	9	10	11	12	13	14	15	16	17	18
	Name	CHANN EL-00	102 Solar	103 Wind speed	104 Wind direction	401 Gas consumption	402 Power consumption	403 Refrigerant flow rate	404 Pressure (high)	405 Refrigerant temperature (high)	406 Temperature of Exhausted Gas	407 Temperature of inlet air 1	408 Temperature of inlet air 2	409 Temperature of inlet air 3	410 Temperature of outlet air 1	411 Temperature of outlet air 2	Temperature of engine room	425 Pressure (low)	426 Refrigerant temperature (low)	427 Temperature of PC room
	Unit	oC	W/m2	m/s	o	Nm3/h	W	L/min	kg/cm2	oC	oC	oC	oC	oC	oC	oC	oC	kg/cm2	oC	oC
	Form	#####0.0	#####0.0	#### 0.0	#####0.0	##0.00 0	##### #0	##0.000	###0.00	###0.0 0	#####0.0	#####0. 0	#####0. 0	#####0.0	#####0. 0	#####0. 0	#####0.0	###0.0 0	##### .0	#### 0.0
37818	0.519803	9999.9	1060.8	3.8	190.2	0.273	836	1.581	11.65	29.3	53.8	27.7	28.1	28.5	32.4	30.2	54.3	4.18	20.6	26.2
37818	0.520498	9999.9	1055.8	3.7	270.7	0.273	839	1.547	11.31	29.2	53.2	26	25.9	26.5	31.2	29.5	54.3	4.18	20.7	26.3
37818	0.521192	9999.9	1059	2.6	266.2	0.273	840	1.561	11.52	29.3	53.2	26.6	26.2	26.6	31.8	29.6	54.1	4.13	20.6	26.2
37818	0.521887	9999.9	1061.6	2.8	307.7	0.273	839	1.561	11.45	29.3	52.9	26.3	26.1	26.4	31.6	29.7	54.2	4.13	20.6	26.3
37818	0.522581	9999.9	1061	2.1	79.6	0.273	838	1.554	11.42	29.2	52.1	27.8	27.8	24.7	31.7	29.3	54.4	4.13	20.5	26.3
37818	0.523275	9999.9	1064	3	352.4	0.273	838	1.547	11.52	28.8	52.3	26.4	24.7	25.3	31.7	29.7	54.5	4.14	20.5	26.2
37818	0.52397	9999.9	1061.2	2.3	264.2	0.273	834	1.561	11.55	28.8	51.7	26.9	26.1	27.3	32.1	30	54.6	4.15	20.6	26.3
37818	0.524664	9999.9	1055.4	2.7	223.3	0.262	845	1.612	11.32	28.9	52.5	26.1	25.4	26.4	31	29	54.2	4.11	20.5	26.3
37818	0.525359	9999.9	1051	2.8	351.7	0.273	841	1.622	11.56	29	53.3	27.7	28.1	27.7	32.3	30.1	53.9	4.14	20.6	26.4
37818	0.526053	9999.9	1052.8	3.2	81.8	0.273	845	1.598	11.43	28.9	53.3	26.7	26.1	25.9	32	29.7	54.1	4.15	20.6	26.3
37818	0.526748	9999.9	1051.8	3.7	228.4	0.273	842	1.615	11.5	29	53.7	26	26.5	26.1	32.1	29.6	54.5	4.16	20.6	26.4
37818	0.527442	9999.9	1050.8	2.9	343	0.273	846	1.663	11.45	29.1	53.4	25.3	24.1	25.4	31.6	29.7	54.1	4.16	20.6	26.3
37818	0.528137	9999.9	1047.2	4.3	13.1	0.273	838	1.581	11.64	29.3	53.2	27.8	27.2	28.5	31.9	30.3	54.4	4.13	20.6	26.4
37818	0.528831	9999.9	1049	3	300.8	0.273	838	1.54	11.47	29	53	27.8	26.3	26.5	31.9	29.6	54.2	4.13	20.6	26.4
37818	0.529525	9999.9	1045.6	4.3	190.7	0.273	830	1.533	11.4	29	52.9	26.5	26.6	26.3	31.7	29.3	54.5	4.13	20.5	26.3
37818	0.53022	9999.9	1045.4	3.3	101.3	0.273	841	1.571	11.51	29.2	53.6	27.1	27.3	25.9	32	29.8	54.3	4.14	20.6	26.5
37818	0.530914	9999.9	1043.8	4.6	159	0.273	837	1.533	11.21	29	53	25.9	24.8	25.6	31.1	29	54.1	4.15	20.6	26.5
37818	0.531609	9999.9	1043.2	4	329.9	0.273	838	1.652	11.56	29	53.7	27.6	27.7	27.5	32.2	30	54	4.13	20.6	26.3
37818	0.532303	9999.9	1045	3.2	329.4	0.273	839	1.564	11.44	29.1	53.3	26.6	26.1	27	31.7	29.8	53.9	4.13	20.6	26.4

37818	0.532998	9999.9	1045.6	4.3	272.6	0.272	835	1.608	11.58	28.9	53.4	26.9	26.9	27.5	32.2	30.3	54.1	4.15	20.6	26.4
37818	0.533692	9999.9	1046.6	3.6	366.9	0.273	835	1.622	11.56	28.8	53.3	27.5	27.9	26.7	32.4	30.5	54.1	4.15	20.6	26.4
37818	0.534387	9999.9	1047.2	5.2	218.1	0.273	830	1.612	11.52	28.7	53.3	27.6	26.6	27.3	32	30.2	54.2	4.15	20.6	26.5
37818	0.535081	9999.9	1041.6	4.3	359.9	0.272	837	1.557	11.39	28.7	52.9	26.7	26.6	27	31.7	30	54	4.13	20.6	26.5
37818	0.535775	9999.9	1037	2.7	68.7	0.273	830	1.622	11.56	28.6	53.4	28.1	28	27.4	32.4	30.5	54.5	4.14	20.6	26.4
37818	0.53647	9999.9	1038.4	5.5	27.2	0.273	838	1.564	11.63	28.7	54	28.4	27.1	27.7	32.6	30.9	54.4	4.21	20.7	26.7
37818	0.537164	9999.9	1039.6	4.7	117.3	0.272	833	1.578	11.25	28.7	52.8	25	25.5	25.6	31.3	29.4	54.3	4.15	20.6	26.5
37818	0.537859	9999.9	1039.2	4.3	245.6	0.273	833	1.584	11.44	29.1	53.2	27.1	26.2	26.8	31.8	29.9	54.3	4.13	20.6	26.6
37818	0.538553	9999.9	1038.6	4.4	334.2	0.272	827	1.591	11.52	29	53.3	27.9	26	27.2	31.5	29.8	54.5	4.13	20.6	26.5
37818	0.539248	9999.9	1034.4	3.4	43.7	0.273	830	1.608	11.47	28.8	53	25.2	25.4	26.2	31.3	29.7	54.5	4.13	20.6	26.5
37818	0.539942	9999.9	1029.2	3.4	6.2	0.273	825	1.574	11.36	28.8	53	25.7	25.1	26.6	31.2	29.4	54	4.13	20.5	26.6
37818	0.540637	9999.9	1029	3.4	282.2	0.272	830	1.571	11.36	28.8	53.2	27.7	26.7	27.4	31.2	29.3	54.2	4.12	20.6	26.5
37818	0.541331	9999.9	1029.6	2.8	245.4	0.272	829	1.561	11.41	28.8	53.3	26.6	26.9	26.9	31.7	29.5	54.6	4.14	20.6	26.6
37818	0.542025	9999.9	1032.8	2.1	229.5	0.273	829	1.639	11.44	28.8	52	27.7	26.5	25.9	31.7	29.2	54.3	4.14	20.6	26.6
37818	0.54272	9999.9	1032.8	2.8	302.2	0.273	825	1.622	11.69	28.9	52.9	27.6	26.9	28	32.3	30.3	54.2	4.17	20.6	26.6
37818	0.543414	9999.9	1033.6	4.2	103.2	0.272	828	1.571	11.84	29.2	54	28.6	27.8	28.3	32.9	31.1	54.4	4.22	20.7	26.6
37818	0.544109	9999.9	1032.4	2.7	23.3	0.263	825	1.615	11.41	29.5	53.3	26.4	26.4	26.4	31.8	29.9	54.3	4.18	20.6	26.6
37818	0.544803	9999.9	1031.4	3.5	272.4	0.272	818	1.578	11.41	29.5	53.3	26.9	25.8	26.4	31.4	29.7	54.1	4.13	20.6	26.6
37818	0.545498	9999.9	1032.2	2.5	343.3	0.273	818	1.632	11.51	29.1	53.6	27.1	27.7	26.8	32.2	30.2	54.6	4.16	20.6	26.8
37818	0.546192	9999.9	1032.4	2.6	318	0.272	821	1.554	11.61	28.8	53.1	26.7	25.5	26	31.9	30.2	54.3	4.16	20.6	26.8
37818	0.546887	9999.9	1034.2	3.4	44.7	0.272	821	1.574	11.6	28.6	53.4	27.9	26.7	27.5	32.2	30.4	54.3	4.16	20.6	26.6
37818	0.547581	9999.9	1031	3.4	305.8	0.272	833	1.601	11.48	28.5	53	26.6	26.2	27.6	31.8	30.2	54.5	4.14	20.6	26.7
37818	0.548275	9999.9	1030.2	2.6	314.1	0.272	832	1.615	11.48	28.6	54	26.4	26.8	26	32.1	30.1	54.2	4.13	20.6	26.6
37818	0.54897	9999.9	1022.4	2.7	305.5	0.273	835	1.625	11.58	28.6	53.5	28	27	28.3	32.2	30.5	54.6	4.12	20.7	26.9
37818	0.549664	9999.9	1024	5.6	108.6	0.273	837	1.618	11.39	28.6	52.9	26.1	25.7	27.9	31.6	29.8	54.2	4.16	20.6	26.7
37818	0.550359	9999.9	1021	3.2	354.6	0.262	833	1.564	11.36	28.7	53.5	26.7	24.6	26.4	31.6	29.8	54.3	4.16	20.7	26.8
37818	0.551053	9999.9	1022.4	2	334.4	0.272	835	1.53	11.35	28.7	53.3	26.4	25.9	26	31.5	29.6	54.3	4.12	20.7	26.8
37818	0.551748	9999.9	1029.6	4.5	355.1	0.272	833	1.625	11.39	28.6	53.4	27	25.4	27.2	31.5	29.5	54.1	4.1	20.6	26.9
37818	0.552442	9999.9	1027.6	4.3	72.3	0.273	839	1.591	11.66	28.5	53.3	27.3	28.9	27.1	32.4	30.2	54.3	4.14	20.7	26.9
37818	0.553137	9999.9	1022.8	3.7	12.5	0.273	828	1.547	11.58	28.5	53.6	26.9	27.1	27.2	32.2	30	54.4	4.19	20.7	27

Table A.4 COP calculation results of cooling operation

Date	Time	Gas Consumption	Electric Consumption	Refrigerant Flow Rate	Pressure 3	Temperature 3	Pressure 1	Temperature 1	Enthalpy 3	Enthalpy 1	Density 3	Cooling Amount	COP
-	-	Nm ³ /h	W	L/min	kg/cm ²	C	kg/cm ²	C	J/kg	J/kg	kg/m ³	W	-
2003/7/16	12:28	0.273	836	1.581	11.65	29.3	4.18	20.6	235724.7	419835.4	1174.06	5695.738	0.591326
2003/7/16	12:29	0.273	839	1.547	11.31	29.2	4.18	20.7	235599.7	419908	1174.258	5580.172	0.578728
2003/7/16	12:30	0.273	840	1.561	11.52	29.3	4.13	20.6	235725.7	419920.5	1173.974	5625.842	0.583262
2003/7/16	12:31	0.273	839	1.561	11.45	29.3	4.13	20.6	235726.2	419920.5	1173.928	5625.604	0.583439
2003/7/16	12:32	0.273	838	1.554	11.42	29.2	4.13	20.5	235598.9	419848	1174.331	5603.971	0.581397
2003/7/16	12:33	0.273	838	1.547	11.52	28.8	4.14	20.5	235088.3	419831	1176.086	5602.029	0.581195
2003/7/16	12:34	0.273	834	1.561	11.55	28.8	4.15	20.6	235088.1	419886.5	1176.105	5654.525	0.587454
2003/7/16	12:35	0.262	845	1.612	11.32	28.9	4.11	20.5	235217.1	419882	1175.533	5832.209	0.621352
2003/7/16	12:36	0.273	841	1.622	11.56	29	4.14	20.6	235342.8	419903.5	1175.269	5863.757	0.607718
2003/7/16	12:37	0.273	845	1.598	11.43	28.9	4.15	20.6	235216.3	419886.5	1175.605	5782.076	0.598426
2003/7/16	12:38	0.273	842	1.615	11.5	29	4.16	20.6	235343.2	419869.5	1175.229	5837.165	0.604753
2003/7/16	12:39	0.273	846	1.663	11.45	29.1	4.16	20.6	235471.1	419869.5	1174.774	6004.161	0.621197
2003/7/16	12:40	0.273	838	1.581	11.64	29.3	4.13	20.6	235724.8	419920.5	1174.054	5698.336	0.591187
2003/7/16	12:41	0.273	838	1.54	11.47	29	4.13	20.6	235343.4	419920.5	1175.209	5567.528	0.577616
2003/7/16	12:42	0.273	830	1.533	11.4	29	4.13	20.5	235343.9	419848	1175.163	5539.813	0.576335
2003/7/16	12:43	0.273	841	1.571	11.51	29.2	4.14	20.6	235598.2	419903.5	1174.391	5667.289	0.587356
2003/7/16	12:44	0.273	837	1.533	11.21	29	4.15	20.6	235345.3	419886.5	1175.038	5540.336	0.574994
2003/7/16	12:45	0.273	838	1.652	11.56	29	4.13	20.6	235342.8	419920.5	1175.269	5972.762	0.619658
2003/7/16	12:46	0.273	839	1.564	11.44	29.1	4.13	20.6	235471.2	419920.5	1174.767	5648.257	0.585789
2003/7/16	12:47	0.272	835	1.608	11.58	28.9	4.15	20.6	235215.2	419886.5	1175.704	5818.78	0.605887
2003/7/16	12:48	0.273	835	1.622	11.56	28.8	4.15	20.6	235088	419886.5	1176.112	5875.524	0.610203
2003/7/16	12:49	0.273	830	1.612	11.52	28.7	4.15	20.6	234961	419886.5	1176.507	5845.277	0.608114
2003/7/16	12:50	0.272	837	1.557	11.39	28.7	4.13	20.6	234961.8	419920.5	1176.422	5646.445	0.587535
2003/7/16	12:51	0.273	830	1.622	11.56	28.6	4.14	20.6	234833.4	419903.5	1176.954	5888.37	0.612597
2003/7/16	12:52	0.273	838	1.564	11.63	28.7	4.21	20.7	234960.2	419856.9	1176.579	5670.686	0.588318
2003/7/16	12:53	2.72E-01	833	1.58E+00	1.13E+01	2.87E+01	4.15E+00	2.06E+01	2.35E+05	4.20E+05	1.18E+03	5.72E+03	5.96E-01

2003/7/16	12:54	2.73E-01	833	1.58E+00	1.14E+01	2.91E+01	4.13E+00	2.06E+01	2.35E+05	4.20E+05	1.17E+03	5.72E+03	5.95E-01
2003/7/16	12:55	2.72E-01	827	1.59E+00	1.15E+01	29	4.13E+00	2.06E+01	2.35E+05	4.20E+05	1.18E+03	5.75E+03	6.01E-01
2003/7/16	12:56	2.73E-01	830	1.61E+00	1.15E+01	2.88E+01	4.13E+00	2.06E+01	2.35E+05	4.20E+05	1.18E+03	5.83E+03	6.06E-01
2003/7/16	12:57	2.73E-01	825	1.57E+00	1.14E+01	2.88E+01	4.13E+00	2.05E+01	2.35E+05	4.20E+05	1.18E+03	5.70E+03	5.94E-01
2003/7/16	12:58	2.72E-01	830	1.57E+00	1.14E+01	2.88E+01	4.12E+00	2.06E+01	2.35E+05	4.20E+05	1.18E+03	5.69E+03	5.94E-01
2003/7/16	12:59	2.72E-01	829	1.56E+00	1.14E+01	2.88E+01	4.14E+00	2.06E+01	2.35E+05	4.20E+05	1.18E+03	5.65E+03	5.90E-01
2003/7/16	13:00	2.73E-01	829	1.64E+00	1.14E+01	2.88E+01	4.14E+00	2.06E+01	2.35E+05	4.20E+05	1.18E+03	5.94E+03	6.18E-01
2003/7/16	13:01	2.73E-01	825	1.62E+00	1.17E+01	2.89E+01	4.17E+00	2.06E+01	2.35E+05	4.20E+05	1.18E+03	5.87E+03	6.12E-01
2003/7/16	13:02	2.72E-01	828	1.57E+00	1.18E+01	2.92E+01	4.22E+00	2.07E+01	2.36E+05	4.20E+05	1.17E+03	5.67E+03	5.91E-01
2003/7/16	13:03	2.63E-01	825	1.62E+00	1.14E+01	2.95E+01	4.18E+00	2.06E+01	2.36E+05	4.20E+05	1.17E+03	5.81E+03	6.21E-01
2003/7/16	13:04	2.72E-01	818	1.58E+00	1.14E+01	2.95E+01	4.13E+00	2.06E+01	2.36E+05	4.20E+05	1.17E+03	5.67E+03	5.94E-01
2003/7/16	13:05	2.73E-01	818	1.63E+00	1.15E+01	2.91E+01	4.16E+00	2.06E+01	2.35E+05	4.20E+05	1.17E+03	5.89E+03	6.16E-01
2003/7/16	13:06	2.72E-01	821	1.55E+00	1.16E+01	2.88E+01	4.16E+00	2.06E+01	2.35E+05	4.20E+05	1.18E+03	5.63E+03	5.89E-01
2003/7/16	13:07	2.72E-01	821	1.57E+00	1.16E+01	2.86E+01	4.16E+00	2.06E+01	2.35E+05	4.20E+05	1.18E+03	5.71E+03	5.98E-01
2003/7/16	13:08	2.72E-01	833	1.60E+00	1.15E+01	2.85E+01	4.14E+00	2.06E+01	2.35E+05	4.20E+05	1.18E+03	5.82E+03	6.06E-01
2003/7/16	13:09	2.72E-01	832	1.62E+00	1.15E+01	2.86E+01	4.13E+00	2.06E+01	2.35E+05	4.20E+05	1.18E+03	5.86E+03	6.11E-01
2003/7/16	13:10	2.73E-01	835	1.63E+00	1.16E+01	2.86E+01	4.12E+00	2.07E+01	2.35E+05	4.20E+05	1.18E+03	5.90E+03	6.13E-01
2003/7/16	13:11	2.73E-01	837	1.62E+00	1.14E+01	2.86E+01	4.16E+00	2.06E+01	2.35E+05	4.20E+05	1.18E+03	5.87E+03	6.09E-01
2003/7/16	13:12	2.62E-01	833	1.56E+00	1.14E+01	2.87E+01	4.16E+00	2.07E+01	2.35E+05	4.20E+05	1.18E+03	5.67E+03	6.07E-01
2003/7/16	13:13	2.72E-01	835	1.53E+00	1.14E+01	2.87E+01	4.12E+00	2.07E+01	2.35E+05	4.20E+05	1.18E+03	5.55E+03	5.78E-01
2003/7/16	13:14	2.72E-01	833	1.63E+00	1.14E+01	2.86E+01	4.10E+00	2.06E+01	2.35E+05	4.20E+05	1.18E+03	5.90E+03	6.15E-01
2003/7/16	13:15	2.73E-01	839	1.59E+00	1.17E+01	2.85E+01	4.14E+00	2.07E+01	2.35E+05	4.20E+05	1.18E+03	5.78E+03	6.00E-01
2003/7/16	13:16	2.73E-01	828	1.55E+00	1.16E+01	2.85E+01	4.19E+00	2.07E+01	2.35E+05	4.20E+05	1.18E+03	5.62E+03	5.85E-01
2003/7/16	13:17	2.72E-01	832	1.58E+00	1.13E+01	2.86E+01	4.14E+00	2.06E+01	2.35E+05	4.20E+05	1.18E+03	5.74E+03	5.98E-01
2003/7/16	13:18	2.73E-01	825	1.59E+00	1.18E+01	29	4.18E+00	2.07E+01	2.35E+05	4.20E+05	1.18E+03	5.75E+03	6.00E-01
2003/7/16	13:19	2.72E-01	831	1.58E+00	1.14E+01	2.91E+01	4.17E+00	2.06E+01	2.35E+05	4.20E+05	1.17E+03	5.70E+03	5.94E-01
2003/7/16	13:20	2.72E-01	835	1.59E+00	1.15E+01	2.91E+01	4.13E+00	2.06E+01	2.35E+05	4.20E+05	1.17E+03	5.75E+03	5.98E-01
2003/7/16	13:21	2.72E-01	833	1.61E+00	1.13E+01	29	4.13E+00	2.06E+01	2.35E+05	4.20E+05	1.18E+03	5.81E+03	6.06E-01
2003/7/16	13:22	2.72E-01	825	1.58E+00	1.14E+01	2.89E+01	4.14E+00	2.07E+01	2.35E+05	4.20E+05	1.18E+03	5.71E+03	5.97E-01

For wintertime, the refrigerant enthalpy at state point 2 and 3 are used to calculate the cooling produced by the GHP. Furthermore, the refrigerant in the GHP system is changed from R22 to R407C since November 2003. The MATLAB program code is shown in the following part. The COP calculation results on typical winter day are shown in Figure A.22. A sample of raw data used for COP calculation is shown in Table A.5 and calculation results are shown in Table A.6.

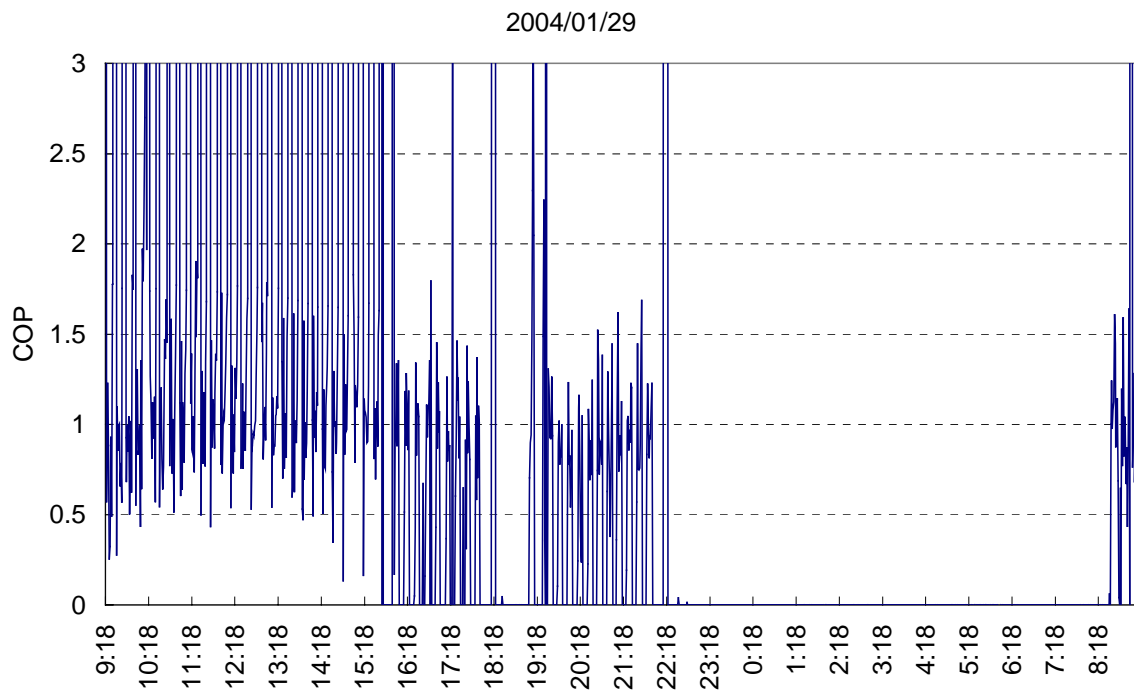


Figure A.22 COP calculation results on typical winter day

Figure A.22 shows that the COP of the GHP system during heating cycle is about 1. This COP is not high compared with catalog COP of 1.37 and shows the potential of improving the performance of the GHP system.

```
%File name:GHPCOP_Winter_StandardTimeStyle.m
%Written by Fulin Wang
%February 25, 2004
%This program is used to calculate a GHP's primary energy COP during heating period in
winter.
%Since October 21, the refrigerant has been changed to R407C(R32:R125:R134a = 23:25:52)
%Measured refrigerant flow rate, pressure and temperature at state points
%3 and 2 are used to calculate the heating amount produce by the GHP.
%The Thermodac Data(RF) files are read to get raw data.
```

```

%Set the current path as the folds where Thermodac Data(RF) data to be analyzed are stored.
%The raw data style of left two columns recording date and time should be standard date/time
value style, for example, 37824 0.519803.
%instead of date/time style, 2003/7/22 12:28:31.
%The data number in every row must be same. Check the first and last row in the raw data file.
clear all
HHV = 90.27; % LPG Higher Heating Value, MJ/Nm3
tic;
for month = 1:12 %Scan and read all the Thermodac(RF) files in current directory.
    if month < 10
        eval(['FileNameMonth = ['0',int2str(month),'];']);
    else
        FileNameMonth = int2str(month);
    end
    for date = 1:31
        if date < 10
            eval(['FileNameDate = ['0',int2str(date),'];']);
        else
            FileNameDate = int2str(date);
        end
        eval(['FileID = fopen('',FileNameMonth,FileNameDate,'1228.csv');']);
        if FileID == -1
            eval(['FileID = fopen('',FileNameMonth,FileNameDate,'1015.csv');']);
            if FileID == -1
                eval(['FileID = fopen('',FileNameMonth,FileNameDate,'0918.csv');']);
                if FileID == -1
                    eval(['FileID =
fopen('',FileNameMonth,FileNameDate,'1849.csv');']);
                end
            end
        end
        if FileID ~= -1
            for line = 1:5
                t = fgets(FileID); %Read five lines table title
            end
            clear RawData P1 T1 P3 T3 H2 H3 Density3 LPGHeat RefFlowRate
CoolingAmount COP
            RawData = fscanf(FileID, '%f%c', [64,inf]);

```

```

%Read raw data. The data style of left two columns recording date and time
%should be standard time value style, 37824 0.519803 instead of date/time style, 2003/7/22
12:28:31.
%The data number in every row must be same. Check the first and last row in the raw data file.
    RawData = RawData';
    RawData = RawData(:,1:2:41); %Eliminate space column
    RowNo = size(RawData);
    for row = 1:RowNo(1,1)
        P2 = RawData(row,19)*9.8E4+101325;
%Refrigerant pressure of State point 2, converted from kg/cm2 to Pa
        P3 = RawData(row,10)*9.8E4+101325;
        T2 = RawData(row,20)+273.15;
%Refrigerant Temperature of State point 2, converted from Centigrade to Kelvin
        T3 = RawData(row,11)+273.15;
        H2(row,1) = property ('H','T',T2,'P',P2,'R32','R125','R134a',[0.23 0.25
0.52]); % Refrigerant enthalpy, J/kg
        H2(row,1) = property ('H','T',T2,'P',P2,'R32','R125','R134a',[0.23 0.25
0.52]); %Because of the bug of refrigerant property calculation program,
        %the first call of the program gives strange answers.
        %So every property has to be calculated two times to get correct results.
        H3(row,1) = property ('H','T',T3,'P',P3,'R32','R125','R134a',[0.23 0.25
0.52]); % Refrigerant enthalpy at state point 4,
        % assumed to be equal to the enthalpy at state point 3
        H3(row,1) = property ('H','T',T3,'P',P3,'R32','R125','R134a',[0.23 0.25
0.52]);
        Density3(row,1) = property ('D','T',T3,'P',P3,'R32','R125','R134a',[0.23 0.25
0.52]); % Refrigerant density at state point 3, kg/m3
        Density3(row,1) = property ('D','T',T3,'P',P3,'R32','R125','R134a',[0.23 0.25
0.52]);
    End
    LPGHeat = RawData(:,7)*HHV*1.0E6/3600; % LPG heat generation, W
    RefFlowRate = RawData(:,9).*Density3*1.0E-3/60; % Refrigerant flow rate,
converted from L/min to kg/s
    CoolingAmount = RefFlowRate.*(H2-H3); % Cooling amount = Refrigerant
flow rate * Delta enthalpy
    COP = CoolingAmount./(LPGHeat+RawData(:,8)./0.3); %convert electric
consumption to primary energy consumption (RawData(:,8)./0.3)
    figure

```

```

plot(COP,'r','LineWidth',1)
grid on
ylabel('COP')
eval(['title('',FileNameMonth,'/',FileNameDate,'')']);
axis auto
fclose(FileID);
set(gca,'ylim',[0 3])
set(gca,'xlim',[0 1440])
set(gca,'xTick',[0:120:1440])
set(gca,'xTickLabel',[0:120:1440])
eval(['hgsave("COP',FileNameMonth,FileNameDate,'.fig")']);
Results = [RawData(:,1) RawData(:,2) RawData(:,7) RawData(:,8) RawData(:,9)
RawData(:,10) RawData(:,11) RawData(:,19) RawData(:,20) H3 H2 Density3 CoolingAmount
COP];

eval(['SaveFileName=["COP',FileNameMonth,FileNameDate,'.csv"];']);
eval(['SaveFileID = fopen('',SaveFileName,'','w");']);
if SaveFileID ~= -1
    TableTitle1 =
['Date,Time,GasConsumption,ElectricConsumption,RefrigerantFlowRate',...
    'Pressure3,Temperature3,Pressure2,Temperature2,Enthalpy3,Enthalpy2,Density3,CoolingAmo
unt,COP'];
    TableTitle2 =
['-',-,Nm3/h,W,L/min,kg/cm2,C,kg/cm2,C,J/kg,J/kg,kg/m3,W,-'];
    fprintf(SaveFileID,'%s,\n',TableTitle1);
    fprintf(SaveFileID,'%s,\n',TableTitle2);
    fprintf(SaveFileID,'%d,%d,%d,%d,%d,%d,%d,%d,%d,%d,%d,%d,%d,%d,%d,\n',Results');
    fclose(SaveFileID);
end
end
end
end
toc;
hours = fix(toc/3600);
minutes = fix(mod(toc,3600)/60);
seconds = mod(mod(toc,3600),60);
['Caculation time: ',int2str(hours),'hours, ',int2str(minutes),'minutes, ',int2str(seconds),'seconds']

```


Table A.5 Raw data for COP calculation of heating operation

29	CH	0	1	2	3	4	5	6	7	8	9	10	11	12	13	14	15	16	17	18
	Name	CHANN EL-00	102 Solar	103 Wind speed	104 Wind direction	401 Gas consumption	402 Power consumption	403 Refrigerant flow rate	404 Pressure (high)	405 Refrigerant temperature (high)	406 Temperature of Exhausted Gas	407 Temperature of inlet air 1	408 Temperature of inlet air 2	409 Temperature of inlet air 3	410 Temperature of outlet air 1	411 Temperature of outlet air 2	Temperature of engine room	425 Pressure (low)	426 Refrigerant temperature (low)	427 Temperature of PC room
	Unit	oC	W/m2	m/s	o	Nm3/h	W	L/min	kg/cm2	oC	oC	oC	oC	oC	oC	oC	oC	kg/cm2	oC	oC
	Form	#####0.0	#####0.0	#### 0.0	#####0.0	##0.00 0	##### #0	##0.000	###0.00	###0.0 0	#####0.0	#####0. 0	#####0. 0	#####0.0	#####0.0	#####0. 0	#####0.0	###0.0 0	#####0. .0	#### 0.0
38015	0.388032	9999.9	116.2	2.4	58.5	0.001	83	1.343	11.57	23.3	9999.9	6.4	5.5	6.8	12	12.6	46.5	9.02	54.7	10.7
38015	0.388727	9999.9	118.6	2.8	199.9	0.261	939	1.343	10.75	23.1	9999.9	5.3	5	6.8	16	13.7	36.1	10.93	55.5	10.5
38015	0.389421	9999.9	115.6	3.1	285.6	0.401	940	3.019	12.36	28.7	9999.9	5.4	5.2	6.7	5.4	6	35.6	14.14	61.6	10.9
38015	0.390116	9999.9	108	2.8	326.8	0.521	932	5.369	13.94	32.7	9999.9	5.1	4.9	6.8	4.1	4.8	34.4	15.39	62.1	10.9
38015	0.39081	9999.9	101	2.2	124.8	0.521	956	3.839	14.46	32.4	9999.9	4.9	4.8	6.8	3.8	4.6	34.6	15.73	63.9	10.8
38015	0.391505	9999.9	95.6	2.1	22.1	0.571	949	4.644	14.56	35.3	9999.9	5	4.7	6.8	3.7	4.6	34.4	16.3	64.9	10.9
38015	0.392199	9999.9	91.4	2.5	254.6	0.591	946	4.349	14.98	36.1	9999.9	5	4.9	6.6	3.6	4.5	35.3	17.11	66.3	10.9
38015	0.392894	9999.9	86.6	2.2	140.7	0.651	952	4.964	14.9	34.8	9999.9	4.9	4.8	6.7	3.3	4.1	36.7	18.13	68.4	10.9
38015	0.393588	9999.9	84.4	2.5	358.8	0.622	940	6.868	13.62	32.6	9999.9	5.1	4.9	6.8	2.8	3.8	37.3	19.73	72.1	11
38015	0.394282	9999.9	84.4	2.5	329.9	0.321	934	4.984	12.48	29	9999.9	4.9	4.8	6.9	3.7	4.6	37.5	19.27	73	10.9
38015	0.394977	9999.9	84.8	2.6	192.9	0.001	916	1.343	12.06	27.6	9999.9	5.3	5.1	7	5.4	6.6	38.9	14.63	68.3	11
38015	0.395671	9999.9	84.2	2.3	286.9	0.001	85	1.343	12.02	25.9	9999.9	5.9	5.2	6.8	9	13.1	45.3	9.56	62.2	10.9
38015	0.396366	9999.9	83	2	105	0.001	87	1.34	11.94	25.2	9999.9	5.9	6.5	6.4	7.9	15.3	45.8	9.52	57.8	10.9
38015	0.39706	9999.9	81.2	2.3	44.6	0.001	83	1.343	11.88	24.4	9999.9	5.8	5.8	6.6	12.4	15.4	46.4	9.26	54.7	11.1
38015	0.397755	9999.9	78	2.3	252	0	82	1.343	11.77	24.5	9999.9	6.1	5.8	6.4	11.3	14.2	46.1	8.92	51.6	11.1
38015	0.398449	9999.9	74.4	2	138.7	0.331	945	0.796	11.44	25.9	9999.9	5.2	4.9	6.5	9.7	8.8	35.4	12.77	57.9	10.8
38015	0.399144	9999.9	71.2	2	100.4	0.471	948	5.76	12.95	30.4	9999.9	5.1	4.8	6.4	4.6	5	35	15.09	59.9	10.9
38015	0.399838	9999.9	72.2	2.4	19.3	0.571	950	4.134	14.45	33.8	9999.9	5.3	5	6.1	3.9	4.8	34.7	15.93	61.1	10.9
38015	0.400532	9999.9	77.2	2.3	11.7	0.501	944	4.277	14.61	33.4	9999.9	5.1	5	6.5	3.9	4.8	35	16.02	62.3	10.9

38015	0.401227	9999.9	83.6	2	345.1	0.542	942	4.655	14.65	34.3	9999.9	5.4	5	6.5	3.7	4.7	35.3	16.49	62.7	11
38015	0.401921	9999.9	88.6	2.1	181.9	0.571	946	3.182	14.91	35	9999.9	5.8	5.1	6.7	3.9	4.9	35.8	17.35	65.5	11
38015	0.402616	9999.9	93.4	2.6	7.3	0.581	941	5.828	14.24	33.9	9999.9	5.8	4.9	6.6	3.5	4.6	35.9	18.56	67.5	10.8
38015	0.40331	9999.9	101.6	2.5	334.8	0.321	956	5.09	12.94	30.8	9999.9	6	5.5	6.8	3.9	5.3	35.9	18.8	69.5	11
38015	0.404005	9999.9	112.6	2	367.1	0.001	917	1.34	12.18	27.3	9999.9	5.8	5.1	7.1	5.3	6.8	37.7	15.79	67.3	11.1
38015	0.404699	9999.9	122	2.1	243.1	0.001	90	1.343	12.14	26.3	9999.9	6.1	5	6.7	7.3	9.3	41.9	10.47	61.2	11
38015	0.405394	9999.9	136.2	2	368.8	0.001	86	1.346	12.07	25.6	9999.9	7	5.5	6.7	10.8	13.6	44.6	9.57	56.6	11.1
38015	0.406088	9999.9	152.4	2.5	209.2	0.001	117	1.34	12.01	24.8	9999.9	7.1	5.9	6.7	12.2	15.1	45.1	9.35	53.3	11.2
38015	0.406782	9999.9	164	2.5	22.1	0.001	82	1.343	11.93	24.4	9999.9	8.5	5.6	7	12.8	11	45.3	9.06	50.5	11.2
38015	0.407477	9999.9	166.8	2.2	16.6	0.271	934	2.298	11.21	24.1	9999.9	5.7	5.1	7.6	14.4	13.3	36.8	10.81	50.8	11
38015	0.408171	9999.9	156	2.3	56	0.372	936	2.581	12.57	29.3	9999.9	5.6	5	7.8	5.6	6.1	35.2	14.43	56.5	11.2
38015	0.408866	9999.9	140.2	2	49.8	0.482	931	4.185	14.06	33.2	9999.9	5.2	5.1	7.5	4.3	5.2	34.9	15.42	58.9	11.3
38015	0.40956	9999.9	129.2	2.8	69.8	0.531	954	3.883	14.53	33.6	9999.9	5.4	5.1	7.7	4.4	5.4	35.1	15.7	60.3	11.1
38015	0.410255	9999.9	123.2	3.1	56.9	0.461	919	4.26	14.55	34.4	9999.9	5.4	5.1	8.2	4.2	5.2	35.1	16	61.6	11.3
38015	0.410949	9999.9	128.4	2.8	22.3	0.502	934	3.958	14.72	35.2	9999.9	5.4	5	8.3	3.9	5	34.3	16.64	62.8	11.4
38015	0.411644	9999.9	145.6	2.6	26.1	0.521	957	4.019	14.48	33.6	9999.9	5.7	5.2	8.2	4	4.9	34.9	17.38	64.6	11.2
38015	0.412338	9999.9	169.4	2.3	59.1	0.491	945	4.175	13.21	30.4	9999.9	5.7	5.2	8.1	3.9	5.2	35.6	18.19	65.3	11.2
38015	0.413032	9999.9	193.4	2.8	108.3	0.28	921	4.845	12.38	29.2	9999.9	5.9	5.1	8.4	4.6	5.8	35.4	17.19	66.2	11.2
38015	0.413727	9999.9	234.2	2.4	326.5	0.291	927	4.75	11.69	25.8	9999.9	6.1	5.2	8.9	5	6.3	36.1	17.47	65.2	11.3
38015	0.414421	9999.9	275	2.1	339.1	0.001	918	1.34	11.58	26.3	9999.9	6	5.4	9.2	6.2	7.4	38	13.01	61	11.3
38015	0.415116	9999.9	236	2	75.5	0.001	86	1.343	11.56	24.3	9999.9	7.5	7	9	11.2	13.4	44	9.51	55.7	11.2
38015	0.41581	9999.9	195	2.1	272.8	0.001	83	1.343	11.52	23.8	9999.9	9.7	6.1	9.4	11.9	14.3	44.2	9.42	52.6	11.1
38015	0.416505	9999.9	200	2.6	56.4	0	81	3.502	11.46	23.1	9999.9	8.4	5.9	9.9	13.3	13.9	44.2	9.16	49.7	11.3
38015	0.417199	9999.9	202.2	2.4	22.7	0.26	940	1.34	10.81	23.7	9999.9	6.5	5.7	10	12.7	13.5	36.5	10.85	50	11.1
38015	0.417894	9999.9	198.6	2.3	32.5	0.381	939	3.73	12.54	28.7	9999.9	6.1	5.5	9.9	6.1	6.7	36	14.36	55.8	11.3
38015	0.418588	9999.9	196.6	2.2	343.7	0.451	947	5.246	14.11	32.5	9999.9	6.5	5.5	10	4.7	6	35.3	15.35	57.2	11.3
38015	0.419282	9999.9	187.4	2.2	73.7	0.492	969	3.604	14.5	33.3	9999.9	6.4	5.8	9.7	5.1	6.2	34.4	15.61	58.6	11.4
38015	0.419977	9999.9	180	2.3	48.8	0.442	932	4.182	14.47	34.4	9999.9	6.1	5.4	9.8	4.4	5.6	34.5	15.79	59.6	11.4
38015	0.420671	9999.9	178.8	2.8	10.2	0.441	966	4.009	14.51	34.4	9999.9	6.2	5.7	10.6	4.6	5.7	35.2	16.18	59.8	11.4
38015	0.421366	9999.9	176.4	2.5	1	0.442	924	4.08	14.23	34.1	9999.9	6.1	5.5	10.6	4.4	5.5	34.6	16.78	60.6	11.5

Table A.6 COP calculation results of heating operation

Date	Time	Gas Consumption	Electric Consumption	Refrigerant Flow Rate	Pressure 3	Temperature 3	Pressure 2	Temperature 2	Enthalpy 3	Enthalpy 2	Density 3	Cooling Amount	COP
-	-	Nm ³ /h	W	L/min	kg/cm ²	oC	kg/cm ²	oC	J/kg	J/kg	kg/m ³	W	-
2004/1/29	9:18	0.001	83	1.343	11.57	23.3	9.02	54.7	234977.1	452914.8	1145.53	5588.091	18.51946
2004/1/29	9:19	0.261	939	1.343	10.75	23.1	10.93	55.5	234683.8	450689.6	1145.834	5540.029	0.572638
2004/1/29	9:20	0.401	940	3.019	12.36	28.7	14.14	61.6	244318.6	451987.6	1008.703	10540.16	0.799199
2004/1/29	9:21	0.521	932	5.369	13.94	32.7	15.39	62.1	249534.1	450445.6	1103.065	19831.16	1.226361
2004/1/29	9:22	0.521	956	3.839	14.46	32.4	15.73	63.9	249040.2	451919.6	1105.035	14344.35	0.882689
2004/1/29	9:23	0.571	949	4.644	14.56	35.3	16.3	64.9	278522.3	452104.9	332.4007	4465.901	0.255469
2004/1/29	9:24	0.591	946	4.349	14.98	36.1	17.11	66.3	271243.9	452358	442.4708	5808.648	0.323194
2004/1/29	9:25	0.651	952	4.964	14.9	34.8	18.13	68.4	252855.1	453099.5	1093.339	18113.23	0.929019
2004/1/29	9:26	0.622	940	6.868	13.62	32.6	19.73	72.1	265588.8	454832.9	426.3945	9236.616	0.493146
2004/1/29	9:27	0.321	934	4.984	12.48	29	19.27	73	243747.1	456671.9	1119.873	19807.14	1.77445
2004/1/29	9:28	0.001	916	1.343	12.06	27.6	14.63	68.3	241577.2	458601.6	1126.171	5470.63	1.777097
2004/1/29	9:29	0.001	85	1.343	12.02	25.9	9.56	62.2	238950.2	459692.3	1134.056	5603.304	18.16846
2004/1/29	9:30	0.001	87	1.34	11.94	25.2	9.52	57.8	237875.7	455285.8	1137.207	5521.7	17.52503
2004/1/29	9:31	0.001	83	1.343	11.88	24.4	9.26	54.7	236651.1	452539	1140.802	5512.691	18.26957
2004/1/29	9:32	0	82	1.343	11.77	24.5	8.92	51.6	236805.8	449939.8	1140.268	5439.818	19.90177
2004/1/29	9:33	0.331	945	0.796	11.44	25.9	12.77	57.9	238961.1	450209	1133.608	3176.999	0.277471
2004/1/29	9:34	0.471	948	5.76	12.95	30.4	15.09	59.9	248783.9	448458.8	860.5961	16496.59	1.101953
2004/1/29	9:35	0.571	950	4.134	14.45	33.8	15.93	61.1	251269.6	448356.2	1098.006	14910.12	0.852762
2004/1/29	9:36	0.501	944	4.277	14.61	33.4	16.02	62.3	250625.1	449586.7	1100.176	15603.41	0.993263
2004/1/29	9:37	0.542	942	4.655	14.65	34.3	16.49	62.7	252062.4	449227.7	1095.655	16759.95	1.001751
2004/1/29	9:38	0.571	946	3.182	14.91	35	17.35	65.5	253176.2	451009.4	1092.321	11460.36	0.655959
2004/1/29	9:39	0.581	941	5.828	14.24	33.9	18.56	67.5	256645.6	451286.8	736.7347	13928.82	0.786706
2004/1/29	9:40	0.321	956	5.09	12.94	30.8	18.8	69.5	264098.1	453273.5	396.3911	6361.432	0.566178
2004/1/29	9:41	0.001	917	1.34	12.18	27.3	15.79	67.3	241109.4	455676.7	1127.676	5403.827	1.753498
2004/1/29	9:42	0.001	90	1.343	12.14	26.3	10.47	61.2	239564.3	457331.4	1132.301	5519.236	16.97835
2004/1/29	9:43	0.001	86	1.346	12.07	25.6	9.57	56.6	238487.8	453987.8	1135.474	5489.314	17.60853

2004/1/29	9:44	0.001	117	1.34	12.01	24.8	9.35	53.3	237261.2	450972.9	1139.084	5436.725	13.09818
2004/1/29	9:45	0.001	82	1.343	11.93	24.4	9.06	50.5	236650.3	448595.9	1140.839	5412.199	18.13689
2004/1/29	9:46	0.271	934	2.298	11.21	24.1	10.81	50.8	236202.7	445945.2	1141.665	9171.154	0.92557
2004/1/29	9:47	0.372	936	2.581	12.57	29.3	14.43	56.5	245510.4	445765.4	983.4881	8472.067	0.680602
2004/1/29	9:48	0.482	931	4.185	14.06	33.2	15.42	58.9	250325.9	446723.7	1100.669	15077.78	0.992646
2004/1/29	9:49	0.531	954	3.883	14.53	33.6	15.7	60.3	250947.1	447839.1	1099.093	14004.85	0.849045
2004/1/29	9:50	0.461	919	4.26	14.55	34.4	16	61.6	252226.6	448811.9	1095.048	15284.19	1.045222
2004/1/29	9:51	0.502	934	3.958	14.72	35.2	16.64	62.8	261369.2	449080	636.0938	7876.531	0.501658
2004/1/29	9:52	0.521	957	4.019	14.48	33.6	17.38	64.6	250948.9	449894.4	1099.046	14645.92	0.901062
2004/1/29	9:53	0.491	945	4.175	13.21	30.4	18.19	65.3	245921.2	449292.7	1113.746	15760.91	1.019344
2004/1/29	9:54	0.28	921	4.845	12.38	29.2	17.19	66.2	260421.7	452105.4	406.1307	6286.277	0.622959
2004/1/29	9:55	0.291	927	4.75	11.69	25.8	17.47	65.2	238802.4	450446.6	1134.262	19004.75	1.829698
2004/1/29	9:56	0.001	918	1.34	11.58	26.3	13.01	61	239575.3	453176.3	1131.865	5399.473	1.750192
2004/1/29	9:57	0.001	86	1.343	11.56	24.3	9.51	55.7	236503.1	453164.2	1141.018	5533.479	17.75021
2004/1/29	9:58	0.001	83	1.343	11.52	23.8	9.42	52.6	235739.9	450146.2	1143.248	5486.592	18.18308
2004/1/29	9:59	0	81	3.502	11.46	23.1	9.16	49.7	234674.2	447615.7	1146.345	14247.56	52.76875
2004/1/29	10:00	0.26	940	1.34	10.81	23.7	10.85	50	235597.7	445028.7	1143.179	5346.981	0.553929
2004/1/29	10:01	0.381	939	3.73	12.54	28.7	14.36	55.8	243277.4	445096.8	1121.355	14069.01	1.109231
2004/1/29	10:02	0.451	947	5.246	14.11	32.5	15.35	57.2	249210.5	444882.2	1104.219	18891.23	1.305951
2004/1/29	10:03	0.492	969	3.604	14.5	33.3	15.61	58.6	250469.6	446030.5	1100.576	12928.13	0.830488
2004/1/29	10:04	0.442	932	4.182	14.47	34.4	15.79	59.6	254364.7	446865.7	914.3129	12267.63	0.864538
2004/1/29	10:05	0.441	966	4.009	14.51	34.4	16.18	59.8	252228.2	446389.3	1095.01	14205.78	0.994936
2004/1/29	10:06	0.442	924	4.08	14.23	34.1	16.78	60.6	264677.3	446230.9	495.1824	6113.345	0.431637
2004/1/29	10:07	0.421	927	4.937	13.1	30.4	17.39	63	245924.3	447974.6	1113.65	18514.85	1.35674
2004/1/29	10:08	0.31	901	5.505	12.34	29.1	16.82	63.5	260731.1	449583.2	398.3006	6901.427	0.64041
2004/1/29	10:09	0.281	909	5.008	11.69	26	16.48	62.9	239110.5	449478.6	1133.339	19900	1.974975
2004/1/29	10:10	0.281	916	4.437	11.05	23.7	16.67	63.5	235594.2	449846.2	1143.355	18115.24	1.793693
2004/1/29	10:11	0.281	925	5.338	10.46	22.6	16.74	64.8	233926.9	451240.9	1147.862	22192.42	2.190891
2004/1/29	10:12	0.281	915	6.457	10.04	21.1	16.81	64.8	231658.5	451120.7	1154.212	27259.94	2.700053
2004/1/29	10:13	0.291	905	7.456	9.61	20.1	17.35	66.3	230154.3	451949.8	1158.296	31924.71	3.095432

A.4 FUTURE RESEARCH

One of the main objectives of this research is to develop model-based commissioning method for GHP systems. Until now the model-based commissioning method for filters in air-conditioner has been completed. In the future, the model-based commissioning methods for other components in GHP system and for whole system commissioning are scheduled to develop. Stylianou (1996) listed that the typical faults occurred in air-conditioner are lack of refrigerant, presence of air in the refrigerating circuit, and presence of refrigerant in the lubricating oil. Accordingly this future research focuses on studying the following commissioning method for GHP system.

- Detecting the fault of lack of refrigerant
- Detecting the fault of presence of air in the refrigerating circuit
- Detecting the fault of presence of refrigerant in the lubricating oil
- Commissioning GHP system using simulated heating/cooling load

ACKNOWLEDGEMENT

I would like to express my sincere thanks to all the people who have helped me to complete this dissertation.

First I would like to express my sincere thanks to my doctoral course supervisor, professor Harunori Yoshida who directed the part II of this dissertation, for his instructive suggestion, fruitful discussion and continuous encouragement. He offers me not only nice conditions to do research, but also continuous supporting to internationally spread the research results. From him, I learned the correct attitude to do research and work, which goes beyond research and can benefit me in my whole life.

I would like to sincerely appreciate my master course supervisor, professor Yi Jiang who directed the part I of this dissertation, for his brilliant direction and useful suggestion. His excellent insight in the specialty smoothed my research. From him I learned the deep understanding of technical knowledge and seriousness of doing research.

I would like to thank professor Naoki Katoh, in Department of Architecture, Faculty of Engineering, Kyoto University, for reviewing this dissertation. Useful advices are obtained from professor Katoh.

I would like to appreciate associate professor Yoshiaki Uetani, in Department of Urban and Environmental Engineering, Faculty of Engineering, Kyoto University. Professor Uetani reviewed this dissertation and gave instructive suggestions.

I would like to express my sincere thanks to professor Yingxin Zhu, in Department of Building Science, Tsinghua University, Beijing, China, for her recommending me to study in Kyoto University and her kind advices for this research.

I would like to sincerely acknowledge professor Kangqi Mi, in Huazhong University of Science and Technology, Wuhan, China, for his recommending me to study in Kyoto University.

I would like to acknowledge all the colleagues in the laboratory of Sustainable Building Environment Engineering, Kyoto University, for their help in not only research but also daily life. Special thanks are given to Mr. Ippei Matsuoka, Mr. Masato Miyata and Mr.

Hiroaki Kitagawa for their help in conducting experiments. Special thanks are given to Mr. Hom Bahadur Rijal, who gave great help to me to complete registration procedure when I arrived in Kyoto University and many helps during daily life. I would like to thank Miss Ai Sato, Mr. Hayato Hosobuchi, Mr. Keiichi Suzuki, Mr. Kazuya Takahashi, Mr. Yasutaka Noda, and Mrs. Rie Nakajima for their helps in many aspects during this research.

I would like to thank all the colleagues in the Department of Building Science, Tsinghua University, Beijing, China, for their help in both research and daily life. Special thanks are given to Dr. Feng Chen, Dr. Weifeng Zhu, Dr. Qingpeng Wei, Mr. Yuchun Deng, Mr. Hongru Wu, Mr. Zhifeng Xu, Mr. Jianjun Xia and Mr. Da Yan.

I would like to express my sincere thanks to Mr. Makoto Tsubaki and Miss Kanako Itou, in Research & Development Department, Yamatake Building Systems Company, Ltd. Without their help, the experiments on studying the commissioning of VAV systems cannot be completed.

I would like to sincerely acknowledge Mr. Keiji Matsumoto and Mrs. Kyoko Goto, in Electronics Development Center, Research & Development Center, YANMAR Company, Ltd. They offered me many helps during conducting experiments on commissioning multi-evaporator GHP systems.

I would like to sincerely thank Annex 40 members for their advices to this research, special thanks to professor Philip Haves in Lawrence Berkeley National Laboratory, USA, and Dr. Jean-Christophe Visier in Centre Scientifique et Technique du Batiment, France.

I would like to express my gratitude to Japanese government for the three years financial support (Scholarship of Monbukagakusho).

Finally, I would like to thank my parents, Keqin Wang and Shufang Yong, and my wife Haiyi Yu for their continuous encouragement and deep love.

May 2004

Fulin Wang